



JAYNE DE ABREU FIGUEIREDO

**ANTHOCYANINS LIPID MICROPARTICLES OBTAINED BY
SPRAY CHILLING GRAPE PEEL EXTRACT**

**LAVRAS-MG
2022**

JAYNE DE ABREU FIGUEIREDO

**ANTHOCYANINS LIPID MICROPARTICLES OBTAINED BY *SPRAY CHILLING*
GRAPE PEEL EXTRACT**

Tese apresentada à Universidade Federal de Lavras, como parte das exigências do Programa de Pós-Graduação em Ciência dos Alimentos, área de concentração em Ciência dos Alimentos para a obtenção do título de Doutora.

Profa. Dra. Soraia Vilela Borges
Orientadora

Prof. Dr. Pedro Henrique Campelo
Coorientador

**LAVRAS-MG
2022**

Ficha catalográfica elaborada pelo Sistema de Geração de Ficha Catalográfica da Biblioteca
Universitária da UFLA, com dados informados pelo(a) próprio(a) autor(a).

Figueiredo, Jayne de Abreu.

Anthocyanins lipid microparticles obtained by spray chilling
grape peel extract / Jayne de Abreu Figueiredo. - 2022.

213 p. : il.

Orientador(a): Soraia Vilela Borges.

Coorientador(a): Pedro Henrique Campelo Felix.

Tese (doutorado) - Universidade Federal de Lavras, 2022.

Bibliografia.

1. Microencapsulação. 2. Pigmentos naturais. 3. Estabilidade. I.
Borges, Soraia Vilela. II. Felix, Pedro Henrique Campelo. III.
Título.

JAYNE DE ABREU FIGUEIREDO

MICROPARTÍCULAS LIPÍDICAS DE ANTOCIANINAS OBTIDAS POR *SPRAY CHILLING* DO EXTRATO DE CASCA DE UVA

ANTHOCYANINS LIPID MICROPARTICLES OBTAINED BY *SPRAY CHILLING* GRAPE PEEL EXTRACT

Tese apresentada à Universidade Federal de Lavras, como parte das exigências do Programa de Pós-Graduação em Ciência dos Alimentos, área de concentração em Ciência dos Alimentos, para a obtenção do título de Doutora.

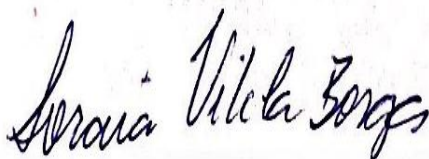
APROVADA em 19 de agosto de 2022.

Dra. Amanda Maria Teixeira Lago UFLA

Dra. Bruna de Souza Nascimento UFLA

Dra. Izabela Dutra Alvim ITAL

Dr. Pedro Henrique Campelo UFV



Profa. Dra. Soraia Vilela Borges
Orientadora

Prof. Dr. Pedro Henrique Campelo
Coorientador

**LAVRAS-MG
2022**

Dedico este trabalho à minha família querida, ao meu companheiro de vida e a meus filhos de quatro patas, em especial ao Nelson e Teodoro José (in memoriam).

AGRADECIMENTOS

Agradeço a Deus por me dar tanta certeza de que eu aguentaria firme. Sem Ele, nada disso seria possível.

Aos meus pais, Zezão e Irani, pelo amor incondicional e por sempre apoiarem as minhas decisões. Aos meus irmãos, Jaqueline e João Vítor, pelo carinho e momentos felizes que sempre me proporcionam. Obrigada, família, por entenderem as minhas faltas e momentos de afastamento. Amo vocês.

Ao meu companheiro de vida, Junior, por ser o meu maior incentivador. Obrigada por me tranquilizar e me distrair nas horas de desespero e desânimo (rs). Agradeço também pela paciência quando esta me faltava (rs). E claro, não poderia deixar de agradecer aos nossos filhos, “cãopanheirinhos” de vida, em especial ao Nelson e Teodoro José (*in memoriam*), por nos ensinar a ser forte e lutar até o “fim” e viver cada dia como se fosse o último, e a Brigitte, por nos dar tanto amor e carinho e deixar tudo mais leve e feliz! Amo muito vocês.

À minha cunhada Juliana e minha sogra Eliana, por não medirem esforços para me verem bem e por vibrarem comigo a cada conquista.

À minha amiga, conselheira, “mãorientadora” e exemplo de pessoa, Profa. Dra. Soraia Vilela Borges, pela orientação desde 2013. Obrigada pela amizade que levarei para o resto da vida, apoio, conselhos, ensinamentos, confiança e paciência. A sua humildade e amor ao próximo fazem o caminho ficar mais leve. Obrigada!

À minha amiga Laís Norcino. Pela companhia, incentivo e toda ajuda no momento em que não tínhamos certeza de nada (pandemia). Você foi essencial para o desenvolvimento deste trabalho! Obrigada pela amizade e principalmente pelas risadas! Conte sempre comigo.

Ao meu coorientador que amolo desde 2015, Prof. Dr. Pedro Henrique Campelo. Obrigada por compartilhar seus conhecimentos com tanta paciência e boa vontade por todos esses anos. Com toda certeza contribuiu muito em minha jornada. Levarei nossa amizade para sempre. Conte sempre comigo!

Aos professores e técnicos do DCA/UFLA, principalmente aos profs. Drs. Diego e Cleiton, por estarem sempre dispostos a ajudar. Obrigada pelos ensinamentos.

Agradeço aos membros da banca, Dra. Amanda, Dra. Bruna e Dra. Izabela, por terem aceitado o convite para participarem desta banca e acrescentarem com suas valiosas contribuições.

Aos amigos do Laboratório de embalagens e encapsulação e do departamento de ciência dos alimentos da UFLA pela troca de conhecimentos, amizade e momentos de distração.

A todos os meus amigos que, direta ou indiretamente, apoiaram-me, auxiliaram-me e torceram por mim.

Às empresas que fizeram doações importantes para o desenvolvimento deste trabalho: Agropalma, Duas Rodas e Danisco. À Dra. Regiane e todos da fazenda em Campos Gerais que gentilmente disponibilizaram as uvas. Muito obrigada!

Ao CNPq pela concessão da bolsa de doutorado. À CAPES, à FAPEMIG e à Universidade Federal de Lavras, especialmente ao Departamento de Ciência dos Alimentos, pela oportunidade.

“O que vale na vida não é o ponto de partida e sim a caminhada.

Caminhando e semeando, no fim terás o que colher.”

(Cora Coralina)

RESUMO GERAL

Com o intuito de aproveitar descartes de cascas de uvas, este trabalho teve como objetivo estudar a microencapsulação por *spray chilling* do extrato de casca de uva, rico em substâncias corantes e antioxidantes. Essas substâncias, além de apresentarem propriedades sensoriais para os alimentos, são valiosas para a saúde humana, pois agem na prevenção de diversas doenças. Entretanto, são sensíveis ao calor, luz e umidade, perdendo-se nas etapas de processamento e estocagem dos alimentos, sendo necessária sua reposição para uma dieta saudável. A microencapsulação por *spray chilling* realiza-se a temperaturas amenas minimizando os danos térmicos e utiliza substâncias lipídicas como materiais encapsulantes. Primeiramente, o teor do emulsificante polirricinoleato de poliglicerol (PGPR) e a homogeneização assistida por ultrassom (160 e 200 W; 4 e 6 min) foram estudados para preparar emulsões contendo o extrato de casca de uva (40%) usando óleo de palma totalmente hidrogenado livre em *trans* (OPH-80%) e óleo de palma (OP- 20%) como materiais encapsulantes. Uma emulsão obtida no agitador magnético (750 rpm/4 min) foi utilizada como controle. As emulsões foram avaliadas quanto à estabilidade cinética, distribuição e tamanho de gotículas, comportamento reológico, microscopia ótica, FTIR, retenção de compostos bioativos e estabilidade oxidativa. O efeito do processo de homogeneização na formação de micropartículas por *spray chilling*, foi investigado, assim como a estabilidade das antocianinas e cor. 4% de PGPR foi eficiente para formar as emulsões. O ultrassom assistido (US) implicou em emulsões mais estáveis, principalmente para as condições de processo de 200 W e 4 minutos. Espectros de FTIR confirmaram a presença dos compostos bioativos e ausência de oxidação lipídica nas emulsões. O teor de compostos fenólicos, a atividade antioxidante, a cinética de degradação das antocianinas e a estabilidade ao armazenamento foram melhorados nas emulsões tratadas pelo US. As micropartículas elaboradas com a emulsão tratada por US (200 W e 4 min) demonstrou melhor aspecto visual, fluidez e estabilidade do pigmento antocianínico quando comparadas aquelas produzidas com a emulsão controle. Depois de otimizar a formulação da emulsão, o efeito de diferentes proporções entre OPTH e OP (90:10; 80:20; 70:30; 60:40 e 50:50) foi avaliado em relação as propriedades físico-químicas, estabilidade ao armazenamento (-18°C, 4°C e 25°C/90 dias) e ao trato gastrointestinal das micropartículas lipídicas microestruturadas (MLMs) obtidas por *spray chilling*. Maior conteúdo de OPTH melhorou a resistência térmica das MLMs e todos os tratamentos levaram a produção de partículas com comportamento cristalino β' e β . A retenção de antocianinas variou de 81,5 – 61,2%, sendo MLM_90:10 apresentando o melhor resultado. O mesmo comportamento foi observado para os compostos fenólicos (1443,1 – 1247,2 mg GAE/100 g) e atividade antioxidante (92,6-86,8%). Durante o armazenamento, as MLMs 80:20, 70:30 e 60:40 (OPH:OP), exibiram melhor retenção de antocianinas e maior estabilidade da cor nas temperaturas estudadas. A simulação gastrointestinal *in vitro* revelou que todos os tratamentos foram capazes de proteger as antocianinas da fase gástrica e mantiveram uma liberação máxima e controlada desse composto na fase intestinal. Esses resultados sugerem promissora aplicação em sistemas alimentícios para finalidades corantes, aromatizantes e antioxidantes.

Palavras-chave: Aditivos naturais. *Spray congealing*. Liberação controlada. Óleo de Palma. Estabilidade.

GENERAL ABSTRACT

This study used spray chilling microencapsulation of grape peel extract, rich in coloring and antioxidant compounds aimed at using discarded grape peels. Besides the sensory properties for use in food, these compounds are valuable for human health, as they act in the prevention of several diseases. However, they are sensitive to heat, light, and humidity, losing their properties in food processing and storage stages, which makes their replacement necessary for a healthy diet. Microencapsulation by spray chilling is performed at mild temperatures, minimizing thermal damage and using lipid compounds as encapsulating materials. First, the polyglycerol polyricinoleate (PGPR) emulsifier content, and the ultrasound-assisted homogenization (160 and 200 W; 4 and 6 min) were studied to prepare stable emulsions containing the grape peel extract (40%) using fully hydrogenated trans-free palm oil (FHPO-80%) and palm oil (PO-20%) as encapsulating agents. An emulsion produced with the aid of a magnetic stirrer (750 rpm/4 min) was used as a control. The emulsions were evaluated for kinetic stability, droplet size and distribution, rheological behavior, optical microscopy, FTIR, retention of bioactive compounds, and oxidative stability. The effect of the homogenization process on the formation of microparticles by spray chilling was also investigated, as well as the anthocyanins and color stability. PGPR proved to be an effective emulsifier at a concentration of 4%. Ultrasound-assisted technique allowed the formation of more stable emulsions, mainly for the process conditions of 200 W and 4 minutes. FTIR spectra confirmed the presence of the bioactive compounds and the absence of lipid oxidation in all emulsions. The phenolic compounds content, antioxidant activity, degradation kinetics of anthocyanins, and storage stability were improved in the US-treated emulsions. The microparticles made with the US-treated emulsion (200 W and 4 min) showed improved visual appearance, flowability, and stability of the anthocyanin pigment when compared to the microparticles made with the control emulsion. After optimizing the emulsion formulation, the effect of different FHPO to PO ratios (90:10; 80:20; 70:30; 60:40, and 50:50) was evaluated concerning the physicochemical properties, storage stability (-18°C, 4°C, and 25°C/90 days) and the resistance to the gastrointestinal tract of spray-chilled microstructured lipid microparticles (MLMs) containing grape peel extract. Increasing the proportion of FHPO improved the thermal resistance of MLMs, although all treatments led to the production of MLMs with β' and β'' crystalline behavior. The anthocyanins retention in the MLMs ranged from 81.5 - 61.2% and the treatment MLM_90:10 showed the best result. Similar behavior was observed for the phenolic compounds content (1443.1 - 1247.2 mg GAE/100 g) and antioxidant activity (92.6-86.8%). During the storage, MLMs containing FHPO to PO ratios of 80:20, 70:30, and 60:40 exhibited better retention of anthocyanins and lower color changes for all temperatures studied. In vitro gastrointestinal simulation revealed that all treatments protected anthocyanins from the gastric phase and maintained a maximum and controlled release of this compound in the intestinal phase. The present results suggest a promising application of MLM in food systems for coloring, flavoring, and antioxidant purposes.

Keywords: Natural additives. Spray congealing. Controlled release. Palm oil. Stability.

SUMÁRIO

	PRIMEIRA PARTE	11
1	INTRODUÇÃO	11
2	REFERENCIAL TEÓRICO	14
2.1	Uva: características gerais	14
2.2	Subprodutos do processamento de uvas	15
2.3	Compostos bioativos e capacidade antioxidante	16
2.3.1	Compostos fenólicos	17
2.3.2	Antocianinas	17
2.3.3	Estabilidade dos compostos bioativos	20
2.4	Microencapsulação	21
2.4.1	Resfriamento por atomização (<i>spray chilling</i>)	22
2.4.1.1	Emulsões	22
2.4.1.2	Homogeneização por ultrassom	23
2.4.2.3	Lipídeos	24
2.4.2.3.1	Cristalização e polimorfismo de lipídeos	25
2.4.2.3.2	Óleo de palma e gordura hidrogenada de palma	29
3	CONSIDERAÇÕES GERAIS	31
	REFERÊNCIAS	32
	SEGUNDA PARTE	42
	ARTIGO 1 – MICROENCAPSULATION BY SPRAY CHILLING IN THE FOOD INDUSTRY: OPPORTUNITIES, CHALLENGES, AND INNOVATIONS	42
	ARTIGO 2 – A COMBINATION OF PGPR AND ULTRASOUND-ASSISTED PRODUCTION OF ANTHOCYANIN-RICH EXTRACT OF GRAPE PEEL EMULSIONS AND ENCAPSULATES	94
	ARTICLE 3 – MICROSTRUCTURED LIPID MICROPARTICLES CONTAINING ANTHOCYANINS: PRODUCTION, CHARACTERIZATION, STORAGE, AND RESISTANCE TO THE GASTROINTESTINAL TRACT	148

PRIMEIRA PARTE

1 INTRODUÇÃO

O desafio das indústrias de alimentos perante ao novo mundo, esperado pelos consumidores, não é somente diante da produção de alimentos saudáveis, com propriedades funcionais, mas, sobretudo, em virtude do bem-estar emocional e mental, transparência, conveniência e os impactos ambientais (EFTIMOV *et al.*, 2020).

A produção de vinhos e sucos geram toneladas de subprodutos, incluindo as cascas que normalmente são descartadas mas que poderiam ser aproveitadas, pois apresentam elevado conteúdo de compostos fenólicos, responsáveis por atividades biológicas, como atividade antioxidante, anti-inflamatória, antimicrobiana, prevenção de doenças coronarianas, inibição de tumores, entre outras (AMENDOLA; DE FAVERI; SPIGNO, 2010; KUCK; NOREÑA, 2016). Além disso, as antocianinas presentes nesses subprodutos desempenham propriedades sensoriais importantes como cor, sabor e adstringência, que podem ser aproveitadas na produção de alimentos (HOGERVORST; MILJIĆ; PUŠKAŠ, 2017).

A inserção de ingredientes funcionais como os compostos fenólicos aos alimentos representa desafios aos profissionais da área, devido à instabilidade ao processamento e armazenamento. Com isso, a microencapsulação juntamente com as tecnologias alimentares pode ser utilizada como alternativa para contornar esse problema e permitir o desenvolvimento de alimentos e nutracêuticos, de forma que a biodisponibilidade e manutenção da funcionalidade dos ingredientes ativos sejam essenciais (ALEMZADEH *et al.*, 2020). A técnica consiste na incorporação de uma substância (ativo) dentro de outra (material encapsulante) que atua como barreira protetora, obtendo partículas nas quais a molécula de interesse é isolada do ambiente externo (GIBBS *et al.*, 1999). Mas a microencapsulação não se limita a isso, pois apresenta outras vantagens como: ingredientes e princípios ativos protegidos contra oxidação, desnaturação térmica, condições extremas de pH, liberação controlada e gradual, mascara odor e sabor indesejáveis e melhora a dispersão dos ingredientes ativos (BOOSTANI; JAFARI, 2021).

Spray chilling é uma técnica de microencapsulação pouco explorada no setor alimentício brasileiro, mas que pode ser promissora, visto que são sistemas práticos para encapsular compostos, apresentam alta eficiência de encapsulação, possibilidade de trabalhar em temperaturas moderadas e ausência de solvente no processo (ALVIM *et al.*, 2016; CONSOLI *et al.*, 2016). O processo consiste na dispersão do material ativo emulsificado ou

solubilizado em uma matriz lipídica fundida. Essa mistura é bombeada para um bico atomizador aquecido, o qual irá aspergir a mistura em uma câmara contendo ar a uma temperatura abaixo do ponto de fusão da matriz lipídica, onde as gotículas se solidificam, formando assim micropartículas lipídicas sólidas (BERTONI; ALBERTINI; PASSERINI, 2019).

A escolha dos materiais lipídicos encapsulantes é uma das etapas mais importantes do processo de microencapsulação por *spray chilling*. É ideal que esses materiais apresentem boa propriedade de cristalização para obter partículas íntegras, capacidade de reter o ativo dentro da estrutura durante o armazenamento e processamento, bem como máxima proteção contra condições ambientais externas e ao trato gastrointestinal, e serem economicamente viáveis (CONSOLI *et al.*, 2016; ORIANI *et al.*, 2018). A mistura de lipídios sólidos e líquidos pode desenvolver micropartículas com núcleo estrutural desorganizado que melhoram a eficiência da microencapsulação ao longo do tempo por permitir que o composto ativo fique aprisionado nessa estrutura desordenada (FIGUEIREDO *et al.*, 2022). O óleo de palma (OP) é um produto versátil muito utilizado em alimentos e facilmente encontrado no mercado, apresenta característica semissólida à temperatura ambiente, é livre de ácidos graxos *trans* e possui ponto de fusão variando de 32-40 °C (LIN, 2002). O óleo de palma totalmente hidrogenado livre em *trans* (OPTH) exibe ponto de fusão variando de 58-65 °C (LIN, 2002). Nesse contexto, a utilização de OPTH em conjunto com OP pode possibilitar a formação de micropartículas lipídicas microestruturadas (MLMs) íntegras, com boas propriedades de retenção do ativo, menor aderência e maior rendimento do processo (PROCOPIO *et al.*, 2018).

Outro ponto chave para o sucesso da microencapsulação por *spray chilling* é a escolha correta do processo de homogeneização da solução a ser atomizada, visando estabilizar o composto ativo durante o processo, aumentando a eficiência e retenção de encapsulação. Técnicas de homogeneização de alta energia como o ultrassom assistido têm demonstrado eficientes resultados na elaboração de emulsões para aplicação em sistemas de encapsulamento, graças ao microcisalhamento gerado pelo colapso de microbolhas formadas durante o fenômeno de cavitação (CAMPELO *et al.*, 2017; ROMANINI *et al.*, 2021).

Embora seja notória a alta potência da técnica para contornar limitações e desenvolver novas aplicações no setor alimentício, estudos envolvendo a microencapsulação de extrato de casca de uva por *spray chilling* ainda são escassos, o que torna o projeto inovador, uma vez que as micropartículas produzidas podem ser aplicadas em alimentos para desempenhar propriedades funcionais, corantes e aromatizantes. Baseado nesse contexto, o presente trabalho teve como objetivos:

- Fazer um estudo de revisão sobre a tecnologia *spray chilling* aplicada na indústria de alimentos, apresentando os conceitos, principais desafios e inovações;
- Otimizar os parâmetros operacionais do processo, potência ultrassônica (W) e tempo de sonicação (min), para a elaboração de emulsões água em óleo pela aplicação da técnica de ultrassom para microencapsular o extrato de casca de uva por meio da técnica de *spray chilling*, utilizando óleo de palma e óleo de palma totalmente hidrogenado na proporção 80:20 como materiais encapsulantes;
- Estudar o efeito de proporções de óleo de palma totalmente hidrogenado e óleo de palma como materiais encapsulantes sobre as características físico-químicas, estabilidade ao armazenamento e ao trato gastrointestinal das micropartículas obtidas por *spray chilling* contendo extrato de casca de uva.

2 REFERENCIAL TEÓRICO

2.1 Uva: características gerais

A uva (*Vitis spp.*) é uma das frutas mais valorizadas, consumidas e industrializadas no mundo. As quatro principais espécies no mundo com relação às variedades são: as europeias (*Vitis vinifera*), as uvas americanas (*Vitis labrusca* e *Vitis rotundifolia*) e as uvas híbridas francesas, cultivadas tanto para o consumo “in natura”, quanto para a elaboração de vinhos e sucos.

A vitivinicultura brasileira se consolidou em meados do século XIX com a introdução do cultivar de uvas americanas *Vitis labrusca* e *Vitis bourquina* por parte dos imigrantes italianos, usadas para a elaboração de vinhos de mesa. Não obstante, a partir do século XX, o Brasil passou a produzir vinhos finos (Cabernet Sauvignon, Cabernet Franc, Merlot, Pinot Noir, Syrah, entre outros), com uvas de variedades *Vitis vinifera*, também conhecidas como uvas finas (CAMARGO; MAIA; RITSCHHEL, 2010).

Segundo a International Organisation of Vine and Wine (OIV, 2022), a produção de uvas em 2019 foi de aproximadamente 77,13 milhões de toneladas produzidas em todo o mundo a cada ano, sendo 75% usadas na produção de vinho. No Brasil a safra de uvas em 2019 foi de 1.445.705 toneladas, sendo a região Sul a maior produtora de uvas, representando 52,91% da produção nacional, a região Nordeste a segunda maior em cultivo de uva, contribuindo com 34,97%, seguida pela região Sudeste, cuja produção de uvas representou 11,72%. A produção nacional de uvas destinadas ao processamento (vinho, suco e derivados) foi estimada em 698.045 toneladas em 2019, representando 48,28% da produção total. O restante da produção (51,72%) destinou-se ao consumo *in natura* (MELLO; MACHADO, 2020).

A uva bordô é uma cultivar da espécie de uva *Vitis labrusca* L., também conhecida como Ives Seedling, Terci, Folha-de-figo ou York Madeira, a depender da região de cultivo. Foi selecionada a partir de sementes de Hartford Prolifi por Henry Ives em 1840, na cidade de Cincinnati, interior dos EUA, e trazida para o Brasil no início do século XX (CAMARGO; MAIA; RITSCHHEL, 2010).

No Brasil, a cultivar bordô se difundiu devido à fácil adaptação à variabilidade climática, boa produtividade, longevidade e apreciável resistência a doenças fúngicas. Sendo assim, tornou-se uma das variedades mais importantes e cultivadas (CASTILHOS *et al.*, 2016). Seu cultivo se destina à produção de sucos, vinhos e também como matéria corante, devido a

sua intensa cor vermelho-púrpura, resultado de seu alto teor de polifenóis, principalmente antocianinas (KUCK; WESOŁOWSKI; NOREÑA, 2017).

Em geral, as uvas são ricas em compostos fenólicos, principalmente as antocianinas, contidos nas cascas de uvas tintas. Os compostos fenólicos têm atividade antioxidante, cuja função é neutralizar e impedir a formação de radicais livres (RICE-EVANS; MILLER; PAGANGA, 1997), podendo resultar em diversos benefícios para a saúde, entre eles propriedades antimicrobianas, anti-inflamatórias, capacidade anticâncer, antidiabética e cardioprotetora (AMORIM *et al.*, 2019; GONÇALVES; LAJOLO; GENOVESE, 2010; KUCK; NOREÑA, 2016; RODRÍGUEZ-ROQUE *et al.*, 2014). Diversos estudos relataram o elevado conteúdo desses compostos provenientes da uva bordô, o que justifica a elevada capacidade antioxidante apresentada por esse fruto (CARMONA-GÓMEZ *et al.*, 2018; CASTILHOS *et al.*, 2016; HAAS *et al.*, 2019; KUCK; WESOŁOWSKI; NOREÑA, 2017; LACERDA *et al.*, 2018).

2.2 Subprodutos do processamento de uvas

O processamento da uva gera uma grande quantidade de subprodutos e/ou bagaço (constituído de casca, semente e engaço), correspondendo cerca de 20 a 30% do peso da uva processada. Esses subprodutos provenientes de uvas podem ser considerados fontes interessantes de antocianinas e podem ser utilizados na produção de pigmentos naturais (ROCKENBACH *et al.*, 2011).

Mundialmente, a produção da indústria vinícola resulta em toneladas de material vegetal processado, que impactam o meio ambiente. E dados estimados indicam que atualmente somente 3% do resíduo da indústria vinícola passa por um processo de aproveitamento, visto que esses subprodutos ainda são considerados de baixo valor econômico, utilizados normalmente como adubo na plantação, ração animal ou, até mesmo, incinerados (DÁVILA *et al.*, 2017).

De acordo com estimativas, 1 kg de bagaço de uva é gerado para cada 6 litros de vinho. Sendo assim, uma tonelada de bagaço de uva é composta por cerca de 430 kg de casca de uva, 250 kg de caule de uva e 230 kg de sementes de uva, a depender do tipo de prensa usada para prensar uvas inteiras, *terroir* e variedade de uva (MENDES *et al.*, 2013). Esse rendimento representa 10,5 a 13,1 milhões de toneladas de bagaço de uva no mundo anualmente (DÁVILA *et al.*, 2017). No Brasil, a quantidade de bagaço de uva gerado da produção de vinhos é próxima

de 59,4 milhões de quilos, considerando 18 kg de bagaço por 100 litros de vinho (ROCKENBACH *et al.*, 2011).

As cascas de uvas provenientes da indústria vinícola representam, em geral, até 65% do bagaço de uvas. Esse subproduto da vinícola era, no passado, usado principalmente como composto ou tratado como lixo inutilizável. No entanto, altas quantidades de compostos fenólicos presentes nas peles de uvas as tornam uma fonte valiosa de fitoquímicos biologicamente ativos (ROCKENBACH *et al.*, 2011).

Diversos estudos comprovaram o potencial antioxidante de bagaço de uva introduzido em diversos produtos alimentícios, como barras de cereais, *muffins*, biscoitos, pão, laticínios, iogurte e frutos do mar (GARCÍA-LOMILLO; GONZÁLEZ-SANJOSÉ, 2017). Além disso, em bebidas e frutas desidratadas, extratos de casca de uva foram adicionados apresentando alta atividade antioxidante (PEDROZA *et al.*, 2012). Também pôde ser comprovada a atividade antimicrobiana de extrato de bagaço de uva contra diferentes patógenos transmitidos por alimentos (XU *et al.*, 2016).

Avaliando as questões ambientais e o elevado potencial dos subprodutos provenientes da viticultura, torna-se viável a realização de estudos que identifiquem formas de aproveitamento desses subprodutos, visto que pouco se sabe sobre suas aplicações para a produção de ingredientes e/ou produtos que possam ser utilizados por indústrias alimentícias, farmacêuticas e cosméticas.

2.3 Compostos bioativos e capacidade antioxidante

Os compostos bioativos são substâncias normalmente presentes nos alimentos. São considerados extranutricionais, ou seja, eles não têm funções estabelecidas como as dos nutrientes, que podem ser facilmente identificados, já que sua falta no organismo causa uma deficiência ou doença. As evidências são de que exercem diferentes ações biológicas, que podem associar-se à promoção da saúde, aumento do bem-estar e menor incidência das doenças crônicas não transmissíveis. Os principais grupos de compostos bioativos são os compostos fenólicos, carotenoides e glicosinolatos. As propriedades funcionais estão associadas, principalmente, a ações anti-inflamatória e antioxidante, colaborando para o bom funcionamento do organismo (SHASHIREKHA; MALLIKARJUNA; RAJARATHNAM, 2015).

2.3.1 Compostos fenólicos

Entre os principais fitoquímicos bioativos encontrados em frutos de uva, vinhos, sucos e subprodutos, podemos destacar os polifenóis (AMENDOLA; DE FAVERI; SPIGNO, 2010). São compostos químicos resultantes do metabolismo secundário das plantas. Compreende vários compostos responsáveis por propriedades sensoriais diferentes, como cor, sabor e adstringência, enquanto numerosos estudos também relataram seus benefícios à saúde (AMORIM *et al.*, 2019; GONÇALVES; LAJOLO; GENOVESE, 2010; KUCK; NOREÑA, 2016; LACERDA *et al.*, 2018).

Com estrutura variável, são caracterizados por meio da presença de estruturas com anéis aromáticos contendo duplas ligações conjugadas, a partir das quais exercem ações antioxidantes (DAMODARAN; PARKIN, 2019).

Os compostos fenólicos presentes nas uvas fazem parte de dois grandes grupos: os não flavonoides (ácidos fenólicos, estilbenos, ácidos benzoicos e ácidos cinâmicos) e os flavonoides (flavonóis, flavonas, antocianinas, flavanóis, catequinas, taninos, procianidinas). As diferenças de estrutura entre ambos os grupos consistem principalmente que os não flavonoides têm um único anel, enquanto que os flavonoides são formados por dois anéis aromáticos unidos por uma cadeia de três átomos de carbono (MATTIVI *et al.*, 2006).

Os subprodutos obtidos no processo de vinificação contêm elevadas quantidades de flavonóis, proantocianidinas, antocianinas, flavanóis, ácidos fenólicos e estilbenos (HOGERVORST; MILJIĆ; PUŠKAŠ, 2017). A capacidade dos flavonóis de reagir com as antocianinas e ácidos fenólicos é responsável pelo fenômeno da copigmentação (MATTIVI *et al.*, 2006).

A concentração de polifenóis em uvas pode variar devido a fatores ambientais e agrônômicos. A concentração de fenólicos totais em cascas de uva bordô em mg de ácido gálico/g de amostra seca foi de 191,8 (SOUZA *et al.*, 2014), 26,26 (KUCK; NOREÑA, 2016) e 10,89 (CARMONA-GÓMEZ *et al.*, 2018), enquanto no bagaço de uvas bordô foi de 211 (MORENO; COCERO; RODRÍGUEZ-ROJO, 2018).

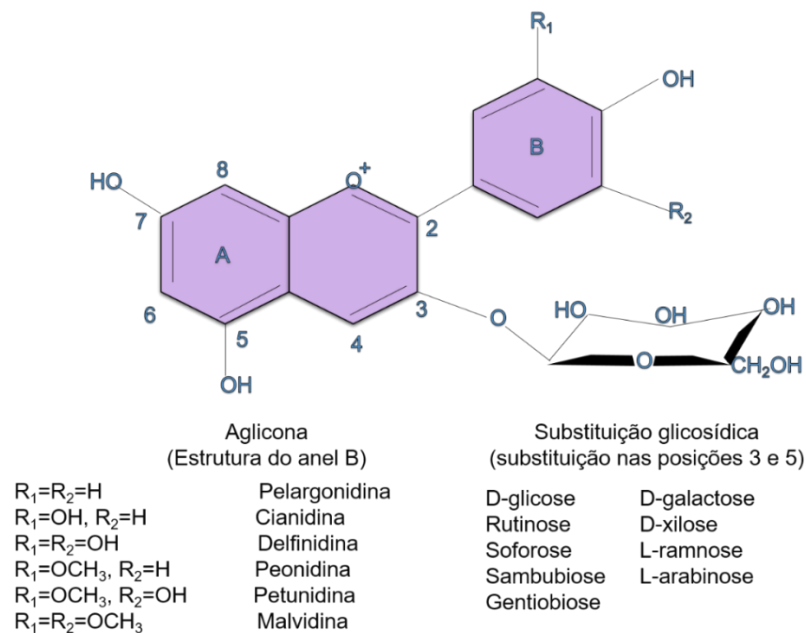
2.3.2 Antocianinas

As antocianinas (do grego *anthos* = flor e *kianos* = azul) são os pigmentos mais importantes do reino vegetal. São atóxicos e de fácil incorporação em meio aquoso, o que os tornam interessantes para uso como corantes naturais solúveis em água. Esses pigmentos são

responsáveis pelas cores laranja brilhante, rosa, vermelho, violeta e azul de muitas frutas e folhas (SINELA *et al.*, 2017). Outra propriedade significativa das antocianinas é a sua atividade antioxidante, que desempenha um papel vital na prevenção de doenças neuronais, cardiovasculares, câncer e diabetes (AH-HEN *et al.*, 2018; MAZZA; MINIATI, 1993; XIA *et al.*, 2010).

As antocianinas pertencem ao grupo dos flavonoides, compostos fenólicos caracterizados pelo núcleo básico flavílio (cátion 2-fenilbenzopirílio) que consiste de dois anéis aromáticos unidos por uma unidade de três carbonos e condensada por um oxigênio. A molécula de antocianina (FIGURA 1) é constituída por duas ou três porções, uma aglicona (antocianidina), um grupo de açúcares e, frequentemente, um grupo de ácidos orgânicos. Elas diferem no número de grupos hidroxila e/ou nos grupos metóxi presentes; tipos, números e sítios de ligação dos açúcares na molécula; e tipos e números de ácidos alifáticos ou aromáticos que estão ligados aos açúcares da molécula (CASTAÑEDA-OVANDO *et al.*, 2009).

Figura 1 - Estruturas químicas das antocianinas.

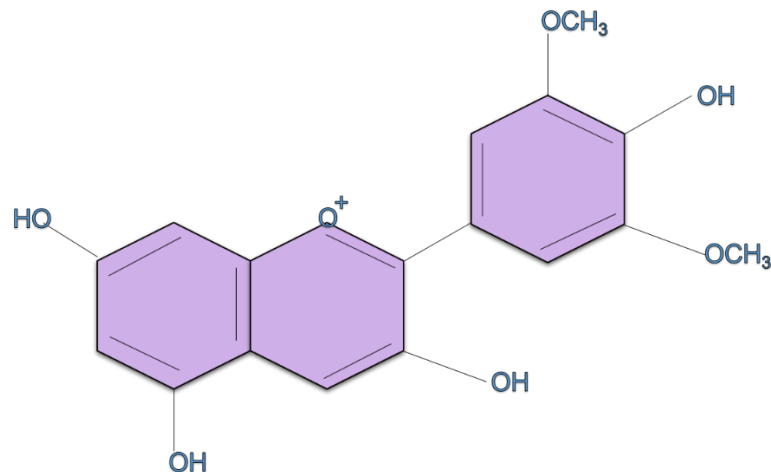


Fonte: Da autora (2022).

Uma antocianina livre de substituições de açúcar é conhecida como antocianidina (a porção aglicona). Existem cerca de 27 antocianidinas de origem natural que compartilham o mesmo esqueleto C₆C₃C₆, das quais 6 derivadas de agliconas costumam ocorrer nos alimentos (pelargonidina, cianidina, delfinidina, peonidina, petunidina e malvidina) (DAMODARAN; PARKIN, 2019).

Nas antocianinas e nas antocianidinas, o número abundante de ligações duplas que são excitadas com facilidade é essencial para a cor, sendo que o tipo e o número da substituição de açúcares e da acilação, também desempenham um papel importante nas características de cor. Em geral, o aumento da hidroxilação das antocianinas diminui a estabilidade, ao passo que o aumento da metoxilação aumenta a estabilidade. A glicosilação também pode aumentar a estabilidade. Geralmente, antocianidinas com grupos hidroxilas na posição 3' e 4' são oxidadas mais rapidamente do que as antocianidinas que não possuem essa estrutura. Por exemplo, malvidina e peonidina são antocianidinas mais estáveis que cianidina, delphinidina e petunidina, devido ao bloqueio dos grupos hidroxilas. Além disso, o número e a posição dos açúcares conectados às antocianidinas também afetam a estabilidade das antocianinas (DAMODARAN; PARKIN, 2019; LOPES *et al.*, 2007). Dentre as antocianidinas encontradas principalmente nas peles das uvas, destacam-se as flavan-3-ols, que estão presentes em concentrações semelhantes nas peles e nas sementes, e a malvidina-3-O-glicosídeo (FIGURA 2) que é a antocianina mais valiosa encontrada nas peles das uvas, seguida pela peonidina-3-O-glicosídeo (HOGERVORST; MILJIĆ; PUŠKAŠ, 2017; XIA *et al.*, 2010).

Figura 2 - Estrutura química da malvidina.



Fonte: Da autora (2022).

Sabe-se que as uvas bordô têm um alto teor de antocianinas, superior às variedades como Cabernet sauvignon, Merlot e Isabel (ROCKENBACH *et al.*, 2011). O vinho da uva bordô é usado para aumentar a intensidade da cor de outros vinhos. Essa característica chama a atenção para os subprodutos dessa variedade de uva como fontes potenciais de pigmentos naturais. De acordo com alguns autores, os teores de antocianinas totais em extratos de cascas de uva bordô

variam entre 20 e 53 mg de malvidina-3,5-diglicosídeo/g de extrato em base seca (KUCK; NOREÑA, 2016; KUCK; WESOLOWSKI; NOREÑA, 2017; SOUZA *et al.*, 2014).

2.3.3 Estabilidade dos compostos bioativos

A estabilidade dos polifenóis é influenciada por diversos fatores. A presença de luz, oxigênio, o processamento e armazenamento, temperatura e umidade podem ser citados como os principais contribuintes para o processo de degradação desses compostos (NAYAK; LIU; TANG, 2015).

As antocianinas são pigmentos relativamente instáveis, com maior estabilidade ocorrendo sob condições ácidas. A degradação das antocianinas pode ocorrer não apenas durante a extração a partir dos tecidos vegetais, mas também durante o processamento e armazenamento. Os principais fatores que governam a degradação das antocianinas são os fatores intrínsecos, como a estrutura química e a copigmentação intramolecular, mas também os fatores extrínsecos, como pH, temperatura, umidade, luz, presença de oxigênio, degradação enzimática, interações entre os componentes dos alimentos, tais como ácido ascórbico, íons metálicos e açúcares (DAMODARAN; PARKIN, 2019).

As reações de degradação normalmente resultam na perda da coloração ou em alterações nas cores de frutas e vegetais, o que quase sempre são indesejáveis no processamento de alimentos (TONON; BRABET; HUBINGER, 2010). Assim, a estabilização dessas moléculas tem sido o foco principal em estudos recentes devido ao seu grande potencial como corantes naturais, por exemplo, em alimentos e cosméticos, e por seus efeitos benéficos para a saúde (FIGUEIREDO *et al.*, 2020b; FREDES *et al.*, 2018; MURALI *et al.*, 2015; REMINI *et al.*, 2015).

A estabilidade das antocianinas pode ser avaliada estudando sua degradação durante o armazenamento. Vários estudos mostraram que a degradação dos compostos fenólicos, entre eles a antocianinas, geralmente segue a cinética de primeira ordem, ou seja, o conteúdo de antocianinas diminui com o tempo (FIGUEIREDO *et al.*, 2020a; KIM *et al.*, 2018; SÓLYOM *et al.*, 2014).

O grande desafio para as indústrias em utilizar pigmentos de origem natural é justamente a instabilidade apresentada por esses compostos. Dessa forma, pesquisadores buscam desenvolver alternativas para proteger esses compostos, como forma de melhorar sua estabilidade durante o armazenamento e processamento, como é o caso da aplicação de tecnologias de encapsulação.

2.4 Microencapsulação

A microencapsulação é uma tecnologia em rápida expansão que oferece inúmeras aplicações benéficas nas indústrias alimentícias, farmacêuticas e cosméticas. Na maioria dos casos o encapsulamento nada mais é do que um processo no qual uma barreira física é aplicada para proteger os componentes bioativos contra qualquer condição ambiental adversa (SAIFULLAH *et al.*, 2019).

O material encapsulado é designado como material de recheio, núcleo, fase interna ou ativo, e o material que o protege ou envolve pode ser chamado de material de parede, revestimento, casca ou carreador (GIBBS *et al.*, 1999). A microencapsulação permite tamanho de partículas de 3 a 800 μm e, de acordo com a morfologia, as micropartículas podem ser classificadas em microcápsulas (com núcleo interno bem definido) ou microesferas, onde o ingrediente ativo é disperso na matriz (ARENAS-JAL; SUÑÉ-NEGRE; GARCÍA-MONTOYA, 2020).

A microencapsulação oferece diferentes vantagens, como: maior estabilidade ao ativo fornecendo proteção aos fatores extrínsecos, proteção contra o sistema gastrointestinal, liberação no momento e local desejado, mascarar sabor e odor indesejáveis, facilidade de manipulação e aplicação, entre outras finalidades (MADENE *et al.*, 2006).

A seleção do material encapsulante no processo de microencapsulação está diretamente relacionada à eficiência do processo. Diferentes tipos de materiais encapsulantes são utilizados como carboidratos (amidos, dextrinas, gomas, quitosana, inulina), proteínas (isolado proteico de soro de leite, gelatina, albumina, caseína) e lipídeos (cera, ácido esteárico, monoglicerídeo, óleos, gorduras hidrogenadas, parafina). A escolha vai depender da técnica de microencapsulação a ser utilizada e o composto a ser encapsulado (BOTREL *et al.*, 2012).

Diversas técnicas são empregadas para a formação das microcápsulas e microesferas, incluindo secagem por atomização (*spray drying*), resfriamento por atomização (*spray chilling*), coacervação, gelificação iônica, emulsificação, revestimento por extrusão, entre outras. Os parâmetros importantes da caracterização da microencapsulação incluem distribuição e tamanho de partículas, morfologia, retenção e/ou eficiência de encapsulação, estudos de perfil de liberação, estabilidade térmica e ao armazenamento (ALEMZADEH *et al.*, 2020).

Estudos revelaram maior proteção de compostos ativos como as antocianinas utilizando a microencapsulação por *spray drying*, liofilização, gelificação iônica e emulsificação (CARMO *et al.*, 2018; FIGUEIREDO *et al.*, 2020a; SILVA *et al.*, 2018; TOLUN; ALTINTAS;

ARTIK, 2016). No entanto, ainda não existem estudos avaliando o potencial uso de *spray chilling* na microencapsulação de extratos antociânicos.

2.4.1 Resfriamento por atomização (*spray chilling*)

Resfriamento por atomização, *spray chilling*, *spray cooling* ou *spray congealing*, é a tecnologia na qual aplica-se um princípio oposto à secagem por *spray*. Nessa técnica também se faz uma dispersão de uma matriz e do ingrediente ativo, mas ao invés de evaporar o solvente, resfria-se a dispersão para permitir a encapsulação. Normalmente, gorduras com alto ponto de fusão são aplicadas nessa tecnologia e, com isso, ar refrigerado é utilizado para a solidificação das partículas (BERTONI; ALBERTINI; PASSERINI, 2019).

Spray chilling já é consolidada pelas indústrias farmacêuticas e de cosméticos, devido a diversos fatores, tais como: capacidade de proteção a compostos hidrofílicos e hidrofóbicos; liberação gradual do ativo por um maior período de tempo, aplicação em sistemas líquidos e sólidos e ausência de toxicidade (SAVOLAINEN *et al.*, 2003). Sua aplicação no setor alimentício é promissora, visto que são sistemas práticos para encapsular compostos como *flavors*, pigmentos, enzimas, probióticos e outros ingredientes funcionais, com o intuito de melhorar a estabilidade ao calor, promover liberação controlada do ativo, converter ingredientes líquidos em materiais em pó com boa capacidade de escoar e melhorar a biodisponibilidade (ALVIM *et al.*, 2013; ORIANI *et al.*, 2018). Mais detalhes acerca dessa tecnologia serão abordados na parte 2 do artigo 1 deste trabalho.

2.4.1.1 Emulsões

A primeira etapa para a microencapsulação por *spray chilling* é baseada na elaboração de uma solução, dispersão ou emulsão, o tipo irá depender da solubilidade entre o composto ativo e os materiais encapsulantes. No caso deste estudo, será necessária a elaboração de uma emulsão do tipo água em óleo (A/O), devido à incorporação de um extrato de casca de uva hidrofílico em uma matriz lipídica. Definimos como emulsão A/O quando gotículas de água são dispersas em meio oleoso. A propriedade física mais importante de emulsões, do ponto de vista tecnológico geral e para processos de microencapsulação, é a sua estabilidade. Pode-se definir estabilidade de uma emulsão como a sua capacidade em resistir a processos de desestabilização que podem carregar na cremeação, sedimentação, floculação ou até mesmo na separação de fases (McCLEMENTS, 2007).

A estabilidade de emulsões é facilitada por agentes surfactantes que atuam na solução, reduzindo a tensão superficial, diminuindo a energia na superfície entre as duas fases, permitindo a formação de novas superfícies quando energia é cedida ao sistema. Uma vez formada a emulsão, o surfactante contribui para a estabilização das gotículas dispersas, impedindo-as da ocorrência de separação de fases.

Cada emulsificante ou surfactante é representado por um número que caracteriza seu balanço hidrofílico-lipofílico (HLB, do inglês *hydrophile-lipophile balance*). Esse número está relacionado à estrutura química de cada surfactante, em termos de grupos hidrofílicos e lipofílicos presentes na molécula, e fornece uma indicação sobre a afinidade de sua molécula às fases aquosa ou oleosa. Um emulsificante com número HLB baixo (entre 3 e 6) tem mais afinidade pela fase oleosa, e por isso é mais adequado para estabilizar emulsões A/O. O oposto ocorre para emulsificantes com números HLB altos (entre 10-18). Valores de HLB intermediários (entre 7 e 9) indicam que o emulsificante não possui afinidade específica pelas fases aquosa ou oleosa, sendo considerados bons agentes umectantes (DAMODARAN; PARKIN, 2019).

O poliglicerol polirricinoleato (PGPR) é um emulsificante de grau alimentício obtido por meio da esterificação de ácidos graxos condensados de óleo de rícino com poliglicerol (WILSON; VAN SCHIE; HOWES, 1998). É considerado um dos emulsificantes oligoméricos mais eficientes para emulsões do tipo A/O (RAVIADARAN *et al.*, 2019; SU; FLANAGAN; SINGH, 2008; USHIKUBO; CUNHA, 2014; ZAFIMAHOVA-RATISBONNE *et al.*, 2014).

Sua principal aplicação na indústria de alimentos é como aditivo em chocolates, visando reduzir a viscosidade desse tipo de produto, auxiliando no controle sobre as propriedades de escoamento. No entanto, no Brasil, a quantidade máxima permitida de PGPR de acordo com o Sistema Internacional de Numeração de Aditivos Alimentares é de 0,4 g/100 g em produtos como cremes vegetais e margarinas, e de 0,5 g/100 g em balas, confeitos, chocolates e similares (BRASIL, 2005).

2.4.1.2 Homogeneização por ultrassom

O preparo da emulsão de alimentação representa um processo significativo da microencapsulação por *spray chilling*, uma vez que a emulsão está relacionada com a retenção e/ou encapsulação do composto ativo. Para a formação de emulsões estáveis é necessária a aplicação de energia, com o intuito de reduzir o tamanho das gotículas, melhorando suas propriedades físico-químicas. O emprego do ultrassom-assistido tem demonstrado bons

resultados na formação de emulsões alimentícias com alta estabilidade (McCLEMENTS, 2020; TADROS *et al.*, 2004).

O mecanismo de formação dessas emulsões a partir do ultrassom se deve à vibração da superfície da emulsão causada pela alta energia desse equipamento. A introdução de ondas sonoras em uma dispersão de água-óleo e/ou óleo-água resulta em uma sucessão de depressões e compressões mecânicas, gerando bolhas de cavitação, tendendo a implodir e formar emulsões com gotículas de tamanho reduzido. O tempo e a potência das ondas do ultrassom são fatores que afetam o tamanho das gotículas formadas durante o processo de homogeneização (TRUJILLO *et al.*, 2014).

O processo de homogeneização por ultrassom apresenta várias vantagens, como eficiência energética, baixo custo de produção, facilidade de manipulação e controle das variáveis de processo. Também é considerado um processo não tóxico para os alimentos e ambientalmente seguro (ZHANG *et al.*, 2020).

As propriedades físicas de emulsões interferem diretamente nas propriedades de retenção de ingredientes ativos. Alguns estudos demonstraram o potencial uso do ultrassom na homogeneização de emulsões alimentícias e sua correlação com as propriedades físico-químicas de alimentos em pó (CONSOLI *et al.*, 2016; FERNANDES *et al.*, 2016; SILVA *et al.*, 2015).

2.4.2.3 Lipídeos

Diferentemente de outras técnicas de microencapsulação, no *spray chilling* os únicos materiais encapsulantes possíveis a serem utilizados devem ser de origem lipídica. Por isso, entender suas características é essencial para o sucesso do processo.

Lipídeos são compostos quimicamente diversos, considerados insolúveis em água, mas solúveis numa variedade de solventes orgânicos. Geralmente são divididos entre óleos (líquidos) e gorduras (sólidos), indicando o estado físico que apresentam à temperatura ambiente. Os lipídios também se apresentam como diversos tipos de moléculas, como por exemplo, ácidos graxos livres, fosfolipídios, triacilgliceróis, esteróis, ceras, terpenos e outros (DAMODARAN; PARKIN, 2019).

Óleos e gorduras são moléculas lipídicas constituídas predominantemente por triacilgliceróis (TAGs), que são originários da reação de esterificação de uma molécula de glicerol e três moléculas de ácidos graxos, e são abundantemente encontrados em produtos alimentícios (DAMODARAN; PARKIN, 2019).

O ponto de fusão de um triacilglicerol puro depende do tamanho da cadeia, do número de insaturações, ramificações e da posição de seus ácidos graxos constituintes em torno da molécula de glicerol. As gorduras comestíveis apresentam uma mistura complexa de diversos tipos de moléculas de triacilgliceróis, cada qual com um ponto de fusão diferente e que, portanto, podem fundir-se normalmente dentro de um amplo intervalo de temperaturas, e não apenas em uma temperatura distinta, como seria o caso de um triacilglicerol puro (DAMODARAN; PARKIN, 2019). O ponto de fusão de ácidos graxos saturados aumenta com a ampliação do comprimento da cadeia de carbonos, pois a estrutura tridimensional promove um melhor empacotamento dos TAGs, o que aumenta as interações moleculares e a força de Van der Waals entre as moléculas. Uma molécula de ácido graxo com uma dupla ligação e com a configuração do tipo *cis* fará com que o ácido graxo se organize em uma configuração curvada, ou seja, os ácidos graxos insaturados não são lineares, dificultando sua auto-orientação em configurações muito empacotadas. Devido ao impedimento espacial para o empacotamento, as interações de Van der Waals entre ácidos graxos insaturados são relativamente fracas, portanto, menos energia é necessária para promover transições de fase sólido-líquido, fazendo seu ponto de fusão diminuir. Quanto mais ligações duplas forem adicionadas, mais curvada se tornará a molécula, mais fracas as interações de Van der Waals e menor o ponto de fusão. Os ácidos graxos com ligações duplas na configuração *trans* são mais lineares que os ácidos graxos na configuração *cis*, o que implica em um empacotamento mais forte das moléculas e em pontos de fusão mais elevados (DAMODARAN; PARKIN, 2019).

2.4.2.3.1 Cristalização e polimorfismo de lipídeos

Para a obtenção das micropartículas lipídicas sólidas por *spray chilling* é necessário que se inicie com a fusão do lipídeo, formação das partículas por atomização, seguidas de resfriamento para fixação da forma das micropartículas. As transições de fases líquido-sólido são uma parte integral de muitas operações de processamento usadas para produção de alimentos, e a qualidade desses produtos dependem de fatores que influenciam na cristalização e fusão dos lipídeos em alimentos.

Sabe-se que a transição de líquido para sólido (cristalização) é exotérmica, pois com o agrupamento das moléculas ocorre a liberação de energia e as interações moleculares são mais intensas. As características de óleos e gorduras são influenciadas pelo complexo comportamento de cristalização dos lipídeos. Quando esses lipídeos são submetidos a temperaturas abaixo de seu ponto de fusão, cristalizam-se. A formação dos cristais é

influenciada por diversos fatores, mas, principalmente, pela taxa de resfriamento a qual os lipídios são submetidos a partir de seu estado líquido (DAMODARAN; PARKIN, 2019).

Para obter cristais a partir do estado líquido é necessário que uma força motriz seja fornecida ao sistema termodinâmico até atingir um estágio de supersaturação. Nesse ponto as moléculas se unem para formar um núcleo mais estável, que começa com o super resfriamento da solução lipídica. O núcleo se inicia quando agrupamentos de moléculas colidem (*clusters*), tornando-se associadas umas às outras através das interações moleculares. O núcleo do cristal se torna estável a partir de certo tamanho, em escala nanométrica, e a etapa subsequente é o crescimento do cristal pela incorporação de moléculas na interface caracterizando assim o processo de cristalização (DAMODARAN; PARKIN, 2019).

No processo de resfriamento lento cristalizam-se primeiro os TAGs com elevado ponto de fusão, que podem se dissolver em outras moléculas de ponto de fusão inferiores. Se um óleo é resfriado de forma rápida, os diferentes TAGs do sistema lipídico se cristalizam simultaneamente, ocorrendo a formação de uma solução sólida com cristais homogêneos (O'BRIEN, 2004).

O arranjo cristalino dos óleos e gorduras tem considerável influência nas suas propriedades físicas (consistência, ponto de fusão, etc.) e é dependente do tipo de TAG presente, da distribuição dos ácidos graxos na molécula lipídica, da pureza e das condições de cristalização (DAMODARAN; PARKIN, 2019).

A organização das moléculas lipídicas no estado sólido pode ocorrer de diversas formas, incluindo a organização geral das moléculas de triacilgliceróis em relação umas às outras, o ângulo de inclinação das moléculas dentro da estrutura do cristal e o empacotamento das cadeias alifáticas. Tais diferenças indicam que os cristais de gordura podem existir em diversas formas cristalinas polimórficas (DAMODARAN; PARKIN, 2019).

O polimorfismo é a capacidade de um material existir sob a forma de diversas estruturas cristalinas com diferentes empacotamentos moleculares. Existem três formas polimórficas mais comuns em que um triacilglicerol pode existir, são as chamadas formas α , β' e β . O comportamento de cristalização do triacilglicerol, tal como a taxa de cristalização, o tamanho dos cristais e sua rede, morfologia e cristalinidade, é influenciado diretamente pelo polimorfismo, o qual é influenciado pela própria estrutura molecular e vários fatores externos, como temperatura, pressão, solvente, taxa de cristalização, presença de impurezas, entre outros (SATO; UENO, 2011).

As formas polimórficas podem ser caracterizadas pela estabilidade térmica, pelo empacotamento das subcélulas e pela estrutura do comprimento das cadeias alifáticas dos

ácidos graxos. A estabilidade térmica, temperatura e entalpia de fusão das formas polimórficas aumentam na ordem $\alpha < \beta' < \beta$. Isso pode ser explicado em termos da energia livre de Gibbs ($G = H - TS$, sendo H, S e T a entalpia, entropia e temperatura, respectivamente). Em uma mesma temperatura, os valores de G são maiores para a forma α , intermediários para a forma β' e menores para a forma β (SATO, 2001). Em condições normais de sub-resfriamento, gorduras com tendência de cristalização na forma β incluem os óleos de soja, amendoim, canola, milho e oliva, além da banha; opostamente, os óleos de palma e algodão, a gordura do leite e o sebo cristalizam geralmente na forma β' (RIBEIRO *et al.*, 2015).

Na maioria das vezes, ácidos graxos e triacilgliceróis são monotrópicos. Ou seja, as transformações das fases polimórficas ocorrem em somente uma direção, de modo que a transformação do material de uma forma polimórfica estável para uma menos estável deva ocorrer através do estado líquido. A estrutura da subcélula define uma forma de empacotamento lateral das cadeias de carbono. As formas polimórficas α , β' e β possuem subcélulas com estruturas hexagonal (H), ortorrômbica perpendicular (O^\perp) e triclínica paralela (T//), respectivamente. Nas subcélulas com estrutura hexagonal, o empacotamento da cadeia de carbono é mais solto, e as interações específicas entre essas cadeias ficam comprometidas por causa da capacidade dos átomos de carbono de rotacionarem vários graus, formando com isso conformações desordenadas das cadeias de carbono. A estrutura de uma subcélula ortorrômbica perpendicular é retangular. Isso representa uma estrutura lamelar fortemente empacotada, onde acontecem interações específicas entre as cadeias. As subcélulas de estrutura triclínica paralela apresentam uma geometria bi-dimensional com ângulo oblíquo, que representa cadeias fortemente empacotadas, nas quais também ocorrem interações específicas entre as cadeias (SATO, 2001).

A estrutura de comprimento de cadeia produz uma sequência repetitiva de cadeias de ácidos graxos envolvidos em célula unitária da lamela ao longo do eixo do seu comprimento. Os TAGs com ácidos graxos iguais ou parecidos tendem a formar uma estrutura de comprimento de cadeia dupla. Uma estrutura de comprimento de cadeia tripla é formada quando as naturezas químicas de um ou dois dos ácidos graxos são muito diferentes entre si. A estrutura do comprimento da cadeia desempenha papéis importantes no comportamento de fases mistas de diferentes tipos de TAGs em fase sólida (SATO, 2001).

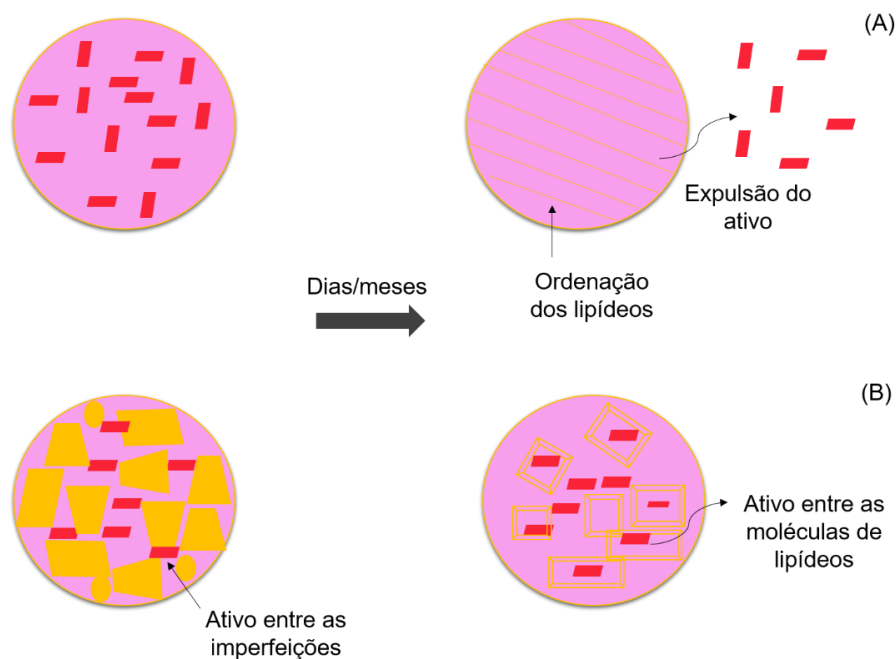
Métodos analíticos são utilizados para o estudo de formas cristalinas de lipídios, entre eles a calorimetria de varredura diferencial (DSC), difração de raios-x (DRX), espectroscopia de infravermelho e ressonância magnética nuclear (NMR). A técnica DSC pode ser utilizada para o estudo do comportamento dos lipídios em transições de fase como fusão e solidificação,

além das transformações entre as várias formas polimórficas. A difração de raios-x (DRX) é utilizada para identificar as diversas formas cristalinas dos lipídios, providenciando informação sobre a estrutura molecular, distância lamelar e estrutura das subcélulas (SATO, 2001; SATO; UENO, 2011).

A propriedade física de transições polimórficas influencia na produção de micropartículas lipídicas sólidas, podendo mostrar baixos valores de eficiência de encapsulação e liberação do núcleo durante o armazenamento, devido à reorganização dos cristais para uma forma polimórfica mais estável (MÜLLER; RADTKE; WISSING, 2002; RIBEIRO; ARELLANO; GROSSO, 2012).

O empacotamento de gorduras sólidas, em que há predominância de ácidos graxos saturados, ocorre de maneira mais organizada. A criação de uma matriz lipídica sólida menos ordenada pode favorecer a permanência do ativo na matriz lipídica. Assim, a utilização de lipídios com moléculas diversas apresenta partículas com estrutura lipídicas com imperfeições, que se acomodam de maneira distintas, favorecendo a permanência do ativo dentro da partícula, ou dependendo da conformação das moléculas de lipídios o ativo pode se incorporar entre as cadeias (MÜLLER; RADTKE; WISSING, 2002). A Figura 3 apresenta esses tipos de partículas.

Figura 3 - (A) Partícula com estrutura ordenada, possível expulsão do ingrediente ativo durante o armazenamento. (B) Partícula com estrutura desordenada, possibilidade de maior retenção do ativo dentro da matriz.



Fonte: Da autora (2022).

2.4.2.3.2 Óleo de palma e gordura hidrogenada de palma

A palma (*Elaeis guineensis jacquin*), ou dendezeiro, como é conhecido no Brasil, é a planta que dá origem ao óleo de palma ou azeite de dendê (extraído da polpa), e o óleo de palmiste (procedente da amêndoa). A diferença entre eles está na predominância de ácido palmítico e oleico no óleo de palma e maior teor de ácido láurico no óleo de palmiste (ASSOCIAÇÃO DOS PRODUTORES DE BIOCOMBUSTÍVEIS DO BRASIL - APROBIO, 2017; LIN, 2002). A Malásia e Indonésia são considerados os maiores produtores de óleo de palma do mundo.

A palma é a oleaginosa de valor econômico mais produtivo de que se tem conhecimento. Sua produtividade média é de 4 toneladas de óleo por hectare/ano, dez vezes mais que o óleo de soja, ou seja, ele é mais competitivo no mercado mundial do que os produtos similares (APROBIO, 2017). É um produto versátil, de fácil acesso e pode ser encontrado em mais de 50% dos produtos nos supermercados, desde óleos de cozinha, margarina, sorvetes, chocolates, biscoitos a detergentes e cosméticos (TEOH, 2010).

Uma das propriedades físicas que torna o óleo de palma interessante para diversas aplicações em alimentos é a sua característica semissólida em temperatura ambiente. Tal característica está relacionada com a composição química de ácidos graxos presentes em uma razão de 50/50 para saturados/insaturados (LIN, 2002).

O óleo de palma apresenta um teor de monoacilglicerol muito baixo (< 0,5%), enquanto os diacilgliceróis variam entre 5% e 8%. Os óleos de palma com alta acidez mostram concentração elevada de diacilgliceróis. Na etapa de refinamento do óleo de palma os ácidos graxos livres são subprodutos do processo. Para ampliar a gama de sua utilização, o óleo de palma processado pode ser fracionado em oleína de palma (fase líquida), que é muito utilizada como óleo de cozinha e em frituras, e na fração de estearina de palma (sólida), com uso para fabricação de alimentos processados como margarinas, biscoitos recheados e gordura vegetal (LIN, 2002).

O principal ácido graxo saturado no óleo de palma é o palmítico (C 16:0), que está distribuído na maioria dos seus ésteres de glicerol e, por isso, suas formas polimórficas são altamente estáveis na forma β' (LIN, 2002).

A estearina de palma corresponde à fração de elevado ponto de fusão do óleo de palma, com ponto de fusão variando entre 32-40°C, sendo uma grande substituta da gordura *trans*. A composição em triacilgliceróis é heterogênea e está concentrada em POP (palmítico-

oleicopalmítico) com 24 a 36% e POO (palmítico-oleico-oleico) com 23 a 30%. A gordura de palma quando cristalizada tende a se apresentar na forma β' (GEE, 2007).

Devido à presença de diacilgliceróis (DAGs), a transição polimórfica da forma α para β' no óleo de palma ocorre de forma lenta se comparada aos demais óleos e gorduras naturais. Dessa forma, com o objetivo de estabilizar o polimorfo β' e acelerar o processo de cristalização do óleo de palma é possível adicionar ao lipídio pequenas quantidades de óleos totalmente hidrogenados (OTH), também conhecidos como *hard fats* (DEMAN; DEMAN; BLACKMAN, 1989).

A hidrogenação de óleos e gorduras para a indústria de alimentos possui dois objetivos principais: aumentar a estabilidade do óleo líquido diminuindo suas insaturações, porém mantendo ainda sua fluidez, e conferir textura a recheios, bolos, sorvetes, etc., através do uso de gorduras sólidas obtidas pela hidrogenação total da matriz lipídica. A hidrogenação catalítica total permite a transformação de óleos líquidos em gorduras completamente saturadas e, portanto, livre em *trans*. Essa transformação dá origem aos chamados *hard fats* que possuem elevado ponto de fusão e são uma alternativa de baixo custo para diversas aplicações em sistemas lipídicos (O'BRIEN, 2004)

Os óleos totalmente hidrogenados são gorduras obtidas a partir do processo de hidrogenação catalítica dos óleos, por meio do qual são eliminadas todas as insaturações presentes nos AGs, através da adição de átomos de hidrogênio. Esses produtos apresentam menor custo de produção industrial e, por possuírem elevado ponto de fusão e composição uniforme de TAGs, são capazes de atuar como sementes de cristalização de óleos e gorduras (O'BRIEN, 2004).

A hidrogenação total do óleo de palma ocorre por meio da conversão completa dos AGs insaturados (oleico, linoleico e linolênico) nos AGs saturados correspondentes. Seu uso como material de semeadura em óleo de palma minimiza os efeitos de incompatibilidade entre os dois lipídios e apresenta a mesma tendência polimórfica (DEMAN; DEMAN; BLACKMAN, 1989; O'BRIEN, 2004).

O óleo de palma totalmente hidrogenado apresenta composição química homogênea e bem definida, apresentando essencialmente os AGs palmítico (56%) e esteárico (44%). Seu ponto de fusão varia de 58 a 65 °C e possui tendência a formar cristais no tipo β' . A presença dos TAGs de alto ponto de fusão e a dominância de AGs de cadeias maiores favorecem a diminuição do tempo de indução da cristalização (LIN, 2002).

3 CONSIDERAÇÕES GERAIS

A microencapsulação do extrato de casca de uva por *spray chilling* proporciona às indústrias vitivinícolas e de alimentos ferramentas para o aproveitamento desse resíduo e o desenvolvimento de produtos com características sensoriais e funcionais melhoradas. As propriedades das emulsões, assim como as diferentes concentrações entre os materiais encapsulantes, estão entre os principais parâmetros relacionados à qualidade do produto final obtido pela técnica de *spray chilling*. Sendo assim, a otimização desses parâmetros e o uso de técnicas analíticas permitem entender o comportamento do processo e estimar as aplicações em alimentos.

REFERÊNCIAS

- AH-HEN, K. S. *et al.* Bioaccessibility of bioactive compounds and antioxidant activity in murta (*Ugni molinae* T.) berries juices. **Journal of Food Measurement and Characterization**, [New York], v. 12, n. 1, p. 602–615, Mar. 2018. Disponível em: <https://link.springer.com/article/10.1007/s11694-017-9673-4>. Acesso em: 22 jan. 2021.
- ALEMZADEH, I. *et al.* Encapsulation of food components and bioactive ingredients and targeted release. **International Journal of Engineering, Transactions A: Basics**, [Argentina], v. 33, n. 1, p. 1–11, Jan. 2020. Disponível em: https://www.ije.ir/article_101141.html. Acesso em: 22 jan. 2021.
- ALVIM, I. D. *et al.* Comparison between the spray drying and spray chilling microparticles contain ascorbic acid in a baked product application. **LWT - Food Science and Technology**, [Amsterdam], v. 65, p. 689–694, Jan. 2016. Disponível em: <https://www.sciencedirect.com/science/article/abs/pii/S0023643815301432>. Acesso em: 05 fev. 2021.
- ALVIM, I. D. *et al.* Use of the spray chilling method to deliver hydrophobic components: Physical characterization of microparticles. **Food Science and Technology**, Campinas, v. 33, n. 1, p. 34–39, Feb. 2013. Disponível em: <https://www.scielo.br/j/cta/a/6wkxyVtygHd9zQQBYHptj8K/?lang=en>. Acesso em: 06 fev. 2021.
- AMENDOLA, D.; DE FAVERI, D. M.; SPIGNO, G. Grape marc phenolics: Extraction kinetics, quality and stability of extracts. **Journal of Food Engineering**, [Oxford], v. 97, n. 3, p. 384–392, Apr. 2010. Disponível em: <https://www.sciencedirect.com/science/article/abs/pii/S0260877409005408>. Acesso em: 19 dez. 2020.
- AMORIM, F. L. *et al.* Grape peel (Syrah var.) jam as a polyphenol-enriched functional food ingredient. **Food Science & Nutrition**, [Hoboken], v. 7, n. 5, p. 1584–1594, Apr. 2019. Disponível em: <https://onlinelibrary.wiley.com/doi/full/10.1002/fsn3.981>. Acesso em: 15 dez. 2020.
- ARENAS-JAL, M.; SUÑÉ-NEGRE, J. M.; GARCÍA-MONTOYA, E. An overview of microencapsulation in the food industry: opportunities, challenges, and innovations. **European Food Research and Technology**, [New York], v. 246, n. 7, p. 1371–1382, Apr. 2020. Disponível em: <https://link.springer.com/article/10.1007/s00217-020-03496-x>. Acesso em: 12 fev. 2021.
- ASSOCIAÇÃO DOS PRODUTORES DE BIOCOMBUSTÍVEIS DO BRASIL. Óleo de Palma no Brasil e suas potencialidades para as indústrias de alimentos, biodiesel e cosméticos. **APROBIO**, São Paulo, 04 jan. 2017, 09:26. Disponível em: <https://aprobio.com.br/noticia/oleo-de-palma-no-brasil-e-suas-potencialidades-para-as-industrias-de-alimentos-biodiesel-e-cosmeticos>. Acesso em: 19 dez. 2020.

BERTONI, S.; ALBERTINI, B.; PASSERINI, N. Spray congealing: an emerging technology to prepare solid dispersions with enhanced oral bioavailability of poorly water soluble drugs. **Molecules**, [Basel], v. 24, n. 19, p. 3471, Sept. 2019. Disponível em: <https://pubmed.ncbi.nlm.nih.gov/31557815/>. Acesso em: 10 fev. 2021.

BOOSTANI, S.; JAFARI, S. M. A comprehensive review on the controlled release of encapsulated food ingredients; fundamental concepts to design and applications. **Trends in Food Science & Technology**, [London], v. 109, p. 303–321, Mar. 2021. Disponível em: <https://www.sciencedirect.com/science/article/abs/pii/S0924224421000418>. Acesso em: 24 fev. 2021.

BOTREL, D. A. *et al.* Evaluation of spray drying conditions on properties of microencapsulated oregano essential oil. **International Journal of Food Science & Technology**, [Malden], v. 47, n. 11, p. 2289–2296, Nov. 2012. Disponível em: <https://ifst.onlinelibrary.wiley.com/doi/abs/10.1111/j.1365-2621.2012.03100.x>. Acesso em: 19 dez. 2020.

BRASIL. Ministério da Saúde. Secretaria de Vigilância Sanitária. a Resolução RDC n° 270, de 22 de setembro de 2005. Aprova o Regulamento Técnico para óleos e vegetais, gorduras vegetais e creme vegetal. **Diário Oficial [da] República Federativa do Brasil**, Poder Executivo, Brasília, DF, 2005.

CAMARGO, U. A.; MAIA, J. D. G.; RITSCHER, P. **Embrapa Uva e Vinho: novas cultivares brasileiras de uva**. Bento Gonçalves: Embrapa Uva e Vinho, 2010. 68 p. Disponível em: <https://www.embrapa.br/busca-de-publicacoes/-/publicacao/1110517/modelo-para-disponibilizacao-e-adocao-de-novas-cultivares-de-videira-ao-setor-produtivo-o-caso-do-programa-de-melhoramento-genetico-uvras-do-brasil>. Acesso em: 19 dez. 2020.

CAMPELO, P. H. *et al.* Use of prebiotic carbohydrate as wall material on lime essential oil microparticles. **Journal of Microencapsulation**, [Abingdon], v. 34, n. 6, p. 535–544, Sept. 2017. Disponível em: <https://pubmed.ncbi.nlm.nih.gov/28795848/>. Acesso em: 22 dez. 2020.

CARMO, E. L. do *et al.* Stability of spray-dried beetroot extract using oligosaccharides and whey proteins. **Food Chemistry**, [Oxford], v. 249, p. 51–59, May 2018. Disponível em: <https://www.sciencedirect.com/science/article/pii/S0308814617320472>. Acesso em: 02 dez. 2020.

CARMONA-GÓMEZ, L. A. *et al.* Separation of polyphenolic compounds by ultrafiltration of bordo grape (*vitis labrusca* var. bordo) skin extract. **Revista Mexicana de Ingeniería Química**, [Mexico], v. 17, n. 1, p. 203–213, Jan./Apr. 2018. Disponível em: <http://rmiq.org/ojs311/index.php/rmiq/article/view/31>. Acesso em: 01 nov. 2020.

CASTAÑEDA-OVANDO, A. *et al.* Chemical studies of anthocyanins: A review. **Food Chemistry**, [Oxford], v. 113, n. 4, p. 859–871, Apr. 2009. Disponível em: <https://www.sciencedirect.com/science/article/abs/pii/S0308814608010674>. Acesso em: 02 nov. 2020.

CASTILHOS, M. B. M. de *et al.* Sensory acceptance drivers of pre-fermentation dehydration and submerged cap red wines produced from *Vitis labrusca* hybrid grapes. **LWT - Food Science and Technology**, [Amsterdam], v. 69, p. 82–90, June 2016. Disponível em: <https://www.sciencedirect.com/science/article/pii/S0023643816300433>. Acesso em: 01 nov. 2020.

CONSOLI, L. *et al.* Gallic acid microparticles produced by spray chilling technique: Production and characterization. **LWT - Food Science and Technology**, [Amsterdam], v. 65, p. 79–87, Jan. 2016. Disponível em: <https://www.sciencedirect.com/science/article/pii/S0023643815300694>. Acesso em: 15 nov. 2020.

DAMODARAN, S.; PARKIN, K. L. **Química de alimentos de Fennema**. Porto Alegre: ArtMed, 2019.

DÁVILA, I. *et al.* **The biorefinery concept for the industrial valorization of grape processing by-products**. Cambridge: Academic Press, 2017. p. 29-53.

DEMAN, L.; DEMAN, J. M.; BLACKMAN, B. Polymorphic behavior of some fully hydrogenated oils and their mixtures with liquid oil. **Journal of the American Oil Chemists' Society**, [New York], v. 66, n. 12, p. 1777–1780, Dec. 1989. Disponível em: <https://link.springer.com/article/10.1007/BF02660746>. Acesso em: 23 nov. 2020.

EFTIMOV, T. *et al.* COVID-19 pandemic changes the food consumption patterns. **Trends in Food Science & Technology**, [London], v. 104, p. 268–272, Oct. 2020. Disponível em: <https://www.sciencedirect.com/science/article/pii/S0924224420305823>. Acesso em: 12 mar. 2021.

FERNANDES, R. V. de B. *et al.* Study of ultrasound-assisted emulsions on microencapsulation of ginger essential oil by spray drying. **Industrial Crops and Products**, [Amsterdam], v. 94, p. 413–423, Dec. 2016. Disponível em: <https://www.sciencedirect.com/science/article/abs/pii/S0926669016305969>. Acesso em: 16 nov. 2020.

FIGUEIREDO, J. de A. *et al.* Encapsulation of camu-camu extracts using prebiotic biopolymers: Controlled release of bioactive compounds and effect on their physicochemical and thermal properties. **Food Research International**, [Amsterdam], v. 137, Nov. 2020b. Disponível em: <https://www.sciencedirect.com/science/article/abs/pii/S0963996920305883>. Acesso em: 08 nov. 2020.

FIGUEIREDO, J. de A. *et al.* Microencapsulation by spray chilling in the food industry: Opportunities, challenges, and innovations. **Trends in Food Science & Technology**, [London], v. 120, p. 274–287, Feb. 2022. Disponível em: <https://www.sciencedirect.com/science/article/abs/pii/S092422442100683X>. Acesso em: 12 jan. 2022.

FIGUEIREDO, J. de A. *et al.* Stability of camu-camu encapsulated with different prebiotic biopolymers. **Journal of the Science of Food and Agriculture**, [Chichester], v. 100, n. 8, p. 3471–3480, June 2020a. Disponível em: <https://onlinelibrary.wiley.com/doi/abs/10.1002/jsfa.10384>. Acesso em: 08 nov. 2020.

FREDES, C. *et al.* Stability and bioaccessibility of anthocyanins from maqui (*Aristotelia chilensis* [Mol.] Stuntz) juice microparticles. **LWT - Food Science and Technology**, [Amsterdam], v. 91, p. 549–556, May 2018. Disponível em: <https://www.sciencedirect.com/science/article/abs/pii/S0023643818301282>. Acesso em: 24 jan. 2021.

GARCÍA-LOMILLO, J.; GONZÁLEZ-SANJOSÉ, M. L. Applications of wine pomace in the food industry: approaches and functions. **Comprehensive Reviews in Food Science and Food Safety**, [Malden], v. 16, n. 1, p. 3–22, Jan. 2017. Disponível em: <https://ift.onlinelibrary.wiley.com/doi/abs/10.1111/1541-4337.12238>. Acesso em: 26 jan. 2021.

GEE, P. T. Analytical characteristics of crude and refined palm oil and fractions. **European Journal of Lipid Science and Technology**, [Weinheim], v. 109, n. 4, p. 373–379, Apr. 2007. Disponível em: <https://onlinelibrary.wiley.com/doi/abs/10.1002/ejlt.200600264>. Acesso em: 23 nov. 2020.

GIBBS, B. F. *et al.* Encapsulation in the food industry: A review. **International Journal of Food Sciences and Nutrition**, [Abingdon], v. 50, n. 3, p. 213–224, May 1999. Disponível em: <https://pubmed.ncbi.nlm.nih.gov/10627837/>. Acesso em: 27 nov. 2020.

GONÇALVES, A. E. de S. S.; LAJOLO, F. M.; GENOVESE, M. I. Chemical composition and antioxidant/antidiabetic potential of brazilian native fruits and commercial frozen pulps. **Journal of Agricultural and Food Chemistry**, [Washington], v. 58, n. 8, p. 4666–4674, Mar. 2010. Disponível em: <https://pubs.acs.org/doi/10.1021/jf903875u>. Acesso em: 29 nov. 2020.

HAAS, I. C. da S. *et al.* Polyphenolic profile, macro- and microelements in bioaccessible fractions of grape juice sediment using *in vitro* gastrointestinal simulation. **Food Bioscience**, [Amsterdam], v. 27, p. 66–74, Feb. 2019. Disponível em: <https://www.sciencedirect.com/science/article/abs/pii/S2212429218305431>. Acesso em: 23 jan. 2021.

HOGERVORST, J. C.; MILJIĆ, U.; PUŠKAŠ, V. **Extraction of bioactive compounds from grape processing by-products**. Cambridge: Academic Press, 2017. p. 105-135.

INTERNATIONAL ORGANISATION OF VINE AND WINE. **State of the world vine and wine sector 2021**. OIV, 2022. 20 p. Disponível em: <https://www.oiv.int/public/medias/8778/eng-state-of-the-world-vine-and-wine-sector-april-2022-v6.pdf>. Acesso em: 19 dez. 2020.

KIM, A.-N. *et al.* Degradation kinetics of phenolic content and antioxidant activity of hardy kiwifruit (*Actinidia arguta*) puree at different storage temperatures. **LWT - Food Science and Technology**, [Amsterdam], v. 89, p. 535–541, Mar. 2018. Disponível em: <https://www.sciencedirect.com/science/article/abs/pii/S0023643817308551>. Acesso em: 28 nov. 2020.

KUCK, L. S.; NOREÑA, C. P. Z. Microencapsulation of grape (*Vitis labrusca* var. Bordo) skin phenolic extract using gum Arabic, polydextrose, and partially hydrolyzed guar gum as encapsulating agents. **Food Chemistry**, [Oxford], v. 194, p. 569–576, Mar. 2016. Disponível em: <https://www.sciencedirect.com/science/article/pii/S0308814615012649>. Acesso em: 28 nov. 2020.

KUCK, L. S.; WESOLOWSKI, J. L.; NOREÑA, C. P. Z. Effect of temperature and relative humidity on stability following simulated gastro-intestinal digestion of microcapsules of Bordo grape skin phenolic extract produced with different carrier agents. **Food Chemistry**, [Oxford], v. 230, p. 257–264, Sept. 2017. Disponível em: <https://www.sciencedirect.com/science/article/pii/S0308814617304016>. Acesso em: 22 jan. 2021.

LACERDA, D. dos S. *et al.* Biochemical and physiological parameters in rats fed with high-fat diet: the protective effect of chronic treatment with purple grape juice (Bordo Variety). **Beverages**, [Basel], v. 4, n. 4, p. 1-13, Dec. 2018. Disponível em: https://lume.ufrgs.br/handle/10183/188775?locale-attribute=pt_BR. Acesso em: 05 nov. 2020.

LIN, S. W. Palm oil. *In*: GUNSTONE, F. D. (ed.). **Vegetable oils in food technology: composition, properties and uses**. Boca Raton: CRC Press LLC., 2002.

LOPES, T. J. *et al.* Anthocyanins: a brief review of structural characteristics and stability. **Revista Brasileira Agrociência**, Pelotas, v. 13, n. 3, p. 291–297, July/Sept. 2007. Disponível em: https://www.academia.edu/28538325/ANTHOCYANINS_A_BRIEF_REVIEW_OF_STRUCTURAL_CHARACTERISTICS_AND_STABILITY. Acesso em: 26 nov. 2020.

MADENE, A. *et al.* Review flavour encapsulation and controlled release – a review. **International Journal of Food Science and Technology**, [Malden], v. 41, n. 1, p. 1–21, Jan. 2006. Disponível em: <https://ifst.onlinelibrary.wiley.com/doi/10.1111/j.1365-2621.2005.00980.x>. Acesso em: 23 jan. 2021.

MATTIVI, F. *et al.* Metabolite profiling of grape: Flavonols and anthocyanins. **Journal of Agricultural and Food Chemistry**, [Washington], v. 54, n. 20, p. 7692–7702, Oct. 2006. Disponível em: <https://pubmed.ncbi.nlm.nih.gov/17002441/>. Acesso em: 25 jan. 2021.

MAZZA, G.; MINIATI, E. **Anthocyanins in fruits, vegetables and grains**. 1st ed. Boca Raton: CRC Press, 1993. p. 471–472.

McCLEMENTS, D. J. Advances in nanoparticle and microparticle delivery systems for increasing the dispersibility, stability, and bioactivity of phytochemicals. **Biotechnology Advances**, [Oxford], v. 38, Jan./Feb. 2020. Disponível em: <https://pubmed.ncbi.nlm.nih.gov/30086329/>. Acesso em: 17 nov. 2020.

McCLEMENTS, D. J. Critical review of techniques and methodologies for characterization of emulsion stability. **Critical Reviews in Food Science and Nutrition**, [Philadelphia], v. 47, n. 7, p. 611–649, Jan. 2007. Disponível em: <https://pubmed.ncbi.nlm.nih.gov/17943495/>. Acesso em: 16 nov. 2020.

MELLO, L. M. R. de; MACHADO, C. A. E. **Vitivinicultura brasileira: Panorama 2019**. Bento Gonçalves: Embrapa Uva e Vinho, 2020. p. 1–21. (Embrapa Uva e Vinho. Comunicado técnico, 214).

MENDES, J. A. S. *et al.* Towards comprehensive utilization of winemaking residues: Characterization of grape skins from red grape pomaces of variety *Touriga Nacional*. **Industrial Crops and Products**, [Amsterdam], v. 43, n. 1, p. 25–32, May 2013. Disponível em: <https://www.sciencedirect.com/science/article/abs/pii/S092666901200369X>. Acesso em: 18 nov. 2020.

MORENO, T.; COCERO, M. J.; RODRÍGUEZ-ROJO, S. Storage stability and simulated gastrointestinal release of spray dried grape marc phenolics. **Food and Bioprocess Technology**, [Rugby], v. 112, p. 96–107, Nov. 2018. Disponível em: <https://www.sciencedirect.com/science/article/abs/pii/S0960308518305996>. Acesso em: 20 nov. 2020.

MÜLLER, R. H.; RADTKE, M.; WISSING, S. A. Nanostructured lipid matrices for improved microencapsulation of drugs. **International Journal of Pharmaceutics**, [Amsterdam], v. 242, n. 1–2, p. 121–128, Ago. 2002. Disponível em: <https://pubmed.ncbi.nlm.nih.gov/12176234/>. Acesso em: 30 out. 2020.

MURALI, S. *et al.* Encapsulation of black carrot juice using spray and freeze drying. **Food Science and Technology International**, [London], v. 21, n. 8, p. 604–612, Dec. 2015. Disponível em: <https://pubmed.ncbi.nlm.nih.gov/25367889/>. Acesso em: 30 out. 2020.

NAYAK, B.; LIU, R. H.; TANG, J. Effect of processing on phenolic antioxidants of fruits, vegetables, and grains—a review. **Critical Reviews in Food Science and Nutrition**, [Philadelphia], v. 55, n. 7, p. 887–919, Jan. 2015. Disponível em: <https://pubmed.ncbi.nlm.nih.gov/24915381/>. Acesso em: 10 nov. 2020.

O'BRIEN, R. D. **Fats and oils: formulating and processing for applications**. New York: CRC Press, 2004. 680 p.

ORIANI, V. B. *et al.* The influence of the storage temperature on the stability of lipid microparticles containing ginger oleoresin. **Food Research International**, [Amsterdam], v. 109, p. 472–480, July 2018. Disponível em: <https://pubmed.ncbi.nlm.nih.gov/29803473/>. Acesso em: 30 out. 2020.

PEDROZA, M. A. *et al.* Waste grape skins thermal dehydration: Potential release of colour, phenolic and aroma compounds into wine. **CYTA - Journal of Food**, [Abingdon], v. 10, n. 3, p. 225–234, Feb. 2012. Disponível em: <https://www.tandfonline.com/doi/full/10.1080/19476337.2011.633243>. Acesso em: 11 nov. 2020.

PROCOPIO, F. R. *et al.* Solid lipid microparticles loaded with cinnamon oleoresin: Characterization, stability and antimicrobial activity. **Food Research International**, [Amsterdam], v. 113, p. 351–361, Nov. 2018. Disponível em: <https://www.sciencedirect.com/science/article/abs/pii/S0963996918305647>. Acesso em: 30 out 2020.

- RAVIADARAN, R. *et al.* Ultrasound-assisted water-in-palm oil nano-emulsion: Influence of polyglycerol polyricinoleate and NaCl on its stability. **Ultrasonics Sonochemistry**, [Amsterdam], v. 52, p. 353–363, Apr. 2019. Disponível em: <https://www.sciencedirect.com/science/article/abs/pii/S1350417718312483>. Acesso em: 31 out. 2020.
- REMINI, H. *et al.* Degradation kinetic modelling of ascorbic acid and colour intensity in pasteurised blood orange juice during storage. **Food Chemistry**, [Oxford], v. 173, p. 665–673, Apr. 2015. Disponível em: <https://pubmed.ncbi.nlm.nih.gov/25466074/>. Acesso em: 15 nov. 2020.
- RIBEIRO, A. P. B. *et al.* Crystallization modifiers in lipid systems. **Journal of Food Science and Technology**, [New Delhi], v. 52, n. 7, p. 3925–3946, July 2015. Disponível em: <https://www.ncbi.nlm.nih.gov/pmc/articles/PMC4486597/>. Acesso em: 31 out. 2020.
- RIBEIRO, M. D. M. M.; ARELLANO, D. B.; GROSSO, C. R. F. The effect of adding oleic acid in the production of stearic acid lipid microparticles with a hydrophilic core by a spray-cooling process. **Food Research International**, [Amsterdam], v. 47, n. 1, p. 38–44, June 2012. Disponível em: <https://www.sciencedirect.com/science/article/abs/pii/S0963996912000415>. Acesso em: 29 out. 2020.
- RICE-EVANS, C.; MILLER, N.; PAGANGA, G. Antioxidant properties of phenolic compounds. **Trends in Plant Science**, [London], v. 2, n. 4, p. 152–159, Apr. 1997. Disponível em: <https://www.sciencedirect.com/science/article/abs/pii/S1360138597010182>. Acesso em: 22 nov. 2020.
- ROCKENBACH, I. I. *et al.* Phenolic compounds content and antioxidant activity in pomace from selected red grapes (*Vitis vinifera* L. and *Vitis labrusca* L.) widely produced in Brazil. **Food Chemistry**, [Oxford], v. 127, n. 1, p. 174–179, July 2011. Disponível em: <https://www.sciencedirect.com/science/article/pii/S0308814611000458>. Acesso em: 18 nov. 2020.
- RODRÍGUEZ-ROQUE, M. J. *et al.* *In vitro* bioaccessibility of health-related compounds from a blended fruit juice-soymilk beverage: Influence of the food matrix. **Journal of Functional Foods**, [Amsterdam], v. 7, n. 1, p. 161–169, Mar. 2014. Disponível em: <https://www.sciencedirect.com/science/article/abs/pii/S1756464614000383>. Acesso em: 15 nov. 2020.
- ROMANINI, E. B. *et al.* Ultrasound assisted extraction of bioactive compounds from BRS Violet grape pomace followed by alginate-Ca²⁺ encapsulation. **Food Chemistry**, [Oxford], v. 338, Feb. 2021. Disponível em: <https://www.sciencedirect.com/science/article/abs/pii/S0308814620319634>. Acesso em: 14 nov. 2020.
- SAIFULLAH, M. *et al.* Micro and nano encapsulation, retention and controlled release of flavor and aroma compounds: A critical review. **Trends in Food Science & Technology**, [London], v. 86, p. 230–251, Apr. 2019. Disponível em: <https://www.sciencedirect.com/science/article/abs/pii/S0924224417307677>. Acesso em: 17 nov. 2020.

SATO, K. Crystallization behaviour of fats and lipids - a review. **Chemical Engineering Science**, [Oxford], v. 56, n. 7, p. 2256–2265, Apr. 2001. Disponível em: <https://www.sciencedirect.com/science/article/pii/S0009250900004589>. Acesso em: 30 out. 2020.

SATO, K.; UENO, S. Crystallization, transformation and microstructures of polymorphic fats in colloidal dispersion states. **Current Opinion in Colloid & Interface Science**, [London], v. 16, n. 5, p. 384–390, Oct. 2011. Disponível em: <https://www.sciencedirect.com/science/article/abs/pii/S135902941100080X>. Acesso em: 31 out. 2020.

SAVOLAINEN, M. *et al.* Evaluation of polar lipid-hydrophilic polymer microparticles. **International Journal of Pharmaceutics**, [Amsterdam], v. 262, n. 1–2, p. 47–62, Aug. 2003. Disponível em: <https://pubmed.ncbi.nlm.nih.gov/12927387/>. Acesso em: 28 out. 2020.

SHASHIREKHA, M. N.; MALLIKARJUNA, S. E.; RAJARATHNAM, S. Status of bioactive compounds in foods, with focus on fruits and vegetables. **Critical Reviews in Food Science and Nutrition**, [Philadelphia], v. 55, n. 10, p. 1324–1339, Oct. 2015. Disponível em: <https://pubmed.ncbi.nlm.nih.gov/24915335/>. Acesso em: 15 nov. 2020.

SILVA, E. K. *et al.* Ultrasound-assisted formation of annatto seed oil emulsions stabilized by biopolymers. **Food Hydrocolloids**, [Oxford], v. 47, p. 1–13, May 2015. Disponível em: <https://www.sciencedirect.com/science/article/abs/pii/S0268005X1500003X>. Acesso em: 31 out. 2020.

SILVA, R. S. *et al.* Physicochemical properties of tucumã (*Astrocaryum aculeatum*) powders with different carbohydrate biopolymers. **LWT - Food Science and Technology**, [Amsterdam], v. 94, p. 79–86, Aug. 2018. Disponível em: <https://www.sciencedirect.com/science/article/abs/pii/S0023643818303530>. Acesso em: 28 nov. 2020.

SINELA, A. *et al.* Anthocyanins degradation during storage of *Hibiscus sabdariffa* extract and evolution of its degradation products. **Food Chemistry**, [Oxford], v. 214, p. 234–241, Jan. 2017. Disponível em: <https://www.sciencedirect.com/science/article/abs/pii/S0308814616310937?via%3Dihub>. Acesso em: 27 out. 2020.

SÓLYOM, K. *et al.* Thermal degradation of grape marc polyphenols. **Food Chemistry**, [Oxford], v. 159, p. 361–366, Sept. 2014. Disponível em: <https://www.sciencedirect.com/science/article/abs/pii/S0308814614004063>. Acesso em: 15 nov. 2020.

SOUZA, V. B. de *et al.* Functional properties and stability of spray-dried pigments from Bordo grape (*Vitis labrusca*) winemaking pomace. **Food Chemistry**, [Oxford], v. 164, p. 380–386, Dec. 2014. Disponível em: <https://pubmed.ncbi.nlm.nih.gov/24996348/>. Acesso em: 28 nov. 2020.

SU, J.; FLANAGAN, J.; SINGH, H. Improving encapsulation efficiency and stability of water-in-oil-in-water emulsions using a modified gum arabic (Acacia (sen) SUPER GUM™). **Food Hydrocolloids**, [Oxford], v. 22, n. 1, p. 112–120, Jan. 2008. Disponível em: <https://www.sciencedirect.com/science/article/abs/pii/S0268005X07000872>. Acesso em: 31 out. 2020.

TADROS, T. *et al.* Formation and stability of nano-emulsions. **Advances in Colloid and Interface Science**, [Amsterdam], v. 108–109, p. 303–318, May 2004. Disponível em: <https://www.sciencedirect.com/science/article/abs/pii/S000186860300157X>. Acesso em: 31 out. 2020.

TEOH, C. H. **Key sustainability issues in the palm oil sector**. A Discussion Paper for Multi-Stakeholders Consultations (commissioned by the World Bank Group). Washington: The World Bank, 2010. 52 p. Disponível em: <http://www.biofuelobservatory.org/Documentos/Otros/Palm-Oil-Discussion-Paper-FINAL.pdf>. Acesso em: 29 out. 2020.

TOLUN, A.; ALTINTAS, Z.; ARTIK, N. Microencapsulation of grape polyphenols using maltodextrin and gum arabic as two alternative coating materials: Development and characterization. **Journal of Biotechnology**, [Amsterdam], v. 239, p. 23–33, Dec. 2016. Disponível em: <https://www.sciencedirect.com/science/article/abs/pii/S0168165616315504>. Acesso em: 15 nov. 2020.

TONON, R. V.; BRABET, C.; HUBINGER, M. D. Anthocyanin stability and antioxidant activity of spray-dried açai (*Euterpe oleracea* Mart.) juice produced with different carrier agents. **Food Research International**, [Amsterdam], v. 43, n. 3, p. 907-914, Apr. 2010. Disponível em: <https://www.sciencedirect.com/science/article/pii/S0963996909003895?via%3Dihub>. Acesso em: 27 out. 2020.

TRUJILLO, F. J. *et al.* Separation of suspensions and emulsions via ultrasonic standing waves - A review. **Ultrasonics Sonochemistry**, [Amsterdam], v. 21, n. 6, p. 2151–2164, Nov. 2014. Disponível em: <https://www.sciencedirect.com/science/article/abs/pii/S1350417714000650>. Acesso em: 27 nov. 2020.

USHIKUBO, F. Y.; CUNHA, R. L. Stability mechanisms of liquid water-in-oil emulsions. **Food Hydrocolloids**, [Oxford], v. 34, p. 145–153, Jan. 2014. Disponível em: <https://www.sciencedirect.com/science/article/abs/pii/S0268005X12002810>. Acesso em: 28 nov. 2020.

WILSON, R.; VAN SCHIE, B. J.; HOWES, D. Overview of the preparation, use and biological studies on Polyglycerol Polyricinoleate (PGPR). **Food and Chemical Toxicology**, [Oxford], v. 36, n. 9–10, p. 711-718, Sept./Oct. 1998. Disponível em: <https://www.sciencedirect.com/science/article/abs/pii/S027869159800057X?via%3Dihub>. Acesso em: 27 out. 2020.

XIA, E.-Q. *et al.* Biological activities of polyphenols from grapes. **International Journal of Molecular Sciences**, [Basel], v. 11, n. 2, p. 622–646, Feb. 2010. Disponível em: <https://www.ncbi.nlm.nih.gov/pmc/articles/PMC2852857/>. Acesso em: 22 nov. 2020.

XU, Y. *et al.* Phenolic compounds, antioxidant, and antibacterial properties of pomace extracts from four virginia-grown grape varieties. **Food Science and Nutrition**, [Hoboken], v. 4, n. 1, p. 125–133, Jan. 2016. Disponível em: <https://pubmed.ncbi.nlm.nih.gov/26788319/>. Acesso em: 23 nov. 2020.

ZAFIMAHOVA-RATISBONNE, A. *et al.* Stability of W/O emulsions encapsulating polysaccharides. **Journal of Dispersion Science and Technology**, [Philadelphia], v. 35, n. 1, p. 38–47, Feb. 2014. Disponível em: <https://www.tandfonline.com/doi/abs/10.1080/01932691.2013.773444>. Acesso em: 27 out. 2020.

ZHANG, K. *et al.* Ultrasonic assisted water-in-oil emulsions encapsulating macro-molecular polysaccharide chitosan: Influence of molecular properties, emulsion viscosity and their stability. **Ultrasonics Sonochemistry**, [Amsterdam], v. 64, June 2020. Disponível em: <https://www.sciencedirect.com/science/article/abs/pii/S1350417719315044>. Acesso em: 29 out. 2020.

SEGUNDA PARTE**ARTIGO 1 – MICROENCAPSULATION BY SPRAY CHILLING IN THE FOOD
INDUSTRY: OPPORTUNITIES, CHALLENGES, AND INNOVATIONS**

Artigo publicado na Revista Trends in Food Science & Technology

Doi: <https://doi.org/10.1016/j.tifs.2021.12.026>

Jayne de Abreu Figueiredo¹, Carlos Ramon de Paula Silva¹, Matheus Felipe Souza Oliveira¹, Laís Bruno Norcino², Pedro Henrique Campelo³, Diego Alvarenga Botrel¹, Soraia Vilela Borges^{1*}

¹Department of Food Science, Federal University of Lavras, P.O. Box 3037, 37200-900, Lavras, MG, Brasil

²Biomaterial Engineering, Federal University of Lavras, P.O. Box, 37200-900, Lavras, MG, Brazil

³Faculty of Agrarian Science, Federal University of Amazonas, 69077-000, Manaus, AM, Brazil

ABSTRACT

Background

The increasing demand for healthy eating habits and the emergence of the COVID-19 pandemic, which resulted in a health crisis and global economic slowdown, has led to the consumption of functional and practical foods. Bioactive ingredients can be an alternative for healthy food choices; however, most functional compounds are sensitive to the adverse conditions of processing and digestive tract, impairing its use in food matrices, and industrial-scale applications. Microencapsulation by spray chilling can be a viable alternative to reduce these barriers in food processing.

Scope and approach

This review discusses the use of spray chilling technique for microencapsulation of bioactive food ingredients. Although this technology is known in the pharmaceutical industry, it has been little exploited in the food sector. General aspects of spray chilling, the process parameters, advantages, and disadvantages are addressed. The feasibility and stability of encapsulated bioactive ingredients in food matrices and the bioavailability in vitro of solid lipid microparticles produced by spray chilling are also discussed.

Main findings and conclusions

Research on the microencapsulation of bioactive ingredients by spray chilling for use in foods has shown the effectiveness of this technique to encapsulate bioactive compounds for application in food matrices. Solid microparticles produced by spray chilling can improve the stability and bioavailability of bioactive ingredients. However, further studies are required, including the use of lipid-based encapsulating agents, process parameters, and novel

formulations for application in food, beverages, and packaging, as well as in vivo studies to prove the effectiveness of the formulations.

Keywords: Bioactive compounds; Spray congealing; Functional foods; Encapsulation; Natural additives; Solid lipid microparticles.

1. Introduction

In March 2020, the Covid-19 pandemic was decreed by the World Health Organization, exposing several challenges for society. Consumer demand will change for years to come due to the pandemic, as longstanding habits, technological acceleration, sanitary and global health protocols, all aimed at providing food safety, health, sustainability, and stability to individuals and countries (LOH; SEAH; LOOI, 2021). Some studies have reported that the consumption pattern has changed, with a drop in the consumption of fast food, and an increase in the intake of fresh, healthy products, soups, frozen foods, and dairy products (CHENARIDES et al., 2021; EFTIMOV et al., 2020; GALANAKIS et al., 2020).

The Covid -19 pandemic accelerated the trend toward food that supports the immune system, including bioactive ingredients, supplements, and nutraceuticals (GALANAKIS et al., 2020) By 2030, innovative and sustainable approaches to the supply chain are expected to be taken by food companies. Over the next 10 years, consumers must become more adept at science and technology as they will ensure more affordable, safer, and nutritious food and beverages (CHO et al., 2020).

Bioactive ingredients in foods exhibit a wide range of biological activities, playing key roles in various industries, including food, pharmaceutical, and cosmetics (RAY; RAYCHAUDHURI; CHAKRABORTY, 2016). However, most of these compounds are very sensitive to processing and adverse environmental conditions such as light, moisture, heat, and oxygen, which represents a great challenge for the use of these compounds on an industrial scale (FIGUEIREDO et al., 2020). Spray chilling technology also known as spray congealing or spray cooling is one of the microencapsulation techniques that have stood out for decades for solving limitations in the delivery of active pharmaceutical and cosmetic ingredients (FAVARO-TRINDADE et al., 2021; HUANG et al., 2019; MÜLLER et al., 2002b, 2007). In particular, the spray chilling technique is an economical strategy and represents an effective

alternative to produce microparticles containing sensitive pigments, flavors, and aromas, antioxidants, and natural preservatives for use in food matrices. Studies have shown that spray chilling encapsulation can maintain the stability of ascorbic acid, vitamin D3, and proanthocyanidins during storage (CARVALHO et al., 2019; PAUCAR et al., 2016; TULINI et al., 2017).

Microencapsulation by spray chilling consists of the formation of solid lipid microparticles through the atomization of active ingredients that can be of hydrophilic or hydrophobic origin, dissolved or dispersed in molten lipid encapsulating materials (ORIANI et al., 2016). It is possible to obtain a solution, emulsion, or dispersion, depending on the solubility of the compounds, which is atomized in a refrigeration chamber, in which the droplets solidify when in contact with cold air, giving rise to solid lipid microparticles with characteristics of a powdered product (SORITA et al., 2021).

Recently, some authors have studied the use of this technology in the food and beverage industry (CARVALHO et al., 2021; NAHUM; DOMB, 2021; QUEIRÓS et al., 2020; TOMŠIK et al., 2019) to overcome challenges related to the stability of sensitive compounds such as vitamins and natural pigments during processing and storage. This technology also allows obtaining fat powders, facilitating the manipulation and the incorporation in different food matrices, besides contributing with lower transport and storage costs due to the smaller volume. In addition, solid lipid microparticles can be added to foods to solve problems related to crystallization events and act as structuring agents (FAVARO-TRINDADE; OKURO; MATOS-JUNIOR, 2015; LANDIM NEVES et al., 2021). However, further studies are required on the application of this technique in the food sector. According to the Web Of Science database, using the search terms “spray chilling” OR “spray cooling” OR “spray congealing” AND “food encapsulation” AND “solid lipid particles”, a total of 731 articles were found.

Review articles and articles that did not fit the spray chilling technology were excluded from the search. Thus, 42 articles were found using this technology for food purposes.

The main objective of this review is to demonstrate the potential of the spray chilling microencapsulation process to improve the applicability, stability, and bioavailability in vitro of bioactive ingredients. The main advantages, challenges, and application potentials of spray chilling will also be addressed

2. Fundamentals of spray chilling technology

2.1 Process steps

Before understanding the steps of the spray chilling process, it is worth noting that this technology is fully scalable from an industrial point of view (CONSOLI et al., 2016). Concerning the atomization equipment and operations, the spray chiller is closely associated with the spray dryer. Typically, the spray dryer system can be used for spray chilling processes with some adaptations. Although the production of particles from both techniques is based on the generation of droplets by spraying a fluid (solution, dispersion, or emulsion), different mechanisms govern the formation of particles by spray drying and spray chilling (ALVIM et al., 2016; JASKULSKI; KHARAGHANI; TSOTSAS, 2018).

Briefly, spray drying consists of converting a fluid into a powdered material by evaporating the solvent, usually water, when sprayed in a chamber containing hot air with a temperature higher than the solvent evaporation temperature (SHISHIR; CHEN, 2017).

In turn, spray cooling is based on the solidification of a fluid (containing high melting molten lipids as encapsulating materials) sprayed in a cooling chamber. In detail, spray cooling consists of two steps. The first step requires the encapsulation of the active compound in a lipid matrix, usually a molten lipid or a water-in-oil emulsion (Fig. 1a) (BERTONI; ALBERTINI; PASSERINI, 2019). In the second step, this mixture is sprayed in the form of droplets, usually

by a heated atomizing nozzle, to maintain the proper temperature and avoid recrystallization of the lipid compounds (Fig. 1b). When the pulverized material comes into contact with a cooled environment (injection of cold air or liquid nitrogen), with a temperature below the lipid melting point, there is a heat transfer between the lipid and the cold air, leading to solidification of the matrix and resulting in the formation of solid lipid particles. Similar to spray drying, the residence time of the sprayed droplets in the cooling chamber is short. The particles are collected in a container below the cooling chamber, while very fine particles are transported by air to a cyclone, and collected in another container (CONSOLI et al., 2016).

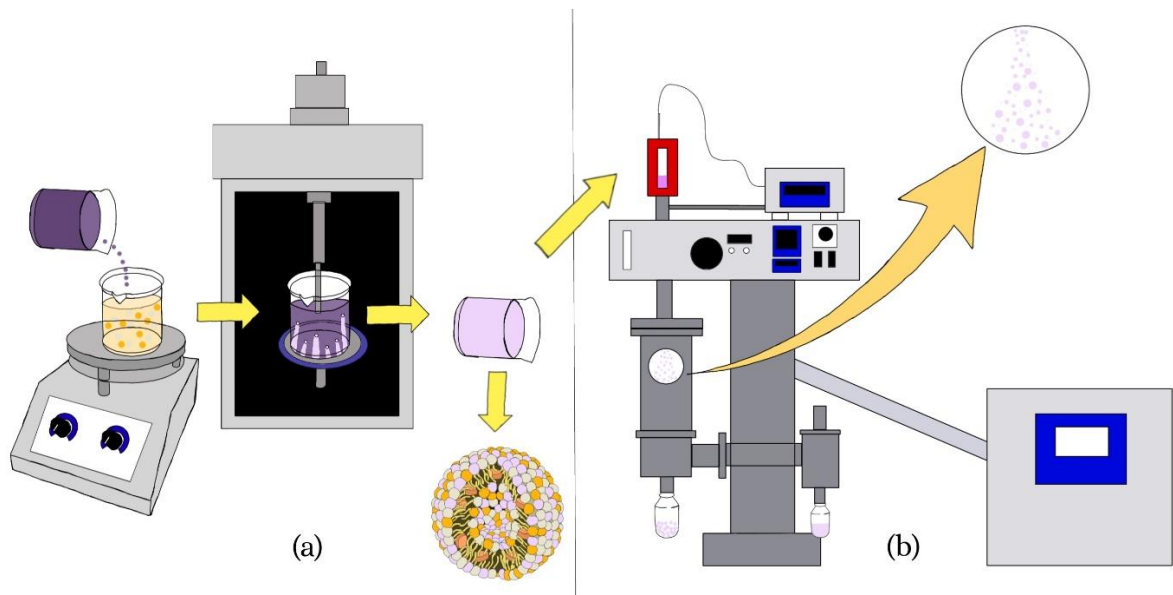


Fig. 1. Production of solid lipid particles by spray chilling. **(a)** Elaboration of a water-in-oil emulsion containing the active ingredient to be atomized in the spray chilling. **(b)** Atomization of the emulsion in the spray chiller and production of solid lipid particles.

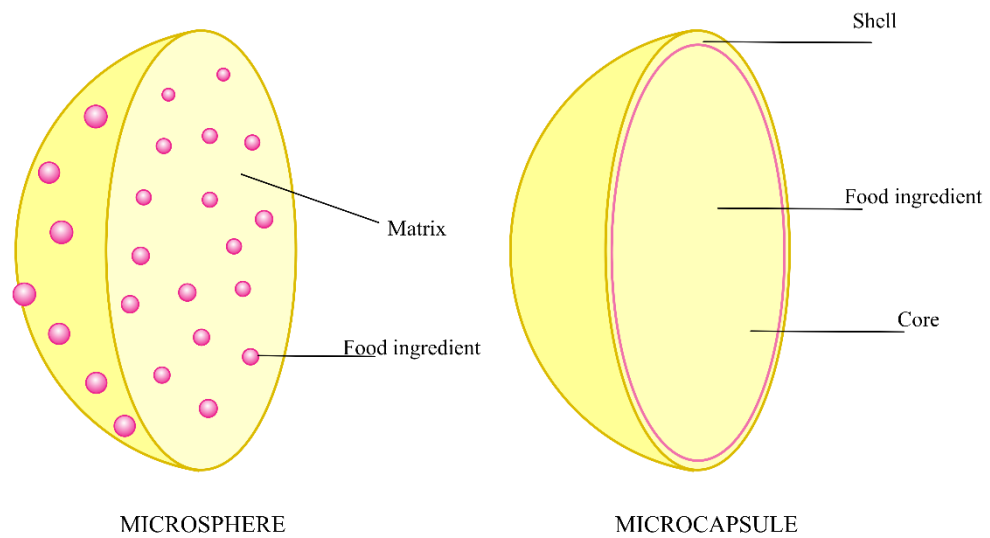
2.2 Structure and Composition

Solid lipid particles are an interesting and versatile tool for the delivery of active compounds. The kinetic stability and rigid morphology are the main advantages of lipid particles over vesicular lipid colloidal systems (liposomes, niosomes, etc.).

As previously mentioned, solid lipid particles are often made from emulsion systems of the W/O type or a dispersion (thermodynamically stable systems), at a temperature above the melting point of the oil droplets, followed by cooling to induce droplet crystallization (MÜLLER; RADTKE; WISSING, 2002b; NAHUM; DOMB, 2021).

Several microencapsulation techniques are used for different purposes, thus allowing the production of microparticles with distinct morphologies. A wide variety of morphologies can be obtained, depending on the desired characteristics and the processing cost (ARENAS-JAL; SUÑÉ-NEGRE; GARCÍA-MONTOYA, 2020). In general, the microparticles are called microcapsules or microspheres (Fig. 2a,b).

(a)



(b)

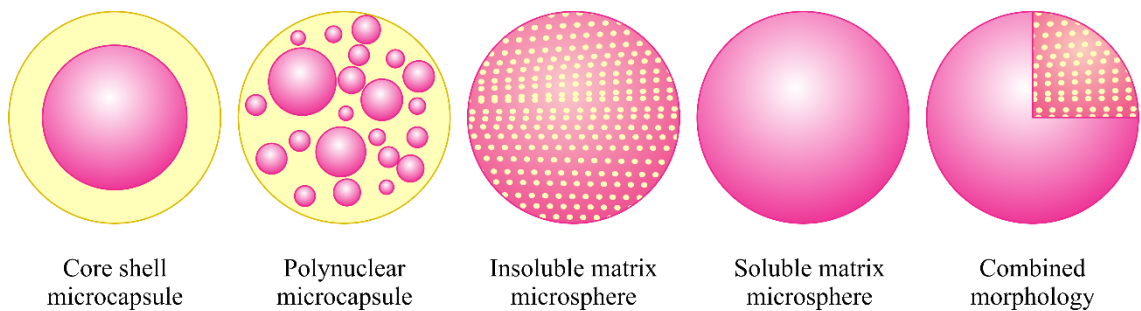


Fig. 2. Main morphology of microspheres and microcapsules. **(a)** Cutout of a microsphere and a microcapsule. **(b)** Different morphologies of microspheres and microcapsules. It is noteworthy that both morphologies can also exhibit an irregular shape.

The microcapsules have a well-defined inner core (active ingredient) and outer shell (encapsulating material). They can have a single core, multiple cores, or multilayers. Generally, this type of microparticle is obtained by microencapsulation processes such as complex

coacervation, polymerization in situ, solvent evaporation, and liposomes (TROJANOWSKA et al., 2017).

Microspheres are another well-known type of microparticles. They are characterized by having the active ingredient dispersed in the encapsulating matrix. Two types of microsphere morphologies differ from each other by the solubility between the active ingredient and the encapsulating material. The microsphere morphology can be selected according to the characteristics desired for the application. Although microcapsules provide better encapsulation, microspheres provide sufficient protection for some applications and can be achieved by a low-cost technique involving fewer unit operations. The spray drying and spray chilling techniques are widely used in the food, pharmaceutical, and cosmetic industries, and produce typical microsphere structures, in addition to other techniques such as freeze-drying, spray coating (fluid bed), extrusion, and emulsion-based processes. It is also possible to obtain microparticles by combining both microcapsules and microspheres (ARENAS-JAL; SUÑÉ-NEGRE; GARCÍA-MONTOYA, 2020).

Furthermore, microspheres can be classified differently, once their physical properties are affected by the polymorphic transitions of fatty materials. The main types of microspheres obtained according to the type and polymorphic behavior of the lipid material are shown in Fig. 3 (MÜLLER; RADTKE; WISSING, 2002b), which shows the microspheres trapping anthocyanin, which is an active food ingredient.

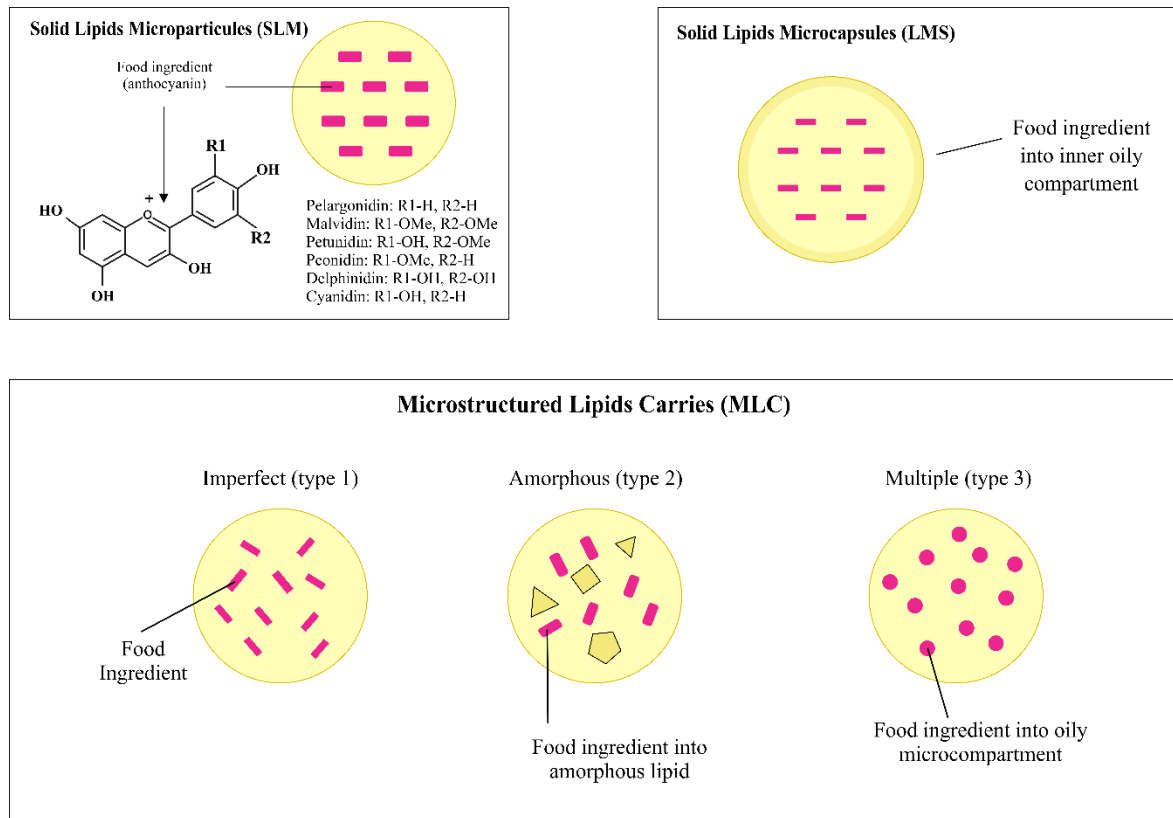


Fig. 3. Main types of lipid microparticles produced by spray chilling.

According to the types of lipids used, the microspheres produced by spray chilling can be named as follows (BATTAGLIA; UGAZIO, 2019; FADINI et al., 2018; MCCLEMENTS, 2020):

- Solid Lipid Microparticles (SLM);
- Microstructured Lipid Carriers (MLC): type 1, type 2, and type 3;
- Solid Lipid Microcapsules (LMS).

2.2.1 Solid Lipid Microparticles (SLM)

Solid lipid microparticles are the best-known type of lipid microspheres. SLM is constituted by solid lipids with a diameter between 3 to 800 μm (MCCLEMENTS, 2020). General ingredients include solid lipid(s), surfactant(s), and water. The term lipid is used in a broad sense and includes triglycerides, partial glycerides, fatty acids, steroids, and waxes. All

classes of surfactants (concerning the load and molecular weight) have been used to stabilize lipid dispersions; however, polyglycerol polyricinoleate has been efficiently used in W/O type emulsions (ZAFIMAHOVA-RATISBONNE et al., 2014).

SLMs were developed in the early 1990s and have long been considered promising drug carrier systems as they are stable from the physicochemical point of view, and can be easily produced on a large industrial scale, while the raw material and production costs are relatively low. A cross-sectional view of SLM delineates that the active ingredient fraction is embedded in the phospholipid layer (Fig.4). The positive aspect of the solid lipid core is that it reduces drug mobility, thus preventing degradation (MÜLLER et al., 2007).

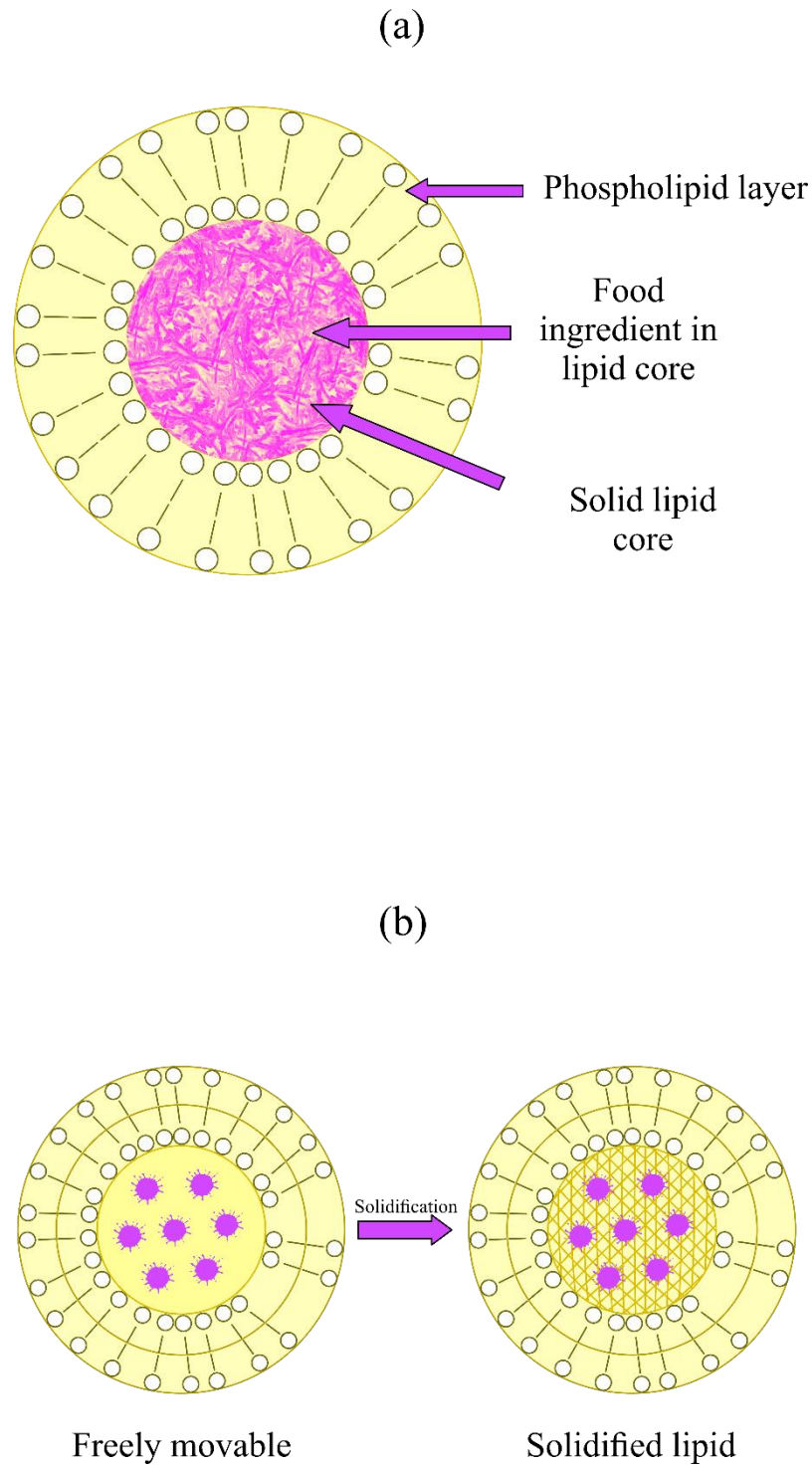


Fig. 4. Production mechanisms (a) and cross-section of SLM (b).

However, several problems have been associated with these particles such as (i) limited drug-carrying capacity and, (ii) drug release during storage (MÜLLER; RADTKE; WISSING, 2002a; SANTOS et al., 2019). This behavior is due to the packaging of solid fats, with a

predominance of saturated fatty acids, which occurs in a more organized manner (SATO; UENO, 2011). These limitations encourage researchers to develop a system known as structured micro (> 1000 nm) and nano (50 to 1000 nm) lipid carriers (BATTAGLIA; UGAZIO, 2019), and this type of microparticle has been used in spray chilling technology for food ingredients (CARVALHO et al., 2019; CONSOLI et al., 2016; RIBEIRO; ARELLANO; GROSSO, 2012).

2.2.2 Microstructured lipid carriers (MLC)

This system is characterized by the production of solid lipid micro or nanoparticles containing not only solid lipids but also a mixture of solid and liquid lipids, spatially incompatible, leading to special lipid structures, called microstructured lipid carriers (>1000 nm) (PEZESHKI et al., 2019).

The formation of a less ordered solid lipid matrix may favor the permanence of the active compound in the lipid matrix. Thus, lipids with different molecules exhibited particles with lipid structure with imperfections, which accommodate differently, favoring the permanence of the active compound inside the particles, which can also be located between the chains, depending on the conformation of the lipid molecules (MÜLLER; RADTKE; WISSING, 2002a).

Micro- or nano-structured lipid microparticles have a higher loading capacity, greater stability during storage, and controlled release of the encapsulated compound (BARROSO et al., 2021). These characteristics are achieved due to the disorganized structure of liquid and solid lipids, which can better accommodate the encapsulated material. The mixture of these lipids from different physical states produces a particle with a low crystallinity index and slower polymorphic transition. The presence of a liquid lipid in the core and the spherical structure of the particle contributes to increasing the efficiency of this system. Thus, the micro/nano-

structured lipid microparticles, in addition to improving the encapsulation yield and physical stability, have proven to be a valuable alternative to increase the controlled release and bioavailability of functional food ingredients, as reported by several authors (CARVALHO et al., 2019; GOMES et al., 2019a; MÜLLER et al., 2007; SADATI BEHBAHANI et al., 2019).

There are 3 main types of micro/nano-structured lipid microparticles (Fig. 3): 1 – imperfect type; 2 – amorphous type, and; 3 - multiple type (MÜLLER; RADTKE; WISSING, 2002a). The imperfect type is obtained when the crystallization of lipids is altered by small amounts of oil. In the amorphous type, the lipid matrix is solid, but not crystalline (amorphous state). In the multiple type, the solid lipid matrix contains tiny oil compartments. These microparticles are obtained by mixing a solid lipid with a larger amount of oil, for example blends containing low amounts of stearic acid and high amounts of oleic acid (BATTAGLIA; UGAZIO, 2019). The principle is that the microstructure of the lipid matrix increases the charge of the encapsulated material, and prevents the release of compounds during storage (MÜLLER et al., 2007; MÜLLER; RADTKE; WISSING, 2002b).

2.2.3 Solid Lipid Microcapsules (LMS)

Lipid microcapsules have a lipid-core shell microstructure. They are composed of an outer shell, formed by solid lipids and emulsifying agents, and an oily core. Unlike multiple-type MLC, which consist of a solid lipid matrix containing multiple oil compartments, LMS has a single lipid core containing the active ingredient, which is surrounded by a thin solid coating (core coating structure) (BATTAGLIA; UGAZIO, 2019).

3. Effect of spray chilling process parameters

3.1 Overview

Knowledge about the effects of the process parameters on the spray chilling technique is important to obtain satisfactory results. Several parameters should be considered, including high process yield, high encapsulation efficiency of the active ingredient, high retention of volatiles, good physical characteristics of the powder, among others (BERTONI; ALBERTINI; PASSERINI, 2019).

The main factors that can be optimized in the spray chilling process include (i) the melting temperature of the lipid compounds; (ii) the temperature of the atomizing air; (iii) the temperature of the cooling chamber; (iv) the atomizing air pressure; and (v) the feed flow rate of the molten mixture (FAVARO-TRINDADE et al., 2021).

3.1.1 Melting temperature of the lipid compounds

The lipid matrix is the basis for the microencapsulation of active compounds. The matrix melting temperature must be above 45°C to ensure some characteristics of the solid lipid microparticles, including the solid state over a wide temperature range, low adhesion rate, good fluidity, and high encapsulation efficiency, as well as ensuring the formation, stability, and high process yield (CONSOLI et al., 2016).

Low melting lipids such as cocoa butter and refined palm oil can cause several problems during and after spray chilling, when used individually (ORIANI et al., 2016), with no formation of solid lipid microparticles, as well as high adhesion in the cooling chamber, and low encapsulation efficiency. After the formation of microparticles, a high powder adhesion, agglomeration, and low microparticle fluidity is required (CARVALHO et al., 2019; CONSOLI et al., 2016; PROCOPIO et al., 2018).

On the other hand, lipids with a high melting point (>70°C) can lead to clogging of the atomizing nozzle, as well as thermal degradation of the active ingredient. In addition, the use of high melting point lipids alone leads to the formation of SLM-type particles, leading to the

release of the active ingredient during storage (MÜLLER; RADTKE; WISSING, 2002a). Modifications in the structure to the more perfect crystal form provide less space to accommodate the active ingredient molecules, leading to ingredient release (BERTONI; ALBERTINI; PASSERINI, 2019). In contrast, the particles obtained with high melting point lipids have excellent fluidity and stability characteristics (ORIANI et al., 2016). Thus, the selection of lipids depends largely on the heat sensitivity of the active ingredient.

3.1.2 Atomizing air temperature

To ensure a continuous and efficient process, the atomizing air temperature must be 10 °C above the highest melting point of the lipids used. If the temperature of the atomizing air is not properly reached, the atomizing nozzle will clog, with no formation of particles (CONSOLI et al., 2016) since the process must be interrupted to clean the atomizing nozzle, with a subsequent restart of the process.

3.1.3 Cooling chamber temperature

The good quality of the microparticles after the spray cooling process is closely related to the solidification step of the atomized droplets in the cooling chamber (FAVARO-TRINDADE et al., 2021), therefore, the lipid materials are largely responsible for the final quality of the product, as also occurring in the encapsulation by spray drying (Fernandes et al., 2014). In spray chilling, knowing the solidification behavior of lipids and the various mixtures is fundamental for the success of the technique.

To ensure that all particles are solidified during spraying, it is recommended to use lipid mixtures with a very narrow melting temperature range (BATTAGLIA; UGAZIO, 2019; CHAMBI et al., 2008). The solidification curve of the molten mixture used as the feed stream must be known. Thus, the material cools down to its solidification temperature when the

atomized droplets come into contact with the cooling air. Thereafter, the temperature remains constant during the heat release of the product, with the subsequent formation of stable solid lipid microparticles (BERTONI; ALBERTINI; PASSERINI, 2019).

For the complete formation of solid lipid microparticles, the pulverized material is subjected to three cooling stages: (i) cooling of the liquid, (ii) solidification, and (iii) cooling of the solid microparticles (FAVARO-TRINDADE et al., 2021).

The solidification of the microparticles happens progressively; first, the temperature of the sprayed droplets decreases as they come into contact with cold air. Then, the droplets reach the solidification temperature and gradually crystallize until complete stability, which will depend on the polymorphic form of the lipid mixture. Therefore, it is recommended to package the solid lipid microparticles at low temperatures after the end of the spray cooling process until they reach stability (BERTONI et al., 2019; CONSOLI et al., 2016).

In lipids, the stability of the polymorphic forms follows the order $\alpha < \beta' < \beta$. In the case of rapid cooling, the lipid is preferably crystallized in its most unstable form (α). On the other hand, at slow cooling, there is a tendency to the stable form β (CARVALHO et al., 2019; SATO, 2001). Therefore, the control and maintenance of the temperature during the solidification of the particles in spray cooling is essential to obtain a high-quality final product.

3.1.4 Atomizing air pressure

The equipment for the production of solid lipid microparticles is a spray dryer adapted for a spray chiller (as shown in Fig. 1), thus the atomizing air pressures between 4 and 6 bar should preferably be used to ensure effective spraying, as recommended by the manufacturer (Labmaq do Brasil, Ribeirão Preto, São Paulo, Brazil).

So far, there are few studies on the effect of spray cooling process variables on the characteristics of the microparticles. Preliminary tests performed by our research team showed

that pressures below 4 bar were not sufficient to promote the atomization of the material, regardless of the type of lipid mixture or type of solution (emulsion or dispersion).

Maschke et al. (2007) evaluated the effects of spray cooling atomization pressure on the characteristics of solid lipid microparticles made from glycerol tripalmitate and insulin. The study showed that increasing the atomization pressure from 5 to 6 bar led to a reduction in the particle size, but higher yields were obtained at pressures of 5.5 and 5.9 bar. Thus, the greater the energy supplied, the smaller the droplet size, with lower efficiency, as very small droplets markedly increase the total surface area.

3.1.5 Feed flow rate of the molten mixture

The feed flow rate of the molten mixture can affect both the process yield and the characteristics of the microparticles (CONSOLI et al., 2016).

The two main factors that affect the flow rate are equipment configurations, for example, with or without a pump system, and the viscosity of the molten mixture, as high viscosities impair atomization, generating larger particles or even clogging of the atomizing nozzle. A high feed rate of the molten mixture increases the particle size while providing greater control of the microparticle size, which can be achieved by controlling the atomizing pressure (CARVALHO et al., 2019; FAVARO-TRINDADE et al., 2021).

However, further studies are required to investigate the effects of the process variables on the spray chilling technology, mainly taking into account the type of equipment as each equipment has minimum and maximum parameters required for an efficient process.

4. Properties of the microencapsulation process by spray chilling

A precise assessment of the spray chilling properties is necessary, as they have a direct impact on the technological behavior of the lipid microparticles. These properties and the techniques used for analysis will be detailed below.

4.1 Type and characteristics of the lipid encapsulating materials

A careful selection of the encapsulating material must be made for all microencapsulation techniques (BOTREL et al., 2014). Encapsulating materials used for the preparation of solid lipid particles are selected for their biocompatibility, availability, and price. For food application purposes, the encapsulating materials are restricted to food grade and must be approved by authorities such as FDA and EFSA or certified as generally recognized as safe (GRAS). Therefore, the alternatives of encapsulating materials are more limited for food products when compared to pharmaceuticals and cosmetics (FURUTA; NEOH, 2020). In addition, they must also preserve the bioactive compounds from decomposition during processing and storage conditions, and not chemically interact with other active agents incorporated into the system (CONSOLI et al., 2016).

In spray chilling, the stability of the microparticles and the encapsulation efficiency are significantly affected by the type and proportion of the encapsulating materials, and food-grade lipids should be used for the development of lipid microparticles for food applications (FAVARO-TRINDADE; OKURO; MATOS-JUNIOR, 2015; OKURO; MATOS-JUNIOR; FAVARO-TRINDADE, 2013).

The selection of the encapsulating material depends on the active ingredient to be encapsulated. For example, for an ingredient sensitive to high temperatures, lipids with a melting point that do not interfere with the properties of the encapsulated material while protecting against the external environment should be used. However, the use of lipid materials with a low melting point may require temperature-controlled storage after the formation of the

particles to ensure integrity until application. Lipids with a melting temperature above 45°C are desirable for the formation and application of lipid microparticles (CONSOLI et al., 2016). Other requirements for the encapsulating materials include (ORIANI et al., 2018; PELISSARI et al., 2016; YIN; CADWALLADER, 2019):

- Stability in equipment operating conditions;
- Process-friendly rheological properties and ease of handling during encapsulation
- Low reactivity in the medium and no reactivity with the active ingredient;
- Ability to retain the active ingredient within its structure during processing and storage;
- Provide maximum protection for the active ingredient against external environmental conditions (light, heat, humidity) and;
- Specific ability to achieve the release of the active ingredient.

Usually, a single encapsulating material is not able to meet all these requirements, thus blends of these materials are generally used (ORIANI et al., 2018). It is also noteworthy that if the active ingredient is not compatible with the matrix material and does not easily settle or separate in the feed tube before spraying, surfactants or dispersing agents can be used.

Various solid and liquid lipids have been widely used in spray chilling technology (BARROSO et al., 2021; BATTAGLIA; UGAZIO, 2019). They can be divided into several categories, including waxes, vegetable oils, fatty acids, fatty alcohols, and triglycerides. Table 1 shows some examples of materials belonging to each group.

Table 1.

Types of lipids used in microencapsulation by spray chilling.

Lipids	Chemical composition	Properties	Examples
Fatty acids	Long-chain fatty acids	Melting point = 60-90 °C	Palmitic acid, stearic acid, behenic acid, lauric acid
Triglycerides	Monoacid triglycerides	Melting point = 46-73 °C	Glyceryl tripalmitate (Dynasan 116), glyceryl trimyristate, glyceryl trilaurate
Waxes	Long-chain fatty acid esters and alcohols	Melting point = 62-86 °C	Carnauba wax, candelilla wax, beeswax, solid paraffin, rice bran wax
Hydrogenated and non-hydrogenated vegetable oils	Mixture of triglycerides, free fatty acids, phospholipids	Hydrogenated - melting point = 60-71 °C	Hydrogenated or non-hydrogenated soy and palm oil
Fatty alcohol	Mixture of fatty alcohols	Non-hydrogenated - melting point = 13°C	Cetyl alcohol, lauryl alcohol, stearyl alcohol, oleyl alcohol

4.2 Determination of the concentration of the active ingredient

The actual or experimental amount of the active compound in the microparticles after the spray chilling is defined as “active ingredient content”, and can be expressed as the percentage by mass (% w/w) (BERTONI; ALBERTINI; PASSERINI, 2019).

The content of this ingredient is closely related to the proportion of the active ingredient used in the production of the microparticles. It is affected by the process (operating parameters and equipment) and formulation variables (e.g. hydrophilic or hydrophobic active ingredient and characteristics of the encapsulating material) (BERTONI; ALBERTINI; PASSERINI, 2019; SORITA et al., 2021).

In general, the microparticles are treated with solvents or heat to dissolve/melt the encapsulating material for the release/extraction of the encapsulated ingredient. The amount of active compound should be determined using an appropriate analytical method, which may vary according to the size of the microparticles and the theoretical value (BERTONI; ALBERTINI; PASSERINI, 2019).

The true concentration of the active ingredient in the microparticles after the spray chilling and the theoretical value is used to estimate the process efficiency, also known as encapsulation efficiency (JAFARI et al., 2008).

Spray chilling has proven to be a very promising technique for presenting very high encapsulation efficiencies. Some authors studied Gallic acid encapsulated by spray chilling in a matrix of fully hydrogenated soybean oil and fat, at 90:10 (fully hydrogenated soybean oil: soybean oil) and 30:70 (Gallic acid: lipid matrix) ratio, and found an encapsulation efficiency of 100% (CONSOLI et al., 2016).

In another study using the same technique, ascorbic acid was encapsulated in a matrix containing fully hydrogenated palm oil and fat. The authors produced microparticles with

different oil and palm fat ratios and reported encapsulation efficiency ranging from 83 to 96% (CARVALHO et al., 2019).

Procopio et al. (2018) evaluated the cinnamaldehyde retention of microencapsulated cinnamon bark oleoresin by spray chilling using fully hydrogenated palm oil and fat. Different concentrations of oleoresin (1 and 2%) and different oil and palm fat ratios were used. The authors reported low retention of cinnamaldehyde, probably due to the use of heating during the atomization process, which may have led to the volatilization of compounds. The maximum percent retention was 69.49% and the minimum 8.28%, with the higher values observed for the formulations containing only fully hydrogenated palm fat, for both concentrations of 1 and 2% oleoresin. However, with the increase in the proportion of liquid oil, higher retention percentages were observed for the concentration of 2% oleoresin when compared to the concentration of 1%. It is worth emphasizing that the microparticles produced only with saturated fat can lead to greater expulsion of the active compound during storage. This behavior is due to the tendency of the lipid crystal chains to reorganize in a more compact structure, thus releasing the active ingredient (MÜLLER; RADTKE; WISSING, 2002a).

Vitamin B12 was encapsulated in a matrix containing vegetable fat with a melting point of approximately 48°C and soy lecithin. The microparticles obtained by spray chilling showed high encapsulation efficiency (76 to 100%). Concentrations of 0.10 and 1% of vitamin B12 and 0, 2.5, and 5.0% of soy lecithin were used, and a more effective encapsulation was observed for the formulations containing higher vitamin concentrations (CHALELLA MAZZOCATO; THOMAZINI; FAVARO-TRINDADE, 2019).

In contrast, Matos-Jr et al. (2015) encapsulated ascorbic acid by spray chilling technique for application of microparticles in an emulsified meat product and reported that the higher the concentration of active material and the smaller the particle diameter, the less effective the encapsulation. Those authors also studied the encapsulation of probiotic microorganisms using

the same technique and reported that the microparticles produced by spray chilling were the matrix type, thus the active material was dispersed throughout the volume of the microparticles rather than inside the particles, such as the reservoir type. Thus, the smaller the size of the microparticles, the greater the surface area and the greater the presence of active material on the surface (OKURO et al., 2013).

These examples demonstrate that the performance of the encapsulation by spray chilling is greatly affected by the proportion and nature of the active ingredient and the lipid materials, suggesting that the concentration of the active ingredient and the encapsulating materials should be carefully selected according to the purpose of application of the microparticles.

4.3 Particle size distribution

Particle size is a fundamental property that directly affects the performance of the encapsulated active ingredient. For example, it influences the fluidity and dissolution of microparticles, particle stability, the controlled release, and the stability of the encapsulated compounds (CAMPELO et al., 2017c).

It can be expressed as mean diameter \pm standard deviation or mean diameter. The mean diameter can be expressed as d50, d10, and d90, which are so-called percentile values, indicating the size below which 10%, 50%, or 90% of all particles are found. The particle size distribution also provides information on the dispersibility of the samples, most commonly mono- or poly-dispersibility of the microparticle batch (BERTONI; ALBERTINI; PASSERINI, 2019).

Studies on spray chilling technique have shown particle diameters ranging from a few microns to hundreds of microns (CARVALHO et al., 2019; CONSOLI et al., 2016; ORIANI et al., 2018; PELISSARI et al., 2016; SILVA et al., 2019). According to those authors, the main factors influencing the particle diameter are the type of atomizing nozzle, atomizing pressure,

feed rate, the nature, and proportion of the active compound and matrix, and the viscosity of the molten liquid to be atomized. Increasing the atomizing pressure can lead to a decrease in the particle size while increasing the feed rate can produce a non-uniform distribution of the particles. The low viscosity of the liquid leads to the production of smaller particles, while a higher viscosity allows for the formation of larger particles.

4.4 Morphology of the solid lipid microparticles

The particle morphology, as well as the particle size, exerts influences on technological properties such as fluidity and performance of the active ingredient (OH et al., 2014). Defects such as cracks can facilitate the release and degradation of the ingredient trapped within the microparticle (BOTREL et al., 2012), while imperfections or irregular shapes can impair the contact surface area available for transfer of the active compound (BERTONI et al., 2019).

Most studies on solid lipid microparticles obtained by spray chilling in the pharmaceutical, cosmetics, and food sectors have reported that the particles are dense and mostly spherical, and free-flowing (ALEMZADEH et al., 2020; OKURO; MATOS-JUNIOR; FAVARO-TRINDADE, 2013; ORIANI et al., 2018), which can explain the high encapsulation efficiency found in those studies.

Some factors are directly related to the morphology of the solid lipid microparticles, including solid to liquid fat ratio, the cooling temperature of the microparticles during atomization, and storage conditions (CARVALHO et al., 2021; HUANG et al., 2019).

Whereas the microparticles produced by spray chilling are based on a lipid matrix, their morphology is closely related to the lipid behavior. Microparticles with high liquid oil content tend to be more agglomerated and undefined in shape. Insufficient cooling for total solidification of the particles during atomization can also potentiate these effects (ORIANI et al., 2016). Similar behavior can occur during storage at temperatures above or near the melting

temperature of the lipid matrix (CARVALHO et al., 2019). The success of the process lies in the correct choice of the lipid materials and process variables, according to the objective of the application of the microparticles.

4.5 Interactions with the active food ingredients

The interactions between the active ingredient and the encapsulating material play a critical role in different aspects and influence the production capacity, physicochemical stability, and performance of the active ingredient. Four types of interactions can occur between the active food ingredient and the encapsulating material, including hydrogen bonding, ionic interaction, dipole-dipole interaction, and Van der Waals interaction, and the formation of hydrogen bonds is the most common type of interaction (BERTONI; ALBERTINI; PASSERINI, 2019).

In spray chilling processes, the encapsulating material and the active ingredient are intimately mixed before atomization, which favors the interactions between the active ingredient and the molecules of the encapsulating agent in the liquid state. Interactions can also occur during the feeding step or persist after solidification of the solid lipid microparticles. Identifying possible interactions between components while still in the molten state is particularly important in spray chilling, as they can affect important properties of the molten mixture, such as viscosity. Furthermore, the specific interactions between the active ingredient and the encapsulating material play a significant role in the formation of eutectic systems (VAN DUONG et al., 2018).

Some authors studied the interactions formed between ascorbic acid and refined oil and fully hydrogenated palm oil as encapsulating materials in spray chilling and reported a marked reduction in ascorbic acid crystallinity after the process (CARVALHO et al., 2019). The reduction in crystallinity may be due to the interactions between the active compound and the

encapsulating agent, or the rapid cooling and solidification of the molten droplets during spray chilling. The rapid solidification of the droplets can prevent the ascorbic acid molecules from reorganizing into their crystalline form. Strong intermolecular bonds between ascorbic acid and the encapsulating materials can provide enough energy to keep the active agent in an "unstable" state, once ascorbic acid remains in an amorphous state or is dispersed at a molecular level within the encapsulating material (BERTONI; ALBERTINI; PASSERINI, 2019).

The Fourier Transform Infrared Spectroscopy (FTIR) can be used to investigate the interaction mechanisms at the molecular level. It allows monitoring the vibrations of the functional groups that characterize the molecular structure in solid state reactions. It is also possible to detect changes in the solid state such as hydrogen bonds or $\pi - \pi$ interactions that are recognized as peak changes of functional groups (VAN DUONG; VAN DEN MOOTER, 2016).

4.6 Solid state properties of the active ingredient and the encapsulating material

It is worth emphasizing that the active ingredient can be present in three different molecular states, including amorphous, crystalline, or semi-crystalline states, as shown in Fig. 3. These molecular states are dependent on the formulation, and directly affect the dissolution performance of the active ingredient and, consequently, its release and bioavailability. As previously discussed, a large part of the mass of solid lipid microparticles is constituted by the encapsulating materials, thus their characteristics play an important role in their properties and behavior (BERTONI; ALBERTINI; PASSERINI, 2019). Therefore, knowledge about the possible polymorphic modifications of lipid materials (for example, from crystalline to semi-crystalline form) during or after the spray chilling process can prevent undesirable reactions in the microparticles.

Furthermore, the mutual effect of the active ingredient and the encapsulating material in its specific solid state should also be considered. Concerning microparticles produced by spray chilling, the following factors contribute to determining the solid state of the active ingredient: (i) active ingredient-encapsulant interaction, as discussed in the previous paragraph; (ii) the nature of the encapsulant, such as its viscosity and tendency to crystallize; (iii) the nature and amount of the active ingredient; (v) the process parameters, mainly the rate and temperature of the cooling phase; and (iv) the storage conditions (BERTONI; ALBERTINI; PASSERINI, 2019; CARVALHO et al., 2019; CONSOLI et al., 2016).

Analytical methods are used to detect changes in the solid state of the active ingredient and the encapsulating agent, as well as the microparticles produced by spray chilling. X-ray diffraction (XRD) provides information about the crystal phase of the sample by the presence of diffraction peaks (SANTOS et al., 2020). The changes in the physical properties of the active ingredient and the encapsulating material can be determined by comparing the diffractograms of each compound separately and the microparticles produced by spray chilling (MÜLLER; RADTKE; WISSING, 2002b). The differential scanning calorimetry (DSC) technique can be used to study the behavior of lipids in phase transitions such as melting and solidification, in addition to the transformations between the various polymorphic forms (SATO, 2001). Nuclear magnetic resonance (NMR) can also predict the overall behavior of lipid and its mixtures, providing solid fat content (SFC) over a wide temperature range. NMR is considered the most accurate technique to identify the absolute content of solid fat content (ORIANI et al., 2016; RIBEIRO; ARELLANO; GROSSO, 2012), and SFC curves can be used to predict the type of fat application. For example, the liquid/solid fractions of a lipid at different temperatures can be identified through an iso-solids diagram, which represents the solids fat content of various compositions at constant temperature (O'BRIEN, 2004; TIMMS, 1985). Therefore, this

information can be used to understand the behavior of lipids and assist in the development of novel fat-based products.

The physical property of the polymorphic transitions affects the production of solid lipid microparticles, with a low encapsulation efficiency and core release during storage, due to crystal reorganization into a more stable polymorphic form (RIBEIRO; ARELLANO; GROSSO, 2012). When the polymorphic form of the active ingredient and the encapsulating agent is maintained, the peaks are formed at the same diffraction angles, while different polymorphs lead to the formation of different angles, which can also be observed in the case of amorphization, i.e., absence of sharp refraction peaks, called an amorphous halo. Finally, the reduction in crystallinity can be detected by the formation of less sharp and less intense diffraction peaks (BERTONI; ALBERTINI; PASSERINI, 2019).

Some authors investigated lycopene dissolved in sunflower oil and encapsulated by spray chilling using fat with a melting point of 51°C. The microparticles were stored at 4 °C for 90 days and analyzed by X-ray diffractometry. The authors reported that both sunflower oil and lycopene solutions appeared as amorphous materials, and the fat presented a crystalline state. On the other hand, the microparticles exhibited as crystalline materials, governed by the fat behavior. The authors also noticed that increasing the concentration of the lycopene solution in the formulations led to a gradual reduction in the relative intensity of the microparticles diffraction peaks. However, they concluded that the fat crystal was not affected by the process or the incorporation of the lycopene/sunflower oil solution for all concentrations studied. Thus, the diffraction peaks of the diffractograms of both fat and microparticles corresponded to the polymorphic phase β' (PELISSARI et al., 2016).

5. Applications in foods

The potential increase in consumer interest in healthier and more natural foods has encouraged the food industry to use natural ingredients such as bioactive compounds. However, the sensitivity to processing, storage, and gastrointestinal conditions of these natural compounds has prompted food scientists to develop technologies to overcome these limitations.

Studies have shown that microencapsulation contributes to the development of novel foods, as well as new structures for food packaging. This stimulating potential has led the industry to invest heavily in the development of encapsulation techniques for delivering food ingredients, such as solid lipid nano/microparticles. Microencapsulation plays a huge impact, transforming essential and conventional foods into fortified processed foods for better nutritional, functional, and controlled delivery.

As reported by Bao et al. (2019), it is estimated that more than 40% of the food industries use the microencapsulation process. A study by the market research and consulting journal *Markets and Markets*, published in March 2020, reported that the global food packaging market was valued at \$9.9 billion in 2020 and is projected to exceed \$14 billion by 2025 with an annual growth rate (CAGR) of 7.5% during the period. This market is mainly driven by the growing demand for encapsulated flavors and dyes in the food and beverage industry, along with the high consumer demand for fortified and functional foods.

Solid lipid microparticles have been proposed for the release of drugs, enzymes, probiotics, vitamins, minerals, flavors, antioxidants, antimicrobials with several purposes (MCCLEMENTS, 2020), ensuring better bioavailability, stability, and delivery at the desired time and place (FREDES et al., 2018). The microparticles also prevent interactions with the food matrix and allow the conversion of ingredients to easily handled and dispersible powders, in addition to masking undesirable odor and taste, improving the retention of volatile compounds, and promoting controlled release by different factors such as dissolution, temperature, pressure, pH and enzymes, depending on the encapsulating material used

(BOTREL, BORGES et al., 2014; CAMPELO-FELIX et al., 2017; CARMO et al., 2018; FERNANDES et al., 2014; FIGUEIREDO et al., 2020).

The most relevant studies using spray chilling technology in the food area are discussed below and can be seen in Table 2.

Table 2.

Application of spray chilling technology for the microencapsulation of food ingredients.

Encapsulating material	Active material	Emulsifier	Reference
Vegetable fat	Vitamin B12	Soy lecithin	(Chalella et al., 2019)
Hydrogenated palm oil and fully hydrogenated vegetable oils	Green tea extract	Not used	(Cutrim; Alvim; Cortez, 2019)
Palmitic acid, oleic acid, and palm fat	Ginger oil resin	Not used	(Oriani et al., 2016)
Refined palm oil and fully hydrogenated palm fat	Ascorbic acid	Not used	(Carvalho et al., 2019)
Vegetable fat and beeswax	Vitamin D3	Soy lecithin	(Paucar et al., 2016)
Hydrogenated palm oil	<i>S. boulardii</i> , <i>L. acidophilus</i> , and <i>B. bifidum</i>	Tween 80	(Arslan-Tontul; Erbas, 2017)
Fully hydrogenated soy fat and refined soy oil	Gallic acid	Polyglycerol polyricinoleate	(Consoli et al., 2016)
Shortening composed of hydrogenated and interesterified cottonseed, soy and palm oils (mp 51°C)	Lycopene	Not used	(Pelissari et al., 2016)
Octacosan paraffin	2-acetyl-1-pyrroline zinc chloride	Not used	(Yin; Cadwallader, 2019)
Fully hydrogenated palm oil and vegetable oil	Fish oil	Polyglycerol polyricinoleate	(Fadini et al., 2019)

Table 2 (continued).

Encapsulating material	Active material	Emulsifier	Reference
Vegetable fat	Guarana seed powder extract	Not used	(Silva et al., 2019)
Stearic acid	Genipap extract	Polyglycerol polyricinoleate	(Neri-Numa et al., 2020)
Fully hydrogenated palm fat and palm fat	Cinnamon Bark Oil Resin	Not used	(Procopio et al., 2018)
Lauric acid and oleic acid	Ascorbic acid	Polyglycerol polyricinoleate	(Sartori et al., 2015)
Interesterified fat from palm oil and corn oil with a melting point of 43°C	Ascorbic acid	Soy lecithin	(Matos-Jr et al., 2017)
Stearic acid and hydrogenated fat with melting point 43°C	Ascorbic acid	Not used	(Alvim et al., 2016)
Vegetable fat with a melting point of 48°C	Cinnamon bark extract, proanthocyanidin, and alpha-tocopherol	Not used	(Tulini et al., 2017)
Vegetable fat with a melting point of 48°C	<i>Lactobacillus acidophilus</i> LA3 (LA) and <i>Bifidobacterium animalis</i> subsp. <i>Lactis</i> BLC1 (BLC)	Gelatin and gum Arabic	(Silva et al., 2018c)
Palm fat	Capsaicin (66.7%)	Soy lecithin and whey protein isolate	(Günel et al., 2021)
Vegetable fat with a melting point of 51°C	Soy Protein Hydrolysate	Polyglycerol polyricinoleate, Tween 80, and soy lecithin	(Salvim et al., 2015)
Beeswax, carnauba wax, and medium-chain triglycerides (Miglyol 812)	Curcumin (85% purity)	Not used	(Sorita et al., 2021)
Fully hydrogenated palm fat (mp 63°C)	Iron, Iodine, and Vitamin A	Soy lecithin	(Wegmüller et al., 2006)

5.1 Vitamins and Minerals

Solid lipid microparticles have great potential to efficiently protect vitamins and minerals against degradation, as they are generally sensitive to light and oxygen (Gu et al., 2016; Matos-Junior et al., 2016). Furthermore, they can improve the bioavailability of these compounds (GOMES et al., 2019a).

Although ascorbic acid is one of the most studied vitamins by spray chilling to date, other vitamins such as, B12, D3, and E have also been investigated. Different studies have shown the potential of spray chilling in the controlled release of vitamins, and greater protection and stability during storage (CARVALHO et al., 2019; CHALELLA MAZZOCATO; THOMAZINI; FAVARO-TRINDADE, 2019; GAMBOA; GONÇALVES; GROSSO, 2011; MATOS-JR et al., 2017; PAUCAR et al., 2016; SARTORI et al., 2015; TULINI et al., 2017).

Ascorbic acid microparticles were obtained by spray chilling using stearic acid and hydrogenated vegetable shortening as encapsulating materials and applied in short dough biscuits. One of the main objectives of the study was to evaluate the stability of ascorbic acid of these microparticles after baking the cookies. The authors reported that the addition of microparticles (0.3 g/100g of dough) did not affect the appearance or the manufacturing stages of the cookies. The microparticles adequately protected the ascorbic acid, preserving more than 85% of the ascorbic acid content, when compared to the compound used in free form (28% loss of ascorbic acid). Therefore, the microparticles are potential protection vehicles in the application of sensitive compounds in bakery products (ALVIM et al., 2016).

Vitamin D supplementation is increasingly common due to consumer awareness of its important biological roles, whose deficiency causes severe health problems (MAURYA; BASHIR; AGGARWAL, 2020). Microencapsulation by spray chilling is an excellent alternative to prevent the rapid degradation of this vitamin and improve its absorption. Vitamin D3 is fat-soluble, thus it requires the use of lipid foods as vehicles, which is not compatible

with the consumer demand for low-fat foods. Therefore, the immobilization of vitamin D3 through fatty encapsulants can overcome this problem. In addition, the release of vitamin D from solid lipid microparticles into the intestine can be regulated by fat digestion, leading to greater bioavailability. Paucar et al. (2016) produced microparticles containing vitamin D3 and vegetable fat and beeswax as encapsulating materials. After a 65-day storage period at 25°C, a vitamin loss of only 14% was observed for the encapsulated vitamin when compared to a 39% loss of the free vitamin. These results are promising and demonstrate the potential of spray chilling for the production of microparticles containing vitamin D3, encouraging future applications in food.

Gallic acid is considered a potent natural antioxidant and was also microencapsulated by spray chilling in a matrix of soybean oil and fully hydrogenated soybean fat. Although the release kinetics and stability studies have not been performed, the authors found encapsulation efficiency greater than 80% (CONSOLI et al., 2016), indicating that this technology can be efficient in the microencapsulation of antioxidant compounds.

Some authors evaluated the encapsulation of green tea extract powder (*C. sinensis*) by spray chilling and ionic gelation. For the production of solid lipid microparticles by spray chilling, the authors used fully hydrogenated palm oil and hydrogenated and interesterified vegetable fat. For the microparticles produced by ionic gelation, amidated low methoxylated pectin, calcium chloride, citric acid, rapeseed oil, and polyglycerol polyricinoleate were used. Satisfactory results were observed and both techniques were able to produce water-insoluble microparticles rich in polyphenols. The spray chilling technology demonstrated greater encapsulation efficiency (approximately 84%) when compared to ionic gelation (73%). Greater antioxidant activity was obtained for solid lipid microparticles (35 IC50 ug/MI) when compared to the microparticles produced by gelation (33 IC50 ug/MI). According to the authors, both

microparticles were considered suitable as ingredients for the incorporation of polyphenols in foods (CUTRIM; ALVIM; CORTEZ, 2019).

Minerals such as iron and zinc play important roles in the body. Iron plays many critical roles in growth and its deficiency leads to anemia, low immunity, and negatively affects mental development. Although iron fortification of foods can minimize this problem, the incorporation of iron in foods can adversely affect their physicochemical and sensory characteristics. Furthermore, for adequate absorption, iron must be bioavailable after ingestion. Thus, encapsulation can be used to increase the stability and bioavailability of iron-fortified foods, as well as providing greater protection against oxidation and controlled release (YANG et al., 2015).

5.2 Natural dyes

Little is known about the effects of spray cooling on the production of natural dyes. In a recent study, turmeric was microencapsulated by spray chilling using beeswax, carnauba wax, and medium-chain triglycerides as encapsulating materials. The results showed that it was possible to incorporate curcumin into encapsulating matrices and obtain suitable microparticles. The highest encapsulation efficiency was 85%, which was dependent on the encapsulating materials. However, further studies on particle stability and its application in food matrices are needed to assess the real applicability of these microparticles (SORITA et al., 2021).

Genipap extract represents an emerging source of blue dyes with wide application possibilities. In a recent study, genipap extract was encapsulated using the spray chilling using stearic acid as an encapsulating agent and polyglycerol polyricinoleate as an emulsifying agent. The microparticles showed intermediate protection against degradation of the genipap extract. These microparticles showed desirable effects on the viability of human cancer cells, as well as on the induction of apoptosis in leukemia cells (at a dosage of 25 µg/mL). However, various issues should be assessed, including the toxicological risks of genipap extract, use of different

encapsulating materials to produce microparticles containing this extract, the particle release under simulated GI conditions, and application of the microparticles in food matrices and therapeutic use (NERI-NUMA et al., 2020).

5.3 Other bioactive compounds

Other types of compounds can be encapsulated by spray chilling for different purposes. Some examples include prebiotics, probiotics, enzymes, microorganisms, peptides, fatty acids (omega 3), essential oils, flavors, fragrances, and antioxidants (quercetin). As discussed above, these compounds, when microencapsulated, can have great potential for the production of fortified foods and beverages (DELSHADI et al., 2020; TAVARES; SANTOS; ZAPATA NOREÑA, 2021; ZANETTI et al., 2018). Functional and fortified foods are one of the new food trends, especially after the catastrophic consequences on the health of consumers after the Covid-19 pandemic. Furthermore, the sensory characteristics of foods can also be improved using this technology.

6. Controlled release mechanisms and bioavailability in vitro

The controlled release is one of the most desirable properties in encapsulation techniques. It prolongs the biological activities of the encapsulated active ingredients, modifies and/or maintains flavors and odors, such as allowing an explosion of flavors or ensuring long-term maintenance, and increases the bioavailability of the compounds after gastrointestinal digestion (ALEMZADEH et al., 2020).

These mechanisms are governed by different physical systems, which aim to modulate the release of the encapsulated active ingredient. In general, this effect is achieved after a specific stimulus, that is, the occurrence of a certain event that allows the particle release. Factors such as the geometry of the active ingredient, the encapsulating material, or the presence of surfactant can determine the particle release mechanism (Figueiredo et al., 2020; Boostani & Jafari, 2021).

In spray chilling technology, the release of the active ingredient usually occurs by erosion and leaching of the matrix, due to its hydrophobic nature (FAVARO-TRINDADE et al., 2021) or by diffusion (CHALELLA MAZZOCATO; THOMAZINI; FAVARO-TRINDADE, 2019; PAUCAR et al., 2016). The presence of surfactants, as well as the temperature conditions, can also affect the release of compounds. In these cases, two distinct concepts stand out. The first is related to temperature sensitivity, which is important for materials that expand or shrink when reaching a critical temperature; the second concept is related to the melting of the encapsulating material in response to an increase in temperature, as observed for microparticles consisting of a modified lipid or waxes (FAVARO-TRINDADE et al., 2021).

Concerning the vitamins, natural pigments, and essential oils, which are potentially oxidizable compounds, the microencapsulation by spray chilling can, in addition to increasing stability, promote the compound release at the desired location and time, for example, after ingestion of food, that is, in the stomach or intestine, once the lipid matrix can promote the enteric release (FAVARO-TRINDADE et al., 2021).

A study evaluated solid lipid microparticles containing vitamin C produced by spray chilling using palm oil and fat, which allowed a slow and controlled vitamin release in an aqueous medium. The authors reported that the different concentrations of the encapsulating materials have also influenced the release of vitamin C. Within 180 minutes, the microparticles containing different palm oil and fat ratios were able to release 15 to 10% of vitamin C. Therefore, it is possible to maintain high vitamin concentration within the microparticles, with a controlled and slower release (CARVALHO et al., 2019). Similar results were observed in another study of controlled release in an aqueous medium of vitamin C lipid microparticles (SARTORI et al., 2015). All authors reported the effects of the lipid materials on the release of vitamin C.

The limited chemical stability of the bioactive compounds present in vitamins, microorganisms, proteins, and peptides, natural dyes, and essential oils leads to low bioavailability, less transfer across the biological membranes, and low stability in the bloodstream (BATTAGLIA; UGAZIO, 2019). Efforts aimed at encapsulation technologies have improved the bioavailability in vitro of these compounds (GHARIBZAHEDI; SMITH, 2021; RODRÍGUEZ-ROQUE et al., 2013; ZHANG et al., 2020b).

For effective intestinal absorption, the microparticles must protect the bioactive compounds against acid and enzymatic degradation when exposed to gastric fluid. That is, the wall materials must be tolerant to gastric stimuli, such as extremely low pH and pepsin present in the stomach. In contrast, when microparticles reach the small intestine, they need to efficiently release core materials (PEDROSO et al., 2013).

The increase in bioavailability in vitro of the active ingredients by spray chilling depends on two effects: (i) effects independent of the physical state of the active ingredient within the microparticles, and (ii) effects resulting from changes in the original crystalline state of the active ingredient. The second category is strictly dependent on the combination between the active compound and the encapsulating material and should be considered on a case-by-case basis, while the first can be ideally explored to increase the bioavailability of all poorly water-soluble drugs (FAVARO-TRINDADE et al., 2021).

Studies on simulated digestion in vitro of the microparticles produced by spray chilling revealed that most microparticles were able to maintain a gradual release in the stomach and especially a greater release in the gut phase, which is an interesting approach since the absorption of bioactive compounds occurs in the intestine. The studies also showed the effect of other variables such as the type of lipid material, use of emulsifiers, and the type of active ingredient in the release and protection of the microparticles in the gastric system (CHALELLA MAZZOCATO; THOMAZINI; FAVARO-TRINDADE, 2019; PAUCAR et al., 2016).

A study has shown that solid lipid microparticles produced with cocoa butter protected *Lactobacillus acidophilus* in gastric fluid and intestine under simulated conditions. However, a 33% loss of microparticles was observed, probably due to the heterogeneous composition and low melting point of cocoa butter. Some triglycerides may have melted at the temperature of the experiment (37°C), causing a premature release of the probiotics into the gastric fluid. The authors reported that the loss of viability of *Bifidobacterium. animalis* subsp. *lactis* and *L. acidophilus* can be prevented by increasing the initial number of viable cells in the microparticles, aimed to release an appropriate number of cells in the intestine. Another approach suggested by the authors is the production of microparticles using a lipid matrix with a higher melting point (BAMPI et al., 2016).

Tulini et al. (2017) reported that the use of soy lecithin as a surfactant in the production of solid lipid microparticles containing vegetable fat and cinnamon extract increased the stability of proanthocyanidins in the gastric fluid, thus increasing the release of this active compound in the intestinal phase.

7. Advantages and disadvantages of spray chilling

The spray chilling technique consumes less time and energy when compared to other methodologies of particle formation, once there is no use of solvents, thus it can be considered an environmentally adequate technique (BERTONI et al., 2018b). Other advantages include simplicity, formation of free-flowing microparticles, high encapsulation efficiency (90-100%) for a lipid matrix composed of solid and liquid lipids, ease of incorporation into different food matrices, non-toxicity, and the possibility of encapsulating hygroscopic and water-sensitive compounds (CHALELLA MAZZOCATO; THOMAZINI; FAVARO-TRINDADE, 2019; OXLEY, 2012; TOMŠIK et al., 2019). From an industrial point of view, it can be performed on an industrial scale and adapted for continuous manufacturing. Concerning the atomizing

equipment and mechanism procedures, spray cooling is closely linked to spray drying, thus the spray drying apparatus can be used for spray chilling processes with some modifications (CONSOLI et al., 2016).

As observed for all technological processes, spray chilling also has some disadvantages. The encapsulated material must be stable at the temperature necessary for melting the lipid matrix, and the possibility of physical changes during the process when using lipids such as glycerides and carnauba wax, affecting the stability and dissolution of the encapsulated compound. Clogging of the atomizer when using highly viscous mixtures can also be a disadvantage of the process (BERTONI et al., 2018a; CHALELLA MAZZOCATO; THOMAZINI; FAVARO-TRINDADE, 2019; OKURO; MATOS-JUNIOR; FAVARO-TRINDADE, 2013; SARTORI et al., 2015).

8. Current challenges of spray chilling

There are several current challenges of spray chilling technology in the production of food ingredients when compared to other processes. The challenges include the search for encapsulating materials of lipid origin that meet the characteristics of an ideal encapsulating agent, such as the food grade, melting point, oxidative stability, maintenance of the encapsulating structure throughout storage and use, among others. Queirós et al. (2020) developed a fully hydrogenated milk fat to be used as an encapsulating material and reported that fat allowed the formation of solid lipid microparticles in the β' form. Further studies are needed for the application of solid lipid microparticles in different foods and beverages.

Other challenges include the applicability of the microparticles produced by spray chilling in different food matrices, as well as the bioavailability in vitro and in vivo.

A forthcoming challenge includes process expansion, as well as optimization in equipment and procedures, to improve the performance in the manufacture of solid lipid microparticles.

9. Innovations

The production of enriched, functional, convenient, and tasty beverages is a major challenge for the food industry. In this context, spray chilling technology can provide innovative and satisfactory results to meet this demand. Most foods are made with a lipid base, thus the addition of solid lipid microparticles containing bioactive compounds, aromas, flavors, microorganisms, among other compounds can be incorporated into the common diet of individuals, such as dairy products, ice cream, cereal bars, meat products, and bakery products, thus providing tasty meals with health benefits. Although few studies have addressed the application of this technology in the food sector, it is known that spray chilling is an innovative technology with great potential to enhance the food and beverage sector.

Some recent studies have shown the improvement of microencapsulation by spray chilling in the food sector with the use of co-encapsulation and different encapsulating agents. Co-encapsulation allows the incorporation of two or more ingredients in the same matrix to be subjected to the encapsulation process. For example, the co-encapsulation of proanthocyanidins from cinnamon extract with α -tocopherol in solid lipid microparticles by spray chilling demonstrated an enhanced scavenging ability of α -tocopherol against reactive oxygen and nitrogen species (TULINI et al., 2017). Therefore, the addition of antioxidant compounds such as α -tocopherol to lipid microparticles produced by spray chilling may be a promising approach, as they can present a synergistic interaction and enhance the biological activities of the compounds (CHAWDA et al., 2017).

The investigation of different sources of encapsulating materials for use in spray chilling, such as edible butters from the Amazon region, can bring innovations to the food industry. In a recent innovative study, some authors developed lipidic microparticles made with anhydrous milk fat and fully hydrogenated soybean oil and reported the potential of the microparticles for

use in foods as crystallization inducers, structuring agents, and as encapsulating material (LANDIM NEVES et al., 2021).

10. Conclusions

Microencapsulation by spray chilling has been relatively little explored in the food sector when compared to spray drying. Although it is not a recent technique, microencapsulation technology has been gaining popularity in the last decade, with a significant increase in studies on the encapsulation of bioactive food ingredients. The increasing demand for healthy foods may have encouraged studies on encapsulated products that allow the incorporation of bioactive ingredients into food matrices. In this context, spray chilling is an expanding technology with many advantages and applications in a wide variety of industries. The technique involves trapping a compound within an encapsulating material of lipid origin, which protects the core material from the surrounding environment. Solid lipid microparticles can enable the production of functional foods and overcome many limitations in the food industry. In addition, the microparticles can increase the stability of aromas, flavors, pigments, and microorganisms, mask undesirable odors and flavors, allow controlled release, and increase the resistance to the GI tract, improving the bioavailability of bioactive compounds, with health benefits for consumers.

Acknowledgments

This study was supported in part by the Coordenação de Aperfeiçoamento de Pessoal de Nível Superior – Brasil (CAPES) – Finance Code 001. The authors thank the Conselho Nacional de Desenvolvimento Científico e Tecnológico - Grant number 578 403803/2016-0 (CNPq, Brasília, Brazil), and Fundação de Amparo à Pesquisa do Estado de Minas Gerais -

Grant number CAG_APQ_02464_16 (FAPEMIG, Belo Horizonte, Brazil), for financial support.

Declaration of interest

The authors declare there is no conflict of interest for this research.

References

- Alemzadeh, I., Hajiabbas, M., Pakzad, H., Sajadi Dehkordi, S., & Vossoughi, A. (2020). Encapsulation of food components and bioactive ingredients and targeted release. *International Journal of Engineering, Transactions A: Basics*, 33(1), 1–11. <https://doi.org/10.5829/ije.2020.33.01a.01>
- Alvim, I. D., Stein, M. A., Koury, I. P., Dantas, F. B. H., & Cruz, C. L. de C. V. (2016). Comparison between the spray drying and spray chilling microparticles contain ascorbic acid in a baked product application. *LWT - Food Science and Technology*, 65, 689–694. <https://doi.org/10.1016/j.lwt.2015.08.049>
- Arenas-Jal, M., Suñé-Negre, J. M., & García-Montoya, E. (2020). An overview of microencapsulation in the food industry: opportunities, challenges, and innovations. *European Food Research and Technology*, 246(7), 1371–1382. <https://doi.org/10.1007/s00217-020-03496-x>
- Arslan-Tontul, S., & Erbas, M. (2017). Single and double layered microencapsulation of probiotics by spray drying and spray chilling. *LWT - Food Science and Technology*, 81, 160–169. <https://doi.org/10.1016/j.lwt.2017.03.060>
- Bampi, G. B., Backes, G. T., Cansian, R. L., de Matos, F. E., Ansolin, I. M. A., Poletto, B. C., Corezzolla, L. R., & Favaro-Trindade, C. S. (2016). Spray Chilling Microencapsulation of *Lactobacillus acidophilus* and *Bifidobacterium animalis* subsp. *lactis* and Its Use in the Preparation of Savory Probiotic Cereal Bars. *Food and Bioprocess Technology*, 9(8), 1422–1428. <https://doi.org/10.1007/s11947-016-1724-z>
- Bao, C., Jiang, P., Chai, J., Jiang, Y., Li, D., Bao, W., Liu, B., Liu, B., Norde, W., & Li, Y. (2019). The delivery of sensitive food bioactive ingredients: Absorption mechanisms, influencing factors, encapsulation techniques and evaluation models. *Food Research International*, 120, 130–140. <https://doi.org/10.1016/j.foodres.2019.02.024>
- Barroso, L., Viegas, C., Vieira, J., Ferreira-Pêgo, C., Costa, J., & Fonte, P. (2021). Lipid-based carriers for food ingredients delivery. *Journal of Food Engineering*, 295, 110451. <https://doi.org/10.1016/j.jfoodeng.2020.110451>
- Battaglia, L., & Ugazio, E. (2019). Lipid nano- and microparticles: An overview of patent-related research. *Journal of Nanomaterials*, 2019, 1-22. <https://doi.org/10.1155/2019/2834941>
- Bertoni, S., Albertini, B., Dolci, L. S., & Passerini, N. (2018). Spray congealed lipid microparticles for the local delivery of β -galactosidase to the small intestine. *European Journal of Pharmaceutics and Biopharmaceutics*, 132, 1–10. <https://doi.org/10.1016/j.ejpb.2018.08.014>
- Bertoni, S., Albertini, B., Ferraro, L., Beggiato, S., Dalpiaz, A., & Passerini, N. (2019). Exploring the use of spray congealing to produce solid dispersions with enhanced indomethacin bioavailability: In vitro characterization and in vivo study. *European Journal of Pharmaceutics and Biopharmaceutics*, 139, 132–141. <https://doi.org/10.1016/j.ejpb.2019.03.020>

- Bertoni, S., Albertini, B., & Passerini, N. (2019). Spray Congealing: An Emerging Technology to Prepare Solid Dispersions with Enhanced Oral Bioavailability of Poorly Water Soluble Drugs. *Molecules*, *24*(19), 3471. <https://doi.org/10.3390/molecules24193471>
- Bertoni, S., Dolci, L. S., Albertini, B., & Passerini, N. (2018). Spray congealing: A versatile technology for advanced drug-delivery systems. *Therapeutic Delivery*, *9*(11), 833–845. <https://doi.org/10.4155/tde-2018-0049>
- Boostani, S., & Jafari, S. M. (2021). A comprehensive review on the controlled release of encapsulated food ingredients; fundamental concepts to design and applications. *Trends in Food Science & Technology*, *109*, 303–321. <https://doi.org/10.1016/j.tifs.2021.01.040>
- Botrel, D. A., Borges, S. V., Barros, R. V. De, & do Carmo, E. L. (2014). Optimization of Fish Oil Spray Drying Using a Protein : Inulin System Optimization of Fish Oil Spray Drying Using a Protein : Inulin System. *Drying Technology*, *32*(3), 279–290. <https://doi.org/10.1080/07373937.2013.823621>
- Botrel, D. A., Borges, S. V., Fernandes, R. V. D. B., Viana, A. D., Costa, J. M. G. da, & Marques, G. R. (2012). Evaluation of spray drying conditions on properties of microencapsulated oregano essential oil. *International Journal of Food Science & Technology*, *47*(11), 2289–2296. <https://doi.org/10.1111/j.1365-2621.2012.03100.x>
- Botrel, D. A., Fernandes, V. D. B., Borges, S. V., & Yoshida, M. I. (2014). Influence of wall matrix systems on the properties of spray-dried microparticles containing fish oil. *FRIN*, *62*, 344–352. <https://doi.org/10.1016/j.foodres.2014.02.003>
- Campelo-Felix, P. H., Souza, H. J. B., Figueiredo, J. D. A., Fernandes, R. V. de B., Botrel, D. A., de Oliveira, C. R., Yoshida, M. I., & Borges, S. V. (2017). Prebiotic Carbohydrates: Effect on Reconstitution, Storage, Release, and Antioxidant Properties of Lime Essential Oil Microparticles. *Journal of Agricultural and Food Chemistry*, *65*(2), 445–453. <https://doi.org/10.1021/acs.jafc.6b04643>
- Campelo, P. H., Figueiredo, J. de A., Ferraz, V., Yoshida, M. I., Fernandes, R. V. D. B., Botrel, D. A., & Borges, S. V. (2017). Hygroscopic thermal and chemical properties of cinnamon essential oil microparticles obtained by spray drying. *Emirates Journal of Food and Agriculture*, *29*(11), 884. <https://doi.org/10.9755/ejfa.2017.v29.i11.1499>
- Carmo, E. L. do, Teodoro, R. A. R., Félix, P. H. C., Fernandes, R. V. de B., Oliveira, É. R. de, Veiga, T. R. L. A., Borges, S. V., & Botrel, D. A. (2018). Stability of spray-dried beetroot extract using oligosaccharides and whey proteins. *Food Chemistry*, *249*, 51–59. <https://doi.org/10.1016/j.foodchem.2017.12.076>
- Carvalho, J. D. dos S., Oriani, V. B., de Oliveira, G. M., & Hubinger, M. D. (2019). Characterization of ascorbic acid microencapsulated by the spray chilling technique using palm oil and fully hydrogenated palm oil. *LWT*, *101*, 306–314. <https://doi.org/10.1016/j.lwt.2018.11.043>
- Carvalho, J. D. dos S., Oriani, V. B., Oliveira, G. M., & Hubinger, M. D. (2021). Solid lipid microparticles loaded with ascorbic acid: Release kinetic profile during thermal stability. *Journal of Food Processing and Preservation*, *45*(6), 1–9. <https://doi.org/10.1111/jfpp.15557>
- Charella Mazzocato, M., Thomazini, M., & Favaro-Trindade, C. S. (2019). Improving stability of vitamin B12 (Cyanocobalamin) using microencapsulation by spray chilling technique. *Food Research International*, *126*, 108663. <https://doi.org/10.1016/j.foodres.2019.108663>
- Chambi, H. N. M., Alvim, I. D., Barrera-Arellano, D., & Grosso, C. R. F. (2008). Solid lipid microparticles containing water-soluble compounds of different molecular mass: Production, characterisation and release profiles. *Food Research International*, *41*(3), 229–236. <https://doi.org/10.1016/j.foodres.2007.11.012>
- Chawda, P. J., Shi, J., Xue, S., & Young Quek, S. (2017). Co-encapsulation of bioactives for food

- applications. *Food Quality and Safety*, 1(4), 302–309. <https://doi.org/10.1093/fqsafe/fyx028>
- Chenarides, L., Grebitus, C., Lusk, J. L., & Printezis, I. (2021). Food consumption behavior during the COVID-19 pandemic. *Agribusiness*, 37(1), 44–81. <https://doi.org/10.1002/agr.21679>
- Cho, T. J., Kim, S. A., Kim, H. W., Park, S. M., & Rhee, M. S. (2020). Changes in Consumers' Food Purchase and Transport Behaviors over a Decade (2010 to 2019) Following Health and Convenience Food Trends. *International Journal of Environmental Research and Public Health*, 17(15), 5448. <https://doi.org/10.3390/ijerph17155448>
- Consoli, L., Grimaldi, R., Sartori, T., Menegalli, F. C., & Hubinger, M. D. (2016). Gallic acid microparticles produced by spray chilling technique: Production and characterization. *LWT - Food Science and Technology*, 65, 79–87. <https://doi.org/10.1016/j.lwt.2015.07.052>
- Cutrim, C. S., Alvim, I. D., & Cortez, M. A. S. (2019). Microencapsulation of green tea polyphenols by ionic gelation and spray chilling methods. *Journal of Food Science and Technology*, 56(8), 3561–3570. <https://doi.org/10.1007/s13197-019-03908-1>
- Delshadi, R., Bahrami, A., Tafti, A. G., Barba, F. J., & Williams, L. L. (2020). Micro and nano-encapsulation of vegetable and essential oils to develop functional food products with improved nutritional profiles. *Trends in Food Science & Technology*, 104, 72–83. <https://doi.org/10.1016/j.tifs.2020.07.004>
- dos Santos, C. A., Carpenter, C. S., Arid, J. D., da Silva, Á. Á., Cardoso, L. P., Ribeiro, A. P. B., & Efraim, P. (2020). Production and characterization of promising β -stable seed crystals to modulate the crystallization of fat-based industrial products. *Food Research International*, 130, 108900. <https://doi.org/10.1016/j.foodres.2019.108900>
- Eftimov, T., Popovski, G., Petković, M., Seljak, B. K., & Kocev, D. (2020). COVID-19 pandemic changes the food consumption patterns. *Trends in Food Science & Technology*, 104, 268–272. <https://doi.org/10.1016/j.tifs.2020.08.017>
- Fadini, A. L., Alvim, I. D., Ribeiro, I. P., Ruzene, L. G., Silva, L. B. da, Queiroz, M. B., Miguel, A. M. R. de O., Chaves, F. C. M., & Rodrigues, R. A. F. (2018). Innovative strategy based on combined microencapsulation technologies for food application and the influence of wall material composition. *LWT - Food Science and Technology*, 91, 345–352. <https://doi.org/10.1016/j.lwt.2018.01.071>
- Fadini, A. L., Dutra Alvim, I., Paganotti, K. B. de F., Bataglia da Silva, L., Bonifácio Queiroz, M., Miguel, A. M. R. de O., & Rodrigues, R. A. F. (2019). Optimization of the production of double-shell microparticles containing fish oil. *Food Science and Technology International*, 25(5), 359–369. <https://doi.org/10.1177/1082013219825890>
- Favaro-Trindade, C. S., de Matos Junior, F. E., Okuro, P. K., Dias-Ferreira, J., Cano, A., Severino, P., Zielńska, A., & Souto, E. B. (2021). Encapsulation of Active Pharmaceutical Ingredients in Lipid Micro/Nanoparticles for Oral Administration by Spray-Cooling. *Pharmaceutics*, 13(8), 1186. <https://doi.org/10.3390/pharmaceutics13081186>
- Favaro-trindade, C. S., Okuro, P. K., & Matos-Junior, F. E. (2015). Encapsulation via Spray Chilling/Cooling/Congelation. *Handbook of Encapsulation and Controlled Release*, 71–87.
- Fernandes, R. V. D. B., Borges, S. V., Botrel, D. A., & Oliveira, C. R. De. (2014). Physical and chemical properties of encapsulated rosemary essential oil by spray drying using whey protein-inulin blends as carriers. *International Journal of Food Science & Technology*, 49(6), 1522–1529. <https://doi.org/10.1111/ijfs.12449>
- Fernandes, R. V. de B., Borges, S. V., & Botrel, D. A. (2014). Gum arabic / starch / maltodextrin / inulin as wall materials on the microencapsulation of rosemary essential oil. *Carbohydrate Polymers*, 101, 524–532. <https://doi.org/10.1016/j.carbpol.2013.09.083>

- Figueiredo, J. de A., Lago, A. M. T., Mar, J. M., da Silva, L. S., Sanches, E. A., de Souza, T. P., A Bezerra, J., Campelo, P. H., Botrel, D. A., & Borges, S. V. (2020). Stability of camu-camu encapsulated with different prebiotic biopolymers. *Journal of the Science of Food and Agriculture*, *100*(8), 3471–3480. <https://doi.org/10.1002/jsfa.10384>
- Figueiredo, J. de A., MT Lago, A., M Mar, J., S Silva, L., A Sanches, E., P Souza, T., A Bezerra, J., H Campelo, P., A Botrel, D., & V Borges, S. (2020). Stability of camu-camu encapsulated with different prebiotic biopolymers. *Journal of the Science of Food and Agriculture*, *100*(8), 3471–3480. <https://doi.org/10.1002/jsfa.10384>
- Figueiredo, J. de A., Teixeira, M. A., Campelo, P. H., Lago, A. M. T., Souza, T. P. de, Yoshida, M. I., Oliveira, C. R. de, Pereira, A. P. A., Pastore, G. M., Sanches, E. A., Botrel, D. A., & Borges, S. V. (2020). Encapsulation of camu-camu extracts using prebiotic biopolymers: Controlled release of bioactive compounds and effect on their physicochemical and thermal properties. *Food Research International*, *137*, 109563. <https://doi.org/10.1016/j.foodres.2020.109563>
- Fredes, C., Osorio, M. J., Parada, J., & Robert, P. (2018). Stability and bioaccessibility of anthocyanins from maqui (*Aristotelia chilensis* [Mol.] Stuntz) juice microparticles. *LWT*, *91*, 549–556. <https://doi.org/10.1016/j.lwt.2018.01.090>
- Furuta, T., & Neoh, T. L. (2020). Microencapsulation of food bioactive components by spray drying: A review. *Drying Technology*, *0*(0), 1–32. <https://doi.org/10.1080/07373937.2020.1862181>
- Galanakis, C. M., Aldawoud, T. M. S., Rizou, M., Rowan, N. J., & Ibrahim, S. A. (2020). Food Ingredients and Active Compounds against the Coronavirus Disease (COVID-19) Pandemic: A Comprehensive Review. *Foods*, *9*(11), 1701. <https://doi.org/10.3390/foods9111701>
- Gamboa, O. D., Gonçalves, L. G., & Grosso, C. F. (2011). Microencapsulation of tocopherols in lipid matrix by spray chilling method. *Procedia Food Science*, *1*, 1732–1739. <https://doi.org/10.1016/j.profoo.2011.09.255>
- Gharibzahedi, S. M. T., & Smith, B. (2021). Legume proteins are smart carriers to encapsulate hydrophilic and hydrophobic bioactive compounds and probiotic bacteria: A review. *Comprehensive Reviews in Food Science and Food Safety*, *20*(2), 1250–1279. <https://doi.org/10.1111/1541-4337.12699>
- Gomes, G. V. L., Sola, M. R., Rochetti, A. L., Fukumasu, H., Vicente, A. A., & Pinho, S. C. (2019). β -carotene and α -tocopherol coencapsulated in nanostructured lipid carriers of murumuru (*Astrocaryum murumuru*) butter produced by phase inversion temperature method: characterisation, dynamic in vitro digestion and cell viability study. *Journal of Microencapsulation*, *36*(1), 43–52. <https://doi.org/10.1080/02652048.2019.1585982>
- Gu, C., Hu, C., Ma, C., Fang, Q., Xing, T., & Xia, Q. (2016). Development and characterization of solid lipid microparticles containing vitamin C for topical and cosmetic use. *European Journal of Lipid Science and Technology*, *118*(7), 1093–1103. <https://doi.org/10.1002/ejlt.201500373>
- Günel, Z., Varhan, E., Koç, M., Topuz, A., & Sahin-Nadeem, H. (2021). Production of pungency-suppressed capsaicin microcapsules by spray chilling. *Food Bioscience*, *40*, 100918. <https://doi.org/10.1016/j.fbio.2021.100918>
- Huang, J., Qian, A., Sun, R., & Xia, Q. (2019). Preparation and characterization of coenzyme Q10 loaded solid lipid-based formulations for enhancement of gastrointestinal solubilization. *Journal of Dispersion Science and Technology*, *40*(10), 1385–1395. <https://doi.org/10.1080/01932691.2018.1515023>
- Jafari, S. M., Assadpoor, E., He, Y., & Bhandari, B. R. (2008). Encapsulation efficiency of food flavours and oils during spray drying. *Drying Technology*, *26*(7), 816–835. <https://doi.org/10.1080/07373930802135972>
- Jaskulski, M., Kharaghani, A., & Tsotsas, E. (2018). Chapter 3- Encapsulation Methods: Spray

- Drying, Spray Chilling and Spray Cooling. In M. K. Krokida (Ed.), *Thermal and Nonthermal Encapsulation Methods*, 67–114. CRC Press.
- Junior Matos, F. E., Thomazini, M., & Fávaro-trindade, C. S. (2016). Aplicação de vitamina C livre e encapsulada por spray chilling em salsicha de carne de frango : características físico-químicas , estabilidade e aceitação sensorial Application of free or encapsulated vitamin C to chicken frankfurter sausage by spray. *Brazilian Journal of Food Technology*, 322–331.
- Landim Neves, M. I., de Souza Queirós, M., Soares Viriato, R. L., Badan Ribeiro, A. P., & Gigante, M. L. (2021). Anhydrous milk fat blended with fully hydrogenated soybean oil as lipid microparticles: Characterization, stability, and trends for application. *LWT*, 152, 112276. <https://doi.org/10.1016/j.lwt.2021.112276>
- Loh, H. C., Seah, Y. K., & Looi, I. (2021). The COVID-19 Pandemic and Diet Change. *Progress In Microbes & Molecular Biology*, 4(1), 1–14. <https://doi.org/10.36877/pmmb.a0000203>
- Maschke, A., Becker, C., Eyrich, D., Kiermaier, J., Blunk, T., & Göpferich, A. (2007). Development of a spray congealing process for the preparation of insulin-loaded lipid microparticles and characterization thereof. *European Journal of Pharmaceutics and Biopharmaceutics*, 65(2), 175–187. <https://doi.org/10.1016/j.ejpb.2006.08.008>
- Matos-Jr, F. E., Comunian, T. A., Thomazini, M., & Favaro-Trindade, C. S. (2017). Effect of feed preparation on the properties and stability of ascorbic acid microparticles produced by spray chilling. *LWT*, 75, 251–260. <https://doi.org/10.1016/j.lwt.2016.09.006>
- Matos-Jr, F. E., Di Sabatino, M., Passerini, N., Favaro-Trindade, C. S., & Albertini, B. (2015). Development and characterization of solid lipid microparticles loaded with ascorbic acid and produced by spray congealing. *Food Research International*, 67, 52–59. <https://doi.org/10.1016/j.foodres.2014.11.002>
- Maurya, V. K., Bashir, K., & Aggarwal, M. (2020). Vitamin D microencapsulation and fortification: Trends and technologies. *Journal of Steroid Biochemistry and Molecular Biology*, 196, 105429. <https://doi.org/10.1016/j.jsbmb.2019.105489>
- McClements, D. J. (2020). Advances in nanoparticle and microparticle delivery systems for increasing the dispersibility, stability, and bioactivity of phytochemicals. *Biotechnology Advances*, 38, 107287. <https://doi.org/10.1016/j.biotechadv.2018.08.004>
- Müller, R. ., Radtke, M., & Wissing, S. . (2002a). Nanostructured lipid matrices for improved microencapsulation of drugs. *International Journal of Pharmaceutics*, 242(1–2), 121–128. [https://doi.org/10.1016/S0378-5173\(02\)00180-1](https://doi.org/10.1016/S0378-5173(02)00180-1)
- Müller, R. H., Petersen, R. D., Hommoss, A., & Pardeike, J. (2007). Nanostructured lipid carriers (NLC) in cosmetic dermal products. *Advanced Drug Delivery Reviews*, 59(6), 522–530. <https://doi.org/10.1016/j.addr.2007.04.012>
- Müller, R. H., Radtke, M., & Wissing, S. A. (2002b). Solid lipid nanoparticles (SLN) and nanostructured lipid carriers (NLC) in cosmetic and dermatological preparations. *Advanced Drug Delivery Reviews*, 54, 131–155. [https://doi.org/10.1016/S0169-409X\(02\)00118-7](https://doi.org/10.1016/S0169-409X(02)00118-7)
- Nahum, V., & Domb, A. J. (2021). Recent developments in solid lipid microparticles for food ingredients delivery. *Foods*, 10(2), 1–25. <https://doi.org/10.3390/foods10020400>
- Neri-Numa, I. A., DellaTorre, A., Oriani, V. B., Franch, G. C., Angolini, C. F. F., Dupas Hubinger, M., Ruiz, A. L. T. G., & Pastore, G. M. (2020). In vitro bioactivity approach of unripe genipap (*Genipa americana* L., Rubiaceae) fruit extract and its solid lipid microparticle. *Food Research International*, 127, 108720. <https://doi.org/10.1016/j.foodres.2019.108720>
- O'Brien, R. D. (2004). Fats and oils: formulating and processing for applications. *New York*, 1–574. <https://doi.org/10.1002/9781118827123>

- Oh, C. M., Guo, Q., Wan Sia Heng, P., & Chan, L. W. (2014). Spray-congealed microparticles for drug delivery-an overview of factors influencing their production and characteristics. *Expert Opinion on Drug Delivery*, *11*(7), 1047–1060. <https://doi.org/10.1517/17425247.2014.915805>
- Okuro, P. K., Matos-Junior, F. E., & Favaro-Trindade, C. S. (2013). Technological challenges for spray chilling encapsulation of functional food ingredients. *Food Technology and Biotechnology*, *51*(2), 171–182.
- Oriani, V. B., Alvim, I. D., Consoli, L., Molina, G., Pastore, G. M., & Hubinger, M. D. (2016). Solid lipid microparticles produced by spray chilling technique to deliver ginger oleoresin: Structure and compound retention. *Food Research International*, *80*, 41–49. <https://doi.org/10.1016/j.foodres.2015.12.015>
- Oriani, V. B., Alvim, I. D., Paulino, B. N., Procópio, F. R., Pastore, G. M., & Hubinger, M. D. (2018). The influence of the storage temperature on the stability of lipid microparticles containing ginger oleoresin. *Food Research International*, *109*, 472–480. <https://doi.org/10.1016/j.foodres.2018.04.066>
- Oxley, J. D. (2012). Spray cooling and spray chilling for food ingredient and nutraceutical encapsulation. In *Encapsulation Technologies and Delivery Systems for Food Ingredients and Nutraceuticals*, 110–130. Elsevier. <https://doi.org/10.1533/9780857095909.2.110>
- Paucar, O. C., Tulini, F. L., Thomazini, M., Balieiro, J. C. C., Pallone, E. M. J. A., & Favaro-Trindade, C. S. (2016). Production by spray chilling and characterization of solid lipid microparticles loaded with vitamin D 3. *Food and Bioproducts Processing*, *100*, 344–350. <https://doi.org/10.1016/j.fbp.2016.08.006>
- Pedroso, D. L., Dogenski, M., Thomazini, M., Heinemann, R. J. B., & Favaro-Trindade, C. S. (2013). Microencapsulation of *Bifidobacterium animalis* subsp. *lactis* and *Lactobacillus acidophilus* in cocoa butter using spray chilling technology. *Brazilian Journal of Microbiology*, *44*(3), 777–783. <https://doi.org/10.1590/S1517-83822013000300017>
- Pelissari, J. R., Souza, V. B., Pigoso, A. A., Tulini, F. L., Thomazini, M., Rodrigues, C. E. C., Urbano, A., & Favaro-Trindade, C. S. (2016). Production of solid lipid microparticles loaded with lycopene by spray chilling: Structural characteristics of particles and lycopene stability. *Food and Bioproducts Processing*, *98*, 86–94. <https://doi.org/10.1016/j.fbp.2015.12.006>
- Pezeshki, A., Hamishehkar, H., Ghanbarzadeh, B., Fathollahy, I., Keivani Nahr, F., Khakbaz Heshmati, M., & Mohammadi, M. (2019). Nanostructured lipid carriers as a favorable delivery system for β -carotene. *Food Bioscience*, *27*, 11–17. <https://doi.org/10.1016/j.fbio.2018.11.004>
- Procópio, F. R., Oriani, V. B., Paulino, B. N., do Prado-Silva, L., Pastore, G. M., Sant'Ana, A. S., & Hubinger, M. D. (2018). Solid lipid microparticles loaded with cinnamon oleoresin: Characterization, stability and antimicrobial activity. *Food Research International*, *113*, 351–361. <https://doi.org/10.1016/j.foodres.2018.07.026>
- Queirós, M. de S., Viriato, R. L. S., Ribeiro, A. P. B., & Gigante, M. L. (2020). Dairy-based solid lipid microparticles: A novel approach. *Food Research International*, *131*, 109009. <https://doi.org/10.1016/j.foodres.2020.109009>
- Ray, S., Raychaudhuri, U., & Chakraborty, R. (2016). An overview of encapsulation of active compounds used in food products by drying technology. *Food Bioscience*, *13*, 76–83. <https://doi.org/10.1016/j.fbio.2015.12.009>
- Ribeiro, M. D. M. M., Arellano, D. B., & Grosso, C. R. F. (2012). The effect of adding oleic acid in the production of stearic acid lipid microparticles with a hydrophilic core by a spray-cooling process. *Food Research International*, *47*(1), 38–44. <https://doi.org/10.1016/j.foodres.2012.01.007>
- Rodríguez-Roque, M. J., Rojas-Graü, M. A., Elez-Martínez, P., & Martín-Belloso, O. (2013). Changes

- in Vitamin C, Phenolic, and Carotenoid Profiles Throughout in Vitro Gastrointestinal Digestion of a Blended Fruit Juice. *Journal of Agricultural and Food Chemistry*, 61(8), 1859–1867. <https://doi.org/10.1021/jf3044204>
- Sadati Behbahani, E., Ghaedi, M., Abbaspour, M., Rostamizadeh, K., & Dashtian, K. (2019). Curcumin loaded nanostructured lipid carriers: In vitro digestion and release studies. *Polyhedron*, 164, 113–122. <https://doi.org/10.1016/j.poly.2019.02.002>
- Salvim, M. O., Thomazini, M., Pelaquim, F. P., Urbano, A., Moraes, I. C. F., & Trindade, C. S. F. (2015). Production and structural characterization of solid lipid microparticles loaded with soybean protein hydrolysate. *Food Research International*, 76, 689–696. <https://doi.org/10.1016/j.foodres.2015.08.003>
- Santos, V. da S., Braz, B. B., Silva, A. Á., Cardoso, L. P., Ribeiro, A. P. B., & Santana, M. H. A. (2019). Nanostructured lipid carriers loaded with free phytosterols for food applications. *Food Chemistry*, 298, 125053. <https://doi.org/10.1016/j.foodchem.2019.125053>
- Sartori, T., Consoli, L., Hubinger, M. D., & Menegalli, F. C. (2015). Ascorbic acid microencapsulation by spray chilling: Production and characterization. *LWT - Food Science and Technology*, 63(1), 353–360. <https://doi.org/10.1016/j.lwt.2015.03.112>
- Sato, K. (2001). Crystallization behaviour of fats and lipids. *Chemical Engineering Science*, 56(7), 2256–2265. [https://doi.org/10.1016/S0009-2509\(00\)00458-9](https://doi.org/10.1016/S0009-2509(00)00458-9)
- Sato, K., & Ueno, S. (2011). Crystallization, transformation and microstructures of polymorphic fats in colloidal dispersion states. *Current Opinion in Colloid & Interface Science*, 16(5), 384–390. <https://doi.org/10.1016/j.cocis.2011.06.004>
- Shishir, M. R. I., & Chen, W. (2017). Trends of spray drying: A critical review on drying of fruit and vegetable juices. *Trends in Food Science and Technology*, 65, 49–67. <https://doi.org/10.1016/j.tifs.2017.05.006>
- Silva, M. P., Thomazini, M., Holkem, A. T., Pinho, L. S., Genovese, M. I., & Fávaro-Trindade, C. S. (2019). Production and characterization of solid lipid microparticles loaded with guaraná (*Paullinia cupana*) seed extract. *Food Research International*, 123, 144–152. <https://doi.org/10.1016/j.foodres.2019.04.055>
- Silva, M. P., Tulini, F. L., Matos-Jr, F. E., Oliveira, M. G., Thomazini, M., & Fávaro-Trindade, C. S. (2018). Application of spray chilling and electrostatic interaction to produce lipid microparticles loaded with probiotics as an alternative to improve resistance under stress conditions. *Food Hydrocolloids*, 83, 109–117. <https://doi.org/10.1016/j.foodhyd.2018.05.001>
- Sorita, G., Santamaria-Echart, A., Gozzo, A., Gonçalves, O., Leimann, F., Bona, E., Manrique, Y., Fernandes, I. P., Ferreira, I. C. F., & Barreiro, M. (2021). Lipid composition optimization in spray congealing technique and testing with curcumin-loaded microparticles. *Advanced Powder Technology*, 32(5), 1710–1722. <https://doi.org/10.1016/j.apt.2021.03.028>
- Tavares, L., Santos, L., & Zapata Noreña, C. P. (2021). Bioactive compounds of garlic: A comprehensive review of encapsulation technologies, characterization of the encapsulated garlic compounds and their industrial applicability. *Trends in Food Science and Technology*, 114, 232–244. <https://doi.org/10.1016/j.tifs.2021.05.019>
- Timms, R. E. (1985). Physical properties of oils and mixtures of oils. *Journal of the American Oil Chemists' Society*, 62(2), 241–249. <https://doi.org/10.1007/BF02541385>
- Tomšik, A., Šarić, L., Bertoni, S., Protti, M., Albertini, B., Mercolini, L., & Passerini, N. (2019). Encapsulations of wild garlic (*Allium ursinum* L.) extract using spray congealing technology. *Food Research International*, 119, 941–950. <https://doi.org/10.1016/j.foodres.2018.10.081>
- Trojanowska, A., Nogalska, A., Valls, R. G., Giamberini, M., & Tylkowski, B. (2017). Technological

- solutions for encapsulation. *Physical Sciences Reviews*, 2(9), 1–20. <https://doi.org/10.1515/psr-2017-0020>
- Tulini, F. L., Souza, V. B., Thomazini, M., Silva, M. P., Massarioli, A. P., Alencar, S. M., Pallone, E. M. J. A., Genovese, M. I., & Favaro-Trindade, C. S. (2017). Evaluation of the release profile, stability and antioxidant activity of a proanthocyanidin-rich cinnamon (*Cinnamomum zeylanicum*) extract co-encapsulated with α -tocopherol by spray chilling. *Food Research International*, 95, 117–124. <https://doi.org/10.1016/j.foodres.2017.03.010>
- Van Duong, T., Lüdeker, D., Van Bockstal, P. J., De Beer, T., Van Humbeeck, J., & Van Den Mooter, G. (2018). Polymorphism of Indomethacin in Semicrystalline Dispersions: Formation, Transformation, and Segregation. *Molecular Pharmaceutics*, 15(3), 1037–1051. <https://doi.org/10.1021/acs.molpharmaceut.7b00930>
- Van Duong, T., & Van den Mooter, G. (2016). The role of the carrier in the formulation of pharmaceutical solid dispersions. Part II: amorphous carriers. *Expert Opinion on Drug Delivery*, 13(12), 1681–1694. <https://doi.org/10.1080/17425247.2016.1198769>
- Wegmüller, R., Zimmermann, M. B., Bühr, V. G., Windhab, E. J., & Hurrell, R. F. (2006). Development, stability, and sensory testing of microcapsules containing iron, iodine, and vitamin A for use in food fortification. *Journal of Food Science*, 71(2). <https://doi.org/10.1111/j.1365-2621.2006.tb08923.x>
- Yang, R., Zhou, Z., Sun, G., Gao, Y., & Xu, J. (2015). Ferritin, a novel vehicle for iron supplementation and food nutritional factors encapsulation. *Trends in Food Science and Technology*, 44(2), 189–200. <https://doi.org/10.1016/j.tifs.2015.04.005>
- Yin, Y., & Cadwallader, K. R. (2019). Spray-chilling encapsulation of 2-acetyl-1-pyrroline zinc chloride using hydrophobic materials: Storage stability and flavor application in food. *Food Chemistry*, 278, 738–743. <https://doi.org/10.1016/j.foodchem.2018.11.122>
- Zafimahova-Ratisbonne, A., Wardhono, E. Y., Lanoisellé, J.-L., Saleh, K., & Clause, D. (2014). Stability of W/O Emulsions Encapsulating Polysaccharides. *Journal of Dispersion Science & Technology*, 35(1), 38–47. <https://doi.org/10.1080/01932691.2013.773444>
- Zanetti, M., Carniel, T. K., Dalcanton, F., dos Anjos, R. S., Gracher Riella, H., de Araújo, P. H. H., de Oliveira, D., & Antônio Fiori, M. (2018). Use of encapsulated natural compounds as antimicrobial additives in food packaging: A brief review. *Trends in Food Science and Technology*, 81, 51–60. <https://doi.org/10.1016/j.tifs.2018.09.003>
- Zhang, R., Zhou, L., Li, J., Oliveira, H., Yang, N., Jin, W., Zhu, Z., Li, S., & He, J. (2020). Microencapsulation of anthocyanins extracted from grape skin by emulsification/internal gelation followed by spray/freeze-drying techniques: Characterization, stability and bioaccessibility. *LWT*, 123, 109097. <https://doi.org/10.1016/j.lwt.2020.109097>

**ARTIGO 2 – A COMBINATION OF PGPR AND ULTRASOUND-ASSISTED
PRODUCTION OF ANTHOCYANIN-RICH EXTRACT OF GRAPE PEEL
EMULSIONS AND ENCAPSULATES**

Artigo submetido as normas da revista científica: Journal of Food Process Engineering

On line ISSN: 1745-4530

(versão preliminar)

**Jayne de Abreu Figueiredo¹, Laís Bruno Norcino², Eloá Lourenço do Carmo¹, Amanda
Maria Teixeira Lago¹, Pedro Henrique Campelo³, Diego Alvarenga Botrel¹, Soraia Vilela
Borges^{1*}**

¹Departament of Food Science, Federal University of Lavras, P.O. Box 3037, 37200-900,
Lavras, MG, Brasil

²Biomaterial Engeneering, Federal University of Lavras, P.O. Box, 37200-900, Lavras, MG,
Brazil

³Faculty of Agrarian Science, Federal University of Amazonas, 69077-000, Manaus, AM,
Brazil

ABSTRACT

This study investigated the effect of PGPR emulsifier (0%, 3%, 4%, and 5%) and ultrasonic treatment (sonication times - 4 min and 6 min and power - 160 W and 200 W) on the properties and stability of water-in-oil (W/O) emulsion of grape peel extract. PGPR (4%) proved to be effective in the kinetic stability of the emulsions. The treatment W/O_200W_4min showed lower droplet size ($3.15 \pm 1.86 \mu\text{m}$) and higher kinetic stability (polydispersity index). The ultrasonic treatment increased the viscosity, the phenolics contents (518 – 502 mg GAE·100 g⁻¹ on a wet basis) and the antioxidant activity (76-68%) of the emulsions, and affected the anthocyanins contents (243-333 mg malvidin-3-diglycoside·100 g⁻¹ on a wet basis). FTIR analysis indicated no changes in the molecular structure of the palm oil and palm fat after sonication, which led to a better encapsulation of the bioactive compounds when compared to the control treatment (made with magnetic stirrer only). The ultrasound-treated emulsions showed a longer half-life (49-56 days) when compared to the control (41 days). The accelerated stability test of the emulsions (65°C/120 h) showed that the ultrasonic treatment increased the stability, provided a controlled release of anthocyanins in the grape peel extract, and reduced the lipid oxidation and the color changes during storage, which is desirable for its application in food systems. The ultrasound treatment also affected the characteristics of the spray-chilled microparticles, showing thinner, more fluid microparticles and less agglomeration when compared to the microparticles made with the control emulsion. It also improved the stability of the anthocyanin pigment in the microparticles during storage. The present study suggests that the ultrasound treatment can be efficient in obtaining stable W/O emulsions containing plant extracts with consequent improvement in the characteristics of microparticles obtained by spray chilling, increasing the storage stability of sensitive compounds.

Keywords: Sonication, Antioxidant, Polyglycerol polyricinoleate, Kinetic stability, Palm oil, Water-in-oil emulsion.

1. Introduction

Grapes peel extract from different species are an abundant source of potent nutraceutical compounds containing different polyphenolics levels (0.5-20% on a dry basis) (Amorim et al., 2019). Anthocyanins are the major red colorant of grape peel extract (Zheng et al., 2021). These phenolic compounds are secondary plant metabolites with health benefits due to their antioxidant, antimicrobial, and anti-viral properties (Mammadova et al., 2020), apoptosis reduction, and improvements in glutathione metabolism (Kerasioti et al., 2017; Maurer et al., 2020).

Anthocyanins from the grape peel extract can be used as natural dyes in dairy products, confectionery, bakery, as well as meat substitutes, among other applications. They can also be used in the food, pharmaceutical, and cosmetic industries due to their antioxidant properties. However, its low stability to oxygen, light, high temperatures, and alkaline pH has limited its application as a food colorant (Zheng et al., 2021). Therefore, the direct application of anthocyanins in the food industry has faced many challenges, and encapsulation techniques such as spray drying (Kuck & Noreña, 2016; Tsali & Goula, 2018), ionic gelation (Romanini et al., 2021), freeze-drying (Mihalcea et al., 2020), and emulsification/internal gelation (R. Zhang et al., 2020) may be a promising approach to increase the anthocyanins stability in processed foods.

To the best of our knowledge, there is no published report on the production of W/O emulsions to encapsulate grape peel extract for the production of stable microparticles using the spray chilling technique. Spray chilling has many advantages when compared to spray drying and other encapsulation techniques, including no need to evaporate the solvent, increased productivity, reduced cost, and easy scale-up (Consoli et al., 2016). The technique consists of converting liquids into powder or powder-like materials using fatty acids, triacylglycerols, waxes, or blends of these materials as carriers. The active material is first

dispersed, emulsified, or solubilized in the molten lipid matrix, which is then fed into a heated nozzle and atomized into a chamber at temperatures below the melting point of the lipid, with solidification of the droplets when in contact with cooled air to form solid lipid microparticles. The final product can be easily incorporated into different food matrices, with different functions.

Recently, W/O emulsions have been studied as encapsulation systems of active compounds, to improve their biological activities, controlled release, and flavor maintenance (Al-Maqtari et al., 2021; Bi et al., 2015; Consoli et al., 2016; Mohammed et al., 2021; K. Zhang et al., 2020), being widely used in food, cosmetics, pharmaceuticals, and chemical areas. The formation and stability of W/O emulsions is a critical step for both the production of microparticles using encapsulation techniques (such as spray chilling) and the direct application into food matrices. For application in spray chilling processes, the emulsion must have good stability at high temperatures until the final production of the microparticles and adequate viscosity for atomization without nozzle clogging (Consoli et al., 2016). The performance of the W/O emulsion is highly dependent on the emulsification parameters (Raviadaran et al., 2019). Ultrasonic homogenization is currently the most promising 'clean technology' for the preparation of emulsions due to its ability to reduce the size of drops at nano levels, high efficiency, and economic performance. Few studies have focused on the effect of ultrasound on W/O emulsions (Al-Maqtari et al., 2021; Mohammed et al., 2021; Nishad et al., 2021; Raviadaran et al., 2019; K. Zhang et al., 2020), with no study using grape peel extract, palm oil, and palm hard fat. The oil phase of this study was composed of palm oil and trans-free hard fat, once it is popular, low cost, and the second most marketed oil in the world after soybean. In addition, studies have shown the health benefits of palm oil, including anticancer properties (Olafisoye et al., 2017; Sambanthamurthi et al., 2000).

The main objective of this study was to investigate the effect of assisted ultrasound (using different times and powers) on the a food emulsion containing grape peel extract and a lipid blend composed of palm oil and fully hydrogenated palm fat (trans-fat free) for further use in the production of functional microparticles by spray chilling. The emulsions were characterized for stability during storage. After selection of the best conditions for emulsion preparation, the spray chilling capacity to form microparticles was investigated, as well as the storage stability of the anthocyanin pigment by colorimetric analysis.

2. Materials and methods

2.1. Materials

The grapes of the Bordo variety (*Vitis labrusca* L.) were supplied by producers from a farm located in Campos Gerais (Minas Gerais, Brazil). Palm oil (PO) (melting point 34 – 40°C) and fully hydrogenated palm oil (FHPO) (trans-fat free) (melting point 55 – 61°C) were kindly donated by Agropalma (Limeira, SP, Brazil). The emulsifier polyglycerol polyricinoleate (Grinsted® PGPR Super, HLB ~ 3.0) was donated by Danisco Brasil Ltda (Cotia, SP, Brazil).

2.2. Preparation of the grape peel extract

The grapes were washed and sanitized. To obtain the grape peel extract, the seeds, peels, and pulps were manually removed. The anthocyanins were extracted from the peel using distilled water and citric acid (1% wt. of water) to a ratio of 1:1 (w/v) (peel: acidified water). The mixture was kept overnight in the dark at 4 ± 1 °C, covered with aluminum foil, for better extraction of anthocyanins. After, the extract was filtered through organza and centrifuged for 5 min at 3000 rpm to eliminate the suspended solids. Finally, the extract was stored in amber flasks at 4 ± 1 °C to prevent the degradation of anthocyanins.

2.3 Preparation of the emulsions

The dispersion of the aqueous grape peel extract into lipid blend characterizes the formation of water-in-oil (W/O) emulsion. To produce kinetically stable emulsions for atomization in spray chilling, a two-step experimental design was performed, using different proportions of emulsifier polyglycerol polyricinoleate (PGPR) and processing conditions (magnetic stirrer and ultrasound-assisted method). Therefore, the study evaluated the effect of different PGPR concentrations and different ultrasound-assisted times and power on the quality of emulsions, using an emulsion obtained by magnetic stirrer as a control treatment.

2.4 Selection of PGPR concentration to obtain stable W/O emulsion

In this part of the study, the continuous phase was composed of a fat blend. A fat blend composed (indicate 60%wt of formulation) of fully hydrogenated palm oil (FHPO) (80 wt%), and palm oil (PO) (20 wt%) was placed in a 250 ml beaker and heated to 70°C using a temperature-controlled water bath (Tecnal, TE-184, Piracicaba, Brazil) until complete melting. Then, PGPR (0, 3, 4, and 5 wt% in relation to lipid materials), and grape peel extract (40 wt%) were added to the fat blend under constant homogenization with a magnetic stirrer at 750 rpm for 4 minutes defined in preliminary tests until complete homogenization. The grape extract concentration of 40% was established in preliminary tests. Immediately after preparation, the emulsions were transferred to a 25 ml graduated cylinder (internal diameter = 17mm), which was sealed and stored for 1 h at 70°C. The phase separation of the emulsions was monitored every 15 minutes for 60 minutes. A ruler was used to measure the height of the emulsion phases. The phase separation was measured for all trials and expressed as sedimentation index (*SI*), which was calculated as a percentage of the ratio between aqueous phase height (*H*), and the total height (*HT*), as shown in Eq. (1).

$$SI = (H / H_T) \times 100 \quad (1)$$

2.5. *Effects of ultrasound-assisted extraction on the formation of W/O emulsion*

2.5.1. *Preparation of W/O emulsions*

First, W/O emulsions were prepared according to Section 2.4, using a 4% PGPR emulsifier (selected in Section 2.4) based on the mass of the fat blend. Emulsions were prepared totaling 170.6 g, of which 100 g corresponded to the lipid blend (FHPO/PO), 66.6 g grape peel extract, and 4 g PGPR. After preparation of the emulsions (Section 2.4), they were immediately subjected to ultrasound-assisted homogenization at different times (4 and 6 minutes) and powers (160 and 200W) defined in preliminary tests, corresponding to the treatments: W/O_160W_4min; W/O_160W_6min; W/O_200W_4min; and W/O_200W_6min. An ultrasonic homogenizer (400W full power, 20 kHz frequency - Brason Ultrasonic, 450, USA) was used, with the probe (\varnothing 13 mm) immersed 24 mm into the liquid. An untreated W/O emulsion (MS_W/O) was used as a control. The control emulsion was prepared using a magnetic stirrer as reported in Section 2.4. The effect of sonication time and powers were varied to obtain the optimum conditions for the production of emulsions. The emulsions were produced in triplicate.

2.5.2. *Characterization and stability of emulsions*

2.5.2.1. *Droplet size and polydispersity index (PDI)*

The emulsions were examined by optical microscopy after emulsification. Aliquots of each sample were placed on glass slides, covered with coverslips, and observed using an optical

microscope (MF-AKS 24 □ 36 Expomet, Carl Zeiss AG, Germany) coupled with a digital camera (Axiocam ICc) at 40× and 100× magnification.

The emulsion samples were previously dispersed in solution containing distilled water and Tween 20 (0.5g of Tween 20 /100g distilled water) (Alvim et al., 2016). Five images of each sample were obtained to generate a representative result. The micrographs were analyzed according to the method described by (Luo et al., 2018), (Alvim et al., 2013), and (Frascareli et al., 2012) with some modifications. Five hundred droplets of each sample were measured using ImageJ software®. The mean droplet size was expressed in terms of Sauter diameter ($D_{3,2}$) and the size distribution (*Span*) was calculated according to Eq (2-3), respectively. The measurements were performed in triplicate.

$$D_{[3,2]} = \frac{\sum n_i \times d_i^3}{\sum n_i \times d_i^2} \quad (2)$$

$$Span = \frac{(d_{90} - d_{10})}{d_{50}} \quad (3)$$

Where d_i is the droplet diameter (μm), n_i is the dimensionless number of droplets between two consecutive diameters. *Span* value is that gives width of size distribution, and the variables d_{90} , d_{10} , and d_{50} are droplet diameters (μm) at 10%, 50%, and 90% cumulative volume, respectively.

2.5.2.2. Emulsion oxidation after the ultrasound treatment

Two protocols were used to evaluate the oxidation and structural changes of the emulsions: the FTIR analysis and peroxide value.

2.5.2.3. FTIR analysis

FTIR spectra were obtained using Perkin Elmer's Frontier FTIR spectrometer. The functional groups of concern were aldehydes (C=O stretch at 1750–1625 cm⁻¹, C–H stretch of C=O at 2850–2800 cm⁻¹, and C–H stretch of C=O at 2750–2700 cm⁻¹), ketones (C=O stretch at 1750–1625 cm⁻¹) and carboxylic acid (C=O stretch at 1730–1650 cm⁻¹, and hydrogen-bonded O–H stretch at 3400–2400 cm⁻¹) (Raviadaran et al., 2019).

2.5.2.4. Peroxide value

Peroxide value for the W/O emulsion was determined in accordance to IDF standard 74A:1991 (1991), with some modifications. For that, 1.0 g of emulsion and 1.5 ml ethanol were mixed in a conical flask, stirred for 60 seconds, and then centrifuged at 3000 rpm for 2 minutes for phase separation. An aliquot of 100 µl of the supernatant was mixed with 4.8 ml of a mixture of chloroform/methanol (7:3) in triplicate. For color development, 25 µl of iron chloride (II) solution and 25 µl of ammonium thiocyanate were added. The sample was kept at rest in the dark for 5 minutes, and absorbance readings were performed at 500 nm in a spectrophotometer - UNICO 2800UV/VIS (United Products & Instruments Inc., New Jersey, USA). The concentrations of hydroperoxides were determined using a standard curve constructed using dilutions of 1 to 30 µg of Fe³⁺, and the correlation coefficient (R²) obtained was 0.989. The peroxide index in peroxide milliequivalent per kilogram of oil was calculated according to to Eq. (4) (Shantha & Decker, 1994).

$$\text{Peroxide value} \left(\frac{\text{meq}}{\text{kg}} \right) = \frac{(A_a - A_b) \times a}{55.84 \times m \times 2} \quad (4)$$

Where, A_a is the absorbance of the sample; A_b is the absorbance of the blank; a is the angular coefficient of the standard curve, and m is the mass of the emulsion.

2.5.2.5. Rheological behavior

The rheological behavior of freshly-prepared emulsions was measured at 70°C (temperature required to prevent hardening of the emulsion) using a rotation viscometer (Brookfield, DV III Ultra, Brookfield Engineering Laboratories, Stoughton, USA) coupled to a thermostatic bath to control the temperature of the samples (Brookfield, EX 200). An adapter 13R/RP and an SC4-18 coaxial shear sensor for small samples were used. Each sample was submitted to an increasing deformation rate ramp (0.01 to 92 s⁻¹). Newton's Law (Eq. 5) and Power Law (Eq. 6) models were adjusted to the experimental data.

$$\sigma = \mu\dot{\gamma} \quad (5)$$

$$\sigma = k\dot{\gamma}^n \quad (6)$$

Where σ is the shear stress in (Pa), μ is the Newtonian viscosity (Pa·s), $\dot{\gamma}$ is the shear rate (s⁻¹), k is the consistency index (Pa·sⁿ), n is the flow behavior index (dimensionless). The viscosity values were recorded in mPa·s.

2.5.2.6. *Sedimentation index (SI)*

The emulsions can lose their stability over time, leading to phase separation. Then, the stability of the emulsions after ultrasound treatment was evaluated for the sedimentation index (*SI*) according to Section 2.4, Eq. (1). The phase separation of the emulsions was monitored every 15 minutes for 120 minutes.

2.6. *Bioactive properties of emulsions*

2.6.1. *Total monomeric anthocyanins*

The total monomeric anthocyanins were determined according to the methodology described by Kuck & Noreña (2016) and Carmo et al. (2021) with modifications. To extract the anthocyanins, 0.5 g of the emulsion was mixed with 5 mL of acidified ethanol (HCL 0.1%, v/v), vortexed for 1 minute, and placed in an ultrasonic bath at 60 °C for 5 minutes. The mixture was centrifuged at 3000 rpm for 2 min to decant the solid material. Absorbance of the supernatant was measured at 520 nm, in triplicate, in a spectrophotometer - UNICO 2800UV/VIS (United Products & Instruments Inc., New Jersey, USA). The results were expressed as mg malvidin-3-glucoside per 100 g sample on a wet basis, using molar absorptivity of 28.000 L/mol.cm, and molecular weight of 493.2g/mol.

2.6.2. Total phenolics content (TPC)

The total phenolics contents were determined using a modified Folin-Ciocalteu colorimetric method Mar et al. (2020), with some modifications. To extract the TPC, 0.5 g of the emulsion was mixed with 5 mL of acidified ethanol (HCL 0.1%, v/v), vortexed for 1 minute, and placed in an ultrasonic bath at 60 °C for 5 minutes. The mixture was centrifuged (2 min/3000 rpm) to decant the solid material. The solution was diluted by adding 1 ml of supernatant to 3 ml of distilled water, and 1 ml of this dilution was added to 1 ml of Folin–Ciocalteu reagent (0.2 N). After 3 min, 1 ml of sodium carbonate solution (4% w/v) was added and the mixture was allowed to stand in the dark for 2 hr at 25°C. The absorbance readings were performed at 765 nm, and quantification of total phenolic content was performed using a Gallic acid (GA) standard curve generated with concentrations of 1, 5, 10, 20, 30, 40, 50, and 60 µg/ml. The result was expressed as mg of gallic acid equivalents (GAE) per 100 g sample on a wet basis.

2.6.3. Antioxidant activity

The antioxidant activity of the emulsions was evaluated using the free radical 2,2-diphenyl-1-picrylhydrazyl (DPPH) assay (Sigma-Aldrich, USA), according to the method of Campelo-Felix et al. (2017), with some modifications. Approximately 5 g of the emulsion was mixed with 5 mL of acidified ethanol (HCL 0.1%, v/v) and vortexed for 1 min. After homogenization, the mixture was placed in an ultrasonic bath at 60 °C for 5 minutes, and centrifuged (2 min/3000 rpm) to decant the solid material. Subsequently, 1.5 ml of supernatant was added to 3.9 mL of DPPH ethanolic solution (0.1 mg/ml), vortexed for 5 s, and stored in the dark for 1 h at 25°C. A blank was prepared by substituting the emulsion solution for 1.5 mL of pure ethanol. The absorbance values of the blank and the samples were measured at 515 nm. The antioxidant activity (%AA) of the emulsions was determined using Eq. (7), where A_0 is the absorbance of blank, and A_E is the absorbance of the sample.

$$AA(\%) = \left(\frac{A_0 - A_E}{A_0} \right) \quad (7)$$

2.7. Accelerated degradation test

To study the emulsion susceptibility to degradation of anthocyanins, the samples were subjected to an accelerated degradation test under standardized conditions according to the method proposed by Poyato et al. (2013), with some modifications. For that, 60 g of emulsion was placed in 250 mL flasks, which were sealed and stored for 120 h under Schaal oven test conditions (65 °C). The samples were taken every 24 h for analysis. It is known that 1 day of storage under this condition is equivalent to 1 month of storage at room (Abou-Gharbia et al., 1996). During the storage period, the anthocyanins contents (Section 2.6.1), the peroxide value (Section 2.5.2.4), and the color parameters (Section 2.7.1) were monitored.

2.7.1. Color measurements

The color parameters of the emulsions were determined using a Konica Minolta CM-5 colorimeter (Minolta Camera Co., Ltd, Osaka, Japan). A white standard color plate ($L^* = 91.76$, $a^* = -0.25$, $b^* = -0.40$) was used for calibration, and the luminosity (L^*) as well as the chromatic coordinates a^* and b^* were determined by reflectance according to the CIE L^* , a^* , and b^* scale. The color parameters were used to calculate the total color difference (ΔE^* , Eq. 8).

$$\Delta E^* = \sqrt{[(\Delta L^*)^2 + (\Delta a^*)^2 + (\Delta b^*)^2]} \quad (8)$$

2.7.2. Degradation kinetics and half-life of anthocyanins

The degradation of anthocyanins was determined according to the anthocyanins contents during the storage (Section 2.7). The half-life ($t^{1/2}$) of anthocyanins was calculated according to Eqs. 9-10, for each treatment, considering that this degradation process is known to follow first-order kinetics (Figueiredo et al., 2020; Moreno et al., 2018; Sinela et al., 2017).

$$kt = -\ln\left(\frac{C_t}{C_0}\right) \quad (9)$$

$$t_{1/2} = \left(\frac{\ln 2}{k}\right) \quad (10)$$

where C_0 and C_t correspond to the initial concentration of anthocyanins in the added extract and final concentrations of anthocyanins (malvidin-3-glucoside) in the emulsions, respectively, at time t (days), and k (days^{-1}) is the first-order reaction rate constant.

2.7.3 Formation capacity of the microparticles by spray chilling, color measurements and, anthocyanins content

To investigate the formation capacity of the microparticles by spray chilling, the best emulsion obtained by the ultrasound treatment and the control emulsion (MS_W/O) were selected to evaluate the effect of the emulsion formation on the characteristics of the microparticles. Thus, the microparticles were evaluated for their visual aspect and the stability of the anthocyanin pigment by color measurements and anthocyanin content when exposed to storage conditions for 30 days.

2.7.3.1 Production of the microparticles by spray chilling

A spray dryer (model MDS 1.0, Labmaq do Brasil, Ribeirão Preto, SP, Brazil) was used for the production of the microparticles, which was adapted for use as a spray chiller. The mixture was fed into the atomizer nozzle (double-fluid model with 3.0 mm diameter) corresponding to a flow rate of 10 ml/min. The temperatures of the samples and the compressed air were 70 °C and 80 °C, respectively. The air flow rate was 35 L/min and the cooling air temperature was 1 °C. The spray chilling parameters were determined in preliminary tests (data not shown), which yielded a free-flowing powder. At the end of the process, the samples were collected in the collecting jar, stored in closed containers, and kept at -18 °C until analysis. The assays were performed in duplicate.

2.7.3.2 Color measurements and anthocyanins content

The microparticles were placed in Petri plates, and the color parameters were determined in a CM-5 colorimeter (Minolta Camera Co., Ltd, Osaka, Japan). The values of Chroma (C^*) and hue angle (h°) were calculated using Equations (11) and (12) respectively, based on the results of the CIE $L^*a^*b^*$ parameters. The color of the samples was defined by

the parameters L^* (0 = black, 100 = white, which indicates the lightness of the sample), C^* (color saturation), and h° (hue: from 0° or 360° = red color, 90° = yellow, 180° = green, and 270° = blue).

Color parameters are fast and effective tools for evaluating the stability of natural pigments (Ahmed et al., 2004; Carvalho et al., 2020; Patras et al., 2010). Thus, to evaluate the stability of the anthocyanin pigment of the microparticles, about 1g of sample was placed in a Petri plate and the color parameters (L^* , a^* , and b^*) were measured immediately after the manufacture (time 0) and after 30 days of exposure to environmental conditions ($25 \pm 3^\circ\text{C}$; RH $55 \pm 3\%$, and contact with oxygen). The total color difference (ΔE^* , Eq. 8) of the samples before and after storage was also determined.

$$C^* = \sqrt{a^{*2} + b^{*2}} \quad (11)$$

$$h^\circ = \tan^{-1} \frac{b^*}{a^*} \quad (12)$$

To extract the anthocyanins, 0.5 g of microparticles was mixed with 5 mL of acidified ethanol (HCL 0.1%, v/v), vortexed for 1 minute, and placed in an ultrasonic bath at 25°C for 60 minutes. The mixture was centrifuged at 3000 rpm for 2 min to decant the solid material. Absorbance of the supernatant was measured at 520 nm, in triplicate, in a spectrophotometer - UNICO 2800UV/VIS (United Products & Instruments Inc., New Jersey, USA). The results were expressed as mg malvidin-3-glucoside per 100 g sample on a wet basis, using molar absorptivity of 28.000 L/mol.cm, and molecular weight of 493.2g/mol.

2.8. Statistical analysis

A completely randomized experimental design was performed to evaluate the effect of sonication time (4 and 6 min) and ultrasound power (160 and 200 W) on the emulsion

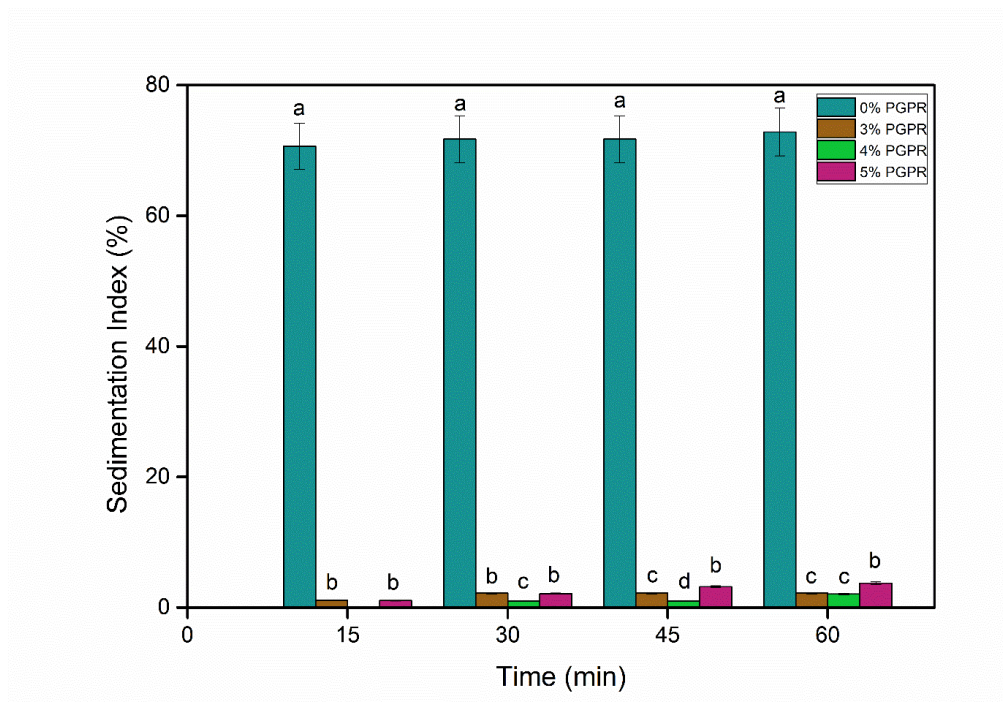
characteristics as well as on the color parameters of the microparticles. All analyses were performed in triplicate and data were evaluated by Analysis of Variance (ANOVA) using the R software package (version 3.6.0). Duncan test was used at a significance level of 5%.

3. *Results and discussion*

The formation of a stable W/O emulsion is dependent on the interaction between the oil and the emulsifier to form a rigid oil-water interface (Raviadaran et al., 2019). After formation emulsion, the emulsifier contributes to the stabilization of the dispersed droplets, preventing phase separation. In a first step, different types of emulsifiers (soy lecithin, tween 60, tween 80, and PGPR) were evaluated in preliminary tests, as well as different homogenization techniques (magnetic stirrer at different times and rotations, and different ultrasound power and exposure times). Preliminary tests indicated that PGPR and the ultrasound-assisted homogenization process were more satisfactory in producing stable emulsions. Polyglycerol polyricinoleate (PGPR) is a food-grade oligomeric emulsifier, and has high affinity for the fat phase due to its low hydrophilic-lipophilic balance number (3 - 6), thus it is a suitable alternative for stabilizing W/O (Ushikubo & Cunha, 2014). The sedimentation index of the emulsion 21/; made without the addition of PGPR was significantly higher ($p \leq 0.05$) when compared with the emulsions made with 3, 4, and 5 g PGPR·100 g⁻¹ of fat blend, as can be seen in Fig. 1A. The emulsion containing 5 g PGPR·100 g⁻¹ showed higher SI when compared to the emulsions made with 4 and 3 PGPR·100 g⁻¹ for the same processing times (45 and 60 min), with significant differences between them ($p \leq 0.05$). This small increase in phase separation of the emulsion containing 5 g PGPR PGPR·100 g⁻¹ may be probably due to the saturation of PGPR at the oil-water interface resulting in an excess of PGPR and micelle formation, leading to a greater reduction in interfacial tension (Raviadaran et al., 2019). The PGPR concentration of 4 g·100 g⁻¹ exhibited the best kinetic stability, thus it was selected for the study. Similar results were found by Consoli

et al. (2016), who evaluated the production of W/O emulsion composed of 30% aqueous phase and 70% oil phase, containing fat and palm oil (80/20 wt%).

(A)



(B)

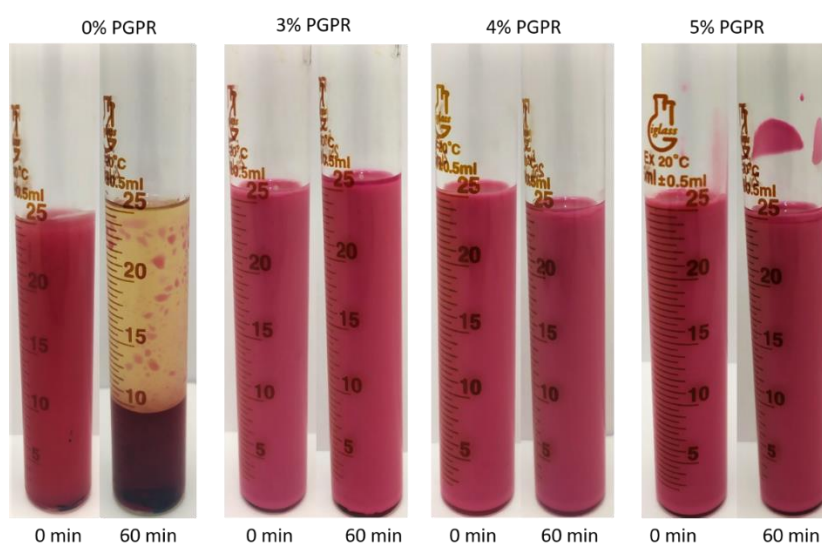


Fig. 1. Effect of the PGPR concentration on the sedimentation index at 70 °C over time. (A) PGPR concentration from 0 to 5 g/100 g. (B) Visual observation of the stability of the emulsions made with different PGPR concentrations over time.

3.1. *Droplet mean diameter, size distribution, and microstructure*

The droplet mean diameter and size distribution are key factors for estimating the emulsifying effect and the emulsion stability. The diameter values ($D_{3,2}$) and the size distribution of the emulsion droplets (Span) can be seen in Table 1. Significant differences ($p \leq 0.05$) were observed for both parameters between the treatments. The lowest mean droplet size was observed for ultrasound-assisted homogenized emulsions. In contrast, the control MS_W/O emulsion presented the highest mean droplet size diameter ($9.01 \pm 0.46 \mu\text{m}$). (Jafari et al., 2007) when compared to the emulsions made using mechanical stirring and ultrasound. The authors reported a three times higher $D_{3,2}$ for the emulsions made by mechanical stirring when compared to the ultrasound-treated emulsion. Emulsion with a higher droplet size tends to present lower steric stabilization. The main force involved in the mechanical stirring is significantly lower when compared to ultrasound (Silva et al., 2018). Similarly, it can promote smaller breaking of the droplets, resulting in larger droplets size (Consoli et al., 2017). Whereas ultrasonic emulsification involves higher energy, the acoustic cavitation phenomenon is responsible for the droplet rupture, which promotes the growth and collapse of microbubbles of gas dissolved in the medium. The collapse of the bubbles leads to strong shock waves propagation into the medium, leading to droplets breakdown (Paniwnyk, 2017). Other authors have also reported similar results when comparing the ultrasound technology with other mechanisms for the production of W/O (Al-Maqtari et al., 2021; Raviadaran et al., 2019; K. Zhang et al., 2020) and O/W (Consoli et al., 2017; Tabibiazar et al., 2015) emulsion systems.

At a fixed sonication time, the higher the power, the lower $D_{3,2}$ diameter. The sonication time affected this parameter differently, once an increase in the mean diameter of the droplet was observed when increasing the sonication time from 4 to 6 minutes at fixed power. This result suggests that there is a limit on the time of ultrasound treatment that still promotes droplet rupture when using the same power. Above this limit, collision, coalescence, and flocculation

of droplets can occur, thus increasing the mean diameter of the droplets (K. Zhang et al., 2020). Excessive energy can lead to over-processing, with an increase in the droplet diameter and re-coalescence, which was reported by K. Zhang et al. (2020) and Consoli et al. (2017). The authors stated that the forces of ultrasonic radiation (referred to as Bjerknes forces) increased with increasing acoustic power, and then the Bjerknes' second forces would drive the emulsion droplets to the nodes and antinodes of the sound field, and the droplets of greater proximity would lead to increased droplet coalescence, and thus the over-processing effect.

In this study, the droplet size distribution (Fig. 2) was more affected by the sonication time rather than the ultrasound power. Long sonication periods expose droplets to high amounts of energy, leading not only to droplet rupture but also droplet collision and thus re-coalescence and flocculation, explaining the larger variability in the droplet size. This tendency of increasing the mean diameter of the droplets with the increase in the sonication time are in accordance with the results reported by K.Zhang et al. (2020) and Raviadaran et al. (2019), who also used ultrasound to produce W/O emulsions.

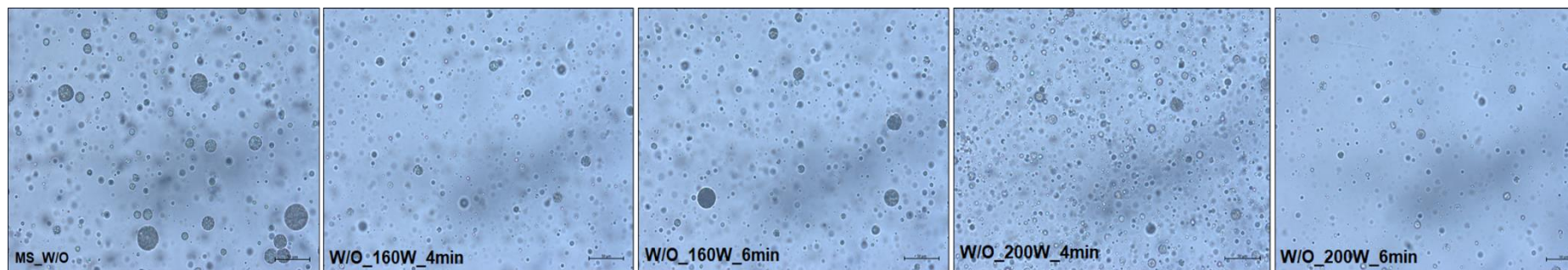
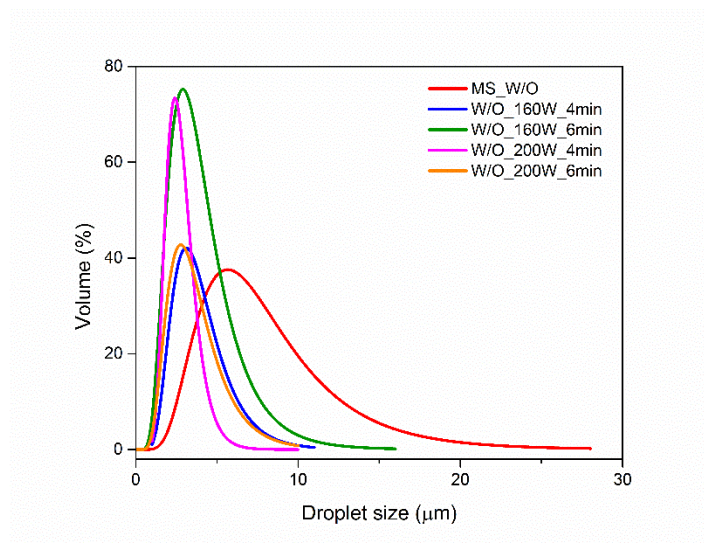


Fig. 2. Surface mean diameter ($D_{3,2}$) and micrographs of the emulsions.

The Span values were used to express the degree of polydispersity in the distribution of droplet size in the emulsions. The smaller the Span values of the emulsion, the narrower the distribution, which implies more uniform and consistent processing (Silva et al., 2015). All emulsions showed small Span values ranging from 0.72 to 1.58, although they differed statistically among them. The lowest Span value was observed for the W/O_200W_4min (Table 1). Span values below 2 typically indicate a narrow and uniform distribution (Alvim, 2016), which can be seen in Fig.2. Furthermore, the droplet size distribution indicated asymmetric curves for both treatments.

The micrographs obtained by optical microscopy (Fig. 2) of the emulsion subjected to the different emulsification processes corroborate the results of the droplet mean diameter and size distribution. Therefore, larger droplets were observed for the control emulsion (MS_W/O), with a higher mean diameter, which highlights the positive effect of the ultrasound process on the average droplet diameter of the emulsions.

3.2. Kinetic stability

In some processes like spray chilling, the emulsions should be atomized immediately after preparation, to minimize the exposure of active compounds to high temperatures (70 °C). For that, it is necessary to maintain the emulsions kinetically stable at least before and during the atomization, which varies according to the amount of sample and the feed rate into the atomizer. According to pre-tests, 15 minutes were required to atomize 150 mL of emulsion. Thus, the time of two hours is suitable to evaluate the kinetic stability of the emulsions, considering their preparation for the production of the particles by spray chilling.

The sedimentation index (SI) provides indirect information about the extent of droplet aggregation in an emulsion. The greater the aggregation, the larger the effective droplet size, and hence the faster the phase separation (Modarres-Gheisari et al., 2019). The SI of the

emulsions was monitored every 15 minutes for 120 minutes. In the first 15 minutes, the control emulsion (MS_W/O) showed kinetic instability with a small oil phase on top (Fig. 3) and 1.33 % of SI. From 30 minutes, a phase separation was observed for the emulsions control (2.67 %), W/O_160W_4min (0.67 %), and W/O_160W_6min (0.40 %), while the emulsions W/O_200W_4min and W/O_200W_6min showed no phase separation. These results suggest that up to 30 minutes the phase separation rate was higher for the control (MS_W/O) and the ultrasound-treated emulsions at lower powers.

Up to the 75-minute period, no changes were observed in the sedimentation levels of the emulsions. After this period, the changes in SI remained stable until the period of 120 minutes, with significant differences ($p \leq 0.05$) between treatments at the end of the period studied. Most emulsions showed phase separation at 120 minutes, except for W/O_200W_4min, which remained stable throughout the period. The higher sedimentation index (120 min) was observed for the untreated emulsion MS_W/O (SI = 3.9 %) followed by W/O_160W_6 min (SI = 2.50 %), W/O_160W_4min (SI = 2.44 %), and W/O_200W_6min (SI = 1.03 %). These results suggest that the sedimentation indices can be directly related to the mean diameter of the emulsion droplets. The emulsion W/O_200W_4min, with the smaller droplet size, showed high stability with no phase separation throughout 120 minutes. The higher droplet size accelerates destabilization processes, such as phase separation, creaming and flocculation (Modarres-Gheisari et al., 2019). According to Stokes law, the speed with which a droplet moves is proportional to the square of its radius, thus reducing the droplet size of an emulsion can increase its stability, thus preventing phase separation (Silva et al., 2015). As previously discussed, unlike ultrasound, the magnetic stirrer promotes a low collision of molecules and, consequently, less droplets breakage, favoring coalescence and separation of phases (Mohammed et al., 2021). As shown in Fig.2, The control emulsion (MS_W/O) showed greater coalescence of the droplets when compared to the ultrasound-treated emulsions. Similar

results were reported by (Silva et al., 2018) in water-oil emulsions subjected to magnetic stirrer and ultrasound, with phase separation for all emulsions over time. However, the phase separation rate and the SI were higher for the emulsion made using magnetic stirrer when compared to the ultrasound-treated emulsions. According to the authors, this behavior is directly related to the average droplet diameter of the emulsions.

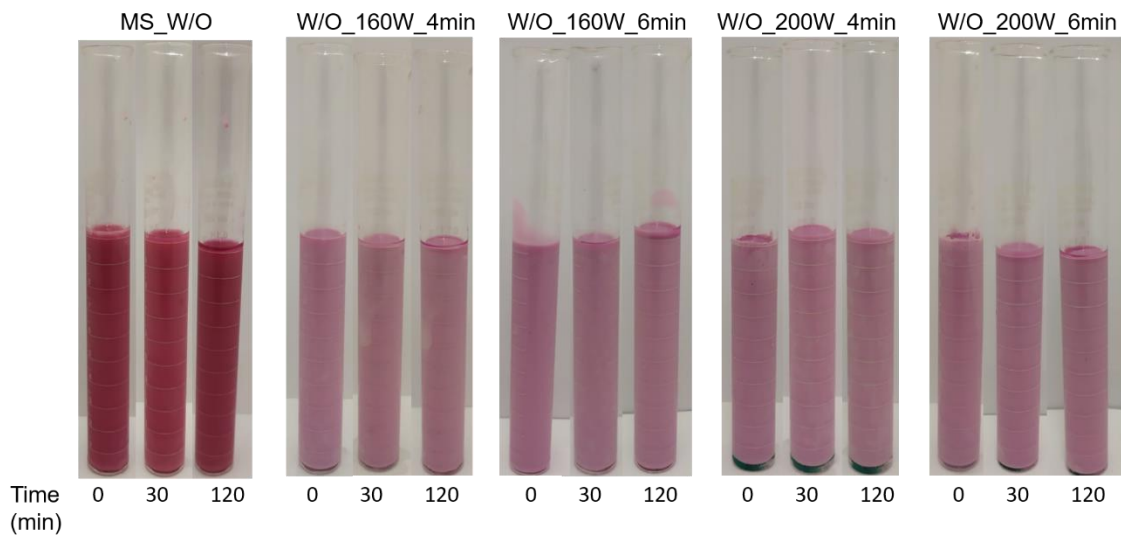


Fig. 3. Visual observation of the stability of W/O emulsions before and after ultrasound treatment for 120 minutes at 70 °C.

3.3. Rheological behavior

Shear viscosity of the emulsions is an important parameter related to fundamental problems of fluid dynamics and has numerous technological implications (Al-Maqtari et al., 2021). The food viscosity can either increase or decrease as a function of the ultrasound intensity, which can be a temporary or permanent effect (Soria & Villamiel, 2010). Flow curves of emulsions are presented in Fig.4, and viscosity values for those samples are outlined in Table 1. Among the models used to describe the rheological behavior of the treatments, Newton's Law model presented the best adjustments to the experimental data, with a high coefficient of determination ($0.9930 \leq R^2 \leq 0.9979$) and low root mean square error ($0.053 \leq RMSE \leq 0.100$)

values. This model has been widely used to describe the rheological behavior of food emulsions as a function of the shear stress applied to the system (Consoli et al., 2016; Lago et al., 2019; Udomrati et al., 2013; Zhang et al., 2020).

The viscosity of the material should be within 500 mPas to not interfere with the atomization process of fluids in spray chilling (Jaskulski et al., 2018). As shown in Table 1, the viscosity values for all emulsions were far below this limit.

For all samples, there was no yield stress, and shear stress responded linearly to shear rate increasing, thus characterizing a Newtonian flow behavior. Such behavior suggests that the viscosity remains constant for a given temperature, regardless of the application time of shear fluid and the shear rate used (Lago et al., 2019). This is important from the perspective of emulsion stability, which is governed by the rate of creaming and/or sedimentation of dispersed-phase droplets under inert or low shear conditions (Mohammed et al., 2021).

Generally, the rheological properties of emulsions are the result of their droplet volume fraction, droplet size distribution, and inter-droplet forces. The viscosity of the ultrasound-treated samples was higher than the corresponding control (MS_W/O), probably due to the high solubilization and smaller droplet sizes (Table 1) of the emulsions. The decreased droplet size may lead to an increase in the total surface area of the W/O emulsions entrapping grape peel extract, thus leading to high viscosity. Moreover, the increase in viscosity can be due to the presence of finely emulsified fat globules generated by the intense shear forces of ultrasound (Yao et al., 2020). Other authors studied W/O emulsions entrapped with chitosan and also reported that the lower the $D_{3,2}$ value, the greater the emulsion viscosity, with an increase in viscosity after the ultrasound treatment. The authors presented a close non-linear relationship between the droplet diameter and the emulsion viscosity, i.e., the emulsion viscosity can be represented as a monotonically decreasing power as a function of the diameter. Thus, in this study, a decrease in particle size yielded a larger interfacial area and a decrease in the mean

distance between particles, which resulted in stronger inter-particle interactions, and smaller particles dispersed better the grape peel extract, consequently resulting in higher viscosity values.

The increase in viscosity due to solubilization (breakdown of macromolecule aggregates into their macromolecules) has been described by some authors in emulsified systems such as avocado puree, tomato pulp, and tomato juice (Anese et al., 2013; Bi et al., 2015; Vercet et al., 2002). The authors reported higher viscosity of these food systems after the ultrasound treatment, probably due to the effect of cavitation that can break particles or molecules and lead to a better interaction between particles, thus increasing the viscosity of these systems. The increase in viscosity observed in the present study can also be due to the solubilization of the cell wall material and the formation of a new network by hydrogen bonds and hydrophobic interactions between the pectin molecules from the grape peel extract after the ultrasound treatment.

Generally, an increase in continuous-phase viscosity leads to a substantial improvement of emulsion stability by decelerating the creaming phenomenon (that causes the rise of oil droplets to the top phase with time) (Modarres-Gheisari et al., 2019). Thus, the inferences from the rheological analysis indicate that the ultrasound treatment emulsions may be more stable than its magnetic stirrer emulsion, this fact has confirmed with stability studies.

Table 1. Emulsion characteristics and kinetic parameters of anthocyanin of emulsions during storage.

<i>Assay</i>	<i>D_{3,2} (μm)</i>	<i>Span</i>	<i>N (Pa.s)</i>	<i>R²</i>	<i>Peroxide value</i>	<i>Anthocyanin (malvidin-3-diglycoside)</i>		
						<i>k (x 10⁻²) (dias⁻¹) *</i>	<i>t^{1/2} (dias)*</i>	<i>R²</i>
<i>MS_W/O</i>	9.01 ± 0.46 ^a	1.31 ± 0.07 ^{b,c}	0.019547	0.9967	4.53 ± 0.15 ^a	1.705	40.654	0.937
<i>W/O_160W_4min</i>	4.50 ± 0.22 ^b	1.07 ± 0.08 ^c	0.032458	0.9950	2.53 ± 0.09 ^b	1.428	48.526	0.950
<i>W/O_160W_6min</i>	4.70 ± 0.13 ^b	1.58 ± 0.13 ^a	0.04143	0.9940	2.76 ± 0.53 ^b	1.311	52.875	0.939
<i>W/O_200W_4min</i>	3.32 ± 0.75 ^c	0.72 ± 0.16 ^d	0.038308	0.9930	2.90 ± 0.13 ^b	1.306	54.447	0.947
<i>W/O_200W_6min</i>	4.06 ± 0.18 ^{b,c}	1.36 ± 0.20 ^{a,b}	0.030885	0.9979	2.98 ± 0.8 ^b	1.248	55.554	0.959

Note: ^{a,b,c,d} Means followed by the same letters in the same column do not differ significantly ($p > .05$) using Duncan's test; k: first-order reaction rate constant; $t_{1/2}$: half-life; R^2 : coefficient of determination.

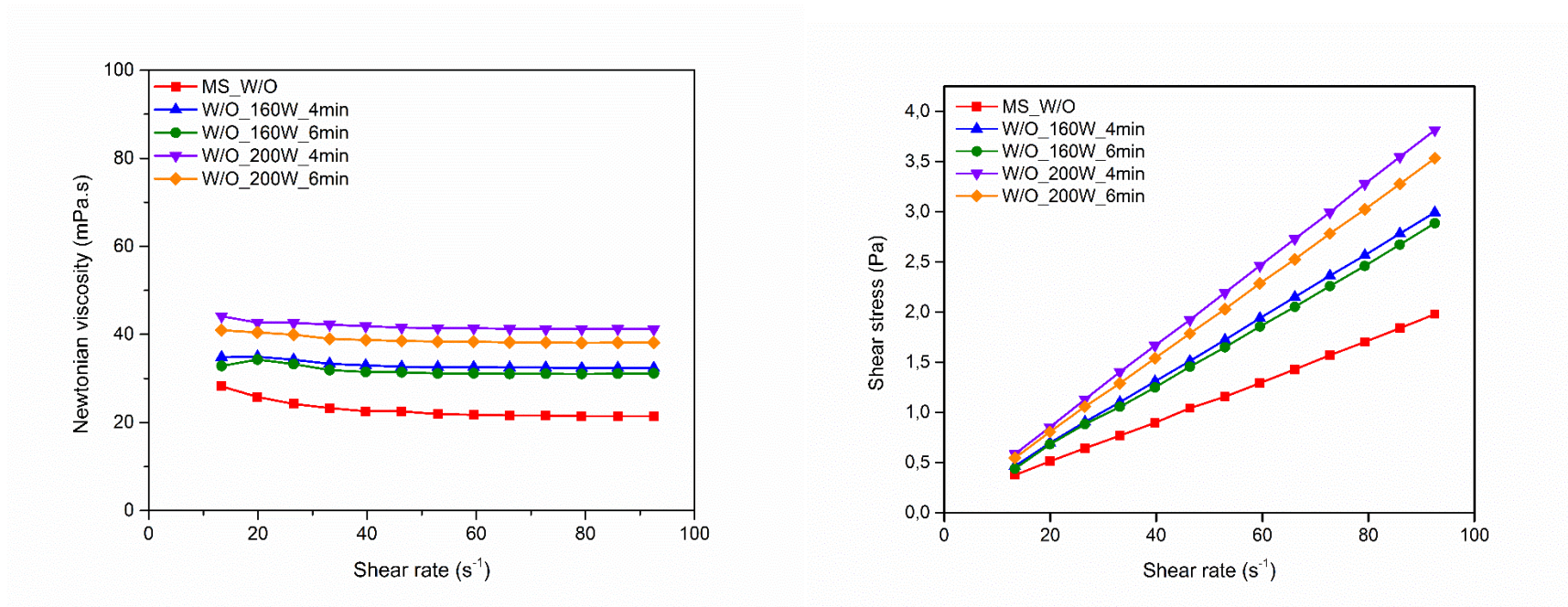


Fig. 4. Rheological behavior and relationship between the shear stress (Pa) and the shear rate (s⁻¹) of the emulsions before and after ultrasound treatment.

3.4. Emulsion oxidation after ultrasound-assisted treatments

FTIR analysis was carried out to determine the structural changes of the emulsions produced by ultrasound-assisted due to hydrolysis and oxidation reactions. Raviadaran et al. (2019) stated that the common functional groups of concern in FTIR spectra are the aldehydes (C–O stretch at 1750–1625 cm^{-1} , C–H stretch of C=O at 2850–2800 cm^{-1} , and C–H stretch of C=O at 2750–2700 cm^{-1}), ketones (C=O stretch at 1750–1625 cm^{-1}) and carboxylic acid (C=O stretch at 1730–1650 cm^{-1} and hydrogen-bonded O–H stretch at 3400–2400 cm^{-1}). Fig. 5 shows the overlapped spectra of the pure lipid materials (FHPO and PO) onto the emulsions, while Fig. 5E shows the spectrum of the grape peel extract. All emulsions showed typical bands of FHPO, PO, and grape peel extract. The FTIR analysis showed the incorporation of the grape peel extract in the emulsions, especially the ultrasound-treated emulsions. The strong peak at around 1600 cm^{-1} found in the grape peel extract can be attributed to the C=C vibration typical of aromatic systems (Nogales-Bueno et al., 2017). Although similar peaks were observed for all emulsions, more pronounced peaks were detected in the ultrasound-assisted emulsions when compared to the control emulsion (MS_W/O). The high energy released by the ultrasound-assisted technology may have contributed to the release of phenolic compounds from the grape peel extract. These results can be correlated with the higher phenolic compounds levels of the ultrasound-treated emulsions when compared to the control treatment. More details are discussed in Section 3.5.

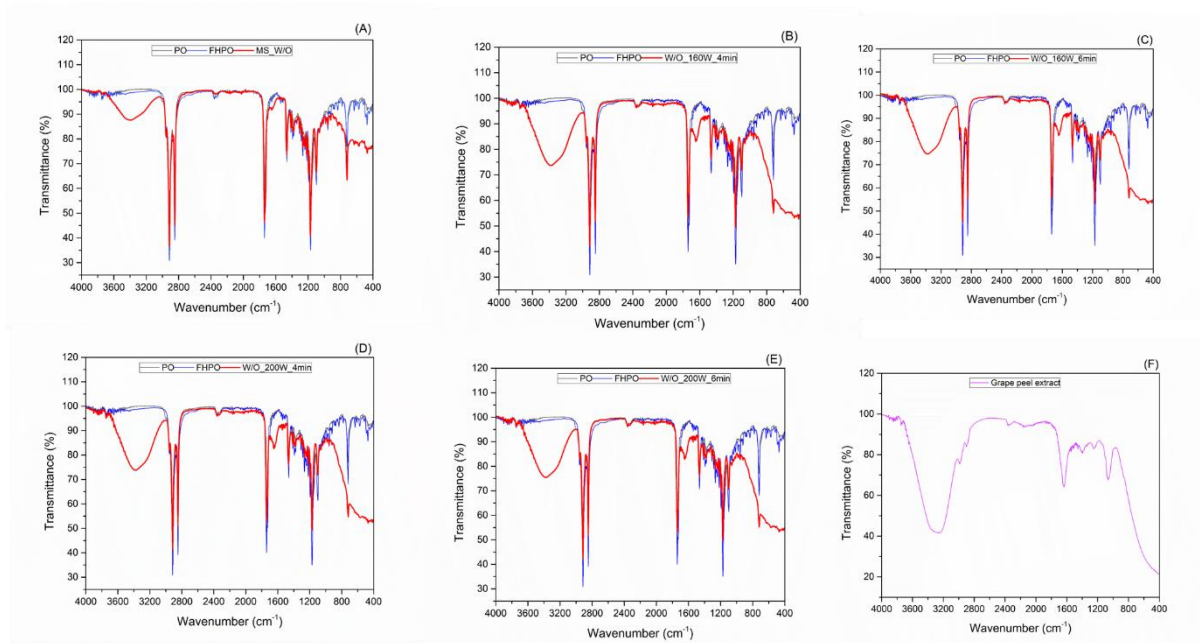


Fig. 5. FTIR spectra of W/O emulsions before and after ultrasound treatment.

The absence of key functional groups showed that no secondary oxidation products were formed due to emulsification process by ultrasound. These results demonstrated that the high energy promoted by ultrasound-assisted at different exposure times and powers led to no undesirable lipid oxidation reactions. Other studies on W/O emulsions found similar results, with no effects of ultrasound treatments on the chemical structures, with no formation of oxidation products (Al-Maqtari et al., 2021; Raviadaran et al., 2019; K. Zhang et al., 2020).

However, some differences in peak intensities were observed between the control and the ultrasound-treated emulsions. According to the literature, regions in the range of 2926–2955 and 2855–2893 cm^{-1} correspond to the symmetric and antisymmetric stretching vibrations of the aliphatic groups ($-\text{CH}_2$ and $-\text{CH}_3$), respectively (Hayati et al., 2005). The control emulsion presented a small increase in the intensity of some bands (2927 and 2855 cm^{-1}). A similar result was also observed for the band near 1746 cm^{-1} , corresponding to vibration of the carbonyl group of triacylglycerol esters. This band has been used to quantify the fat content in butter and mayonnaise products. It is usually detected in the infrared spectrum of palm oil, once both

aliphatic and carbonyl groups give a very strong absorption in the corresponding regions (Lim et al., 2018). Therefore, the more unstable emulsion is likely to demonstrate stronger band absorption in these regions due to the physical separation of the oil phase. Physical separation results from an increase in molecular interactions at the interfacial region, making these groups more available for vibration. This finding reveals that the physical destabilization of emulsions due to phase separation can be due to the increase in vibrations of aliphatic groups and carbonyls close to these regions (Hayati et al., 2005). In this study, the control emulsion showed the highest physical instability (measured as sedimentation index), that is, a greater separation of the oil phase was observed when compared to the ultrasound-treated emulsions.

The peroxide value was determined to evaluate possible oxidation of the fatty acid fractions by the high energy generated by ultrasound (Pandit & Joshi, 1993). As shown in Table 1, a significantly higher peroxide value ($p \leq 0.05$) was observed for the control emulsion (MS_W/O) when compared with the ultrasound-assisted emulsions. Ultrasound-assisted emulsions presented similar peroxide values, which indicate that the higher energy produced by ultrasound did not provide the lipid oxidation. This finding corroborates the findings of Raviadaran et al. (2019). Moreover, the different ultrasound exposure times and powers did not cause significant difference in this parameter ($p \geq 0.05$). The higher peroxide value of the control emulsion may be due to the greater separation of the oil phase when compared to the other treatments. As previously mentioned, the peaks related to triacylglycerol ester bonds may be associated with emulsion instability. The oxygen molecules of the triacylglycerol ester bonds provide many hydrogen bonding sites for alcohols and hydroperoxides (Daoud et al., 2019), which may have led to an increase in the peroxide value of this treatment.

3.5. Bioactive compounds, degradation test, and accelerated oxidation

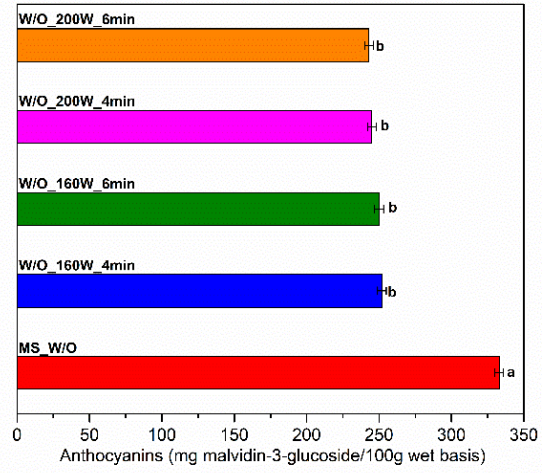
Grape peel is an important source of polyphenols, like phenolic acids, flavonoids, anthocyanins, proanthocyanidins and resveratrol. Approximately 60–65% of phenolic compounds remain in the grape pomace after juice or red wine production, which could be processed, and used as a source of antioxidants, but it is usually discarded as waste or employed as animal feed (Mammadova et al., 2020; Romanini et al., 2021).

The bioactive compounds contents (anthocyanins and total phenolic compounds) and the antioxidant activity of the emulsions before (control treatment) and after homogenization by ultrasound are shown in Fig. 6A, 6C, and 6E. The degradation kinetics of anthocyanins, the total color changes, and the peroxide values of the emulsions were monitored during storage, aimed to assess the degradation rate and the oxidative stability of the emulsions, and are shown in Fig. 6B, 6D, and 6F, respectively.

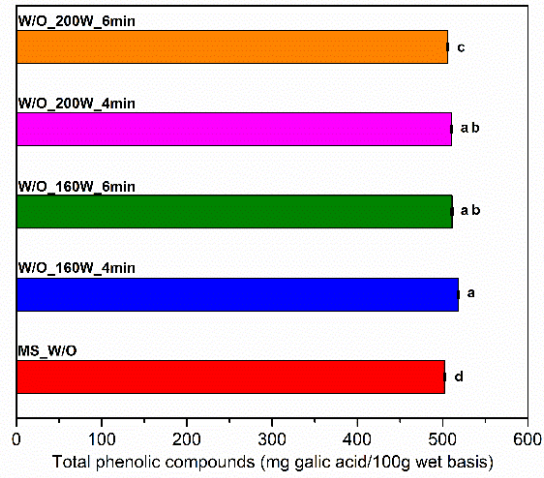
The effect of the ultrasound processing on the phenolic compound's concentration in the emulsions is shown in Fig. 6C. A positive and significant effect ($p \leq 0.05$) was noted when the ultrasound was applied when compared to the control (MS_W/O). During ultrasound processing, increased mass transfer rates and possible rupture of the cell wall (presents in the extract) due to the formation of microcavities can result in the release of phenolic compounds. Probably, this increase may be due to sonochemically generated hydroxyl radicals (OH.) in the aromatic ring of phenolic compounds (Romanini et al., 2021). According to Wang et al. (2019), in general, the peak of compounds containing hydroxyl (OH.) groups, such as phenolic compounds, occurs between 2900 and 3550 cm^{-1} . As shown in Fig. 5, a peak increase corresponding to the hydroxyl compounds was observed for the ultrasound treated emulsions. This result indicates that the increase in OH. groups can be due to the increase in phenolics contents after the ultrasound treatment, which corroborates the results of the quantitative Folin-Ciocalteu method. In addition, other peaks with greater intensity, related to aromatic rings of the phenolic compounds (1600 cm^{-1}) (Nogales-Bueno et al., 2017) were also observed in the

ultrasound-treated emulsions. Similar effects of ultrasound treatments on phenolic compounds were reported in blueberry juice (Wu et al., 2021), mulberry juice (Kwaw et al., 2018), and grape pomace (Romanini et al., 2021).

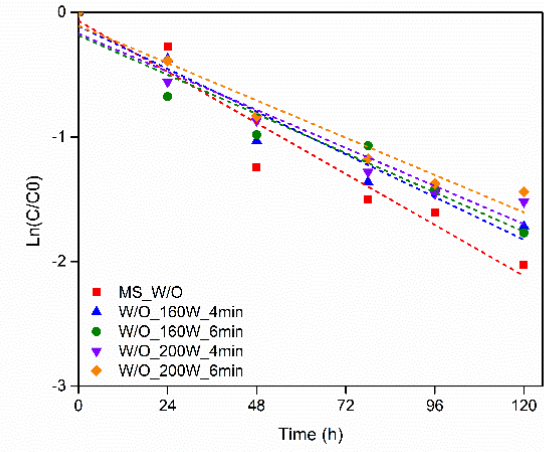
(A)



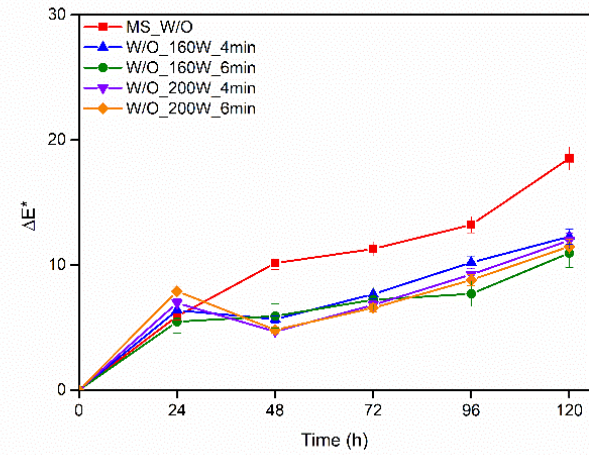
(C)



(B)



(D)



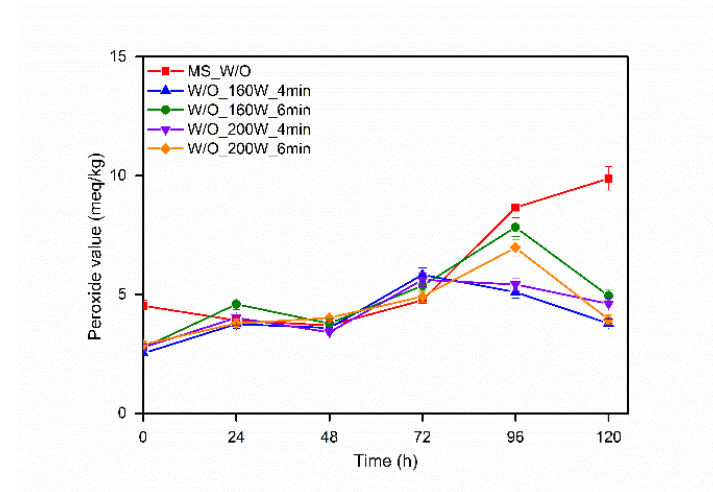
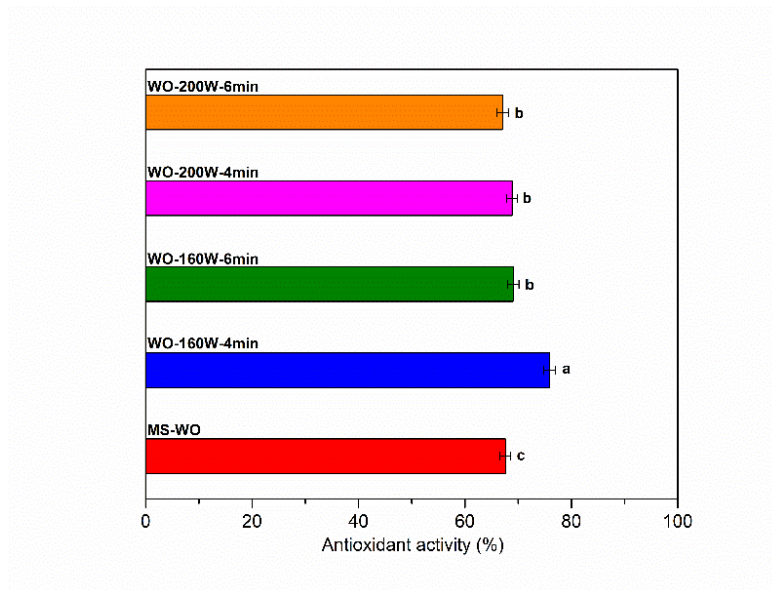


Fig. 6. Anthocyanins content (A), degradation kinetics of anthocyanins (B), antioxidant activity (C), total phenolics content (D), total color differences ΔE (E), and peroxide values (F) of the emulsions.

Concerning the ultrasound-treated emulsions, both sonication time and power affected ($p \leq 0.05$) the content of phenolic compounds, and the emulsion W/O_200W_6min exhibited the lowest total phenolic compounds levels. Therefore, the increase in the exposure time from 4 to 6 minutes for the highest power used in this study may have led to degradation of the phenolic compounds. The ultrasound processing conditions such as power, exposure time, and frequency may induce chemical reactions related to degradation, such as pyrolysis within cavitation bubbles, which causes degradation of polar compounds, and generation of hydrogen ions, hydrogen peroxide, and free radicals that are produced by cavitation effect (Chemat et al., 2011; Paniwnyk, 2017).

The antioxidant activity of the emulsions is related to the content of phenolic compounds in the grape peel extract. The antioxidant activity values ranged from 76 to 68%. (Fig. 6E), and the emulsion W/O_160W_4min presented a higher antioxidant activity, with significant differences ($p \leq 0.05$) from the other treatments. In contrast, the control emulsion (MS_W/O) exhibited the lowest antioxidant activity. The increase in antioxidant capacity could be attributed to the increase in phenolic compounds and the probable presence of components with proton-donating properties that can react with DPPH radicals (Kwaw et al., 2018). As shown in FTIR analysis, ultrasound increased the OH groups related to phenolic compounds in the emulsions. Studies have shown that the presence of a second hydroxyl group at the ortho or para positions may increase the antioxidant activity of the phenolic molecules (Carvalho et al., 2020). These improvements have already been described by other authors for fruit extracts subjected to ultrasound treatments. González-Centeno et al. (2015) reported an improvement in the extraction of phenolic compounds and antioxidant capacity of grape peel extracts subjected to ultrasound when compared to conventional extraction (with mechanical agitation), reaching concentrations 2.4 to 3.4 times higher, respectively. Ultrasound can modify the structure of the

grape peel extract, increasing the phenolic compounds and improving the antioxidant activity (Romanini et al., 2021).

The use of natural colorants as additives has received increasing attention in recent years. Anthocyanins are included in the class of natural colorants that provide a wide range of colors from green/yellow to violet/blue (Lopes et al., 2007). In grapes, these compounds are present mainly in the peels. Anthocyanins are synthesized via the phenylpropanoid and flavonoid pathways, have the typical C₆-C₃-C₆ flavonoid skeleton consisting of two aromatic rings and a heterocyclic benzopyran ring (Yang et al., 2021). Recent studies have reported that the major anthocyanins present in Maple grape peels are malvidin-3,5-diglucoside, cyanidin-3,5-diglucoside, and malvidin-3-O-glucoside (Gomes et al., 2019; Haas et al., 2019).

In the present study, the anthocyanin contents ranged from 333 to 243 mg malvidin-3-glucoside/100 g on a wet basis. The control emulsion (MS_W/O) made using a magnetic stirrer had a higher anthocyanin level ($p \leq 0.05$), when compared to the ultrasound-treated emulsions, with no significant differences between them. The use of ultrasound can affect the anthocyanins contents in plant extracts, leading to positive (improved extraction) and/or negative (degradation) results. The negative effects of ultrasound on anthocyanin contents have been reported in studies on red grape (Tiwari et al., 2010), grape (Yang et al., 2021), star fruit extract (Annegowda et al., 2012), and strawberry juice (Dubrovic et al., 2011). All those studies reported a tendency of degradation of anthocyanins when subjected to ultrasound treatment at high exposure times and powers.

Tiwari et al. (2010) reported that cyanidin-3-O-glycoside, delphinidin-3-O-glycoside, and malvidin-3-O-glycoside were the major anthocyanins affected by ultrasound power and exposure time of grape juice (*Vitis vinifera* L.), while other anthocyanins were not affected by sonication. According to the authors, higher power levels and exposure times have adverse effects on the anthocyanin contents of grape juice, which is also affected by the type of

anthocyanin. It has been shown that prolonged exposure of anthocyanins to high temperatures can accelerate the formation of chalcone, leading to degradation of anthocyanins (Ahmed et al., 2004; Rehman et al., 2017; Turturică et al., 2016). The high local temperatures can result in free radicals by the cleavage of the water molecules, which can interact with the pyrilium rings of the molecular structure of anthocyanins, resulting in glycosylated chalcones. These chalcones can rapidly degrade to phenolic acids and aldehydes due to their thermosensitivity (Carvalho et al., 2020). In addition, the exposure to high temperatures during the ultrasound treatment may have degraded the anthocyanins, reducing their content. Although no significant differences were observed between the ultrasound-treated emulsions, the emulsions subjected to higher power (W/O_200W_4min and W/O_200W_6min) showed 2% more loss of anthocyanins when compared to the emulsions subjected to lower power (W/O_160W_4min and W/O_160W_6min).

The higher anthocyanins content of the control emulsion (MS_W/O) may also be due to the extraction process during the quantification of this compound. As observed in the kinetic stability of the emulsions, the treatment MS_W/O was less stable when compared to the ultrasound-treated emulsions. Therefore, the magnetic stirrer was less able to form a stable and strongly bound system among the grape peel extract, the emulsifier, and the lipid materials. This less stable system may easily allow migration of the grape peel extract and/or the palm oil to the emulsion surface, facilitating the release of the anthocyanins from the W/O_MS emulsion during quantification. In contrast, the extraction of anthocyanins from the ultrasound-treated emulsions was impaired since ultrasound allowed the formation of stable and strongly bound systems.

The degradation kinetics of anthocyanins is an important tool to prevent the loss of the characteristic color of these compounds and their functional properties (Zhou et al., 2017). Thus, the degradation kinetics of anthocyanins was used in this study as a complementary

analysis to select the best condition for making a stable emulsion to be subjected to spray chilling, and to protect the bioactive compounds.

The study of the degradation kinetics of anthocyanins of the emulsions (Fig. 6B) followed first-order kinetics ($0.937 \leq R^2 \leq 0.959$), and revealed that the ultrasound-assisted processing led to a lower degradation rate (k) and an increase in the half-life ($t^{1/2}$) (Table 1) of this compound during storage. The ultrasound treated emulsions showed smaller droplet size, higher viscosity, and greater kinetic stability when compared to the control (MS_W/O). These characteristics may explain the greater stability of anthocyanins in the ultrasound treated emulsions during the storage since these emulsions are more homogeneous, thin, with small molecular mobility due to higher viscosity, which can protect the sensitive compounds such as anthocyanins from adverse reactions such as temperature, light, oxygen, and moisture during storage. The emulsion made using a magnetic stirrer (MS_W/O) showed higher particle diameter ($D_{3,2}$), lower viscosity, lower kinetic stability, which can cause an increase in energy in the interfacial area of the emulsions, releasing the bioactive compounds to the surface more easily, and quickly and making it more susceptible to oxidation throughout the storage period.

In a similar study on the controlled release of phenolic compounds from *Pulicaria jaubertii* extract W/O emulsion, the authors reported that the ultrasound treated emulsions showed greater encapsulation efficiency and lower release of phenolic compounds during storage (Al-Maqtari et al., 2021). Therefore, the use of ultrasound can be efficient for improving the stability and allowing controlled delivery systems for bioactive compounds such as anthocyanins.

In addition to the degradation kinetics, the parameter total color difference (ΔE) can be used as a quality parameter (Figueiredo et al., 2020). The increase in ΔE values indicates the loss of the initial characteristic color of the product due to different factors, including the degradation of bioactive compounds. The results of total color difference of the emulsions

during storage are shown in Fig. 6D. All emulsions showed ΔE values between 5 and 7 in the first 24 hours of storage, which indicates a noticeable change visible to the naked eye since ΔE values above 3.0 represent the color difference threshold (Buvé et al., 2018). The total color changes of the ultrasound treated emulsions were similar, with a greater change in the first 24 hours. After this period, the emulsions presented a stable color change behavior, that is, the variations in the ΔE values were subtle, reaching ΔE of 11 - 12. Greater instability in this parameter was observed for the control emulsion MS_W/O during storage, with an increase in the ΔE values, reaching the maximum value ($\Delta E = 19$). Many factors can affect the color during the storage of the emulsions, such as the oxidation and degradation reactions of palm oil and fat, and the bioactive compounds present in the grape peel extract. The control emulsion showed a higher degradation rate when compared to the ultrasound-treated emulsions, thus the degradation process may have contributed to higher ΔE values observed for MS_W/O. The degradation of anthocyanins by heat during storage leads to the formation of enzymes such as glycosidases, which first oxidize other phenolic compounds in the medium to the corresponding quinone forms, which react with the anthocyanins, resulting in the degradation of anthocyanins and the formation of darkly colored condensation products (Fredes et al., 2018).

The peroxide value of the emulsions were determined during the storage to monitor the lipid oxidation (Poyato et al., 2013). A Fig. 6F shows the peroxide values of the emulsions during storage. Initially, the ultrasound-treated emulsions exhibited similar peroxide values, which was lower than the values found for the control emulsion MS_W/O. Although all emulsions exhibited close peroxide values during the first 72 hours, the control had a higher peroxide value at the end of storage (96 and 120 hours). As can be seen in the anthocyanins degradation kinetics, the ultrasound can improve the stability of sensitive compounds during storage, which explains the lower peroxide values of the ultrasound treated emulsions. Probably, the antioxidant compounds present in the grape extract were released gradually,

protecting the palm oil and fat from lipid oxidation during storage. Moreover, as can be observed in this study, the control emulsion exhibited the highest kinetic instability (sedimentation index) over time, indicating greater phase separation. Thus, it is believed that the lipid phase migrated to the emulsion surface maintaining greater contact of the lipids with the oxygen, leading to an increase in the peroxide value. The interaction between atmospheric oxygen and the double bonds of unsaturated fatty acids leads to the formation of free radicals, with the consequent formation of peroxides and hydroperoxides, which in turn are responsible for the lipid oxidation (Ahmed et al., 2016).

It is worth mentioning that the peroxide values of all emulsions are in accordance with the limit established by the legislation ($<15.0 \text{ meq.kg}^{-1}$) even after the end of the storage (BRASIL, 2005). However, the control emulsion showed double the peroxide value (9.88 meq.kg^{-1}) when compared to the ultrasound-treated emulsion ($3.78 - 4.94 \text{ meq.kg}^{-1}$). These results infer that the ultrasound treatment has also improved the oxidation stability of the emulsions during the storage.

3.6. Formation of the microparticles, color measurements and anthocyanins content

As shown in this study, the use of ultrasound technique led to a higher kinetic stability of the emulsions (sedimentation index), and decreased the degradation rate of anthocyanins during the storage, which consequently contributed to the oxidative stability and color of the emulsions. These results suggest that the use of ultrasound is effective for the production of emulsions to be atomized by spray chilling since the emulsion stability can interfere with the quality of the final product (Campelo et al., 2017).

Therefore, the emulsion W/O_200W_4min was selected among the other ultrasound-treated emulsions for the microparticle forming ability test when compared to emulsion the MS_W/O due to its smaller average diameter ($D_{3,2}$) and higher kinetic stability (SI).

Both emulsions were able to form the microparticles by spray chilling (Fig.7), with no interferences during the process, even with different viscosities. However, phase separation was observed for the control emulsion after 10 minutes of atomization, which was expected since the kinetic stability study showed phase separation in the first 15 minutes for this treatment. In contrast, no phase separation was observed for the ultrasound-treated emulsion during the entire atomization process.

The visual aspect of the microparticles can be seen in Fig.7. The microparticles of both emulsions exhibited characteristics of a powdered product. Finer particles with better flowability were observed for the emulsion W/O_200W_4min when compared to the MS_W/O. These differences may be due to the phase separation in MS_W/O during atomization. During the phase separation, the lower melting point fat (palm oil) may have migrated to the surface of the particles, which may not have been fully crystallized during crystallization of the lipid matrix in spray cooling. The spray chilling process is very fast, thus the low melting point palm oil may have not crystallized, leading to the formation of a product with more agglomerated and sticky particles, which can impair the application and handling. In addition, the higher the stickiness of the microparticles, the lower the process yield (Carvalho et al., 2019; Favaro-trindade et al., 2015; Procopio et al., 2018).

Significant differences were observed for anthocyanin content ($p < 0.05$) in the two treatments, suggesting that homogenization influences the characteristics of bioactive compounds in the microparticles throughout storage. The microparticles produced with the emulsion subjected to W/O_200W_4min ultrasound showed a 42% loss of anthocyanins over 30 days, while the MS_W/O microparticles showed a 62% loss. As previously mentioned, ultrasound provided a more effective incorporation of the grape peel extract in the emulsion, which may have contributed to a better protection of anthocyanins against adverse storage conditions.

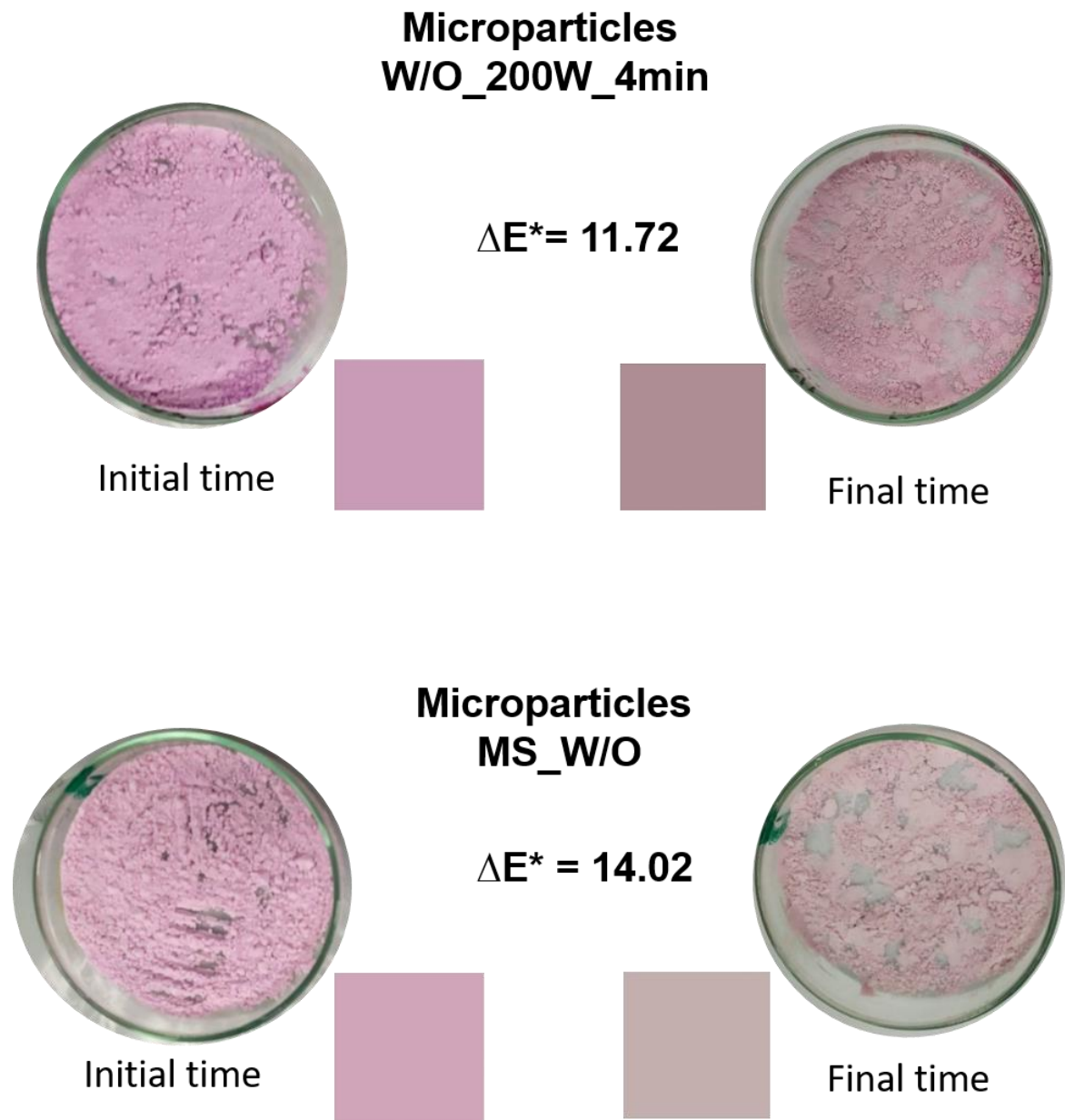


Fig.7. Visual aspects of the microparticles obtained by spray chilling immediately after production and after 30 days of storage.

The visual color parameters such as CIE $L^*a^*b^*$ and Hunter $L^*C^*h^*$ are more advantageous in food processes once they are on-line quality control methods (Yang et al., 2008). The color of the microparticles was evaluated before and after 30 days of storage, and the results are presented in Table 2. Significant differences ($p \leq 0.05$) were observed between the treatments for both storage time of 0 and 30 days.

Table 2. Storage stability of anthocyanins in microparticles based on the color parameters.

Time (days)	L*	a*	b*	C*	h*	ΔE
Microparticles obtained by magnetic stirring (MS_W/O)						
0	77.2 ± 0.90 ^a	17.9 ± 0.17 ^b	-4.2 ± 0.3 ^b	17.7 ± 0.3 ^b	12.95 ± 0.1 ^b	0
30	72.8 ± 0.6 ^a	6.2 ± 0.3 ^b	3.1 ± 0.1 ^b	6.93 ± 0.1 ^b	26.56 ± 0.0 ^a	14.47 ± 0.2 ^a
Microparticles obtained by assisted ultrasound (W/O_200W_4min)						
0	70.2 ± 1.44 ^b	21.4 ± 0.26 ^a	-7.9 ± 0.12 ^a	22.8 ± 0.17 ^a	19.79 ± 1.04 ^a	0
30	67.6 ± 0.1 ^b	15.7 ± 0.4 ^a	2.0 ± 0.1 ^a	15.8 ± 1.0 ^a	7.23 ± 0.7 ^b	11.72 ± 0.3 ^b

Note: ^{a,b}Means followed by the same letters in the same column do not differ significantly ($p > .05$) using Duncan's test.

Initially, the ultrasound-treated microparticles showed a more intense purple-pink color when compared to the control microparticles (Fig.7). Higher L^* values indicate lower brightness, higher a^* (+) and h^* values indicate higher intensity of red color and tone, respectively, while higher b^* (-) values indicate blue color, and C^* indicate higher saturation of the sample. Therefore, it can be inferred that the ultrasound-treated microparticles contained a higher concentration of bioactive compounds. This finding corroborates with other studies that showed lower anthocyanins levels in the emulsions obtained by ultrasound when compared to the control due to the efficient encapsulation which consequently hindered the release during the extraction of anthocyanins from the emulsions. These color parameters are commonly used to infer the presence of phenolic compounds such as anthocyanins in different samples, with higher values for a higher content of these compounds (Carvalho et al., 2020; Jiménez-Aguilar et al., 2011; Stoll et al., 2016).

Anthocyanins can undergo basic changes during a certain period of storage, such as color, which gradually becomes less intense due to the loss of saturation and/or changing tones after the formation of degradation compounds (Ahmed et al., 2004). After 30 days of storage, changes in color were observed for both samples, with a greater variation for the control treatment. A tendency to lower L^* , a^* , C^* values was observed for both treatments after 30 days of storage, i.e., there was a loss of coloration of the microparticles, corroborating other studies that reported that these parameters are associated with the anthocyanins content of the samples (Carmo et al., 2021; Moura et al., 2019; Carvalho et al., 2020). Several factors including light, humidity, and oxygen can accelerate the degradation of anthocyanins, leading to changes in their structures and causing the loss of color or the formation of dark pigments (Patras et al., 2010).

Hue values ranging from $h^* = 0^\circ$ (or 360°) to $h^* = 90^\circ$ indicate red to yellow tones, respectively. An increase in h^* was observed during the storage of the microparticles MS_W/O.

This behavior may be due to a color shift from red anthocyanin towards yellowish-brown colored compounds. As reported by Yang et al. (2008), there is a linear correlation between this parameter and the degradation of anthocyanins, associated with the formation of yellowish chalcone species. A distinct behavior was observed for the microparticles W/O_200W_4min, with a decrease in the h^* value, indicating lower intensity of the red color, and probably anthocyanins degradation.

Regarding the color parameter b^* that measures the difference between blue (-) and yellow (+), both treatments showed an increase in this parameter during storage, indicating loss of blue color due to anthocyanins degradation. According to Zheng et al. (2021), malvidin is the most important anthocyanidin for the blue color. Souza et al. (2015) also observed an increase in the b^* parameter in anthocyanins from Bordo grapes during storage. However, the authors reported that this result was due to the brown color of the samples throughout the storage, with an increase in yellow color (increase in b^*) due to the anthocyanins degradation.

The overall change in color of the samples is represented by the ΔE values, which relates the L^* , a^* and b^* parameters and expresses the weakening of the color during the storage. The greater color variation was observed for the microparticles MS_W/O, which indicates greater instability of these microparticles to the storage conditions, when compared to the microparticles W/O_200W_4min. In spray drying and spray chilling microencapsulation processes, the production of a quality emulsion directly interferes with the quality of the microparticles. As reported in this study, the ultrasound-treated emulsions showed better properties (higher kinetic stability, smaller particle size, and lower degradation rate of anthocyanins) when compared to the control emulsion. These results may be due to the higher stability of anthocyanins represented by the color parameters of the microparticles of this treatment, once a higher kinetic stability indicates a better emulsified system, and consequently better encapsulation of anthocyanins, impairing their interaction with degradation compounds.

A possible inactivation of oxidative enzymes during sonication may also have influenced the higher storage stability of the anthocyanin pigment in the microparticles made using the ultrasound treated emulsion, which may not have occurred with the control emulsion. In the presence of oxygen, enzymes such as polyphenoloxidase catalyze the oxidation of chlorogenic acid (CG) to the corresponding o-quinone (chlorogenoquinone, CGQ), which reacts with anthocyanins to form brown condensation products (Patras et al., 2010). This report corroborates the results of the degradation kinetics of anthocyanins in emulsions, with a higher degradation rate for the control treatment. It can also explain the greater variation of the parameters responsible for the brown color and the greater total color variation of the microparticles.

In general, it can be inferred that the ultrasound technique contributed to the characteristics of the microparticles obtained by spray chilling, producing fine, fluid microparticles, and with better stability of the anthocyanin pigment.

4. Conclusion

In this study, different PGPR concentrations and ultrasound exposure times and amplitudes were used to make W/O emulsions from grape peel extract to produce functional microparticles by spray chilling. The ultrasound played an essential role in the production of stable emulsions, mainly for the process conditions of 200W for 4 minutes. The ultrasound-treated emulsions exhibited smaller droplet sizes and higher viscosity. In addition, the different sonication times and amplitudes provided no lipid oxidation of the emulsions. FTIR spectra showed the encapsulation efficiency of the bioactive compounds of the extract in the emulsions, mainly for the ultrasound-treated emulsions, which showed higher content of phenolic compounds and antioxidant activity when compared to the control emulsion not subjected to the ultrasound treatment (MS_W/O). The storage test showed a longer half-life and lower

degradation of anthocyanins in the ultrasound-treated emulsions as well as lower lipid peroxidation and higher color stability. The results showed that the application of ultrasound effectively improved the emulsion stability, which can be used in a rational design of emulsion release systems based on plant extracts with better functional properties. The microparticles made with the emulsion W/O_200W_4min showed better characteristics regarding the visual aspects, fluidity, and stability of the anthocyanin pigment upon storage when compared to the microparticles produced with the control emulsion. The present study can provide an ecological and facile route to convert plant extracts into emulsions, which can later be transformed into powder products by spray chilling, with great potential for applications in the food industry.

References

- Abou-Gharbia, H. A., Shehata, A. A. Y., Youssef, M., & Shahidi, F. (1996). Oxidative stability of sesame paste (tehina). *Journal of Food Lipids*, 3(2), 129–137. <https://doi.org/10.1111/j.1745-4522.1996.tb00060.x>
- Ahmed, J., Shivhare, U. S., & Raghavan, G. S. V. (2004). Thermal degradation kinetics of anthocyanin and visual colour of plum puree. *European Food Research and Technology*, 218(6), 525–528. <https://doi.org/10.1007/s00217-004-0906-5>
- Ahmed, M., Pickova, J., Ahmad, T., Liaquat, M., Farid, A., & Jahangir, M. (2016). Oxidation of Lipids in Foods. *Sarhad Journal of Agriculture*, 32(3), 230–238. <https://doi.org/10.17582/journal.sja/2016.32.3.230.238>
- Al-Maqtari, Q. A., Ghaleb, A. D. S., Mahdi, A. A., Al-Ansi, W., Noman, A. E., Wei, M., ... Yao, W. (2021). Stabilization of water-in-oil emulsion of *Pulicaria jaubertii* extract by ultrasonication: Fabrication, characterization, and storage stability. *Food Chemistry*, 350: 129249. <https://doi.org/10.1016/j.foodchem.2021.129249>
- Alvim, I. D., Souza, F. da S., Koury, I. P., Jurt, T., & Dantas, F. B. H. (2013). Use of the spray chilling method to deliver hydrophobic components: Physical characterization of microparticles. *Food Science and Technology*, 33(SUPPL.1), 34–39. <https://doi.org/10.1590/S0101-20612013000500006>
- Alvim, I. D., Stein, M. A., Koury, I. P., Dantas, F. B. H., & Cruz, C. L. de C. V. (2016). Comparison between the spray drying and spray chilling microparticles contain ascorbic acid in a baked product application. *LWT - Food Science and Technology*, 65, 689–694. <https://doi.org/10.1016/j.lwt.2015.08.049>
- Amorim, F. L., Cerqueira Silva, M. B., Cirqueira, M. G., Oliveira, R. S., Machado, B. A. S., Gomes, R. G., ... Umsza-Guez, M. A. (2019). Grape peel (Syrah var.) jam as a polyphenol-enriched functional food ingredient. *Food Science & Nutrition*, 7(5), 1584–1594. <https://doi.org/10.1002/fsn3.981>

- Anese, M., Mirolo, G., Beraldo, P., & Lippe, G. (2013). Effect of ultrasound treatments of tomato pulp on microstructure and lycopene in vitro bioaccessibility. *Food Chemistry*, *136*(2), 458–463. <https://doi.org/10.1016/j.foodchem.2012.08.013>
- Annegowda, H. V., Bhat, R., Min-Tze, L., Karim, A. A., & Mansor, S. M. (2012). Influence of sonication treatments and extraction solvents on the phenolics and antioxidants in star fruits. *Journal of Food Science and Technology*, *49*(4), 510–514. <https://doi.org/10.1007/s13197-011-0435-8>
- Bi, X., Hemar, Y., Balaban, M. O., & Liao, X. (2015). The effect of ultrasound on particle size, color, viscosity and polyphenol oxidase activity of diluted avocado puree. *Ultrasonics Sonochemistry*, *27*, 567–575. <https://doi.org/10.1016/j.ultsonch.2015.04.011>
- Buvé, C., Kebede, B. T., De Batselier, C., Carrillo, C., Pham, H. T. T., Hendrickx, M., ... Van Loey, A. (2018). Kinetics of colour changes in pasteurised strawberry juice during storage. *Journal of Food Engineering*, *216*, 42–51. <https://doi.org/10.1016/j.jfoodeng.2017.08.002>
- Brasil. Ministério da Saúde. Secretaria de Vigilância Sanitária. a Resolução RDC nº 270, de 22 de setembro de 2005. Aprova o Regulamento Técnico para óleos e vegetais, gorduras vegetais e crème vegetal. *Diário Oficial [da] República Federativa do Brasil*, Poder Executivo, Brasília, DF, 2005.
- Campelo-Felix, P. H., Souza, H. J. B., Figueiredo, J. D. A., Fernandes, R. V. de B., Botrel, D. A., de Oliveira, C. R., ... Borges, S. V. (2017). Prebiotic Carbohydrates: Effect on Reconstitution, Storage, Release, and Antioxidant Properties of Lime Essential Oil Microparticles. *Journal of Agricultural and Food Chemistry*, *65*(2), 445–453. <https://doi.org/10.1021/acs.jafc.6b04643>
- Campelo, P. H., Carmo, E. L., Zacarias, R. D., Yoshida, M. I., Ferraz, V. P., de Barros Fernandes, R. V., ... Borges, S. V. (2017). Effect of dextrose equivalent on physical and chemical properties of lime essential oil microparticles. *Industrial Crops and Products*, *102*, 105–114. <https://doi.org/10.1016/j.indcrop.2017.03.021>
- Carmo, E. L., Teixeira, M. A., Souza, I. S., Figueiredo, J. de A., Fernandes, R. V. de B., Botrel, D. A., & Borges, S. V. (2021). Co-encapsulation of anthocyanins extracted from grape skins (*Vitis vinifera* var. Syrah) and α -tocopherol via spray drying. *Journal of Food Processing and Preservation*, *45*(12), 1–11. <https://doi.org/10.1111/jfpp.16038>
- Carvalho, J. D. dos S., Oriani, V. B., de Oliveira, G. M., & Hubinger, M. D. (2019). Characterization of ascorbic acid microencapsulated by the spray chilling technique using palm oil and fully hydrogenated palm oil. *LWT*, *101*:306–314. <https://doi.org/10.1016/j.lwt.2018.11.043>
- Carvalho, L. M. de S., Lemos, M. C. M., Sanches, E. A., da Silva, L. S., de Araújo Bezerra, J., Aguiar, J. P. L., ... Campelo, P. H. (2020). Improvement of the bioaccessibility of bioactive compounds from Amazon fruits treated using high energy ultrasound. *Ultrasonics Sonochemistry*, *67*, 105148. <https://doi.org/10.1016/j.ultsonch.2020.105148>
- Chemat, F., Zill-E-Huma, & Khan, M. K. (2011). Applications of ultrasound in food technology: Processing, preservation and extraction. *Ultrasonics Sonochemistry*, *18*(4), 813–835. <https://doi.org/10.1016/j.ultsonch.2010.11.023>
- Consoli, L., Furtado, G. de F., Cunha, R. L., & Hubinger, M. D. (2017). High solids emulsions produced by ultrasound as a function of energy density. *Ultrasonics*

- Sonochemistry*, 38, 772–782. <https://doi.org/10.1016/j.ultsonch.2016.11.038>
- Consoli, L., Grimaldi, R., Sartori, T., Menegalli, F. C., & Hubinger, M. D. (2016). Gallic acid microparticles produced by spray chilling technique: Production and characterization. *LWT - Food Science and Technology*, 65, 79–87. <https://doi.org/10.1016/j.lwt.2015.07.052>
- Haas, I. C. da S., Toaldo, I. M., Gomes, T. M., Luna, A. S., de Gois, J. S., & Bordignon-Luiz, M. T. (2019). Polyphenolic profile, macro- and microelements in bioaccessible fractions of grape juice sediment using in vitro gastrointestinal simulation. *Food Bioscience*, 27:66–74. <https://doi.org/10.1016/j.fbio.2018.11.002>
- Daoud, S., Bou-maroun, E., Dujourdy, L., Waschatko, G., Billecke, N., & Cayot, P. (2019). Fast and direct analysis of oxidation levels of oil-in-water emulsions using ATR-FTIR. *Food Chemistry*, 293:307–314. <https://doi.org/10.1016/j.foodchem.2019.05.005>
- Dubrovic, I., Herceg, Z., Jambrak, A. R., Badanjak, M., & Dragovic-Uzelac, V. (2011). Effect of High Intensity Ultrasound and Pasteurization on Anthocyanin Content in Strawberry Juice. *Food Technology and Biotechnology*; 49(2), p.196-204.
- Favaro-trindade, C. S., Okuro, P. K., & Matos-Junior, F. E. (2015). Encapsulation via Spray Chilling/Cooling/Congeeing. *Handbook of Encapsulation and Controlled Release*, 71–87.
- Figueiredo, J. de A., MT Lago, A., M Mar, J., S Silva, L., A Sanches, E., P Souza, T., ... V Borges, S. (2020). Stability of camu-camu encapsulated with different prebiotic biopolymers. *Journal of the Science of Food and Agriculture*, 100(8), 3471–3480. <https://doi.org/10.1002/jsfa.10384>
- Frascareli, E. C., Silva, V. M., Tonon, R. V., & Hubinger, M. D. (2012). Effect of process conditions on the microencapsulation of coffee oil by spray drying. *Food and Bioproducts Processing*, 90(3),413–424. <https://doi.org/10.1016/j.fbp.2011.12.002>
- Fredes, C., Osorio, M. J., Parada, J., & Robert, P. (2018). Stability and bioaccessibility of anthocyanins from maqui (*Aristotelia chilensis* [Mol.] Stuntz) juice microparticles. *LWT*, 91:549–556. <https://doi.org/10.1016/j.lwt.2018.01.090>
- Gomes, T. M., Toaldo, I. M., Haas, I. C. da S., Burin, V. M., Caliari, V., Luna, A. S., ... Bordignon-Luiz, M. T. (2019). Differential contribution of grape peel, pulp, and seed to bioaccessibility of micronutrients and major polyphenolic compounds of red and white grapes through simulated human digestion. *Journal of Functional Foods*, 52:699–708. <https://doi.org/10.1016/j.jff.2018.11.051>
- González-Centeno, M. R., Comas-Serra, F., Femenia, A., Rosselló, C., & Simal, S. (2015). Effect of power ultrasound application on aqueous extraction of phenolic compounds and antioxidant capacity from grape pomace (*Vitis vinifera* L.): Experimental kinetics and modeling. *Ultrasonics Sonochemistry*, 22:506–514. <https://doi.org/10.1016/j.ultsonch.2014.05.027>
- Hayati, I. N., Man, Y. B. C., Tan, C. P., & Aini, I. N. (2005). Monitoring peroxide value in oxidized emulsions by Fourier transform infrared spectroscopy. *European Journal of Lipid Science and Technology*, 107(12), 886–895. <https://doi.org/10.1002/ejlt.200500241>
- Jafari, S. M., He, Y., & Bhandari, B. (2007). Production of sub-micron emulsions by ultrasound and microfluidization techniques. *Journal of Food Engineering*, 82(4), 478–

488. <https://doi.org/10.1016/j.jfoodeng.2007.03.007>
- Jaskulski, M., Kharaghani, A., & Tsotsas, E. (2018). Chapter 3- Encapsulation Methods: Spray Drying, Spray Chilling and Spray Cooling. In M. K. Krokida (Ed.), *Thermal and Nonthermal Encapsulation Methods* (pp. 67–114). London: CRC Press.
- Jiménez-Aguilar, D. M., Ortega-Regules, A. E., Lozada-Ramírez, J. D., Pérez-Pérez, M. C. I., Vernon-Carter, E. J., & Welti-Chanes, J. (2011). Color and chemical stability of spray-dried blueberry extract using mesquite gum as wall material. *Journal of Food Composition and Analysis*, *24*(6), 889–894. <https://doi.org/10.1016/j.jfca.2011.04.012>
- Kerasioti, E., Terzopoulou, Z., Komini, O., Kafantaris, I., Makri, S., Stagos, D., ... Kouretas, D. (2017). Tissue specific effects of feeds supplemented with grape pomace or olive oil mill wastewater on detoxification enzymes in sheep. *Toxicology Reports*, *4*, 64–372. <https://doi.org/10.1016/j.toxrep.2017.06.007>
- Kuck, L. S., & Noreña, C. P. Z. (2016). Microencapsulation of grape (*Vitis labrusca* var. Bordo) skin phenolic extract using gum Arabic, polydextrose, and partially hydrolyzed guar gum as encapsulating agents. *Food Chemistry*, *194*, 569–576. <https://doi.org/10.1016/j.foodchem.2015.08.066>
- Kwaw, E., Ma, Y., Tchabo, W., Apaliya, M. T., Sackey, A. S., Wu, M., & Xiao, L. (2018). Impact of ultrasonication and pulsed light treatments on phenolics concentration and antioxidant activities of lactic-acid-fermented mulberry juice. *LWT*, *92*, 61–66. <https://doi.org/10.1016/j.lwt.2018.02.016>
- Lago, A. M. T., Neves, I. C. O., Oliveira, N. L., Botrel, D. A., Minim, L. A., & de Resende, J. V. (2019). Ultrasound-assisted oil-in-water nanoemulsion produced from *Pereskia aculeata* Miller mucilage. *Ultrasonics Sonochemistry*, *50*, 339–353. <https://doi.org/10.1016/j.ultsonch.2018.09.036>
- Lim, S. Y., Abdul Mutalib, M. S., Khaza'ai, H., & Chang, S. K. (2018). Detection of fresh palm oil adulteration with recycled cooking oil using fatty acid composition and FTIR spectral analysis. *International Journal of Food Properties*, *21*(1), 2428–2451. <https://doi.org/10.1080/10942912.2018.1522332>
- Lopes, T. J., Xavier, M. F., Quadri, M. G. N., & Quaid, M. B. (2007). Anthocyanins: a brief review of structural characteristics and stability. *Revista Brasileira Agrociência*, *13*(3), 291–297. <https://doi.org/10.18539/cast.v13i3.1375>
- Luo, X., Cao, J., Yin, H., Yan, H., & He, L. (2018). Droplets banding characteristics of water-in-oil emulsion under ultrasonic standing waves. *Ultrasonics Sonochemistry*, *41*, 319–326. <https://doi.org/10.1016/j.ultsonch.2017.09.055>
- Mammadova, S. M., Fataliyev, H. K., Gadimova, N. S., Aliyeva, G. R., Tagiyev, A. T., & Baloglanova, K. V. (2020). Production of functional products using grape processing residuals. *Food Science and Technology*, *40*(suppl 2), 422–428. <https://doi.org/10.1590/fst.30419>
- Moura, S. C. S. R., Berling, C. L., Garcia, A. O., Queiroz, M. B., Alvim, I. D., & Hubinger, M. D. (2019). Release of anthocyanins from the hibiscus extract encapsulated by ionic gelation and application of microparticles in jelly candy. *Food Research International*, *121*, 542–552. <https://doi.org/10.1016/j.foodres.2018.12.010>
- Mar, J. M., da Silva, L. S., Lira, A. C., Kinupp, V. F., Yoshida, M. I., Moreira, W. P., ...

- Sanches, E. A. (2020). Bioactive compounds-rich powders: Influence of different carriers and drying techniques on the chemical stability of the Hibiscus acetosella extract. *Powder Technology*, 360, 383–391. <https://doi.org/10.1016/j.powtec.2019.10.062>
- Maurer, L. H., Cazarin, C. B. B., Quatrin, A., Nichelle, S. M., Minuzzi, N. M., Teixeira, C. F., ... Emanuelli, T. (2020). Dietary fiber and fiber-bound polyphenols of grape peel powder promote GSH recycling and prevent apoptosis in the colon of rats with TNBS-induced colitis. *Journal of Functional Foods*, 64, 103644. <https://doi.org/10.1016/j.jff.2019.103644>
- Mihalcea, L., Barbu, V., Enachi, E., Andronoiu, D. G., Râpeanu, G., Stoica, M., ... Stănciuc, N. (2020). Microencapsulation of Red Grape Juice by Freeze drying and Application in Jelly Formulation. *Food Technology and Biotechnology*, 58(1), 20–28. <https://doi.org/10.17113/ftb.58.01.20.6429>
- Modarres-Gheisari, S. M. M., Gavagsaz-Ghoachani, R., Malaki, M., Safarpour, P., & Zandi, M. (2019). Ultrasonic nano-emulsification – A review. *Ultrasonics Sonochemistry*, 52, 88–105. <https://doi.org/10.1016/j.ultsonch.2018.11.005>
- Mohammed, A. N., Ishwarya, S. P., & Nisha, P. (2021). Nanoemulsion Versus Microemulsion Systems for the Encapsulation of Beetroot Extract: Comparison of Physicochemical Characteristics and Betalain Stability. *Food and Bioprocess Technology*, 14(1), 133–150. <https://doi.org/10.1007/s11947-020-02562-2>
- Moreno, T., Cocero, M. J., & Rodríguez-Rojo, S. (2018). Storage stability and simulated gastrointestinal release of spray dried grape marc phenolics. *Food and Bioprocess Technology*, 112, 96–107. <https://doi.org/10.1016/j.fbp.2018.08.011>
- Nishad, J., Dutta, A., Saha, S., Rudra, S. G., Varghese, E., Sharma, R. R., ... Kaur, C. (2021). Ultrasound-assisted development of stable grapefruit peel polyphenolic nano-emulsion: Optimization and application in improving oxidative stability of mustard oil. *Food Chemistry*, 334, 127561. <https://doi.org/10.1016/j.foodchem.2020.127561>
- Nogales-Bueno, J., Baca-Bocanegra, B., Rooney, A., Miguel Hernández-Hierro, J., José Heredia, F., & Byrne, H. J. (2017). Linking ATR-FTIR and Raman features to phenolic extractability and other attributes in grape skin. *Talanta*, 167, 44–50. <https://doi.org/10.1016/j.talanta.2017.02.008>
- Olafisoye, O. B., Oguntibeju, O. O., & Osibote, O. A. (2017). Trace elements and radionuclides in palm oil, soil, water, and leaves from oil palm plantations: A review. *Critical Reviews in Food Science and Nutrition*, 57(7), 1295–1315. <https://doi.org/10.1080/10408398.2014.886032>
- Pandit, A. B., & Joshi, J. B. (1993). hydrolysis of fatty oils: effect of cavitation. *Chemical Engineering Science*, 48(19), 3440–3442. [https://doi.org/10.1016/0009-2509\(93\)80164-L](https://doi.org/10.1016/0009-2509(93)80164-L)
- Paniwnyk, L. (2017). Applications of ultrasound in processing of liquid foods: A review. *Ultrasonics Sonochemistry*, 38, 794–806. <https://doi.org/10.1016/j.ultsonch.2016.12.025>
- Patras, A., Brunton, N. P., O'Donnell, C., & Tiwari, B. K. (2010). Effect of thermal processing on anthocyanin stability in foods; mechanisms and kinetics of degradation. *Trends in Food Science & Technology*, 21(1), 3–11. <https://doi.org/10.1016/j.tifs.2009.07.004>

- Poyato, C., Navarro-Blasco, I., Calvo, M. I., Cavero, R. Y., Astiasarán, I., & Ansorena, D. (2013). Oxidative stability of O/W and W/O/W emulsions: Effect of lipid composition and antioxidant polarity. *Food Research International*, *51*(1), 132–140. <https://doi.org/10.1016/j.foodres.2012.11.032>
- Procopio, F. R., Oriani, V. B., Paulino, B. N., do Prado-Silva, L., Pastore, G. M., Sant'Ana, A. S., & Hubinger, M. D. (2018). Solid lipid microparticles loaded with cinnamon oleoresin: Characterization, stability and antimicrobial activity. *Food Research International*, *113*, 351–361. <https://doi.org/10.1016/j.foodres.2018.07.026>
- Raviadaran, R., Ng, M. H., Manickam, S., & Chandran, D. (2019). Ultrasound-assisted water-in-palm oil nano-emulsion: Influence of polyglycerol polyricinoleate and NaCl on its stability. *Ultrasonics Sonochemistry*, *52*, 353–363. <https://doi.org/10.1016/j.ultsonch.2018.12.012>
- Rehman, R. N. U., You, Y., Zhang, L., Goudia, B. D., Khan, A. R., Li, P., & Ma, F. (2017). High temperature induced anthocyanin inhibition and active degradation in Malus profusion. *Frontiers in Plant Science*, *8*, 1–10. <https://doi.org/10.3389/fpls.2017.01401>
- Romanini, E. B., Rodrigues, L. M., Finger, A., Chierrito, T. P. C., Scapim, M. R. da S., & Madrona, G. S. (2021). Ultrasound assisted extraction of bioactive compounds from BRS Violet grape pomace followed by alginate-Ca²⁺ encapsulation. *Food Chemistry*, *338*, 128101. <https://doi.org/10.1016/j.foodchem.2020.128101>
- Sambanthamurthi, R., Sundram, K., & Tan, Y. A. (2000). Chemistry and biochemistry of palm oil. In *Progress in Lipid Research* (Vol. 39). [https://doi.org/10.1016/S0163-7827\(00\)00015-1](https://doi.org/10.1016/S0163-7827(00)00015-1)
- Shantha, N. C., & Decker, E. A. (1994). Rapid, Sensitive, Iron-Based Spectrophotometric Methods for Determination of Peroxide Values of Food Lipids. *Journal of AOAC INTERNATIONAL*, *77*(2), 421–424. <https://doi.org/10.1093/jaoac/77.2.421>
- Silva, E. K., Costa, A. L. R., Gomes, A., Bargas, M. A., Cunha, R. L., & Meireles, M. A. A. (2018). Coupling of high-intensity ultrasound and mechanical stirring for producing food emulsions at low-energy densities. *Ultrasonics Sonochemistry*, *47*, 114–121. <https://doi.org/10.1016/j.ultsonch.2018.04.020>
- Silva, E. K., Gomes, M. T. M. S., Hubinger, M. D., Cunha, R. L., & Meireles, M. A. a. (2015). Ultrasound-assisted formation of annatto seed oil emulsions stabilized by biopolymers. *Food Hydrocolloids*, *47*, 1–13. <https://doi.org/10.1016/j.foodhyd.2015.01.001>
- Sinela, A., Rawat, N., Mertz, C., Achir, N., Fulcrand, H., & Dornier, M. (2017). Anthocyanins degradation during storage of Hibiscus sabdariffa extract and evolution of its degradation products. *Food Chemistry*, *214*, 234–241. <https://doi.org/10.1016/j.foodchem.2016.07.071>
- Soria, A. C., & Villamiel, M. (2010). Effect of ultrasound on the technological properties and bioactivity of food: a review. *Trends in Food Science & Technology*, *21*(7), 323–331. <https://doi.org/10.1016/j.tifs.2010.04.003>
- Stoll, L., Costa, T. M. H., Jablonski, A., Flôres, S. H., de Oliveira Rios, A., Maria, T., ... Flôres, S. H. (2016). Microencapsulation of Anthocyanins with Different Wall Materials and Its Application in Active Biodegradable Films. *Food and Bioprocess Technology*, *9*(1), 172–181. <https://doi.org/10.1007/s11947-015-1610-0>

- Souza, V. B., Thomazini, M., Balieiro, J. C. D. C., & Fávoro-Trindade, C. S. (2015). Effect of spray drying on the physicochemical properties and color stability of the powdered pigment obtained from vinification byproducts of the Bordo grape (*Vitis labrusca*). *Food and Bioprocess Technology*, *93*, 39–50. <https://doi.org/10.1016/j.fbp.2013.11.001>
- Tabibiazar, M., Davaran, S., Hashemi, M., & Homayonirad, A. (2015). Food Hydrocolloids Design and fabrication of a food-grade albumin-stabilized nanoemulsion. *Food Hydrocolloids*, *44*, 220–228. <https://doi.org/10.1016/j.foodhyd.2014.09.005>
- Tiwari, B. K., Patras, A., Brunton, N., Cullen, P. J., & O'Donnell, C. P. (2010). Effect of ultrasound processing on anthocyanins and color of red grape juice. *Ultrasonics Sonochemistry*, *17*(3), 598–604. <https://doi.org/10.1016/j.ultsonch.2009.10.009>
- Tsali, A., & Goula, A. M. (2018). Valorization of grape pomace: Encapsulation and storage stability of its phenolic extract. *Powder Technology*, *340*, 194–207. <https://doi.org/10.1016/j.powtec.2018.09.011>
- Turturică, M., Stănciuc, N., Bahrim, G., & Râpeanu, G. (2016). Effect of thermal treatment on phenolic compounds from plum (*prunus domestica*) extracts - A kinetic study. *Journal of Food Engineering*, *171*, 200–207. <https://doi.org/10.1016/j.jfoodeng.2015.10.024>
- Udomrati, S., Ikeda, S., & Gohtani, S. (2013). Rheological properties and stability of oil-in-water emulsions containing tapioca maltodextrin in the aqueous phase. *Journal of Food Engineering*, *116*(1), 170–175. <https://doi.org/10.1016/j.jfoodeng.2012.10.032>
- Ushikubo, F. Y., & Cunha, R. L. (2014). Stability mechanisms of liquid water-in-oil emulsions. *Food Hydrocolloids*, *34*, 145–153. <https://doi.org/10.1016/j.foodhyd.2012.11.016>
- Vercet, A., Sánchez, C., Burgos, J., Montañés, L., & Lopez Buesa, P. (2002). The effects of manothermosonication on tomato pectic enzymes and tomato paste rheological properties. *Journal of Food Engineering*, *53*(3), 273–278. [https://doi.org/10.1016/S0260-8774\(01\)00165-0](https://doi.org/10.1016/S0260-8774(01)00165-0)
- Wang, J., Wang, J., Ye, J., Vanga, S. K., & Raghavan, V. (2019). Influence of high-intensity ultrasound on bioactive compounds of strawberry juice: Profiles of ascorbic acid, phenolics, antioxidant activity and microstructure. *Food Control*, *96*, 128–136. <https://doi.org/10.1016/j.foodcont.2018.09.007>
- Wu, Y., Xu, L., Liu, X., Hasan, K. M. F., Li, H., Zhou, S., ... Zhou, Y. (2021). Effect of thermosonication treatment on blueberry juice quality: Total phenolics, flavonoids, anthocyanin, and antioxidant activity. *LWT*, *150*, 112021. <https://doi.org/10.1016/j.lwt.2021.112021>
- Yang, W., Kaimainen, M., Järvenpää, E., Sandell, M., Huopalahti, R., Yang, B., & Laaksonen, O. (2021). Red beet (*Beta vulgaris*) betalains and grape (*Vitis vinifera*) anthocyanins as colorants in white currant juice – Effect of storage on degradation kinetics, color stability and sensory properties. *Food Chemistry*, *348*, 128995. <https://doi.org/10.1016/j.foodchem.2020.128995>
- Yang, Z., Han, Y., Gu, Z., Fan, G., & Chen, Z. (2008). Thermal degradation kinetics of aqueous anthocyanins and visual color of purple corn (*Zea mays* L.) cob. *Innovative Food Science & Emerging Technologies*, *9*(3), 341–347. <https://doi.org/10.1016/j.ifset.2007.09.001>

- Yao, Y., Pan, Y., & Liu, S. (2020). Power ultrasound and its applications: A state-of-the-art review. *Ultrasonics Sonochemistry*, *62*. <https://doi.org/10.1016/j.ultsonch.2019.104722>
- Zhang, K., Mao, Z., Huang, Y., Xu, Y., Huang, C., Guo, Y., ... Liu, C. (2020). Ultrasonic assisted water-in-oil emulsions encapsulating macro-molecular polysaccharide chitosan: Influence of molecular properties, emulsion viscosity and their stability. *Ultrasonics Sonochemistry*, *64*, 105018. <https://doi.org/10.1016/j.ultsonch.2020.105018>
- Zhang, R., Zhou, L., Li, J., Oliveira, H., Yang, N., Jin, W., ... He, J. (2020). Microencapsulation of anthocyanins extracted from grape skin by emulsification/internal gelation followed by spray/freeze-drying techniques: Characterization, stability and bioaccessibility. *LWT*, *123*, 109097. <https://doi.org/10.1016/j.lwt.2020.109097>
- Zheng, W., Alim, A., Bai, Y., Feng, Z., Zhang, J., Xia, N., & Ding, Z. (2021). Effect of postharvest dehydration on the microstructure and anthocyanin content of grapes. *Horticulture Environment and Biotechnology*, *62*(3), 423-434 <https://doi.org/10.1007/s13580-020-00331-w>
- Zhou, M., Chen, Q., Bi, J., Wang, Y., & Wu, X. (2017). Degradation kinetics of cyanidin 3-O-glucoside and cyanidin 3-O-rutinoside during hot air and vacuum drying in mulberry (*Morus alba* L.) fruit: A comparative study based on solid food system. *Food Chemistry*, *229*, 574–579. <https://doi.org/10.1016/j.foodchem.2017.02.131>

ARTICLE 3 – MICROSTRUCTURED LIPID MICROPARTICLES CONTAINING ANTHOCYANINS: PRODUCTION, CHARACTERIZATION, STORAGE, AND RESISTANCE TO THE GASTROINTESTINAL TRACT

Artigo submetido as normas da revista científica: Food Research International

ISSN: 0963-9969

(versão preliminar)

Jayne de Abreu Figueiredo¹, Laís Bruno Norcino², Pedro Henrique Campelo³, Diego Alvarenga Botrel¹, Sérgio Michielon de Souza⁴, Cassiano Rodrigues de Oliveira⁵, Soraia Vilela Borges¹

¹*Department of Food Science, Federal University of Lavras, P.O. Box 3037, 37200-900, Lavras, MG, Brasil*

²*Biomaterial Engeneering, Federal University of Lavras, P.O. Box, 37200-900, Lavras, MG, Brazil*

³*Faculty of Agrarian Science, Federal University of Amazonas, 69077-000, Manaus, AM, Brazil*

⁴*Department of Physics, Federal University of Amazonas, Manaus, Amazonas 69077-000, Brazil*

⁵*Department of Chemistry, Federal University of Viçosa, 38810-100 Rio Paranaíba, MG, Brazil*

Abstract

Anthocyanins from grape peel extract have several biological properties and can act as a natural colorant and antioxidant agent. However, these compounds are susceptible to degradation by light, oxygen, temperature, and the gastrointestinal tract. Thus, this study produced microstructured lipid microparticles (MLMs) containing anthocyanins by the spray chilling technique and evaluated the particle stability. Trans-free fully hydrogenated palm oil (FHPO) and palm oil (PO) were used as encapsulating materials in the ratios 90:10, 80:20, 70:30, 60:40, and 50:50, respectively. The concentration of grape peel extract was 40% (w/w) in relation to the encapsulating materials. PGPR (polyglycerol polyricinoleate) emulsifier at 4% by weight relative to lipid materials was used to produce the emulsions to be subjected to atomization. The microparticles were evaluated for thermal behavior by DSC, polymorphism, FTIR, size distribution and particle diameter, bulk density, tapped density, flow properties, morphology, phenolic compounds content, antioxidant capacity, and retention of anthocyanins. Furthermore, the storage stability of the microparticles was investigated at different temperatures (-18, 4, and 25 °C), and the anthocyanins retention capacity, kinetic parameters (half-life time and degradation constant rate), total color difference, and visual aspects were evaluated during 90 days of storage. The resistance of MLMs to the gastrointestinal tract was also evaluated. In general, higher FHPO concentrations increased the thermal resistance of the MLMs and both showed defined peaks of β' and β forms. The FTIR analysis showed that the MLMs preserved the original forms of their constituent materials even after atomization, with interactions between them. The increase in the PO concentration directly affected the increased mean particle diameter, agglomeration, and cohesiveness, as well as lower bulk density, tapped density, and flowability. The retention of anthocyanins in MLMs ranged from 81.5 to 61.3% and was influenced by the particle size, with a better result observed for the treatment MLM_90:10. The same behavior was observed for the phenolic compounds content (1443.1 - 1247.2 mg GAE/100g) and antioxidant capacity (92.6-86.8 %). During the storage, MLMs

made with FHPO to PO ratios of 80:20, 70:30, and 60:40 showed the highest stability for anthocyanin retention and color changes at both temperatures. The gastrointestinal simulation *in vitro* revealed that all treatments were resistant to gastric phase and maintained a maximum and controlled release in the intestinal phase, demonstrating that FHPO together with PO are effective to protect anthocyanins during gastric digestion, and can improve the bioavailability of this compound in the human organism. Thus, the spray chilling technique may be a promising alternative for the production of anthocyanins-loaded microstructured lipid microparticles with functional properties for various technological applications.

Keywords: Functional foods; Spray congealing; Natural additives; Stability; Innovation.

1 Introduction

The increasing awareness of consumers about the benefits provided by foods beyond meeting basic nutrition needs has driven the food industries to produce healthier and more natural foods.

Grape pomace, considered an agro-industrial waste, represents about 25% (w/w) of the weight of the processed grapes, reaching more than 9 million tons per year. The vast majority of this waste is disposed of inefficiently, thus the transformation of these materials into useful resources can contribute to the environment and improve the health of the population (Sirohi et al., 2020).

Grape peel can be considered a rich co-product, due to its large amounts of essential bioactive compounds, such as polyphenols, which are responsible for biological properties such as antioxidant activity, anti-inflammatory, antimicrobial, prevention of coronary heart disease, tumor inhibition, among others (Amendola et al., 2010; Kuck & Noreña, 2016). In addition, these compounds have important sensory properties such as color, flavor, and astringency that can be used in food production (Hogervorst et al., 2017).

The insertion of functional ingredients such as phenolic compounds and anthocyanins into foods represents industrial challenges due to the instability to processing and storage. In addition, to act with biological properties, these compounds must be resistant to the gastric system to allow greater bioavailability to the human body (Carbonell-Capella et al., 2014; Haas et al., 2019).

Thus, the microencapsulation technique together with other food processing technologies can be an alternative to circumvent this problem, providing foods and nutraceuticals with bioavailability and maintenance of the functionality of active ingredients (Alemzadeh et al., 2020). Microencapsulation consists in the incorporation of a substance (active compound) inside another (encapsulating material) that acts as a protective barrier,

obtaining particles that can protect the molecule of interest from the external environment (Saifullah et al., 2019). Other advantages of the microencapsulation include the protection of ingredients against oxidation, thermal denaturation, extreme pH conditions, as well as controlled and gradual release, masking of undesirable odor and flavor, and improved dispersion of active ingredients (Madene & Jacquot, 2006; Ray et al., 2016; Usha & Cánovas, 1995).

Spray chilling is one of the microencapsulation techniques little explored in the food sector, which can be a promising alternative since it consists in practical systems to encapsulate compounds, has high encapsulation efficiency, and possibility to process at moderate temperatures, without the need to use solvents (Figueiredo et al., 2022). The technology consists in the dispersion of the emulsified or solubilized active material in a molten lipid matrix, which is pumped into a heated atomizing nozzle, followed by sprinkling in a chamber containing air at a temperature below the melting point of the lipid matrix, allowing the solidification of the droplets forming solid lipid microparticles. These microparticles have high added value and can be used in food formulations with the function of colorant, antioxidant, flavoring, providing a controlled release of these components at the desired time and site (Nahum & Domb, 2021; Oriani et al., 2016).

Various lipid materials can be used in the production of lipid microparticles by spray chilling. The lipid encapsulating material should have good crystallization properties, low cost, good rheological properties, ability to retain the active agent within the structure during storage and processing, maximum protection against external environmental conditions, and ability to achieve specific active release properties (Consoli et al., 2016; Oriani et al., 2018).

Palm oil and its derivatives are low-cost lipids easily found on the market with ideal sensory characteristics for incorporation into many types of foods. Lipid blends containing fully hydrogenated trans-free palm oil (FHPO) and palm oil (PO) may be promising alternatives for

the production of lipid microparticles by spray chilling due to the possibility of operation with melting point higher than 45 °C, allowing the formation of microparticles with favorable structure in the retention of the active compound, lower adhesion, higher process yield, and ease of handling (Procopio et al., 2018).

The present study aimed at investigating the spray chilling technique for the production of microstructured lipid microparticles (MLMs) containing anthocyanins from grape peel extract. Blends of palm oil (PO) and trans-free fully hydrogenated palm oil (FHPO) were analyzed as encapsulating materials. The microparticles were evaluated for simulated GI digestion and storage stability at different temperatures.

2 Material and Methods

2.1 Materials

The grapes of the Bordo variety (*Vitis labrusca* L.) were supplied by producers from a farm located in Campos Gerais (Minas Gerais, Brazil). Palm oil (PO) (melting point 34 – 40°C) and fully hydrogenated palm oil (FHPO) (trans-fat free) (melting point 55 – 61°C) were kindly donated by Agropalma (Limeira, SP, Brazil). The emulsifier polyglycerol polyricinoleate (Grinsted® PGPR Super, HLB ~ 3.0) was donated by Danisco Brasil Ltda (Cotia, SP, Brazil).

2.2. Preparation of the grape peel extract

The grapes were washed and sanitized. To obtain the grape peel extract, the seeds, peels, and pulps were manually removed. The anthocyanins were extracted from the peel using distilled water and citric acid (1% wt. of water) to a ratio of 1:1 (w/v) (peel: acidified water). The mixture was kept overnight in the dark at 4 ± 1 °C, covered with aluminum foil, for better extraction of anthocyanins. After, the extract was filtered through organza and centrifuged for

5 min at 3000 rpm to eliminate the suspended solids. Finally, the extract was stored in amber flasks at 4 ± 1 °C to prevent the degradation of anthocyanins.

2.3 Characterization of pure lipid materials

2.3.1 Fatty acids composition

The AOCS methodology, method 2-66 (AOCS, 2004) was used for the determination of the fatty acid composition through gas chromatography of the fatty acid methyl esters, in a capillary gas chromatograph. The operating conditions were: column flow rate of 1.00 mL/min; linear speed of 24 cm/s. The detector and injector temperatures were 280 °C and 250 °C, respectively. The oven temperature was programmed to start at 110 °C for 5 minutes, followed by a 5 °C/min ramp up to 215 °C, remaining at this temperature for 24 minutes, resulting in a total run time of 48 minutes. Helium was used as the carrier gas, and the injected volume was 1 µL. The identification of the compounds was performed by comparing the retention times of the peaks with the respective standards.

2.4 Preparation of the emulsion

An experimental design was performed to establish the processing conditions for the formation of stable emulsions before atomization. The emulsifier concentration and the homogenization method (magnetic stirrer and ultrasound) were selected as variables for study. PGPR (polyglycerol polyricinoleate) was used as an emulsifier, which is suitable for stabilizing W/O emulsions due to its low hydrophilic-lipophilic balance (between 1.5 and 2.0). Based on preliminary tests (data not shown) a concentration of 4% of PGPR (4% by weight relative to lipid materials) was used. Blends composed of FHPO and PO (90:10; 80:20; 70:30; 60:40; and 50:50) (% by weight) were placed in a 250 ml beaker and heated to 70 °C in a temperature

controlled water bath (Tecnal, TE-184, Piracicaba, Brazil) until complete melting. Then, PGPR and grape peel extract (40% by weight relative to the total formulation) was added to the fat blend under constant stirring on a magnetic stirrer at 750 rpm for 4 minutes. Then, the emulsions were homogenized in ultrasound (Ultrasound Digital Sonifier, Model 450 - Branson Ultrasonic Corporation, Brookfield, USA) for 4 minutes at 200 W power and 20kHz to ensure greater stability. The emulsions were immediately subjected to atomization in a spray chiller.

2.5 Production of the microparticles by spray chilling

A spray dryer (model MDS 1.0, Labmaq do Brasil, Ribeirão Preto, SP, Brazil) was used for the production of the microparticles, which was adapted for use as a spray chiller. The mixture was fed into the atomizer nozzle (double-fluid model with 3.0 mm diameter) corresponding to a flow rate of 10 ml/min. The temperatures of the samples and the compressed air were 70 °C and 80 °C, respectively. The air flow rate was 35 L/min and the cooling air temperature was 1 °C. The spray chilling parameters were determined in preliminary tests (data not shown), which yielded a free-flowing powder. At the end of the process, the samples were collected in the collecting jar, stored in closed containers, and kept at -18 °C until analysis. The assays were performed in duplicate.

2.6 Characterization of microstructured lipid microparticles (MLMs)

2.6.1 Thermal analysis

Thermal analysis was performed by Differential Scanning Calorimetry (DSC) using a DSC 2920 modulated thermal analyzer (TA Instruments, New Castle, Delaware, USA) as described by AOCS Cj1-94 (AOCS, 2004) to obtain melting and crystallization curves of the MLMs and the lipid materials. The samples were weighed (~10 mg) into hermetically sealed

aluminum pans. The operation conditions were: heating to 80 °C for 10 min, cooling to -70 °C (10 °C/min) for 30 min, and then again heating at a rate of 10 °C/min to 80 °C, and finally held at this temperature for 10 min. The melting curves were obtained at the second heating. The software Origin was used to obtain the thermal curves and to define the crystallization and melting parameters.

2.6.2 Polymorphism

The polymorphic forms of MLMs and lipids were determined by AOCS (2004) method Cj 2-9527. The samples were analyzed in an XRD-6000 x-ray diffractometer (Shimadzu, Kyoto, Japan) using the Bragg - Breton ($\theta:2\theta$) geometry with Cu-K α radiation ($k=1.5418$ Å, 40 KV voltage and 30 mA current). Measurements were taken with interval at angle 2θ from 5 to 40°, with step size of 0.02° every 2 seconds. The Rietveld method was applied considering the widening of peaks due to crystallite size and microtensions. The percentage of crystallinity was calculated as described by Pinto et al. (2020).

2.6.3 Fourier Transform Infrared Spectroscopy (FTIR)

FTIR measurements were performed for the crude grape peel extract and the pure lipid encapsulating materials and the MLMs at room temperature from 400 to 4000 cm⁻¹ (4 cm⁻¹ resolution and 64-scan accumulation) on an accessory Total Attenuated Reflectance (ATR) spectrometer (Jasco 4100, Tokyo, Japan).

2.6.4 Physical properties

2.6.4.1 Mean particle diameter and polydispersity index (Span)

MLMs were mixed with a Tween 20 aqueous solution (0.5 g Tween 20 /100 g) as a dispersion medium using a sonicator (Model S-450D, Branson Ultrasonics Corporation, Danbury, USA) for 1 min at 200 W. Mean Brouckere diameter ($D_{4,3}$) and polydispersity index (Span) were determined using a Mastersizer (Model 3000E, Malvern Instruments Inc., Worcestershire, U.K.) according to Equations 1 and 2, respectively.

$$[D_{4,3}] = \frac{\sum ni \times d_i^4}{\sum ni \times d_i^3} \quad (1)$$

$$Span = \frac{(d_{90} - d_{10})}{d_{50}} \quad (2)$$

where $[D_{4,3}]$ is the volume-weighted mean diameter of microparticles (μm), d is the diameter of microparticles (μm), n is the dimensionless number of microparticles between two consecutive diameters. Span indicates polydispersion, and the variables d_{90} , d_{10} , and d_{50} correspond to the particle diameters (μm) at 10%, 50%, and 90% of the accumulated volume, respectively.

2.6.4.2 Density and flowability (bulk and tapped density; Haunser ratio; Carr's index)

The density of the MLMs was measured as both bulk density and tapped density. Bulk density was determined by weighing a 10 mL graduated cylinder filled with the MLMs, without compaction, to a set level, and expressed as the weight of MLMs (kg) per volume of powder (m^3). The tapped density was measured in the beaker containing the MLMs that was gently tapped on a table until a negligible difference in volume was observed between successive measurements. Then, the new volume after tapping was determined in the measuring cylinder, and expressed as the weight of MLMs (kg) per volume of tapped MLMs (m^3). The flowability

and cohesiveness were expressed as Carr's index (CI), also called compressibility index, and Hausner ratio (HR), respectively, using the following expressions (Pugliese et al., 2017): $CI = ((\text{tapped density} - \text{bulk density}) / \text{tapped density})$; $HR = \text{tapped density} / \text{bulk density}$).

2.6.4.3 Morphology of MLMs

The surface of the MLMs was analyzed on a scanning electron microscope (SEM) (LEO EVO 40 XVP; Carl Zeiss, Jena, Germany) with an accelerating voltage of 20 Kv and a beam current of 50 Pa. The samples were placed in aluminum stubs with double-sided carbon tape, covered with gold sputter coating (Bal-Tec SCD 050 Sputter Coater; Capovani Brothers Inc., Balzers, Liechtenstein). Micrographs were obtained at 1080x magnification.

2.6.5 Total monomeric anthocyanins

The total monomeric anthocyanins were determined according to the methodology described by Kuck & Noreña (2016) and Carmo et al. (2021) with modifications. To extract the anthocyanins, 0.5 g of the emulsion was mixed with 5 mL of acidified ethanol (HCL 0.1%, v/v), vortexed for 1 minute, and placed in an ultrasonic bath at 60 °C for 5 minutes. The mixture was centrifuged at 3000 rpm for 2 min to decant the solid material. Absorbance of the supernatant was measured at 520 nm, in triplicate, in a spectrophotometer - UNICO 2800UV/VIS (United Products & Instruments Inc., New Jersey, USA). The results were expressed as mg malvidin-3-glucoside per 100 g sample on a wet basis, using molar absorptivity of 28.000 L/mol.cm, and molecular weight of 493.2g/mol.

2.6.6 Encapsulation retention of the anthocyanins content

The total encapsulation retention (RE) was determined as proposed by Figueiredo et al. (2020) with modifications. The RE was defined as the ratio of the total anthocyanins present in the microparticles (CTAM) to the total anthocyanins present in the grape peel extract (CTAE) initially added to the emulsions before the spray chilling, as shown in Equation 3. The quantification of the anthocyanins in the MLMs was performed as described in Section 2.6.5.

$$RE(\%) = \frac{CTAM}{CTAE} \times 100 \quad (3)$$

2.6.7 Total phenolics content (TPC)

The total phenolics contents were determined using a modified Folin-Ciocalteu colorimetric method Mar et al. (2020), with some modifications. To extract the TPC, 0.5 g of the emulsion was mixed with 5 mL of acidified ethanol (HCL 0.1%, v/v), vortexed for 1 minute, and placed in an ultrasonic bath at 60 °C for 5 minutes. The mixture was centrifuged (2 min/3000 rpm) to decant the solid material. The solution was diluted by adding 1 ml of supernatant to 3 ml of distilled water, and 1 ml of this dilution was added to 1 ml of Folin–Ciocalteu reagent (0.2 N). After 3 min, 1 ml of sodium carbonate solution (4% w/v) was added and the mixture was allowed to stand in the dark for 2 hr at 25°C. The absorbance readings were performed at 765 nm, and quantification of total phenolic content was performed using a Gallic acid (GA) standard curve generated with concentrations of 1, 5, 10, 20, 30, 40, 50, and 60 µg/ml. The result was expressed as mg of gallic acid equivalents (GAE) per 100 g sample on a wet basis.

2.6.8 Antioxidant capacity

The antioxidant activity of the emulsions was evaluated using the free radical 2,2-diphenyl-1-picrylhydrazyl (DPPH) assay (Sigma-Aldrich, USA), according to the method of Campelo-Felix et al. (2017), with some modifications. Approximately 5 g of the emulsion was mixed with 5 mL of acidified ethanol (HCL 0.1%, v/v) and vortexed for 1 min. After homogenization, the mixture was placed in an ultrasonic bath at 60 °C for 5 minutes, and centrifuged (2 min/3000 rpm) to decant the solid material. Subsequently, 1.5 ml of supernatant was added to 3.9 mL of DPPH ethanolic solution (0.1 mg/ml), vortexed for 5 s, and stored in the dark for 1 h at 25°C. A blank was prepared by substituting the emulsion solution for 1.5 mL of pure ethanol. The absorbance values of the blank and the samples were measured at 515 nm. The antioxidant activity (%AA) of the emulsions was determined using Eq.(4), where A_0 is the absorbance of blank, and A_E is the absorbance of the sample.

$$CA(\%) = \frac{A_0 - A_E}{A_0} \quad (4)$$

2.6.9 Storage conditions and stability of MLMs

After the production of the MLMs, the samples were stored in transparent polypropylene zip lock plastic packages (55 x 55 mm) protected from light, under three different temperatures, as follows: -18 °C (freezing temperature, to study the behavior of MLMs in frozen products), 4 °C (cooling temperature (refrigerated products) and at 25 °C (room temperature).

The MLMs were stored for 90 days and characterized for anthocyanins content (Section 2.6.7), which was expressed as the anthocyanin retention defined as the ratio between anthocyanins concentration at a given time (C_t , mg.100g⁻¹) and its concentration just after production - time zero (C_0 , mg.100g⁻¹). In addition, considering that anthocyanins follow first-order kinetics kinetics (Figueiredo et al., 2020; Yang et al., 2021), the half-life time ($t_{1/2}$) and

the degradation constant rate (k) were determined according to Equations 6 and 7 (Carmo et al., 2018).

$$kt = -\ln\left(\frac{C_t}{C_0}\right) \quad (6)$$

$$t_{1/2} = \left(\frac{\ln 2}{k}\right) \quad (7)$$

where k (days^{-1}) is the first order rate constant, t (days) is the storage period, and $t_{1/2}$ (days) is the time required to degrade 50% of the initial anthocyanin concentration.

2.6.9.1 Color measurements

The color parameters L^* (brightness), a^* (green to red), and b^* (blue to yellow) were determined using a colorimeter (CR-300 Chroma Meter; Konica Minolta, Tokyo, Japan), and the color differences (ΔE^*) over time were calculated using the L^* , a^* , and b^* values according to Equation 8.

$$\Delta E^* = \sqrt{(\Delta L^*)^2 + (\Delta a^*)^2 + (\Delta b^*)^2} \quad (8)$$

where ΔE^* indicates the magnitude of the color difference between the samples over the storage time, classified as: very different ($\Delta E^* > 3$); different ($1.5 > \Delta E^* < 3$); and little different ($\Delta E^* < 1.5$) (Patras et al., 2011).

2.10 Simulated gastrointestinal digestion in vitro

The gastric and intestinal juices were prepared as described by Flores et al. (2014). The pH of the digestive juices was adjusted with 1M HCl or 1M NaOH. Before the simulated digestion, anthocyanins were determined in the grape peel extract and MLMs as described in Section 2.6.7. The samples (2.0 g) were placed in 250 mL Erlenmeyer flasks and 25 mL of simulated gastric juice was added. The pH was adjusted to 1.2 with 1M HCl and the solution was incubated at 37 °C in a bath with stirring set at 200 rpm for 2 hours. At different times, aliquots (1 mL) were taken for anthocyanin analysis and replaced with the same amount of fresh medium, and the reaction was stopped by cooling the test tubes on ice. At the end of the gastric digestion, the pH was adjusted to 7.4 with 1M NaOH before the addition of the pancreatin solution and bile salts. The solution with each sample was incubated at 37°C in a shaking bath for another 2 h. At different times, aliquots were taken for anthocyanin analysis and the reaction was stopped by cooling the test tubes on ice. The samples taken during intestinal digestion were immediately acidified at pH 2.0 to ensure the stability of the anthocyanins present in the reaction mixture (Minekus et al., 2014; Tagliacruzchi et al., 2010). The test tubes were then centrifuged at 3000 rpm for 5 min and the supernatants were removed for the determination of the anthocyanins concentration. For that, 1 mL of the supernatant was mixed with 3 mL of acidified ethanol (HCl 0.1%, v/v) and the mixture was centrifuged (3000 rpm/2 min). The absorbance of the supernatant was measured in a UNICO 2800UV/VIS spectrophotometer (United Products & Instruments Inc., New Jersey, USA) at 520 nm. To determine the percent loss, the initial anthocyanins content of the samples was compared to the loss of anthocyanins during the release study.

3.0 Statistical analysis

The effects of the different treatments were evaluated by ANOVA and test of means (Duncan, $p < 0.05$) using the software R (version 3.6.0). Data were plotted using OriginPro v9.9 (Origin Lab, Northampton, United States).

4.0 Results and Discussion

4.1 Characterization of fully hydrogenated palm oil (FHPO) and refined palm oil (PO)

4.1.1 Fatty acids composition

PO and FHPO are materials with a great diversity of fatty acids. Each fatty acid can occupy different positions in the molecule, allowing a complex mixture of triacylglycerols (TAGs) with distinct molecular arrangements. Small differences in fatty acid composition significantly influence the TAG composition and consequently the melting profile and crystallization of oils and fats (Sato & Ueno, 2011). Table 1 shows the fatty acid composition of the lipid materials used in this study.

Table 1. Fatty acid composition of fully hydrogenated palm oil (FHPO) and palm oil (PO).

Fatty acids composition (%)		
Fatty acids	FHPO	PO
C12:0 Lauric	0.39 ± 0.04	0.32 ± 0.01
C14:0 Myristic	1.03 ± 0.02	1.02 ± 0.00
C16:0 Palmitic	42.75 ± 0.06	42.82 ± 0.03
C16:1 Palmitoleic	---	0.14 ± 0.00
C18:0 Stearic	55.06 ± 0.04	4.42 ± 0.02
C18:1 Oleic	0.25 ± 0.04	40.99 ± 0.02
C18:2 Linoleic	0.06 ± 0	9.41 ± 0.02
C18:3 Linolenic	---	0.31 ± 0.01
C20:0 Arachidonic	0.46 ± 0	0.33 ± 0.00
<i>Σ Saturated</i>	99.71 ± 0.04	48.91 ± 0.01
<i>Σ Unsaturated</i>	0.31 ± 0.04	51.09 ± 0.01

The fatty acid composition of PO and FHPO was in agreement with the literature and according to their characteristic composition (O'Brien, 2004). FHPO presented 99.71% of saturated fatty acids (55.06% stearic acid and 42.75% palmitic acid), which confers a solid consistency and high oxidation stability. It is worth noting that all unsaturated fatty acid bonds become saturated after total hydrogenation, forming fully hydrogenated oil. Therefore, fully hydrogenated oils do not contain trans isomers. The PO had balanced proportions of saturated fatty acids (48.91%, of which 42.82% palmitic acid and 4.42% stearic acid) and unsaturated fatty acids (51.09%, of which 40.99% oleic acid and 9.41% linoleic acid). This composition confers semi-solid and plastic characteristics, in addition to good stability against the oxidation reactions.

The physical properties of oils and fats are related to the structure of their TAGs, i.e., the fatty acid composition and their distribution within the TAG molecules (Timms, 1985).

According to the literature, PO is composed of molecules with carbon number distribution between C46 and C54 with high contents of monounsaturated (41 to 59%) and diunsaturated (32 to 54%) TAGs. The presence of mono- and diglycerides may contribute to slower crystallization of PO. In turn, FHPO presents a carbon distribution between C48 to C54, most often with a prevalence of trisaturated fatty acids (93 to 99%) (Carvalho et al., 2019; O'Brien, 2004; Procopio et al., 2018).

In the spray chilling microencapsulation, the selection of FHPO as a high melting point lipid is important due to the presence of fatty acids with chain lengths compatible with those of the fatty acids present in PO. Research advances have shown that blends made with liquid and solid oils develop disordered structures after microencapsulation, with better retention capacity of bioactive compounds when compared to the structures formed only by saturated lipids, giving rise to the known microstructured lipid microparticles (MLMs) (Müller et al., 2007; Nahum & Domb, 2021).

4.2 Characterization of microstructured lipid microparticles (MLMs)

4.2.1 Thermal properties

Fig. 1 and Table 2 show the melting and crystallization curves as well as the DSC parameters of the lipid materials (FHPO and PO) and the MLMs loaded with grape peel extract. The melting and crystallization parameters include, respectively, initial temperature (T_{if} and T_{ic}), which refers to the onset of phase transition; peak temperature (T_f and T_c), with maximal thermal effect; final temperature (T_{df} and T_{dc}), which indicates the completion of the thermal effect; and melting and crystallization enthalpy (ΔH_f and ΔH_c), which is measured by the area under the curve.

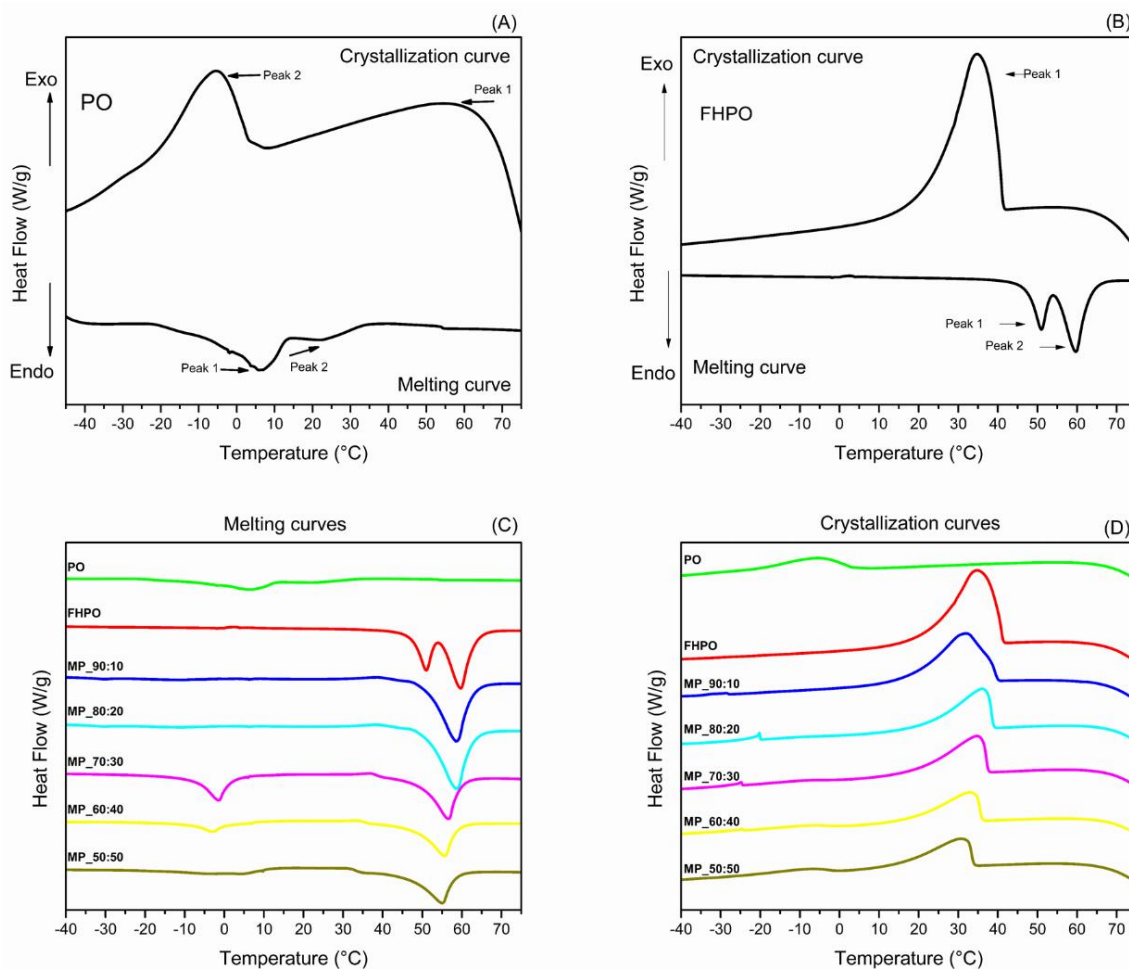


Fig. 1. Melting and crystallization curves of the lipid materials (PO and FHPO) and the MLMs with grape peel extract. 90:10, 80:20, 70:30, 60:40, and 50:50 correspond to PO and FHPO ratios in the microparticles.

The melting and crystallization curves of the pure lipid materials were evaluated separately and the results were similar to those reported in the literature (O'Brien, 2004). Two melting peaks (Fig. 1 A and C) were observed for PO, the first at 6.04 °C related to the melting of the unsaturated fatty acid fraction, and a second peak at 23.27 °C corresponding to the melting of the saturated fraction of this lipid. Due to its varied fatty acids composition (Table 1), peaks in different regions were expected, representing low and medium melting points (Lin, 2002). For FHPO, two well-defined peaks were found at 50.96 and 59.72 °C (Fig. 1B). These two intense peaks are attributed to the presence of 99.1% saturated fatty acids in this lipid, characterizing a high melting point. The melting enthalpy is associated with the amount of

energy absorbed to melt the fat crystals. The more homogeneous the crystals and their structure, the more energy required to break the crystals (Ribeiro et al., 2015). Therefore, the total melting enthalpy of FHPO (12.46 J/g) was higher than the enthalpy of PO (3.85 J/g).

Regarding the crystallization curves, the PO exhibited a single peak at $-5.35\text{ }^{\circ}\text{C}$, which can also be observed in Fig. 1D. This peak is related to lipid fractions rich in unsaturated fatty acids, corresponding to low melting point triacylglycerols. No crystallization peaks related to the tri-unsaturated lipid fraction were observed in the PO, probably due to the low concentration of this triacylglycerol, corresponding to peaks with melting points between 12 and $28\text{ }^{\circ}\text{C}$ (Gee, 2007; Omar et al., 2015).

For FHPO, a well-defined crystallization peak was found at $34.74\text{ }^{\circ}\text{C}$ representing the trisaturated triacylglycerol fraction (Carvalho et al., 2019). Crystallization is an exothermic event, with energy release from the sample during the process. The total crystallization enthalpy related to the FHPO peak was 56.97 J/g when compared to 8.78 J/g observed for OP. Therefore, the energy dissipated for the FHPO crystallization was higher than that of PO, confirming that this property is extensive and proportional to the amount of crystalline material formed.

Table 2. DSC crystallization and melting behavior of palm oil, fully hydrogenated palm oil, and the microstructured lipid microparticles containing grape peel extract.

	Thermal properties	Peak	FHPO	PO	MLM_90:10	MLM_80:20	MLM_70:30	MLM_60:40	MLM_50:50
MELTING	T _{if} (°C)	1	45.40	-17.53	5.71	4.71	-10.88	-11.79	-15.20
		2	53.80	19.43	44.42	47.79	40.15	40.79	39.56
	T _{peak} (°C)	1	50.96	6.04	6.24	6.23	-1.44	-3.08	4.37
		2	59.72	23.27	58.49	58.32	56.56	55.65	55.04
	T _{df} (°C)	1	53.80	14.42	20.58	7.73	5.26	2.60	13.47
		2	68.35	33.31	65.31	67.22	64.66	62.61	60.68
	Total melting enthalpy (J/g)		12.46	3.85	16.71	17.26	17.83	11.38	11.83
CRYSTALLIZATION	T _{ic} (°C)	1	45.02	7.61	42.51	41.09	39.78	36.66	34.67
		2	-	-	-27.81	-19.61	-24.33	-24.07	-1.47
	T _{peak} (°C)	1	34.74	-5.35	31.65	35.43	34.56	32.89	30.62
		2	-	-	-28.78	-20.22	-24.88	-24.67	-10.61
	T _{dc} (°C)	1	15.99	-20.37	11.03	17.81	12.5	7.91	4.55
		2	-	-	-30.82	-22.81	-27.07	-26.58	-22.85
	Total crystallization enthalpy (J/g)		56.97	25.23	45.34	28.76	30.82	23.58	22.27

T_i: melting/crystallization onset temperature; T_{peak}: melting/crystallization peak temperature and T_d: melting/crystallization final temperature. 90:10, 80:20, 70:30, 60:40, and 50:50 correspond to the FHPO to PO ratio in the microparticles.

In general, MLMs with higher FHPO concentrations showed a significant increase in T_{if} , T_{peak} , and T_{df} (Table 2) indicating slower MLM melting. This finding is confirmed by the shift of the curves (2nd peak) to the right (Fig. 1C) of the MLMs with higher FHPO concentration. In addition, the melting enthalpies were substantially higher for the MLMs containing FHPO concentration $\geq 70\%$. These results suggest a possible correlation with the presence of thermodynamically more stable polymorphic forms, which have higher melting temperatures and require higher energy levels for phase transition (Oliveira et al., 2015).

The first melting peak (from left to right) of the MLMs was less intense for all treatments. However, more pronounced peaks were observed around -3 to 4 °C in the MLMs containing 30, 40, and 50% PO. This result may be due to the fractionated melting of fatty acids from the MLMs with the addition of high PO concentrations. The presence of high PO concentrations initially induced the melting of lower melting point triacylglycerols in the system, followed by the second more intense and defined transition event (2nd peak), related to the melting of partially or fully saturated triacylglycerols. Carvalho et al. (2019) reported similar results of thermal behavior of spray chilled MLMs containing ascorbic acid using FHPO and PO as encapsulating materials.

The curves in Fig. 1D confirm that the addition of palm fat to the MLMs led to an acceleration of crystallization events as a function of the PO concentration. As can be seen in Table 2, the onset crystallization temperatures (peak 1) were above 40°C for MLM_90:10 and MLM_80_20, while the other MLMs exhibited onset crystallization between 39 and 32 °C, confirming the decrease of the onset of crystallization. This first crystallization peak is associated with the higher melting point triacylglycerols present in FHPO, which promoted a decrease in the nucleation period. The second and lower intensity peak represents the unsaturated fatty acids of PO. These fractions were much lower in the MLMs containing 90 and 80% FHPO. Overall, the energy release for solidification of the MLMs was proportional to the

FHPO content, with greater energy dissipated for the microparticles containing higher palm fat content.

4.2.2 Polymorphism

Fig. 2 shows the X-ray diffraction measurements of the pure lipid materials and the MLMs. The PO showed a nearly amorphous pattern, evidenced by the wide halo between $2\theta \sim 10^\circ$ and 30° . Amorphous materials do not have atoms arranged periodically, i.e., they are disordered, and consequently do not produce a diffraction pattern, hindering the correct interpretation of the location of peaks in the sample (Sato; Ueno, 2011). In turn, the diffraction pattern of FHPO was well identified by the CSD (Cambridge Structural Database) as the β' polymorph (Groom et al., 2016). According to the literature, the formation of β' crystals is related to the presence of high concentrations of palmitic acid (Omar et al., 2015), which represented 42.75% and 42.82% of the total fat content of FHPO and PO, respectively..

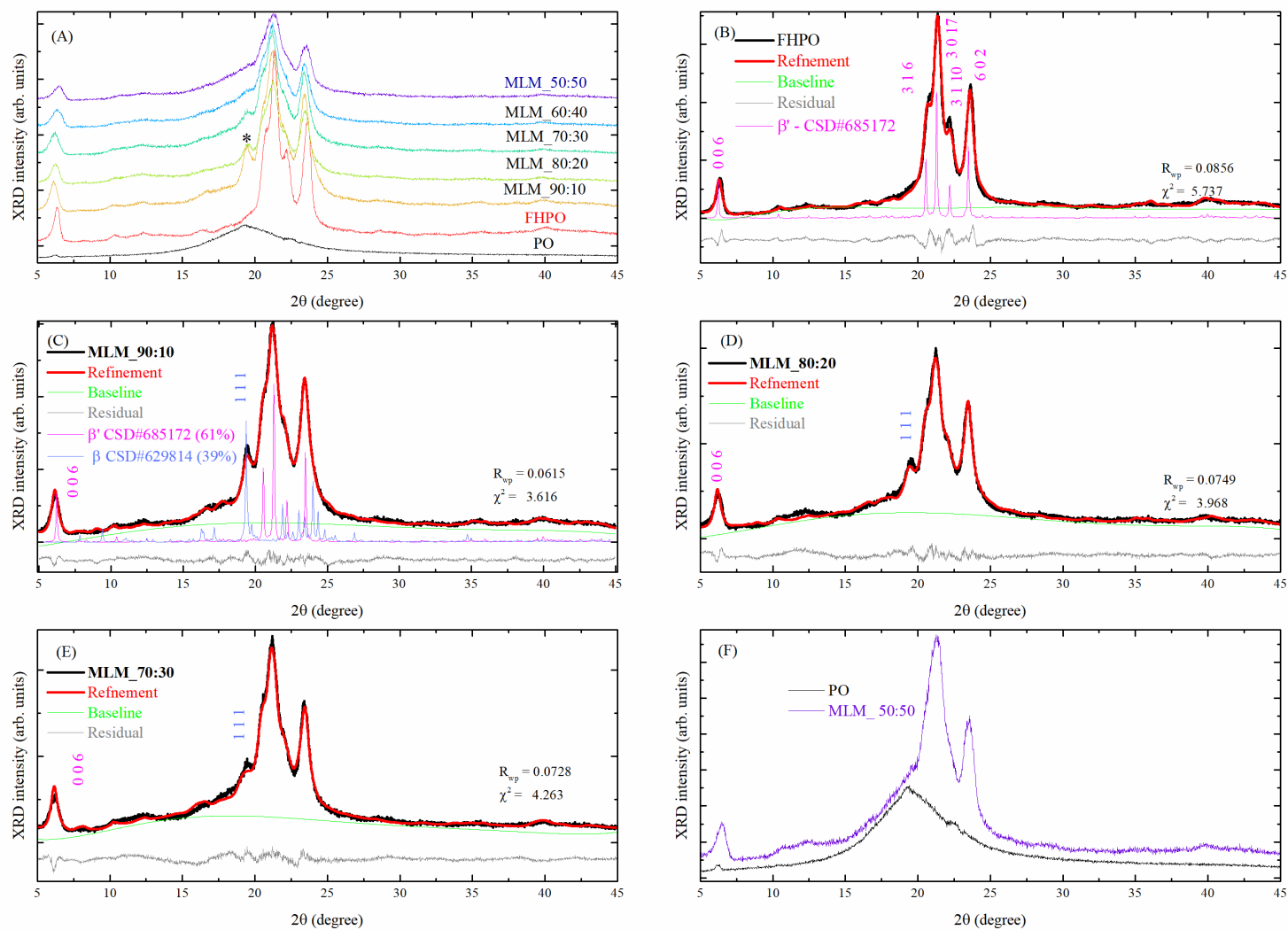


Fig. 2. (A) XRD patterns of MLMs, FHPO, and PO, (b) normalized XRD patterns for FHPO, (C) normalized XRD patterns for MLM_90:10 and calculation of percent crystallinity, (D) normalized XRD patterns for MLM_80:20, (E) normalized XRD patterns for MLM_70:30, and (F) normalized XRD patterns of PO and MLM_50:50.

As can be seen in Fig. 2B, all peaks of the FHPO sample are satisfied according CSD (Groom et al., 2016) as well as the structural refinement shows excellent agreement in addition to good convergence factors (Toby, 2006). The unit cell parameters in Table 3 provide the structure dimensions before the addition of PO. The asterisk in Fig. 2A points out the appearance of a peak around $2\theta = 19.45^\circ$ when PO was added to the formulation MLM_90:10. This peak, in turn, coincides with the peak referring to the (1 1 1) lattice plane of the polymorph β (Groom et al., 2016). Figure 4C shows the result of the Rietveld refinement considering the polymorphs β' and β . The agreement with the experimental data indicates that the PO addition led to a partial transition in the β' structure. Given this hypothesis, we believe that the PO molecules destabilized the β' crystals on the surface of the crystallites, forming a cap of β crystals over the β' crystals. However, the β' phase was preserved in all MLMs. Moreover, although PO affected the formation of more stable β -crystals, it probably remained in the semisolid phase, while crystallization was observed for FHPO. Despite the high crystallization rate due to the rapid pulverization of the lipid material in cold room at $\sim 13^\circ\text{C}$, according to the thermal properties of PO (Table 2) its peak melting temperature of highest intensity was relatively low (around 6.04°C). Therefore, this semi-solid phase may have allowed a higher diffusion rate of the triacylglycerol molecules and their continuous rearrangement to reach crystal conformations of higher density and stability (Santos et al., 2020).

In addition, the widths of the halos suggest the broadening of the β peak with increasing PO concentration, making the diffractograms typical of amorphous materials, and impairing the Rietveld refinements. The lower intensity of peak 1 1 1 led to an increase in the deviations of the cell parameter values, with lower agreement between the experimental and calculated deviation, as shown in Figs. 2D and E and Table 3.

A refinement was not possible for the MLMS 60:40 and 50:50, suggesting an amorphous behavior similar to pure PO, which can be confirmed by the thermal behavior.

Fig.2F shows the X-ray diffraction pattern at the highest PO concentration, superimposed on the pattern of the pure PO. In this fraction, the β phase became indistinguishable, corresponding only to a shoulder of the peak 3 1 6 of the β' phase, in the same region as the maximum intensity of the amorphous halo of the XRD pattern of PO.

Table 3. Rietveld-refined unit cell parameters of the β' and β polymorphs and unit cell volume (V).

Treatments	Polymorph	a (Å)	b (Å)	c (Å)	β (°)	V(Å ³)
FHPO	β'	22.669(3)	5.652(2)	84.46(5)	91.25(5)	10820(5)
90:10	β'	22.802(4)	5.623(2)	86.47(4)	91.96(4)	11081(8)
	β	5.346(3)	117.5(2)	8.302(9)	87.54(9)	5211(9)
80:20	β'	22.745(9)	5.665(3)	85.20(6)	91.853	10973(7)
	β	5.350(9)	118.8(2)	8.35(9)	87.8(9)	5312(18)
70:30	β'	22.769(6)	5.683(2)	85.50(5)	91.751(6)	11059(7)
	β	5.53(1)	133.0(2)	8.23(9)	89.355(9)	6060(28)

Gamboa et al. (2011) studied the microencapsulation of tocopherol by spray chilling and found the β form by XRD in the microparticles from interesterified cottonseed oil mixed with fully hydrogenated palm and soybean oils. Santos et al. (2020) also reported that the addition of canola oil or D-limonene to fully hydrogenated soybean oil to produce the spray-chilled microparticles led to microparticles with crystals in both β' and β polymorphic forms. These results suggest that spray chilling technology can produce lipid microparticles with crystals in the two most stable polymorphic forms, and dilution of fats with oils induces the formation of more stable polymorphs. It is worth noting that these characteristics depend on

many other factors, such as the interactions between the lipid materials, the active compound, and the process parameters, including the cooling rate.

In general, all MLMs exhibited well-defined peaks referring to the polymorphic β' form, and more intense peaks were observed in the MLMs containing higher FHPO concentration. Ensuring the stability of the β' form in products made with palm oil is a matter of great industrial interest. The stabilization of the β' form and the reduction of crystal size allow the incorporation of a greater amount of liquid oil into the crystal network, providing a shiny and uniform surface and even a smooth texture. This fat profile contributes to the use of palm oil in margarines and fats. In addition, the incidence of β crystals favors the use of palm oil as an alternative ingredient to cocoa butter (Carvalho et al., 2019).

4.2.3 FTIR

FTIR analysis is an effective tool to qualitatively evaluate the encapsulation of bioactive compounds and the identification of important functional groups, and can demonstrate lipid oxidation or other interactions between the materials after spray chilling. The FTIR spectra of the grape peel extract, the microparticles, the palm oil and palm fat are shown in Fig. 3.

FTIR analysis showed that the grape peel extract was efficiently encapsulated by the encapsulating materials for all formulations. The spectrum of the grape peel extract and the MLMs made with different FHPO and PO showed several bands between 1650 cm^{-1} and 1000 cm^{-1} characteristic of phenolic compounds. The strong peak at 1643 cm^{-1} found in the sample can be due to the vibration of the $=\text{C}=\text{C}$ bond, typical of aromatic compounds (Nogales-Bueno et al., 2017). Although this peak did not appear in pure FHPO and PO, it was visible in the formulations. The large band from 3000 to 3600 cm^{-1} in all samples except for FHPO and PO

is related to hydrogen bonded O-H stretching of carbohydrates, carboxylic acids, and residual water (Moreno et al., 2018).

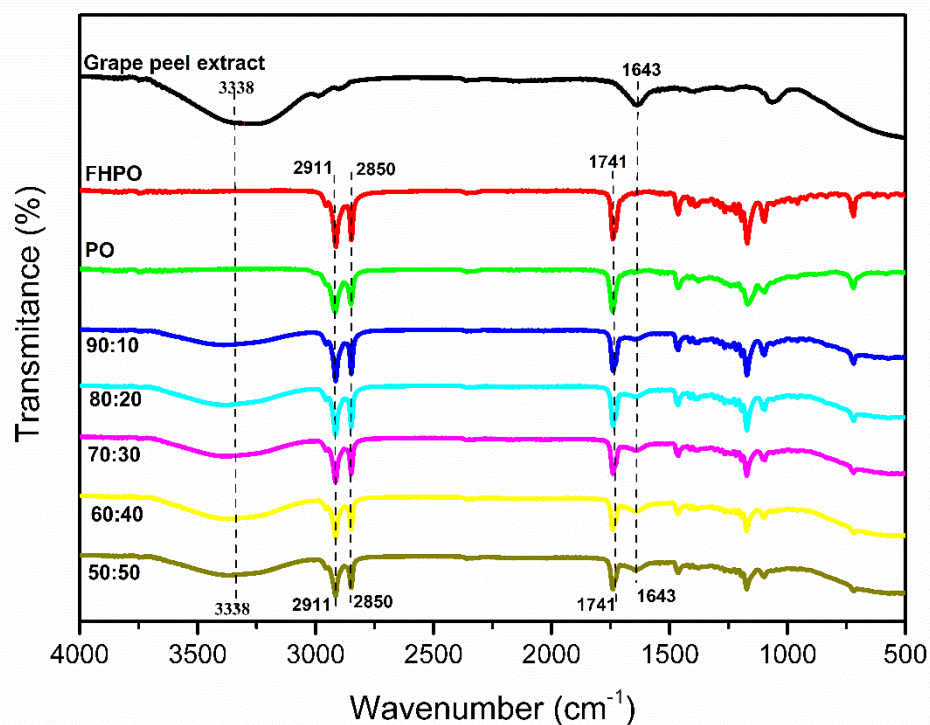


Fig. 3. FTIR spectra of the grape peel extract, fully hydrogenated palm oil (FHPO), palm oil (PO) and the microstructured lipid microparticles with different FHPO to PO ratios.

The peaks located between 1741, 2850, and 2911 cm⁻¹ are characteristic of fully hydrogenated palm oil (FHPO) and pure palm oil (PO), which were also found in the microparticles. These bands are related to the presence of carbonyl compounds, more specifically carboxylic acids that are present in the triacylglycerol molecules, which are predominant in FHPO and PO (Oriani et al., 2016). The bands corresponding to the ester bond stretching vibration of the triacylglycerols appeared between 1300 and 1000 cm⁻¹ (approximately 1170 cm⁻¹ in the present study) (Pelissari et al., 2016). Overall, the spectra of the microparticles were consistent with the ingredients used, showing characteristic peaks of grape peel extract, FHPO, and PO for all treatments studied.

4.2.4 Mean particle diameter, span, and morphology

The diameter of the MLMs has a great influence on the products since the crystal size can have direct implications on the sensory properties of the product. The mean diameter values and polydispersity index of the MLMs are presented in Table 4.

The MLMs showed a mean diameter (expressed as $D_{4.3}$) between 23.30 and 30.12 μm . Significant differences ($p < 0.05$) were observed among treatments, except for the samples made with 80 and 70 % FHPO. The increase in the proportion of lower melting point (OP) lipid in the MLMs led to an increase in the mean particle diameter. As reported by Carvalho et al. (2019) and Procopio et al. (2018), a higher PO concentration has been related to larger diameter of ascorbic acid and cinnamon oleoresin loaded MLMs produced by spray chilling. The authors found similar mean diameter values to this study and reported that the higher concentration of unsaturated fatty acids of PO decreased the melting point of the MLMs, causing agglomeration. A higher agglomeration of the MLMs (Fig. 4) was observed after spray cooling, in which the unsaturated fatty acids of PO allowed a lipid to remain liquid, accommodated on the surface of the microparticles or trapped in the crystal network formed by the high melting point lipids, causing disruption in the crystal network. These perturbations caused by the natural disorganization of liquid lipids may be due to the larger diameter values of the samples containing higher PO concentrations.

The polydispersity index (Span) indicates the particle size variation, and particles with lower Span values are more homogeneous. As observed in Table 4, the span of the MLMs was in the range 1.19 - 1.26, indicating a unimodal behavior with a narrow size distribution of the MLMs (Patra & Routray, 2018).

Table 4. Physical properties of the microstructured lipid microparticles.

Treatment	Variables					
	D _{4.3} (μm)	<i>Span</i>	Bulk density (kg/ m ³)	Tapped density (kg/m ³)	Carr's Index (%)	Hausner ratio
MLM_90:10	23.30 ± 0.48 ^d	1.22 ± 0.01 ^{b, c}	322 ± 0.02 ^a	449 ± 0.02 ^a	28 ± 1.37 ^b	1.4 ± 0.02 ^b
MLM_80:20	25.92 ± 0.27 ^c	1.19 ± 0.01 ^c	314 ± 0.00 ^a	441 ± 0.00 ^a	28 ± 1.51 ^b	1.4 ± 0.02 ^b
MLM_70:30	25.98 ± 0.23 ^c	1.28 ± 0.01 ^a	306 ± 0.01 ^a	441 ± 0.00 ^a	31 ± 1.50 ^b	1.4 ± 0.03 ^b
MLM_60:40	27.74 ± 0.34 ^b	1.21 ± 0.01 ^{b, c}	279 ± 0.02 ^c	437 ± 0.01 ^a	36 ± 1.64 ^a	1.6 ± 0.14 ^a
MLM_50:50	30.12 ± 0.81 ^a	1.26 ± 0.03 ^{a, b}	253 ± 0.01 ^b	399 ± 0.00 ^b	37 ± 1.01 ^a	1.6 ± 0.02 ^a

Lower case letters in each column represent significant difference (p<0.05). 90:10, 80:20, 70:30, 60:40, and 50:50 correspond to the FHPO to PO ratios in the microparticles.

Other studies have shown the variability ($D_{4.3}$) in mean particle size of spray chilled particles (181 - 20.52 μm) (Carvalho et al., 2019; Consoli et al., 2016; Gamboa et al., 2011; Matos-Jr et al., 2017; Oriani et al., 2018; Procopio et al., 2018). These studies confirmed that several factors can influence the distribution and size of spray-chilled particles, such as the characteristics and proportion of the active material, viscosity of the atomization fluid, equipment settings, and spray cooling parameters. However, the diameter values of this study were satisfactory since for food applications the crystal size should be below 30 μm to prevent a sandy mouthfeel (Barbas et al., 1998).

The MLMs and the respective photomicrographs obtained by scanning electron microscope at a magnification of 1800X are shown in Fig. 4. In general, all treatments presented characteristics of spray-chilled particles, i.e., the vast majority had a spherical shape, slightly rough surface, absence of pores and size variation (Alvim et al., 2016; Consoli et al., 2016).

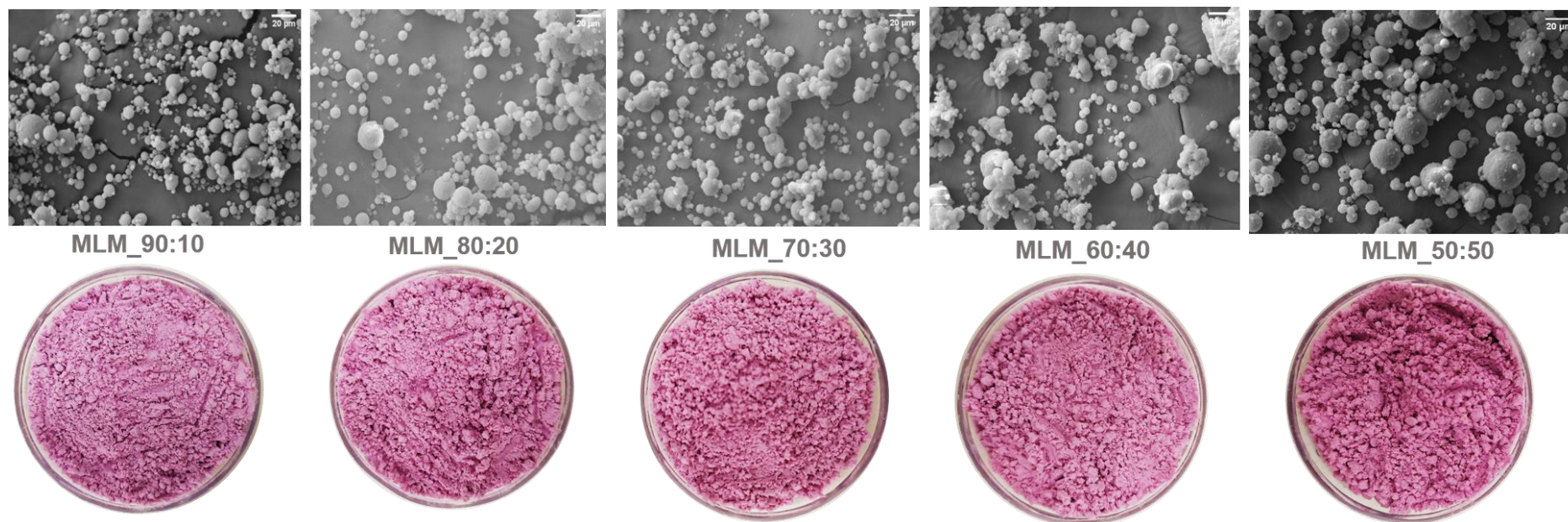


Fig. 4. SEM images and visual aspects of spray-chilled MLMs with grape peel extract at 1800x. 90:10, 80:20, 70:30, 60:40, and 50:50 correspond to the FHPO to PO ratios in the microparticles.

The MLMs with higher PO concentrations (40 and 50 %) exhibited more agglomerated particles, more rough, with larger diameters. In addition, some holes were found in the MLMs with 50% PO, which may facilitate the degradation of bioactive compounds in the particles due to the passage of oxygen, light, humidity, among other factors. The roughness suggests an inefficient crystallization of the particles, caused by the higher amount of unsaturated fatty acids in PO, leading to a lower melting point of the MLMs. Thus, the particles require a longer time for complete solidification when compared to those with higher FHPO content. The incomplete solidification can generate a larger amount of particles in an amorphous state. This behavior was observed by Wegmüller et al. (2006) in the encapsulation of vitamin A, iodine, and iron by spray chilling technology using FHPO as an encapsulating material. The authors observed the presence of roughness and agglomerates due to incomplete solidification of the microparticles during the process.

In addition, higher adhesion of smaller particles on the surface of larger particles was also observed in these two treatments, leading to deformation of the final morphology of MLMs. Carvalho et al. (2019) and Procopio et al. (2018) studied the microencapsulation of ascorbic acid and cinnamon oleoresin using spray chilling and FHPO and PO as encapsulating materials and reported this change due to melting point of the microparticles during solidification in the atomization process. The higher agglomeration and adhesion of the formulations with higher PO concentrations (40 and 50%) can lead to so-called caking, which is the formation of lumps that cause defect in powder products, resulting in loss of quality (Fitzpatrick, 2013).

4.2.5 Bulk and tapped density, Carr's index, and Hausner ratio

The values of bulk and tapped density, flowability (Carr's index), and cohesiveness (Hausner ratio) of the samples are shown in Table 4. These parameters are indispensable to evaluate powder products, as they help in predicting the size and design of the packaging and assist in the correct application of the MLMs. The lowest bulk density values were obtained for the MLMs containing 40 and 50% PO, which were significantly different ($p < 0.05$) from the other treatments. Tapped density also decreased with increasing PO concentration; however, only the treatment with 50% PO was significantly different ($p < 0.05$) from the others.

During crystallization of MLMs on spray cooling, the higher concentration of saturated lipids (higher presence in FHPO) is associated with a more compact crystalline structure. Crystallization of liquid lipids leads to a volume contraction of the lipid molecules, while melting of solid lipids leads to volume expansion (Sato; Ueno, 2011). Therefore, the lower density values in MLMs with 40 and 50% PO may be due to lower crystallinity when compared to the other MLMs (30, 20, and 10 % OP), allowing the formation of less compact structures with lower densities. In addition, the mixing of solid (FHPO) and liquid (PO) lipids may lead to the formation of microstructured lipid microparticles of type 1 (imperfect), type 2 (amorphous), and/or type 3 (multiple) (Müller et al., 2002b). Probably, the treatments containing higher proportions of FHPO (90:10, 80:20, and 70:30) fit the type 1, i.e., the MLMs are formed when the fat crystallization is altered by small amounts of oil. This event explains the higher bulk density and tapped values of these treatments, which can also be due to the smaller particle diameters. The more organized and crystalline the structure, the higher the bulk and tapped density of the MLMs. The MLMs with lower FHPO concentrations (60:40 and 50:50) are type 2 (amorphous), in which the lipid matrix is solid, but not crystalline (amorphous state), occupying a greater volume.

The bulk and tapped densities were used to calculate the empirical parameters Carr's index and Hausner ratio, which characterize the flowability and the cohesive forces of a powder,

respectively. These parameters can explain trends in reconstitution properties since they indicate inter-particle interactions that can affect the dispersion of the powder (VU et al., 2003). The flowability of the microparticles was compared with reference values, while the flowability of the powders was classified by the Carr's Index (CI) values as very good (< 15), good (15-20), regular (20-35), bad (35-45) and very bad (> 45) flowability. Cohesiveness was classified by the Hausner ratio (HR) as low (< 1.2), intermediate (1.2-1.4) and high (>1.4) (Geldart et al., 1984).

According to the results, the CI and HR values of the samples differed statistically ($p < 0.05$) and ranged from 28-37% and 1.4-1.6, respectively, indicating that MLMs were more cohesive and have intermediate flowability. These values are close to those found for high-fat powder products such as whole and skim milk (CI = 23.5 to 29%; HR= 1.31 to 1.40) (Pugliese et al., 2017) and honey powder using biopolymers as carriers (CI = 23.03 to 26.59% ; HR= 1.23 to 1.33) (Mutlu et al., 2020).

In this study, increasing the PO concentrations in the MLMs resulted in larger mean particle diameter, which may be related to the worse flow properties of the MLMs containing 40 and 50% PO when compared to the others. Lipids in general have a high adhesion capacity, which may contribute to a lower flowability of microparticles, especially those containing higher content of liquid lipid (PO), resulting in deformed particles, as seen in the SEM micrographs, increasing the contact area and the attractive forces between them, resulting in agglomerated particles (Pugliese et al., 2017). Similar behavior was reported by Procopio et al. (2018) in the microencapsulation of cinnamon oleoresin by spray chilling, using FHPO and PO as encapsulating materials. According to those authors, most microparticles were rated with reasonable flowability and intermediate cohesiveness, except for the formulation containing only FHPO, which exhibited better flow properties. Rennie et al. (1999) also reported that

higher fat contents and larger particle sizes can impact negatively the flow properties of dairy powders.

4.3 Anthocyanins content, total phenolic compounds, and antioxidant capacity of MLM.

The content of total monomeric anthocyanins and their retention, as well as the content of total phenolic compounds and antioxidant capacity of microstructured lipid microparticles are shown in Table 5. The results indicated that the concentration of the encapsulating materials (FHPO and PO) affected the anthocyanins and phenolic compounds ($p < 0.05$) rather than the antioxidant capacity.

The highest retention and content of anthocyanins, phenolic compounds, and antioxidant capacity were observed for the treatment with the highest FHPO concentration (MLM_90:10). Procopio et al. (2018) reported that higher FHPO concentration in FHPO/PO blends led to higher encapsulation efficiency of cinnamon oleoresin. The authors stated that saturated lipids with the same chain size crystallize faster, which may contribute to higher encapsulation efficiency. The thermal behavior of the MLMs in this study revealed a higher crystallization enthalpy of MLM_90:10 when compared to the others, showing that these MLMs exhibited a larger amount of crystalline material, which may have favored the entrapment of bioactive compounds. However, crystal chains are more compact and may lead to greater release of the active compound during storage. Further studies are needed to understand the actual encapsulation behavior of bioactive compounds in MLMs during storage.

Table 5. Total monomeric anthocyanins, anthocyanin retention, total phenolic compounds, and antioxidant capacity of lipid microparticles with grape peel extract.

Treatment	Total monomeric anthocyanins (mg/100g)	Anthocyanin retention (%)	Total phenolic compounds (mg GAE/100g)	Antioxidant capacity (%)
MLM_90:10	706.3 ± 0.03 ^a	81.5 ± 0.03 ^a	1443.1 ± 0.01 ^a	92.6 ± 0.81 ^b
MLM_80:20	531.0 ± 0.01 ^b	61.3 ± 0.01 ^d	1247.2 ± 0.01 ^e	84.0 ± 0.04 ^a
MLM_70:30	547.5 ± 0.01 ^c	63.2 ± 0.01 ^c	1272.0 ± 0.01 ^d	86.1 ± 0.01 ^a
MLM_60:40	556.2 ± 0.00 ^d	64.2 ± 0.00 ^b	1386.1 ± 0.01 ^c	86.6 ± 0.06 ^a
MLM_50:50	558.0 ± 0.01 ^e	64.4 ± 0.01 ^b	1400.3 ± 0.01 ^b	86.8 ± 0.04 ^a

Values are given as mean ± standard deviation. The same letters in the same column indicate no significant differences ($p > 0.05$) by Duncan's test. 90:10, 80:20, 70:30, 60:40, and 50:50 correspond to the FHPO to PO ratio in the microparticles.

As shown in Table 5, the results of bioactive compounds and antioxidant capacity were proportional to the PO concentration in the MLMs, except for MLM_90:10. The polymorphic form of the fat crystals after solidification exerts direct influence on the entrapment of the active compound within the particles. According to the literature, in structured lipid matrices, the solid and liquid lipid ratio generates different types of MLMs, which can be classified as imperfect, amorphous, and multiple (Barroso et al., 2021; Figueiredo et al., 2022; Müller et al., 2002a).

Thus, it is believed that the MLMs with PO concentration above 10% generated amorphous microparticles, which are not crystalline despite being solid, creating imperfect structures that facilitate the accommodation of bioactive compounds, confirming that the higher the PO concentration, the higher the anthocyanins content, phenolics retention, and antioxidant capacity. This hypothesis is confirmed in the X-ray diffraction, which revealed that the higher the PO concentration, the higher the amorphous fraction of MLMs, although all treatments showed polymorphic β' and β crystals. Several studies on the production of micro and nano

structured lipid particles have reported that particles containing both β' and β' forms provide better accommodation of the active agent, due to the spatial organization of the crystals in the matrix (Carvalho et al., 2019; Consoli et al., 2016; Müller et al., 2002b; Patra & Routray, 2018).

In general, the microencapsulation process of grape peel extract by spray chilling using FHPO and PO as encapsulating materials proved to be effective since higher antioxidant capacity and anthocyanins retention in the MLMs were observed. Satisfactory results have also been reported in the microencapsulation of different compounds by spray chilling. Encapsulation efficiencies between 101 and 76 % were obtained in the microencapsulation of vitamin B12 using vegetable fat (Chalella Mazzocato et al., 2019). A solution containing 40% glucose was encapsulated with different stearic acid and oleic acid ratios, with efficiencies ranging from 96 to 75.1%. A phytosterol blend was encapsulated using low-trans hydrogenated vegetable fat and stearic acid. Some authors have studied microencapsulation of ascorbic acid by spray drying and spray chilling, comparing both techniques regarding the protection of the microparticles containing the active ingredient in baked cookies and reported high encapsulation efficiencies for both techniques. The addition of the microparticles to the cookie formulations inhibited the formation of dark spots associated with the degradation of ascorbic acid. Despite the higher protection of ascorbic acid in the spray drying technology, there was a reduction of almost half of the loss when compared to the free ascorbic acid added to the product. Thus, both microencapsulation methods can be used in the protection of active compounds in bakery products (Alvim et al., 2016).

4.4 Stability of MLMs upon storage

The study of the stability of MLMs to storage at different temperatures allows the choice of the best conditions for application and maximum use of MLMs. Table 6 shows the anthocyanins retention in MLMs, and Fig. 5 shows the anthocyanin contents in MLMs as well

as the half-life time values (days). Fig. 6 shows the ΔE^* (total color difference) values, and Fig. 7 presents the visual aspects of the MLMs during the storage.

Table 6. Anthocyanins retention (%) in the microparticles with grape peel extract with different FHPO to PO ratios, over 90 days of storage at -18°C, 4°C, and 25°C.

Treatment	Temperature (°C)	0	7	15	30	45	60	75	90
MLM_90:10	-18°C		99.58	94.22	81.95	73.77	72.21	63.19	57.26
MLM_80:20			92.84	86.44	75.33	72.69	70.06	69.68	58.00
MLM_70:30		100	94.89	92.88	76.64	75.91	74.27	62.04	58.94
MLM_60:40			94.24	93.17	83.99	78.42	76.80	64.03	59.53
MLM_50:50			96.71	90.12	86.14	71.75	68.98	50.61	48.70
MLM_90:10	4°C		91.40	84.34	79.13	70.66	66.57	56.84	56.14
MLM_80:20			99.62	85.88	75.14	73.07	72.88	55.74	54.80
MLM_70:30		100	99.27	90.51	77.19	75.36	72.08	57.85	56.75
MLM_60:40			98.74	90.47	83.45	80.22	78.42	59.71	55.58
MLM_50:50			98.44	90.64	87.00	72.44	59.27	54.59	45.58
MLM_90:10	25°C		71,37	56.84	44.99	42.74	36.53	34.70	30.18
MLM_80:20			79,28	70.06	57.25	51.22	47.65	45.01	43.88
MLM_70:30		100	78,10	68.98	59.12	51.28	45.26	41.97	38.87
MLM_60:40			77,34	67.99	53.24	52.34	49.82	42.81	39.57
MLM_50:50			73,14	59.10	46.79	46.45	40.21	35.53	31.02

90:10, 80:20, 70:30, 60:40, and 50:50 correspond to the FHPO to PO ratios in the microparticles.

In general, the anthocyanins degradation was proportional to the storage time, i.e., the longer the time, the greater the degradation of this pigment. The temperature also affected the degradation of anthocyanins, with lower degradation rates at -18°C and 4°C when compared to samples stored at 25°C . Temperature is one of the main factors causing degradation of natural pigments. The degradation of anthocyanins by heat is initiated by the hydrolysis of glycosidic bonds, which leads to the loss of glycosyl radicals and the formation of the most unstable form of anthocyanins, inducing color changes (Fredes et al., 2018). This phenomenon is shown through the color parameter ΔE^* (Fig. 6) and the visual aspects in Fig. 7. At 25°C , the highest ΔE^* values were observed and consequently the greatest color changes of the MLMs.

As shown in Table 6, until the day 30 of storage at -18°C and 4°C , the MLMs showed high anthocyanins retention (86-75 %). In contrast, different behavior was observed at 25°C , reaching lower retention values on day 15 of storage. At the end of the storage, the anthocyanins retention at -18°C and 4°C was close for all formulations, with values between 59 and 45 %. As expected, at 25°C the MLMs exhibited a lower capacity to retain anthocyanins (43-30%), reinforcing that temperature is a key factor in the stability of this compound.

The degradation of anthocyanins followed first-order kinetics ($0.832 \leq R^2 \leq 0.978$). The degradation rate constant ($k \times 10^{-2}$) ranged from -0.008 to -0.005 days^{-1} at -18°C ; -0.010 to -0.006 days^{-1} at 4°C , and -0.011 to -0.008 days^{-1} at 25°C . The half-life times can be seen in Figs. 5 A, B, C, D, and E. The longest half-lives (consequently the lowest degradation rates) were achieved for MLMs stored at -18°C , 4°C and finally 25°C .

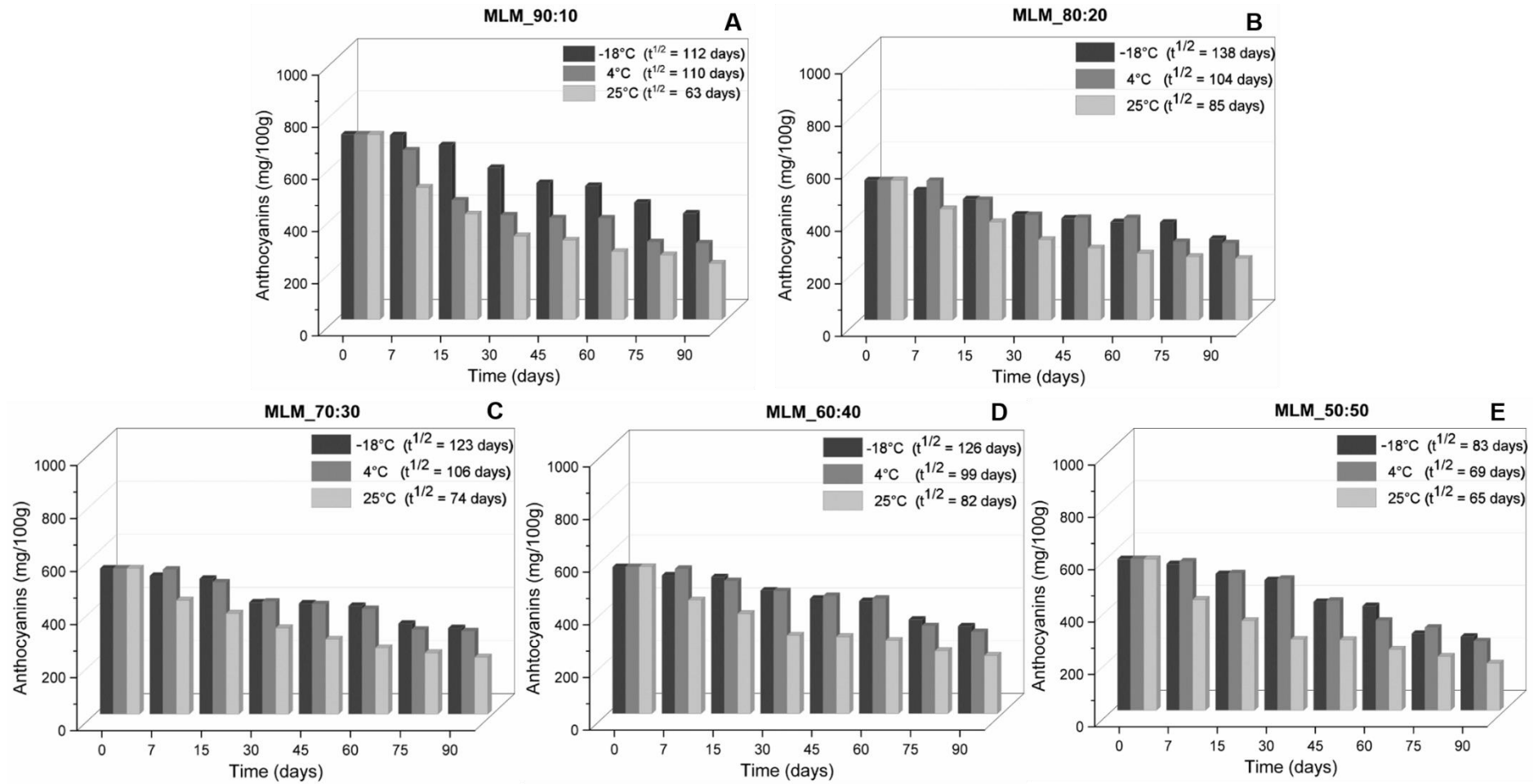


Fig. 5. Anthocyanins contents and half-life ($t^{1/2}$) of spray-chilled MLMs with grape peel extract with different FHPO to PO ratios, stored at -18 °C, 4 °C, and 25 °C for 90 days.

Regarding the MLMs stored at -18 °C and 4 °C, close anthocyanin half-life times were obtained for most treatments, except for MLM_50:50 that showed lower $t^{1/2}$ values at both temperatures. These results suggest that the high PO concentration had negative impacts on the anthocyanins retention during storage, probably due to the polymorphic instability of MLM. The polymorphic transitions always occur towards the most stable form (α , β' , and β). As shown in the XRD plots (Fig. 2A and F) the high concentration of unsaturated fatty acids in PO led to the formation of amorphous MLMs, which were less thermodynamically stable. Therefore, it is believed that during storage, MLM_50:50 underwent rapid changes from less stable to more stable polymorphic forms. However, an early transition from less stable (α and β') to the most stable (β) forms is not interesting for MLMs, once it may lead to an early expulsion of the active compound due to restructuring the polymorph to more organized and energetically favorable levels, leading to a lack of space in the microstructure of the lipid matrix, which causes the release of the active ingredient from the MLMs (Carvalho et al., 2019; Müller et al., 2002b).

A higher anthocyanins retention was observed for the MLMs with higher FHPO concentrations stored at -18 and 4 °C, thus the presence of large amounts of saturated fatty acids in the MLMs may have affected the stabilization of the polymorphic β' form during storage, contributing to the better retention of the anthocyanins from the grape peel extract.

Ribeiro et al. (2015) state that α and β' forms can be formed at constant temperatures in almost all vegetable oils, and the β form can be developed through liquid-solid or solid-solid structures during storage. Santos et al. (2020a) studied the polymorphic behavior of MLMs from blends of fully hydrogenated soybean oil and canola oil during storage at 25 °C. The authors found that the higher the oil content added to the fully hydrogenated soybean oil, the faster the polymorphic transition from the less stable to the more stable form.

The polymorphic behavior of MLMs containing blends of anhydrous milk fat and fully hydrogenated soybean oil in the ratios of 90:10 and 80:20 during storage at 5, 10, and 25 °C

was evaluated. The authors reported polymorphic modifications to the most stable forms in the MLMs during storage. The higher the storage temperature, the greater the tendency for β -form since the more unstable polymorphic forms were melted and eliminated at higher temperatures (Landim Neves et al., 2021).

Lower $t_{1/2}$ values were observed for all MLMs stored at 25 °C. However, MLMs containing the highest FHPO concentration (MLM_90:10; $t^{1/2} = 63$ days) and those with the highest PO concentration (MLM_50:50; $t^{1/2} = 65$ days) exhibited the lowest $t_{1/2}$ among all treatments. It is believed that much of the less stable polymorphic form of the formulation MLM_50:50 was melted at 25 °C, giving rise to the more stable β -form, leading to greater expulsion of the anthocyanins in the MLMs. For the MLM_90:10, the high saturated fatty acids concentration led to the formation of particles with a more compact structure, therefore with a greater expulsion of anthocyanins to the surface during storage, facilitating their degradation. Procópio et al. (2018) reported that the absence of unsaturated fatty acids in spray-chilled MLMs loaded with cinnamon oleoresin led to rapid crystallization of the MLMs, with a greater expulsion of the active ingredient during storage.

Tulini et al. (2017) evaluated the stability of MLMs obtained by spray chilling from vegetable fat (melting point 48 °C) loaded with proanthocyanidins and alpha-tocopherol. The MLMs were stored at different storage temperatures (5, 25, and 37 °C) for 90 days. At 25 and 37 °C there were the lowest retention of proanthocyanidins and alpha-tocopherol. During storage, especially at higher temperatures, the MLMs underwent polymorphic changes to an amorphous phase due to the fat melting, which may have contributed to the greater degradation of the bioactive compounds.

Thus, the formulations MLM_80:20, MLM_70:30, and MLM_60:40 were the most stable at all temperatures of storage, with better anthocyanins retention. This result reinforces that blends made with solid and liquid lipids can change the particle structure, favoring the

entrapment of the active compound. In this study, there was a better FHPO to PO ratio for the anthocyanins retention in the grape peel extract, due to it allowed the maintenance of β' crystals during storage (Müller et al., 2002b).

The results of the total color difference ΔE^* of the MLMs show that the anthocyanins degradation was highly influenced by the storage temperature. In general, the MLMs stored at the three temperatures showed oscillations of the ΔE^* values (Fig. 6) probably due to reactions of the anthocyanin pigment that is able to be regenerated continuously since some pathways are reversible (Berland & Andersen, 2021; Maciel et al., 2018).

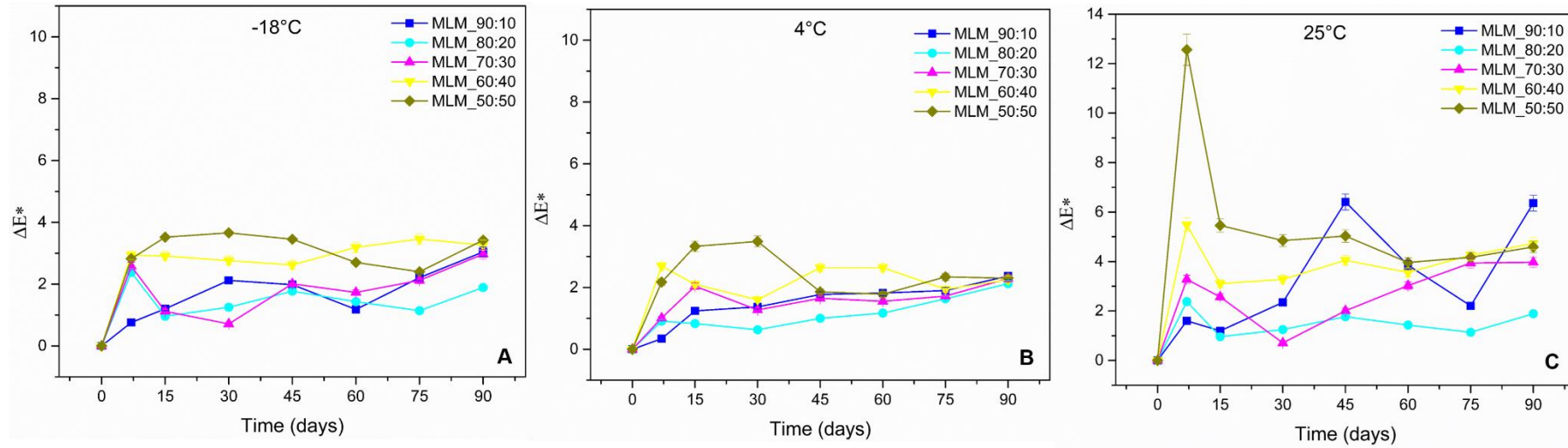


Fig. 6. ΔE^* values of spray-chilling MLMs containing grape peel extract made with different FHPO to PO ratios, during storage at: (A) -18 °C, (B) 4 °C, and (C) 25 °C.

However, the reactions were irreversible after a certain period of storage, with an increase in ΔE^* for most treatments. The smallest oscillations in ΔE^* observed for the treatments stored at -18°C and 4°C , corroborating the results of the anthocyanins retention during storage. As can be seen in Figs. 6A, B, and C, the MLMs containing 40 and 50% PO showed the greatest changes in ΔE^* throughout the storage for all temperatures, while the MLM containing 10% PO demonstrated high color instability at 25°C . MLMs containing higher concentrations of unsaturated fatty acids crystallized in the less unstable form, with reorganization to more stable polymorphic forms during storage, generating instability in the particle structures and favoring anthocyanins degradation and consequently greater color changes. Moreover, the high saturated fatty acids concentration in MLM_90:10 led to the anthocyanins release during storage at 25°C , causing the degradation of this pigment, as shown in the ΔE^* values.

However, at the end of storage at -18°C and 4°C , most treatments showed similar ΔE^* values below 4. In turn, the values were slightly higher at 25°C , due to the instability of the anthocyanin pigment at higher temperatures. It is worth noting that the formulation MLM_80:20 stood out with higher color stability at all temperatures, maintaining a more stable behavior. Fig. 7 shows the visual color changes of the MLMs, with emphasis on the treatments stored at 25°C , with a great tendency of color loss.

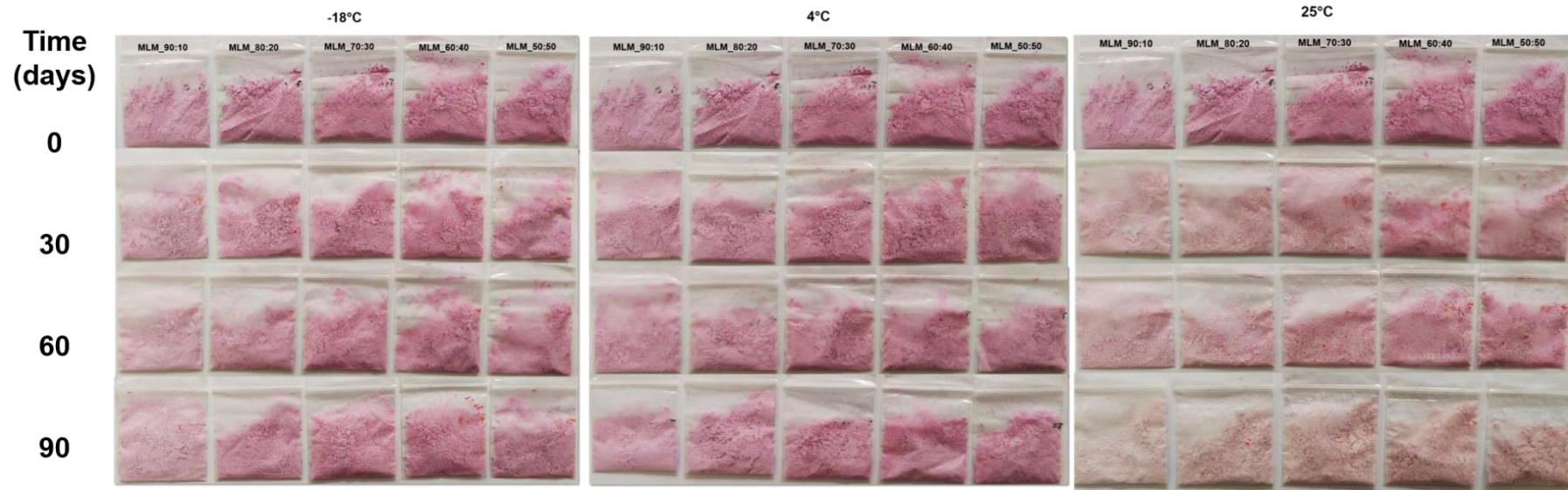


Fig.7. Visual aspects of spray-chilled MLMs containing grape peel extract made with different FHPO to PO ratios, stored at -18 °C, 4 °C, and 25 °C for 90 days.

4.5 Stability of MLMs in the gastrointestinal tract in vitro

To evaluate the protection of anthocyanin from degradation when passing through an unfavorable environment in the gastrointestinal tract, the release of anthocyanins from MLMs and the free grape peel extract was studied under simulated gastric and intestinal juices. As shown in Fig. 8, the anthocyanins release was effectively controlled by the protective coating of the encapsulating materials. The lack of protection led to a higher release of anthocyanins from the free extract in the simulated gastric juice when compared to the MLMs. In the first 20 min of gastric simulation, the extract released more than 70 % of the anthocyanins, remaining constant until 120 min.

The maximum anthocyanins release from MLMs ranged from 12 to 2 %, which was dependent on the proportion of the encapsulating materials (FHPO and PO). In an acidic environment, anthocyanins are in the flavyl cation form with red color and are relatively stable, which explains the stable behavior of anthocyanins in both the extract and the MLMs when subjected to the simulated gastric conditions (Fredes et al., 2018).

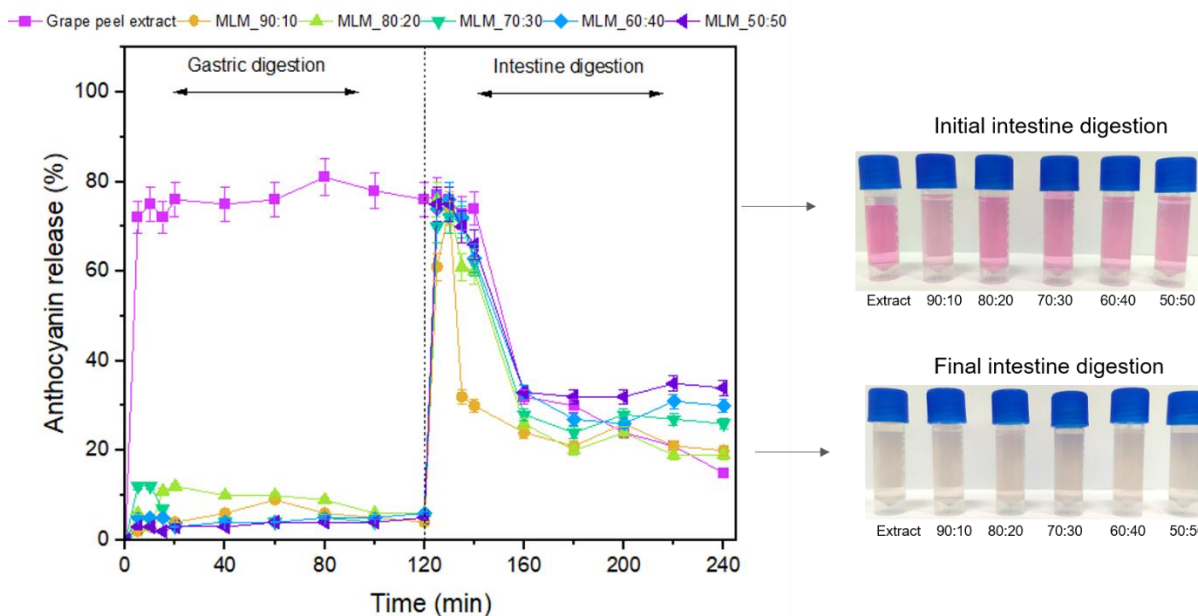


Fig. 8. (A) Anthocyanin release profile of the free grape peel extract and the microstructured lipid microparticles with different FHPO to PO ratios subjected to the simulated GI conditions. (B) Visible aspect of the intestinal juices of the free extract and the microparticles at the beginning (10 min) and at the end of the intestinal digestion *in vitro*.

However, the results suggested that the anthocyanins in the MLMs were more resistant to the gastric environment of the stomach and protected the bioactive compounds during passage through the simulated gastric system due to the structural barriers provided by the encapsulating materials. This hypothesis is evidenced by the color of the digestive juice in Fig. 9. At the onset of digestion, the simulated gastric juice referring the free extract exhibited red color, indicating the presence of anthocyanins, while the gastric juices of the MLMs showed a slight pink color, indicating low anthocyanins release. As shown in Fig. 9, the gastric juice of the free extract maintained its coloration at the end of gastric digestion, while the juices referring to the MLMs continued with a light pink color, with a greater intensity when compared to the initial time, indicating a more controlled release of anthocyanins over time. The particle stability at acidic pH and the pepsin hydrolysis may be due to the steric stabilization effect of the non-ionic surfactant PGPR, once nonionic surfactants show resistance to flocculation and coalescence at low pH values due to their molecular structure (Van Aken et al., 2011).

Studies have shown that the release of active compounds in nano- and/or micro-structured lipid particles usually occurs by diffusion of the active agent from the matrix or erosion of the matrix due to lipid degradation, and may be associated with different factors (Figueiredo et al., 2022; Sadati Behbahani et al., 2019). In the present study, the highest anthocyanins release from MLMs in the simulated gastric conditions may be due to three major factors, including the size, morphology, and lipid composition of the microparticles.

In the first 20 minutes, higher anthocyanins release from MLMs was observed for the treatments containing 20, 30, and 40% PO, with release percentages of 5, 9, and 5%, respectively. This rapid release may be due to the anthocyanins adsorbed on the particle surface. After this period, smaller MLMs presented greater anthocyanins release in the gastric system up to 100 minutes. The higher anthocyanin release from smaller particles may be due to the larger surface area of the particles, which may be controlled by the diffusion of the anthocyanins through the lipid matrix (Sadati Behbahani et al., 2019).

However, the higher release was not proportional to the smaller particle size. Although the formulation MLM_90:10 presented the lower particle size, a higher anthocyanins release was observed for the MLMs containing 20% PO. Therefore, the higher PO concentration in the MLMs led to further erosion and weakening of the particle matrix structure over time due to the partial melting of PO induced by simulated acidic gastric conditions and temperature (37 °C), thus facilitating the anthocyanins release. This behavior was observed at 120 min, when the MLMs containing a higher PO concentration (40 and 50%) showed a greater anthocyanins release. The images of the gastric juice at the end of digestion (Fig. 9) corroborate these results, with a higher intensity of pink color for the gastric juice referring to MLM_60:40 and MLM_50:50. However, these MLMs showed high resistance to the simulated gastric conditions up to 100 minutes probably due to the physical characteristics of the MLMs. The larger sizes, high agglomeration, and particle adhesion may have hindered the interaction and mobility with

the aqueous medium mainly at the beginning of the digestion, preventing the diffusion of anthocyanins into the matrix, with a lower release of this active compound. With increasing digestion time, the partial melting of PO facilitated the controlled anthocyanins release from the MLMs. This greater agglomeration and less interaction with the gastric juice can be seen in Figure 9.

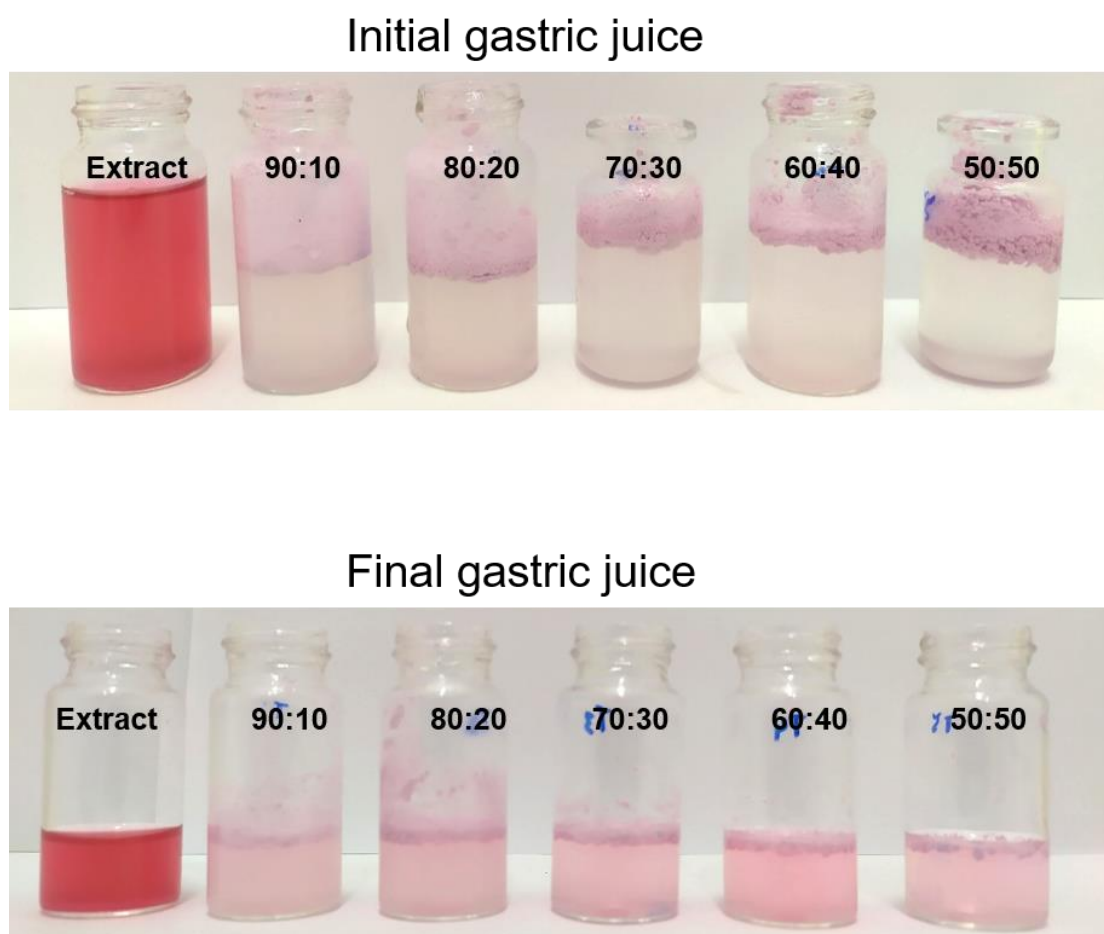


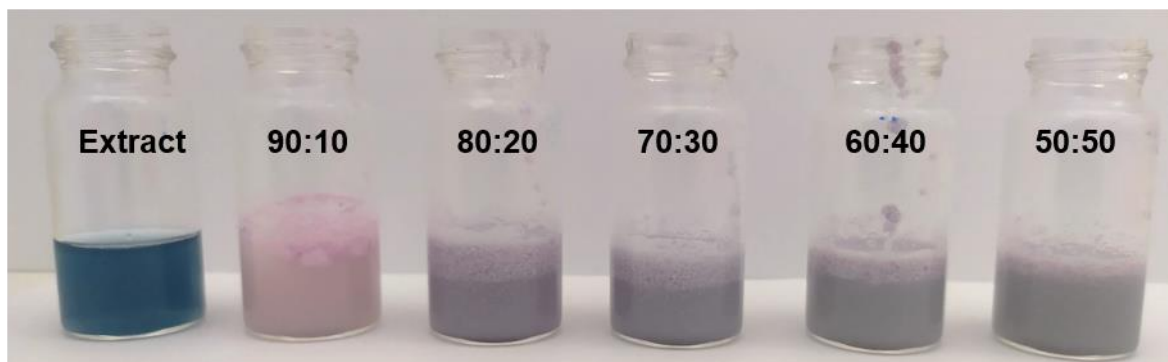
Fig. 9. Visible aspect of the gastric juices of the free grape peel extract and the microparticles with different FHPO to PO ratios, at the beginning (10 minutes) and at the end (120 minutes) of the gastric simulation in vitro.

For the intestinal simulation (Fig. 8), the amount of anthocyanin released from the free extract and the MLMs reached maximum values in the first 20 minutes. After this period, there was a decrease in the amount of anthocyanins for all treatments, probably due to the degradation of this compound (Tagliazucchi et al., 2010). Anthocyanins are unstable at high pH, and the

change from acidic pH (pH 1.2) in the stomach to neutral pH in the duodenum (pH 7.4) may be responsible for the hydrolysis and/or degradation of anthocyanins due to the partial disintegration of the encapsulating materials (Fig. 10). However, when anthocyanins are encapsulated, they are more protected in the gastrointestinal tract, as demonstrated in this study. This behavior was not observed for the free extract, which showed a linear decrease in anthocyanins content over time. Similar findings were reported by Fredes et al. (2018) for the free extract of maqui berry juice rich in anthocyanins encapsulated by spray drying. The authors stated that the encapsulating materials acted as an additional protective effect to the anthocyanins in the GI tract. The control of anthocyanin release under these conditions is beneficial for the absorption of the bioactive compound into the intestinal cells (Ahmad et al., 2018).

In the intestinal phase, the treatment MLM_{90:10} took a longer time to disintegrate the particles completely, especially early in the simulation (Fig. 10), followed by the treatments MLM_{80:20} and MLM_{70:30}. These results suggest that large amounts of the higher melting point lipid (FHPO) may provide greater physical resistance to the microparticles, maintaining a controlled anthocyanins release. MLMs with lower FHPO concentrations (MLM_{60:40} and MLM_{50:50}) exhibited the highest anthocyanin release in the intestinal phase, suggesting that the presence of lower melting point lipids can improve the disintegration of MLMs during digestion.

Initial intestine juice



Final intestine juice

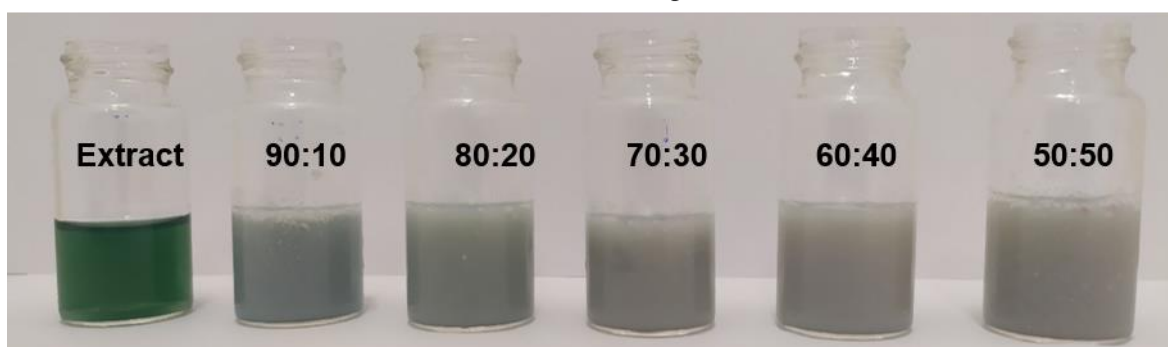


Fig. 10. Visible aspect of the intestinal juices of the free grape peel extract and the microparticles with different FHPO to PO ratios, at the beginning (10 minutes) and at the end (120 minutes) of the GI simulation *in vitro*.

For anthocyanins and other phenolic compounds, an effective digestion, absorption, and metabolization is necessary to exert their bioactive activities (Bao et al., 2019). The GI simulation *in vitro* of this study showed that the spray chilling microencapsulation can increase the bioaccessibility of anthocyanins. The results showed that MLMs with different FHPO to PO ratios effectively prevented the anthocyanins release under gastric conditions, while maintaining a higher release in the intestinal phase, where this compound is better absorbed, thus conferring health benefits (Donhowe et al., 2014; Mihalcea et al., 2020).

5. Conclusion

The use of spray chilling technique for the production of microstructured lipid microparticles containing anthocyanins from grape peel extract using blends of fully hydrogenated palm oil (FHPO) and palm oil (PO) as encapsulating materials may be a promising approach. Higher FHPO concentrations decreased the mean particle diameter and improved the flowability and cohesiveness of the particles. The highest anthocyanins retention, phenolic compounds content, and antioxidant capacity of the microparticles (MLMs) before storage were observed for the treatment with 90% FHPO and 10% PO (81.5%; 1443.1 mg GAE.100g⁻¹; 92.6%), respectively. All MLMs showed high melting temperatures (< 50 °C), however a higher thermal resistance of the microparticles was observed for higher FHPO concentrations. X-ray diffraction revealed that the MLMs mostly exhibited β' and β'' polymorphs. Regarding the storage stability of the microparticles, the retention and half-life times of anthocyanins were most affected at 25 °C. The microparticles made with 80:20; 70:30, and 60:40 of FHPO:PO stored at -18 °C, 4 °C, and 25 °C for 90 days can be considered more stable concerning the anthocyanins content and color changes, demonstrating a high potential for application in food products such as yogurts, ice cream, powder preparations, vegan and vegetarian products, and supplements. In turn, the microparticles made with 90:10 and 50:50 of FHPO:PO can be used in foods requiring early release of bioactive compounds and pigments. The gastrointestinal simulation *in vitro* showed that MLMs increased the bioaccessibility of anthocyanins. All treatments were able to protect the anthocyanins from the gastric phase, allowing greater release of this compound in the intestinal phase, which was greater with increasing PO concentrations. These results suggest that spray chilling is an effective alternative for the production of microparticles with biological and techno-functional properties.

References

- Ahmad, M., Ashraf, B., Gani, A., & Gani, A. (2018). Microencapsulation of saffron anthocyanins using β glucan and β cyclodextrin: Microcapsule characterization, release behaviour & antioxidant potential during in-vitro digestion. *International Journal of Biological Macromolecules*, *109*, 435–442.
<https://doi.org/10.1016/j.ijbiomac.2017.11.122>
- Alemzadeh, I., Hajiabbas, M., Pakzad, H., Sajadi Dehkordi, S., & Vossoughi, A. (2020). Encapsulation of food components and bioactive ingredients and targeted release. *International Journal of Engineering, Transactions A: Basics*, *33*(1), 1–11.
<https://doi.org/10.5829/ije.2020.33.01a.01>
- Alvim, I. D., Stein, M. A., Koury, I. P., Dantas, F. B. H., & Cruz, C. L. de C. V. (2016). Comparison between the spray drying and spray chilling microparticles contain ascorbic acid in a baked product application. *LWT - Food Science and Technology*, *65*, 689–694.
<https://doi.org/10.1016/j.lwt.2015.08.049>
- Amendola, D., De Faveri, D. M., & Spigno, G. (2010). Grape marc phenolics: Extraction kinetics, quality and stability of extracts. *Journal of Food Engineering*, *97*(3), 384–392.
<https://doi.org/10.1016/j.jfoodeng.2009.10.033>
- AOCS - American oil Chemists' Society. Official methods and recommended practices of the AOCS. (2004) 5. ed. Champaign: AOCS, p. 1200.
- Bao, C., Jiang, P., Chai, J., Jiang, Y., Li, D., Bao, W., Liu, B., Liu, B., Norde, W., & Li, Y. (2019). The delivery of sensitive food bioactive ingredients: Absorption mechanisms, influencing factors, encapsulation techniques and evaluation models. *Food Research International*, *120*, 130–140. <https://doi.org/10.1016/j.foodres.2019.02.024>
- Barbas, C., Herrera, E. (1998). Lipid composition and vitamin E content in human colostrum

and mature milk. *J Physiol Biochem.* 54(3), 167-73.

- Barroso, L., Viegas, C., Vieira, J., Ferreira-Pêgo, C., Costa, J., & Fonte, P. (2021). Lipid-based carriers for food ingredients delivery. *Journal of Food Engineering*, 295, 110451. <https://doi.org/10.1016/j.jfoodeng.2020.110451>
- Berland, H., & Andersen, Ø. M. (2021). Characterization of a Natural, Stable, Reversible and Colourful Anthocyanidin Network from Sphagnum Moss Based Mainly on the Yellow Trans-Chalcone and Red Flavylium Cation Forms. *Molecules*, 26(3), 709. <https://doi.org/10.3390/molecules26030709>
- Campelo-Felix, P. H., Souza, H. J. B., Figueiredo, J. D. A., Fernandes, R. V. de B., Botrel, D. A., de Oliveira, C. R., Yoshida, M. I., & Borges, S. V. (2017). Prebiotic Carbohydrates: Effect on Reconstitution, Storage, Release, and Antioxidant Properties of Lime Essential Oil Microparticles. *Journal of Agricultural and Food Chemistry*, 65(2), 445–453. <https://doi.org/10.1021/acs.jafc.6b04643>
- Carbonell-Capella, J. M., Buniowska, M., Barba, F. J., Esteve, M. J., & Frígola, A. (2014). Analytical methods for determining bioavailability and bioaccessibility of bioactive compounds from fruits and vegetables: A review. *Comprehensive Reviews in Food Science and Food Safety*, 13(2), 155–171. <https://doi.org/10.1111/1541-4337.12049>
- Carmo, E. L. do, Teodoro, R. A. R., Félix, P. H. C., Fernandes, R. V. de B., Oliveira, É. R. de, Veiga, T. R. L. A., Borges, S. V., & Botrel, D. A. (2018). Stability of spray-dried beetroot extract using oligosaccharides and whey proteins. *Food Chemistry*, 249, 51–59. <https://doi.org/10.1016/j.foodchem.2017.12.076>
- Carmo, E. L., Teixeira, M. A., Souza, I. S., Figueiredo, J. de A., Fernandes, R. V. de B., Botrel, D. A., & Borges, S. V. (2021). Co-encapsulation of anthocyanins extracted from grape skins (*Vitis vinifera* var. Syrah) and α -tocopherol via spray drying. *Journal of*

Food Processing and Preservation, 45(12), 1–11. <https://doi.org/10.1111/jfpp.16038>

Carvalho, J. D. dos S., Oriani, V. B., de Oliveira, G. M., & Hubinger, M. D. (2019).

Characterization of ascorbic acid microencapsulated by the spray chilling technique using palm oil and fully hydrogenated palm oil. *LWT*, 101, 306–314.

<https://doi.org/10.1016/j.lwt.2018.11.043>

Chalella Mazzocato, M., Thomazini, M., & Favaro-Trindade, C. S. (2019). Improving

stability of vitamin B12 (Cyanocobalamin) using microencapsulation by spray chilling technique. *Food Research International*, 126, 108663.

<https://doi.org/10.1016/j.foodres.2019.108663>

Consoli, L., Grimaldi, R., Sartori, T., Menegalli, F. C., & Hubinger, M. D. (2016). Gallic acid

microparticles produced by spray chilling technique: Production and characterization.

LWT - Food Science and Technology, 65, 79–87.

<https://doi.org/10.1016/j.lwt.2015.07.052>

Donhowe, E. G., Flores, F. P., Kerr, W. L., Wicker, L., & Kong, F. (2014). LWT - Food

Science and Technology Characterization and in vitro bioavailability of β -carotene :

Effects of microencapsulation method and food matrix. *LWT - Food Science and*

Technology, 57(1), 42–48. <https://doi.org/10.1016/j.lwt.2013.12.037>

Figueiredo, J. de A., MT Lago, A., M Mar, J., S Silva, L., A Sanches, E., P Souza, T., A

Bezerra, J., H Campelo, P., A Botrel, D., & V Borges, S. (2020). Stability of camu-camu encapsulated with different prebiotic biopolymers. *Journal of the Science of Food and*

Agriculture, 100(8), 3471–3480. <https://doi.org/10.1002/jsfa.10384>

Figueiredo, J. de A., Silva, C. R. de P., Souza Oliveira, M. F., Norcino, L. B., Campelo, P. H.,

Botrel, D. A., & Borges, S. V. (2022). Microencapsulation by spray chilling in the food

industry: Opportunities, challenges, and innovations. *Trends in Food Science &*

Technology, 120, 274–287. <https://doi.org/10.1016/j.tifs.2021.12.026>

Fitzpatrick, J. (2013). Powder properties in food production systems. In *Handbook of Food*

Powders: Processes and Properties, 285–308. Elsevier.

<https://doi.org/10.1533/9780857098672.2.285>

Flores, F. P., Singh, R. K., Kerr, W. L., Pegg, R. B., & Kong, F. (2014). Total phenolics content and antioxidant capacities of microencapsulated blueberry anthocyanins during in vitro digestion. *Food Chemistry*, 153, 272–278.

<https://doi.org/10.1016/j.foodchem.2013.12.063>

Fredes, C., Osorio, M. J., Parada, J., & Robert, P. (2018). Stability and bioaccessibility of anthocyanins from maqui (*Aristotelia chilensis* [Mol.] Stuntz) juice microparticles. *LWT*,

91, 549–556. <https://doi.org/10.1016/j.lwt.2018.01.090>

Gamboa, O. D., Gonçalves, L. G., & Grosso, C. F. (2011). Microencapsulation of tocopherols in lipid matrix by spray chilling method. *Procedia Food Science*, 1, 1732–1739.

<https://doi.org/10.1016/j.profoo.2011.09.255>

Gee, P. T. (2007). Analytical characteristics of crude and refined palm oil and fractions.

European Journal of Lipid Science and Technology, 109(4), 373–379.

<https://doi.org/10.1002/ejlt.200600264>

Geldart, D., Harnby, N., & Wong, A. C. (1984). Fluidization of cohesive powders. *Powder*

Technology, 37(1), 25–37. [https://doi.org/10.1016/0032-5910\(84\)80003-0](https://doi.org/10.1016/0032-5910(84)80003-0)

Groom, C.R., Bruno, I. J., Lightfoot, M. P., Ward, S.C. (2016). The Cambridge Structural

Database. *Acta Cryst. B*72, 171-179. <https://doi.org/10.1107/S2052520616003954>

Haas, I. C. da S., Toaldo, I. M., Gomes, T. M., Luna, A. S., de Gois, J. S., & Bordignon-Luiz,

M. T. (2019). Polyphenolic profile, macro- and microelements in bioaccessible fractions of grape juice sediment using in vitro gastrointestinal simulation. *Food Bioscience*, 27,

66–74. <https://doi.org/10.1016/j.fbio.2018.11.002>

Hogervorst, J. C., Miljić, U., & Puškaš, V. (2017). Extraction of Bioactive Compounds from Grape Processing By-Products. In *Handbook of Grape Processing By-Products*, 105–135. Elsevier. <https://doi.org/10.1016/B978-0-12-809870-7.00005-3>

Kuck, L. S., & Noreña, C. P. Z. (2016). Microencapsulation of grape (*Vitis labrusca* var. Bordo) skin phenolic extract using gum Arabic, polydextrose, and partially hydrolyzed guar gum as encapsulating agents. *Food Chemistry*, *194*, 569–576. <https://doi.org/10.1016/j.foodchem.2015.08.066>

Landim Neves, M. I., de Souza Queirós, M., Soares Viriato, R. L., Badan Ribeiro, A. P., & Gigante, M. L. (2021). Anhydrous milk fat blended with fully hydrogenated soybean oil as lipid microparticles: Characterization, stability, and trends for application. *LWT*, *152*, 112276. <https://doi.org/10.1016/j.lwt.2021.112276>

Lin, S. W. (2002). Palm Oil. In: Gunstone, F.D. (Ed), *Vegetable Oils in Food Technology: Composition, Properties and Uses*. In *Encyclopedia of Food and Health*. CRC Press LLC. <https://doi.org/10.1016/B978-0-12-384947-2.00514-6>

Maciel, L. G., do Carmo, M. A. V., Azevedo, L., Daguer, H., Molognoni, L., de Almeida, M. M., Granato, D., & Rosso, N. D. (2018). Hibiscus sabdariffa anthocyanins-rich extract: Chemical stability, in vitro antioxidant and antiproliferative activities. *Food and Chemical Toxicology*, *113*, 187–197. <https://doi.org/10.1016/j.fct.2018.01.053>

Madene, A., & Jacquot, M. (2006). Review Flavour encapsulation and controlled release – a review. *International Journal of Food Science and Technology*, *41*(1), 1–21. <https://doi.org/10.1111/j.1365-2621.2005.00980.x>

Mar, J. M., da Silva, L. S., Lira, A. C., Kinupp, V. F., Yoshida, M. I., Moreira, W. P., Bruginski, E., Campos, F. R., Machado, M. B., de Souza, T. P., Campelo, P. H., de

- Araújo Bezerra, J., & Sanches, E. A. (2020). Bioactive compounds-rich powders: Influence of different carriers and drying techniques on the chemical stability of the Hibiscus acetosella extract. *Powder Technology*, *360*, 383–391. <https://doi.org/10.1016/j.powtec.2019.10.062>
- Matos-Jr, F. E., Comunian, T. A., Thomazini, M., & Favaro-Trindade, C. S. (2017). Effect of feed preparation on the properties and stability of ascorbic acid microparticles produced by spray chilling. *LWT*, *75*, 251–260. <https://doi.org/10.1016/j.lwt.2016.09.006>
- Mihalcea, L., Barbu, V., Enachi, E., Andronoiu, D. G., Râpeanu, G., Stoica, M., Dumitraşcu, L., & Stănciuc, N. (2020). Microencapsulation of Red Grape Juice by Freeze drying and Application in Jelly Formulation. *Food Technology and Biotechnology*, *58*(1), 20–28. <https://doi.org/10.17113/ftb.58.01.20.6429>
- Minekus, M., Alming, M., Alvito, P., Ballance, S., Bohn, T., Bourlieu, C., Carrière, F., Boutrou, R., Corredig, M., Dupont, D., Dufour, C., Egger, L., Golding, M., Karakaya, S., Kirkhus, B., Le Feunteun, S., Lesmes, U., Macierzanka, A., Mackie, A., ... Brodkorb, A. (2014). A standardised static *in vitro* digestion method suitable for food – an international consensus. *Food Funct.*, *5*(6), 1113–1124. <https://doi.org/10.1039/C3FO60702J>
- Moreno, T., Cocero, M. J., & Rodríguez-Rojo, S. (2018). Storage stability and simulated gastrointestinal release of spray dried grape marc phenolics. *Food and Bioprocess Processing*, *112*, 96–107. <https://doi.org/10.1016/j.fbp.2018.08.011>
- Müller, R., Radtke, M., & Wissing, S. . (2002a). Nanostructured lipid matrices for improved microencapsulation of drugs. *International Journal of Pharmaceutics*, *242*(1–2), 121–128. [https://doi.org/10.1016/S0378-5173\(02\)00180-1](https://doi.org/10.1016/S0378-5173(02)00180-1)
- Müller, R. H., Petersen, R. D., Hommos, A., & Pardeike, J. (2007). Nanostructured lipid

- carriers (NLC) in cosmetic dermal products. *Advanced Drug Delivery Reviews*, 59(6), 522–530. <https://doi.org/10.1016/j.addr.2007.04.012>
- Müller, R. H., Radtke, M., & Wissing, S. A. (2002b). Solid lipid nanoparticles (SLN) and nanostructured lipid carriers (NLC) in cosmetic and dermatological preparations. *Advanced Drug Delivery Reviews*, 54(SUPPL.), 131–155. [https://doi.org/10.1016/S0169-409X\(02\)00118-7](https://doi.org/10.1016/S0169-409X(02)00118-7)
- Mutlu, C., Koç, A., & Erbaş, M. (2020). Some physical properties and adsorption isotherms of vacuum-dried honey powder with different carrier materials. *LWT*, 134, 110166. <https://doi.org/10.1016/j.lwt.2020.110166>
- Nahum, V., & Domb, A. J. (2021). Recent developments in solid lipid microparticles for food ingredients delivery. *Foods*, 10(2), 1–25. <https://doi.org/10.3390/foods10020400>
- Nogales-Bueno, J., Baca-Bocanegra, B., Rooney, A., Miguel Hernández-Hierro, J., José Heredia, F., & Byrne, H. J. (2017). Linking ATR-FTIR and Raman features to phenolic extractability and other attributes in grape skin. *Talanta*, 167, 44–50. <https://doi.org/10.1016/j.talanta.2017.02.008>
- O'Brien, R. D. (2004). *Fats and oils: formulating and processing for applications*. New York: CRC Press, 1–574. <https://doi.org/10.1002/9781118827123>
- Oliveira, G. M., Badan Ribeiro, A. P., dos Santos, A. O., Cardoso, L. P., & Kieckbusch, T. G. (2015). Hard fats as additives in palm oil and its relationships to crystallization process and polymorphism. *Lwt*, 63(2), 1163–1170. <https://doi.org/10.1016/j.lwt.2015.04.036>
- Omar, Z., Hishamuddin, E., Miskandar, M. S., Fauzi, S. H. M., Noor Lida, H. M. D., Ramli, M. R., & Abd Rashid, N. (2015). Palm oil crystallisation: A review. *Journal of Oil Palm Research*, 27(2), 97–106.
- Oriani, V. B., Alvim, I. D., Consoli, L., Molina, G., Pastore, G. M., & Hubinger, M. D.

- (2016). Solid lipid microparticles produced by spray chilling technique to deliver ginger oleoresin: Structure and compound retention. *Food Research International*, *80*, 41–49.
<https://doi.org/10.1016/j.foodres.2015.12.015>
- Oriani, V. B., Alvim, I. D., Paulino, B. N., Procópio, F. R., Pastore, G. M., & Hubinger, M. D. (2018). The influence of the storage temperature on the stability of lipid microparticles containing ginger oleoresin. *Food Research International*, *109*, 472–480.
<https://doi.org/10.1016/j.foodres.2018.04.066>
- Patra, N., & Routray, S. B. (2018). Solid Lipid-based Delivery System for Oral. *Asian Journal of Pharmaceutical Sciences*, *12*(4), 1135–1145.
- Patras, A., Brunton, N. P., Downey, G., Rawson, A., Warriner, K., & Gernigon, G. (2011). Application of principal component and hierarchical cluster analysis to classify fruits and vegetables commonly consumed in Ireland based on in vitro antioxidant activity. *Journal of Food Composition and Analysis*, *24*(2), 250–256.
<https://doi.org/10.1016/j.jfca.2010.09.012>
- Pelissari, J. R., Souza, V. B., Pigoso, A. A., Tulini, F. L., Thomazini, M., Rodrigues, C. E. C., Urbano, A., & Favaro-Trindade, C. S. (2016). Production of solid lipid microparticles loaded with lycopene by spray chilling: Structural characteristics of particles and lycopene stability. *Food and Bioproducts Processing*, *98*, 86–94.
<https://doi.org/10.1016/j.fbp.2015.12.006>
- Pinto, C. C., Campelo, P. H., & Michielon, S. de S. (2020). Rietveld-based quantitative phase analysis of B-type starch crystals subjected to ultrasound and hydrolysis processes. *Journal of Applied Polymer Science*, *137*(47), 49529. <https://doi.org/10.1002/app.49529>
- Procopio, F. R., Oriani, V. B., Paulino, B. N., do Prado-Silva, L., Pastore, G. M., Sant’Ana, A. S., & Hubinger, M. D. (2018). Solid lipid microparticles loaded with cinnamon

- oleoresin: Characterization, stability and antimicrobial activity. *Food Research International*, 113, 351–361. <https://doi.org/10.1016/j.foodres.2018.07.026>
- Pugliese, A., Cabassi, G., Chiavaro, E., Paciulli, M., Carini, E., & Mucchetti, G. (2017). Physical characterization of whole and skim dried milk powders. *Journal of Food Science and Technology*, 54(11), 3433–3442. <https://doi.org/10.1007/s13197-017-2795-1>
- Ray, S., Raychaudhuri, U., & Chakraborty, R. (2016). An overview of encapsulation of active compounds used in food products by drying technology. *Food Bioscience*, 13, 76–83. <https://doi.org/10.1016/j.fbio.2015.12.009>
- Rennie, P. R., Chen, X. D., Hargreaves, C., Mackereth, A. R. (1999). A study of cohesion of dairy powders. *Journal of Food Engineering*, 39, 277–284. [https://doi.org/10.1016/S0260-8774\(98\)00158-7](https://doi.org/10.1016/S0260-8774(98)00158-7)
- Ribeiro, A. P. B., Masuchi, M. H., Miyasaki, E. K., Domingues, M. A. F., Stroppa, V. L. Z., de Oliveira, G. M., & Kieckbusch, T. G. (2015). Crystallization modifiers in lipid systems. *Journal of Food Science and Technology*, 52(7), 3925–3946. <https://doi.org/10.1007/s13197-014-1587-0>
- Sadati Behbahani, E., Ghaedi, M., Abbaspour, M., Rostamizadeh, K., & Dashtian, K. (2019). Curcumin loaded nanostructured lipid carriers: In vitro digestion and release studies. *Polyhedron*, 164, 113–122. <https://doi.org/10.1016/j.poly.2019.02.002>
- Saifullah, M., Shishir, M. R. I., Ferdowsi, R., Tanver Rahman, M. R., & Van Vuong, Q. (2019). Micro and nano encapsulation, retention and controlled release of flavor and aroma compounds: A critical review. *Trends in Food Science and Technology*, 86, 230–251. <https://doi.org/10.1016/j.tifs.2019.02.030>
- Santos, C. A., Carpenter, C. S., Arid, J. D., da Silva, Á. Á., Cardoso, L. P., Ribeiro, A. P. B., & Efraim, P. (2020). Production and characterization of promising β -stable seed crystals

- to modulate the crystallization of fat-based industrial products. *Food Research International*, 130, 108900. <https://doi.org/10.1016/j.foodres.2019.108900>
- Sato, K., & Ueno, S. (2011). Crystallization, transformation and microstructures of polymorphic fats in colloidal dispersion states. *Current Opinion in Colloid & Interface Science*, 16(5), 384–390. <https://doi.org/10.1016/j.cocis.2011.06.004>
- Sirohi, R., Tarafdar, A., Singh, S., Negi, T., Gaur, V. K., Gnansounou, E., & Bharathiraja, B. (2020). Green processing and biotechnological potential of grape pomace: Current trends and opportunities for sustainable biorefinery. *Bioresource Technology*, 314, 123771. <https://doi.org/10.1016/j.biortech.2020.123771>
- Tagliazucchi, D., Verzelloni, E., Bertolini, D., & Conte, A. (2010). In vitro bio-accessibility and antioxidant activity of grape polyphenols. *Food Chemistry*, 120(2), 599–606. <https://doi.org/10.1016/j.foodchem.2009.10.030>
- Timms, R. E. (1985). Physical properties of oils and mixtures of oils. *Journal of the American Oil Chemists' Society*, 62(2), 241–249. <https://doi.org/10.1007/BF02541385>
- Toby, B. H. (2006). R factors in Rietveld analysis: How good is good enough? *Powder Diffraction*, 21(1), 67–70. <https://doi.org/10.1154/1.2179804>
- Tulini, F. L., Souza, V. B., Thomazini, M., Silva, M. P., Massarioli, A. P., Alencar, S. M., Pallone, E. M. J. A., Genovese, M. I., & Favaro-Trindade, C. S. (2017). Evaluation of the release profile, stability and antioxidant activity of a proanthocyanidin-rich cinnamon (*Cinnamomum zeylanicum*) extract co-encapsulated with α -tocopherol by spray chilling. *Food Research International*, 95, 117–124. <https://doi.org/10.1016/j.foodres.2017.03.010>
- Usha R. Pothakamury, & Gustavo V. Barbosa-Cánovas. (1995). Fundamental aspects of controlled release in foods. *Trends in Food Science and Technology*, 6(12), 397–406.

- van Aken, G. A., Bomhof, E., Zoet, F. D., Verbeek, M., & Oosterveld, A. (2011). Differences in in vitro gastric behaviour between homogenized milk and emulsions stabilised by Tween 80, whey protein, or whey protein and caseinate. *Food Hydrocolloids*, 25(4), 781–788. <https://doi.org/10.1016/j.foodhyd.2010.09.016>
- Vu, T. ., Galet, L., Fages, J., & Oulahna, D. (2003). Improving the dispersion kinetics of a cocoa powder by size enlargement. *Powder Technology*, 130(1–3), 400–406. [https://doi.org/10.1016/S0032-5910\(02\)00242-5](https://doi.org/10.1016/S0032-5910(02)00242-5)
- Wegmüller, R., Zimmermann, M. B., Bühr, V. G., Windhab, E. J., & Hurrell, R. F. (2006). Development, stability, and sensory testing of microcapsules containing iron, iodine, and vitamin A for use in food fortification. *Journal of Food Science*, 71(2). <https://doi.org/10.1111/j.1365-2621.2006.tb08923.x>
- Yang, W., Kaimainen, M., Järvenpää, E., Sandell, M., Huopalahti, R., Yang, B., & Laaksonen, O. (2021). Red beet (*Beta vulgaris*) betalains and grape (*Vitis vinifera*) anthocyanins as colorants in white currant juice – Effect of storage on degradation kinetics, color stability and sensory properties. *Food Chemistry*, 348, 128995. <https://doi.org/10.1016/j.foodchem.2020.128995>